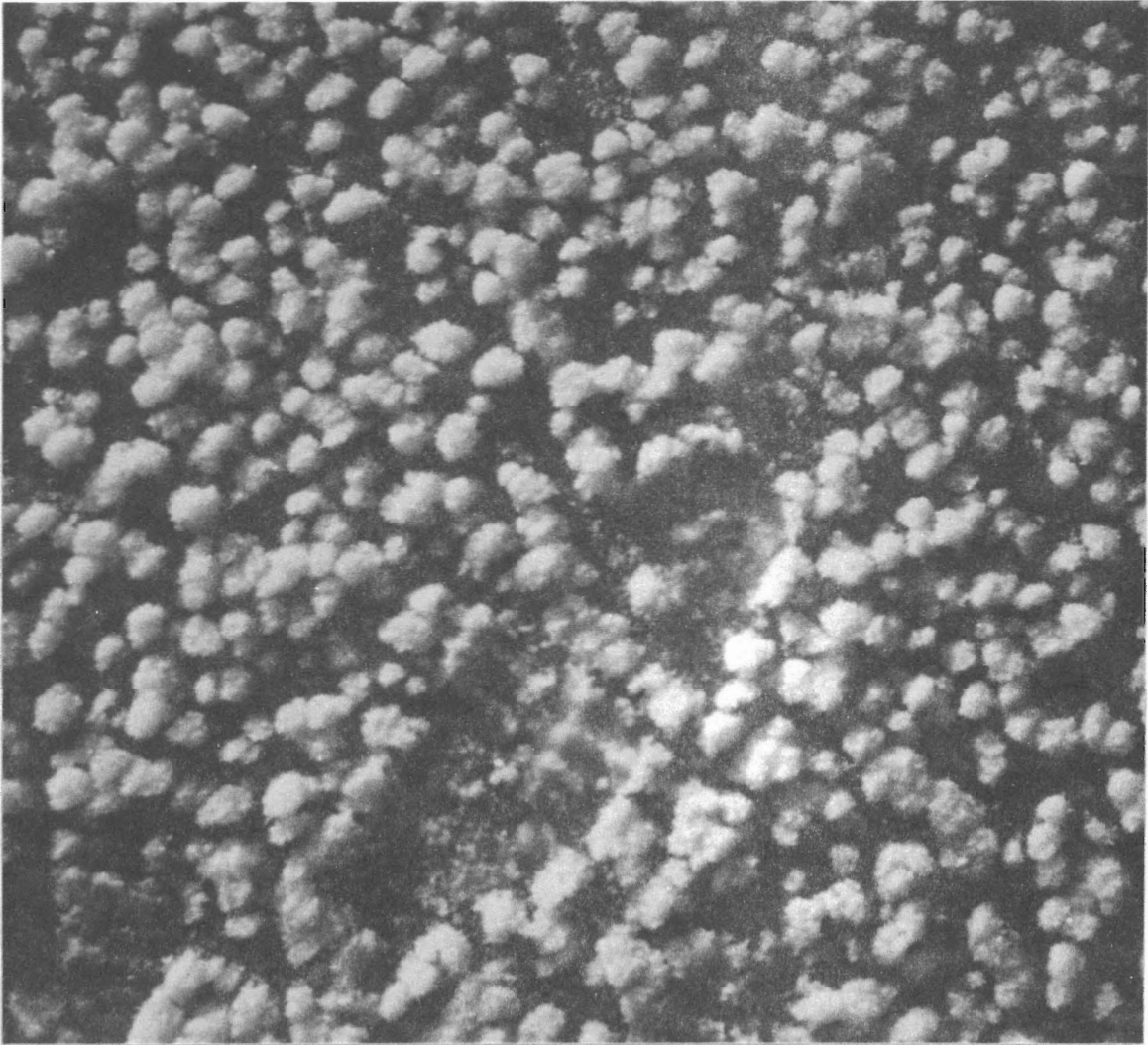


**Sea Ice Dynamics and Regional Meteorology for the
Arctic Polynya Experiment (APEX) - Bering Sea 1985**



Frontispiece.--Salt flowers of order 2.0 cm diameter, spaced on about 2.5 cm centers at floe marked with ARGOS buoy 2327. Note boot print in midframe.

NOAA Technical Memorandum ERL PMEL-64

SEA ICE DYNAMICS AND REGIONAL METEOROLOGY FOR THE
ARCTIC POLYNYA EXPERIMENT (APEX) - BERING SEA 1985

Carol H. Pease
Michael Reynolds
George A. Galasso
V. Lynn Long
Sigrid A. Salo
Bruce D. Webster

Pacific Marine Environmental Laboratory
Seattle, Washington
October 1985



**UNITED STATES
DEPARTMENT OF COMMERCE**

**Malcolm Baldrige,
Secretary**

**NATIONAL OCEANIC AND
ATMOSPHERIC ADMINISTRATION**

**Anthony J. Calio,
Administrator**

**Environmental Research
Laboratories**

**Vernon E. Derr,
Director**

NOTICE

Mention of a commercial company or product does not constitute an endorsement by NOAA/ERL. Use of information from this publication concerning proprietary products or the tests of such products for publicity or advertising purposes is not authorized.

CONTENTS

ABSTRACT.....	1
1. INTRODUCTION.....	2
2. EQUIPMENT AND METHODS.....	5
2.1 ARGOS.....	5
2.2 GOES.....	8
2.3 Deployment.....	8
3. ICE TRAJECTORIES AND REGIONAL CONDITIONS.....	16
4. METEOROLOGY.....	35
4.1 Regional Meteorology.....	35
4.2 Meteorology Station Results.....	48
5. OCEANOGRAPHY.....	56
5.1 Regional Oceanography.....	56
5.2 Oceanography Station Results.....	56
6. SUMMARY.....	61
7. ACKNOWLEDGMENTS.....	62
8. REFERENCES.....	63
Appendix A. METLIB Meteorological Data.....	65
- Surface Air Temperature and Sea-level Pressure Fields	
Appendix B. METLIB Meteorological Data.....	86
- Sea-level Pressure Fields and Surface Wind Vectors	
Appendix C. GOES Meteorological Data.....	107
Appendix D. GOES Oceanography Data.....	117

TABLES

1. ARGOS Buoy Position Accuracy.....6
2. Flight Operations.....14
3. GOES Station Deployment Information.....15
4. ARGOS Buoy Deployment Information.....15

FIGURES

1. Bathymetry of eastern Bering Sea and topography of St. Lawrence.....3
2. Photograph of ARGOS buoy 2328.....7
3. Frequency distribution of ARGOS buoy fixes.....7
4. Schematic of PMEL GOES ice station.....10
5. Current meter developed by PMEL for under-ice measurements.....11
6. Plot of battery voltage with time for the four GOES stations.....11
7. ARGOS buoy positions on 20 February 1985.....12
8. ARGOS buoy positions on 24 February 1985.....13
9. ARGOS buoy drift west of St. Lawrence Island.....18
10. ARGOS buoy drift east of St. Lawrence Island before 31 March.....24
11. ARGOS buoy drift east of St. Lawrence Island after 31 March.....30
12. Sea-level pressure analyses.....38
13. Meteorological time series plot for GOES station A.....49
14. Meteorological time series plot for GOES station B.....51
15. Meteorological time series plot for GOES station C.....53
16. Meteorological time series plot for GOES station D.....54
17. Oceanographic time series plot for GOES station A.....58
18. Oceanographic time series plot for GOES station B.....60

SEA ICE DYNAMICS AND REGIONAL METEOROLOGY FOR THE
ARCTIC POLYNYA EXPERIMENT (APEX) - BERING SEA 1985¹

Carol H. Pease, Michael Reynolds², George A. Galasso,
V. Lynn Long, Sigrid A. Salo, and Bruce D. Webster³

Pacific Marine Environmental Laboratory
National Oceanic and Atmospheric Administration
7600 Sand Point Way NE, Bin C15700, Building 3
Seattle, Washington 98115-0070

ABSTRACT. This memorandum summarizes the deployment of drifting ARGOS buoys, some with GOES ice stations in the northern Bering Sea, and stationary GOES meteorological stations on St. Lawrence Island in support of the Arctic Polynya Experiment (APEX). Weather conditions during January 1985 over the eastern Bering Sea and western Alaska were extremely anomalous with the warmest air temperatures on record and the least ice ever recorded for the month, both due to prolonged southerly winds throughout the month. During the last three weeks in February, the wind shifted to northerly, air temperatures dropped to -20 to -30°C, and the ice recovered its previous maximum both by freezing *in situ* and by the return of Bering Sea ice from the Chukchi Sea. Flying conditions were generally very good during this period, so all the buoys and drifting stations were deployed between 19 and 23 February.

The ARGOS buoys initially drifted south to southwestward. The buoys deployed on the west side of St. Lawrence Island turned and drifted northward on 27 February and the buoys deployed on the east side of the island turned on 28 February. This is consistent with the idea that reversals (periods of southward flow) in Anadyr Strait are of shorter duration than in Shpanberg Strait, although this was certainly one of longest reversals ever observed for Anadyr Strait. After 7 March, the buoys on the west side of St. Lawrence again drifted southwestward and the buoys on the east side of the island drifted southward. There was considerable strain over the arrays. Particularly, the eastern array lost two ARGOS buoys on the southward transit past St. Lawrence Island, one on the northward transit and one along the western end of Nunivak Island due to crushing or shear. Both arrays exhibited greater deformation than the MIZEX-West array did while passing St. Matthew Island during 1983.

¹ Contribution No. 807 from Pacific Marine Environmental Laboratory.

² Present Affiliation: Coastal Climate Company, Ltd., 316 2nd Avenue South, Seattle, Washington 98104.

³ Affiliation: Fairweather Forecasting, 6601 S. Airpark Place, Anchorage, Alaska 99502.

1. INTRODUCTION

Over the last decade, experimental studies of ice motion in the Bering Sea have indicated that sea ice floes are typically created along the coastlines of Alaska and Siberia and drift in the mean toward the southwest under the influence of northeasterly to easterly winds. Observations supporting this general view were made in 1979 (Salo et al., 1980; Pease, 1980), 1981 (Macklin et al., 1984; Pease et al., 1983), and 1983 (Reynolds et al., 1985) along the marginal ice zone of the eastern Bering Sea shelf and for the entire eastern Bering Sea shelf from satellite images for a variety of years (Muench and Ahlnäs, 1976; McNutt, 1981). However, ice motion studies made in the northern Bering Sea in 1980 (Pease and Salo, 1981), 1981 (Thomas and Pritchard, 1981) and 1982 (Reynolds and Pease, 1984; Aagaard et al., 1985) have tempered the simple conveyor belt picture of coastal ice formation, drift toward the south and west, and ice-edge decay. In some winters and possibly many springs for all or part of the northern Bering Sea, there is a net export of ice northward through the Bering Strait. Where and under what meteorological conditions the bifurcation of ice drift occurs and what role St. Lawrence Island plays are open questions. Clearly, the background currents are a factor (Salo et al., 1983; Schumacher et al., 1983; Aagaard et al., 1985; Muench and Schumacher, 1985), as are interannual variations in the meteorological forcing (Overland and Pease, 1982; Aagaard et al., 1985).

The purpose of this project, the Arctic Polynya Experiment (APEX), is to investigate physical processes in the atmosphere, sea ice, and ocean in the vicinity of St. Lawrence Island in the northern Bering Sea (Figure 1) and to observe the interaction of a wind-created polynya with regional dynamics and thermodynamics. The relative importance on sea ice motion of baroclinic currents due to brine rejection during the freezing of ice in the polynya, barotropic currents due to set-up on the shelf, internal ice stress due to the presence of St. Lawrence Island, wind stress, and Coriolis force are being considered through a measurement and modeling program. The measurement program included a variety of field measurements from ocean moorings, from the sea ice, and from St. Lawrence Island. The regional scale measurements looked particularly at differences between Anadyr Strait and Shpanberg Strait, on either side of St. Lawrence Island.

Nine ocean moorings were deployed with various configurations of instruments. They generally determined current velocities, water salinities, water temperatures, and ocean bottom pressure. Eight of these moorings were deployed from the R/V *Alpha Helix* during October, 1984 and were recovered by the R/V *Alpha Helix* in July, 1985. One mooring in Bering Strait was deployed in late November by commercial helicopter and was also recovered by the R/V *Alpha Helix*. The ocean mooring work was conducted jointly by Science Applications International Corp. of Bellevue, Washington and PMEL/NOAA.

The remainder of this report will detail deployment operations of equipment on the sea ice and on St. Lawrence Island during January and February, 1985 and provide preliminary interpretations of the results. The equipment included 15 ARGOS position buoys, 10 of which were fitted with air temperature sensors; 2 GOES shore meteorological stations with anemometers and air temperature sensors; and 2 GOES ice stations with the meteorological sensors plus air pressure transducers, current meters, water temperature sensors, floe rotation compasses, and LORAN-C receivers.

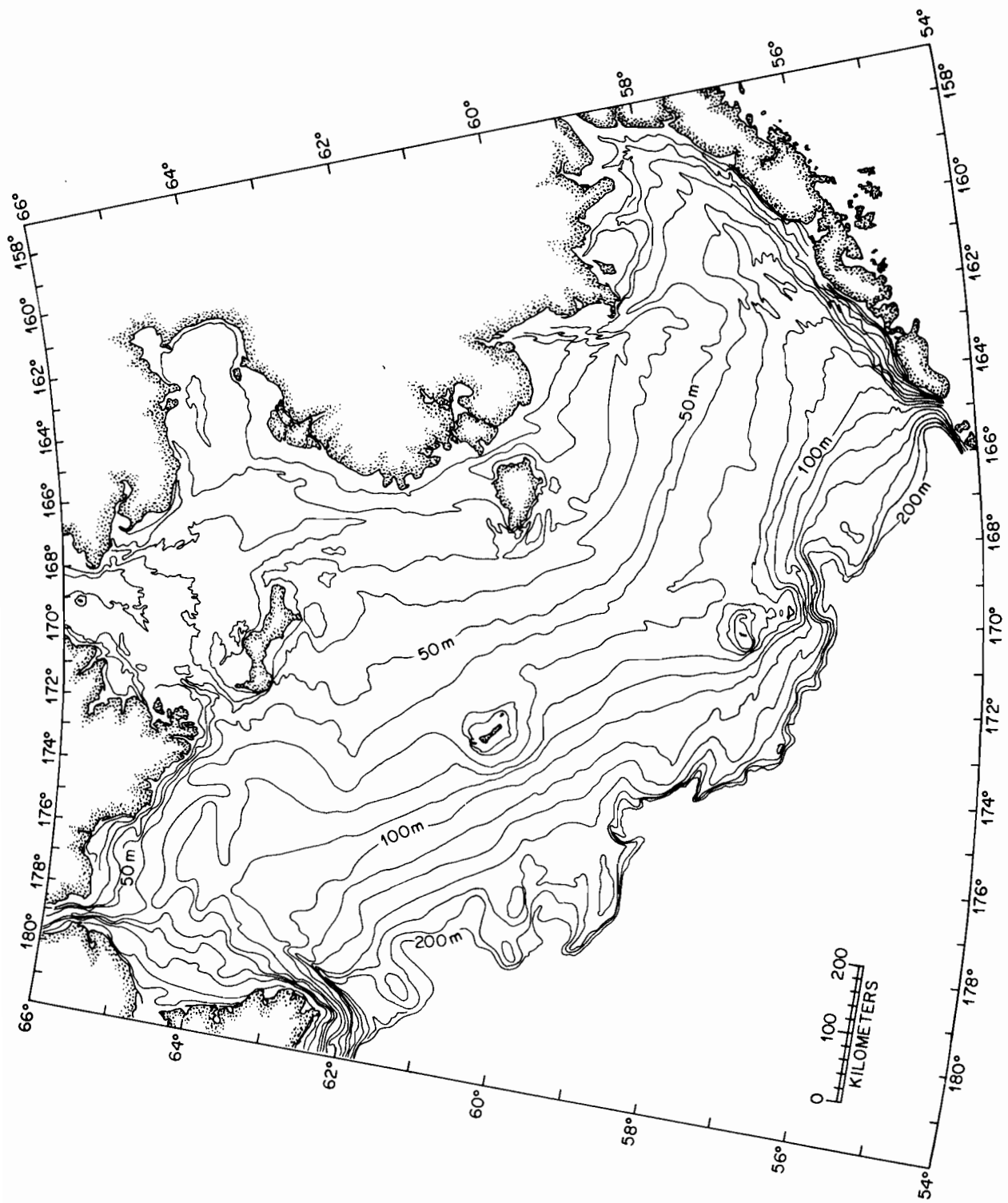


Figure 1a.--Bathymetry of the eastern Bering Sea. St. Lawrence Island is the large island centered approximately at 63.5°N, 171°W, south of Bering Strait.

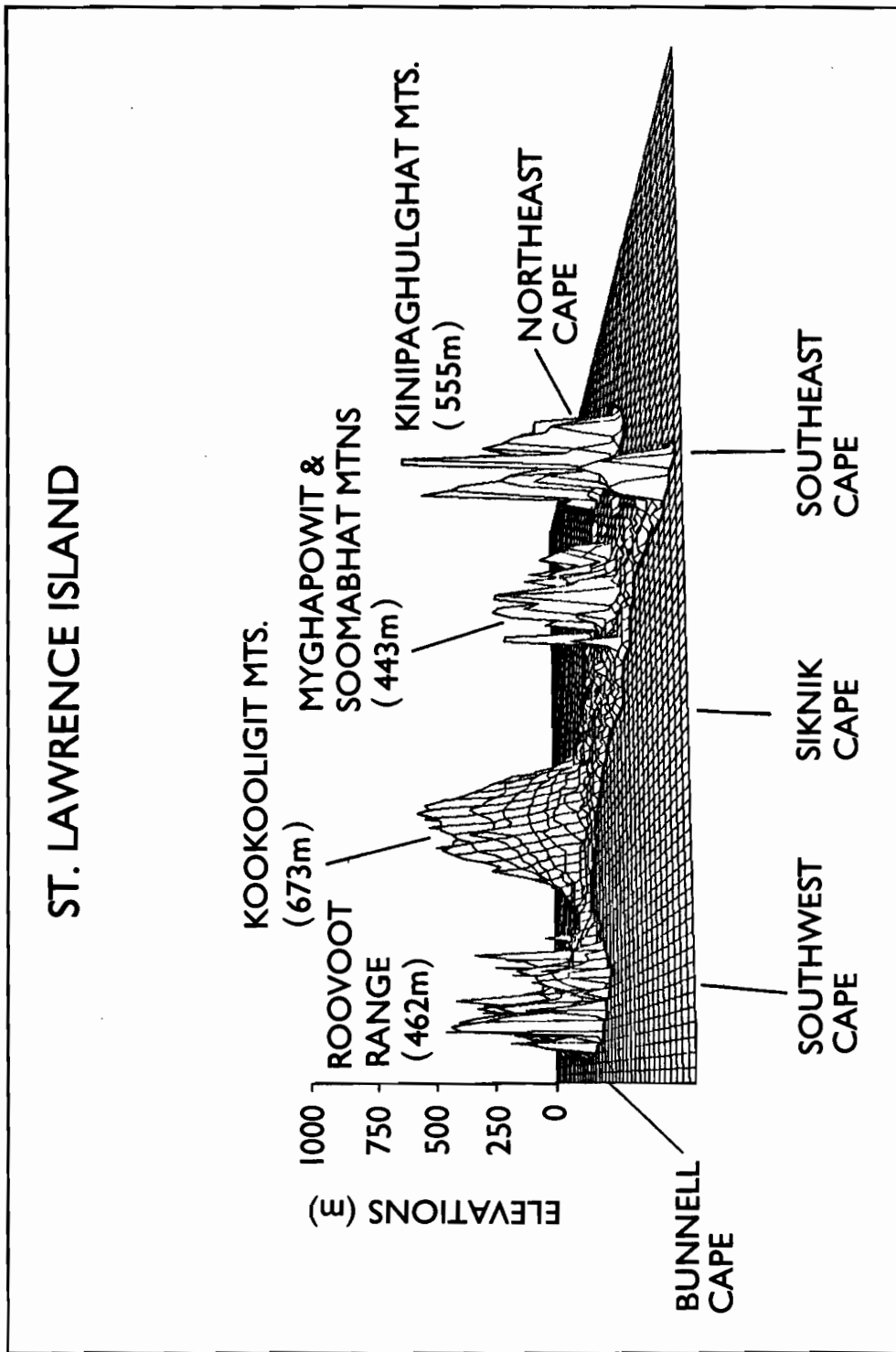


Figure 1b.--Topography of St. Lawrence Island. Elevations (m) are plotted on a 4-km grid looking toward the north-northeast, the principal direction from which the wind blows while the St. Lawrence polynya is open. The vertical exaggeration is about 125 times horizontal.

2. EQUIPMENT AND METHODS

2.1 ARGOS

The location of each ice buoy was determined by satellite with a transponder called an ARGOS Data Acquisition Platform (ADAP). We had 9 units (model 901) manufactured by Polar Research Laboratory; 4 of these were retrofitted by PRL with an air temperature probe inside a finned radiation shield and 5 of these were standard (without temperature). All of the PRL units were housed in rugged, waterproof polyethylene cases. We also had 6 units (model 2101A) manufactured by Synergetics and enclosed in wooden boxes built at PMEL (Figure 2). Each of these ADAP's was fitted with a linearized thermistor probe (model 44020) and precision resistor (model 44312) from Yellow Springs Instrument Company, inside of a gill-type radiation shield (model 44312) from R.M. Young. The nominal accuracy of the air temperature measurements was $\pm 0.1^{\circ}\text{C}$ over the full scale of -50°C to $+50^{\circ}\text{C}$. The ARGOS buoys were powered by (model LDD-1) lithium thionyl chloride batteries manufactured by Power Systems Operations.

Each ADAP transmitted independently at $401.650\text{ MHz} \pm 3.2\text{ kHz}$ at 55-s intervals for less than 1-s duration. The NOAA polar-orbiting satellites receive these transmissions when in view of the ADAP, record the transmissions on tape, and then retransmit them to one of three ground stations as they pass over. Service ARGOS then processes these transmissions for the Doppler shift to calculate buoy position, and the user receives bi-weekly tapes and real-time access to the data via the Service ARGOS computer.

The number of satellite passes over a given location is a function of latitude. For the vicinity of the central Bering Sea (58° - 64°N), the number of high quality fixes is typically 8 or 9 per day, with a highly non-Gaussian time-separation distribution (Figure 3). Figure 3 is based on all of the first and second quality fixes from Service ARGOS for the 12 long-lived buoys from the time of deployment until they quit transmitting. The times between successive fixes for each buoy were accumulated in registers, normalized by the total number of observation pairs for that buoy, and then the 12 buoys were averaged to produce Figure 3. The one standard-deviation distribution is also given in Figure 3. Nearly 60% of the observations were separated by less than 2 hours, and cumulatively 80% were separated by less than 4 hours. However, there is a very long tail on the time-separation distribution with significant data gaps at all separation intervals under 11 hours and for the 13-14 and 15-16 hour intervals for all buoys (Figure 3). Although each of these longer intervals accounts for only a few percent of the observation pairs, they constitute the greatest problem for designing a resampling scheme in order to compare ice velocities with other measurements.

The position accuracy of the ARGOS buoys is dependent on oscillator stability which varies greatly from transponder to transponder and must be obtained from intercalibrations at a fixed site prior to deployment. ARGOS position accuracy for the northern Bering Sea was tested from 1 to 19 February by looking at the position stability and biases of individual buoys next to the Army National Guard hanger at the Nome Airport. Table 1 summarizes these results for several buoys. The number of fixes per buoy vary both because some of the buoys were not turned on through the entire period and because some of the lower quality transmitters obtained fewer fixes. Some of the

buoys gave less accurate positions while part of the group than while dispersed in the field (e.g., 2335 performed as well as 2332 after the other buoys were deployed), in part because there are problems with so many buoys transmitting as a group, even if some care is taken so there are no overlapping transmission times. These problems are caused by the ARGOS data collection and location system having a limited reception capability (WMO, 1983). Informally it seemed that 8 buoys were the maximum number for intercomparison at one place and time. Except for the two highest quality buoys (2333 and 2334) which had very low correlations between latitude and longitude and one of the lower quality buoys (2336) which had an unusually high correlation, the quality of the position fix was inversely related to the correlation of latitude and longitude at a fixed point.

Table 1.--ARGOS buoy position accuracy for a fixed point during the period of 1 to 19 February 1985 at 64.51°N latitude for all non-duplicate fixes received from Service ARGOS.

Buoy ID	Buoy Type	Buoy Number of Fixes	Mean Latitude °N	Mean Longitude °E	Standard Deviation Latitude (km)	Standard Deviation Longitude (km)	Correlation Coefficient lat.-long.
2324	PRL-T	183	64.5103	194.5735	0.0037 (0.41)	0.0096 (0.46)	-0.21
2325	Syn-T	133	64.5100	194.5723	0.0031 (0.34)	0.0046 (0.22)	-0.57
2326	PRL-T	167	64.5100	194.5726	0.0032 (0.36)	0.0066 (0.32)	-0.38
2327	Syn-T	145	64.5105	194.5722	0.0043 (0.48)	0.0092 (0.44)	-0.28
2328	Syn-T	151	64.5102	194.5726	0.0030 (0.33)	0.0063 (0.30)	-0.49
2329	Syn-T	155	64.5103	194.5726	0.0030 (0.33)	0.0055 (0.26)	-0.58
2330	Syn-T	0					
2331	PRL-T	170	64.5105	194.5724	0.0026 (0.29)	0.0063 (0.30)	-0.42
2332	Syn-T	133	64.5102	194.5721	0.0064 (0.71)	0.0162 (0.77)	-0.15
2333	PRL-T	68	64.5107	194.5721	0.0008 (0.09)	0.0025 (0.12)	-0.10
2334	PRL-N	49	64.5104	194.5717	0.0019 (0.21)	0.0037 (0.18)	+0.05
2335	PRL-N	16	64.5048	194.5649	0.0195 (2.17)	0.0443 (2.12)	+0.09
2336	PRL-N	27	64.5095	194.5754	0.0041 (0.46)	0.0226 (1.08)	+0.54
2337	PRL-N	41	64.5112	194.5719	0.0047 (0.52)	0.0068 (0.33)	+0.22
2338	PRL-N	51	64.5098	194.5710	0.0031 (0.34)	0.0072 (0.34)	+0.24

¹ PRL-T is a Polar Research Laboratory ADAP model 901 modified for us by PRL to transmit air temperature. Syn-T is a Synergetics ARGOS transmitter and antenna built into a wooden box at PMEL and fitted with air temperature. PRL-N is a PRL ADAP model 901, not fitted with air temperature.

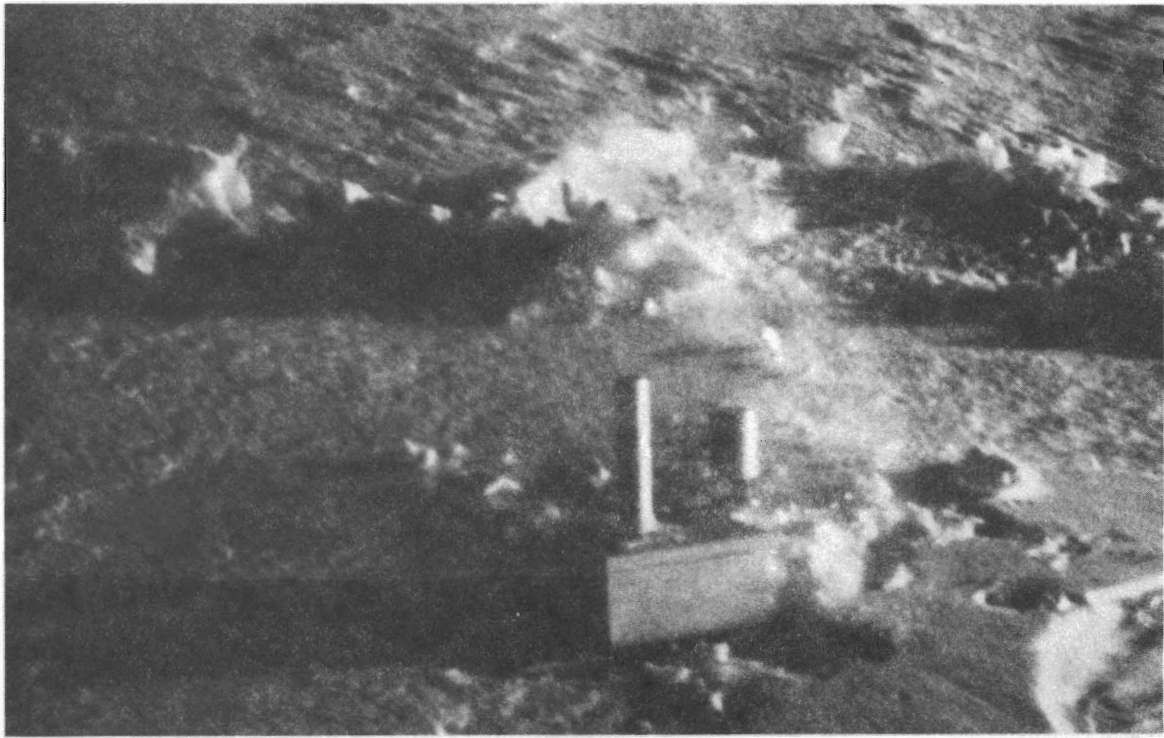


Figure 2. Photograph of ARGOS buoy 2328, typical of those buoys used for part of the deployment. Other buoys were off-the-shelf models directly from a manufacturer.

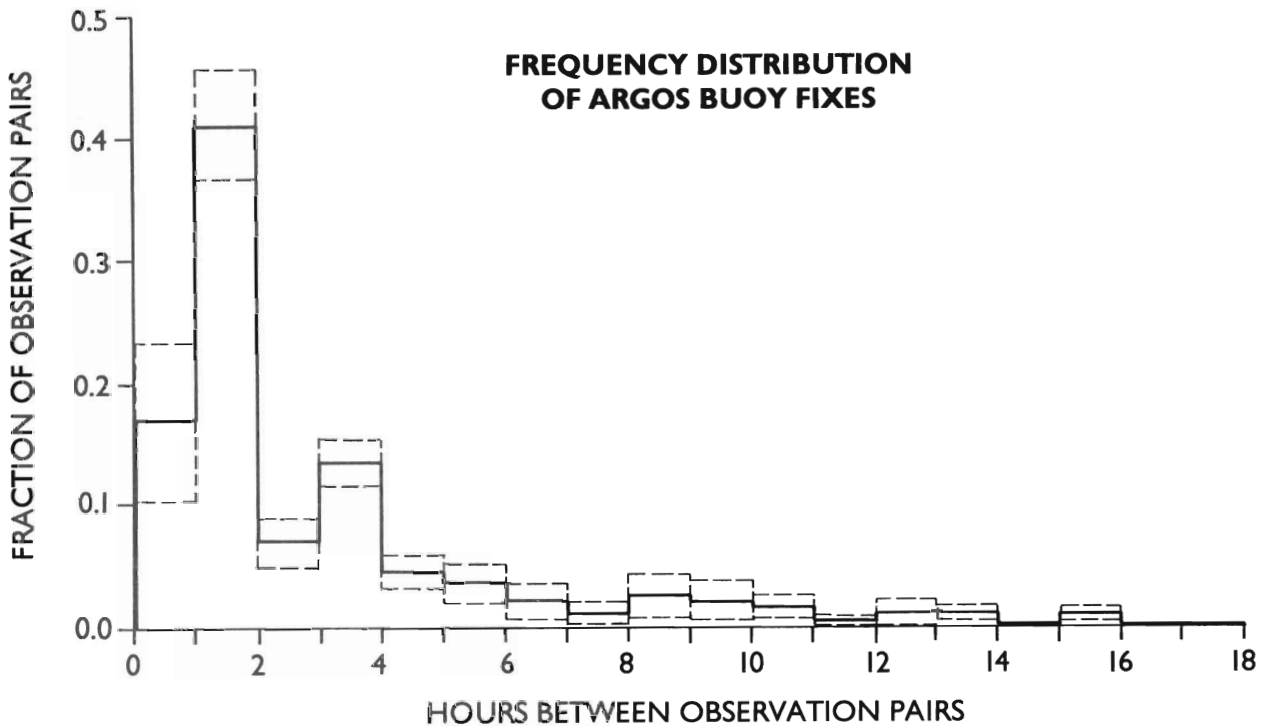


Figure 3. Frequency distribution of ARGOS buoy fixes between 58° and 64°N latitudes and from deployment until last transmission for 12 long-lived buoys. ARGOS fixes of quality levels 1 and 2 were included. The dashed lines are the one standard-deviation distributions. See text for additional information.

2.2 GOES

There were two styles of GOES transponder stations: meteorological stations at fixed sites on shore and drifting stations on ice floes. GOES transponders transmit data to the Geostationary Satellite positioned over Hawaii, which then retransmits to a ground station. The ground station computer transfers the data in near real time to a dissemination computer which the user directly accesses to retrieve the data. All of our GOES stations used the same basic configuration (Reynolds, 1983) with a model 3421A transmitter and a model 3401A master control module manufactured by Synergetics set in a wooden box built at PMEL. The stations sampled data hourly and then transmitted three samples at one time.

The shore stations had an anemometer affixed to a tower at 3 m and an air temperature sensor inside of a radiation shield just below the anemometer. The anemometer was a model 05103 wind monitor from R.M. Young. The air temperature probes and the radiation screen were the same as were used on the ARGOS buoys. The ice stations (Figure 4) had the same anemometer and air temperature set up as the shore stations, but had several additional instruments, including a compass, a barometer, a current meter, a water temperature probe, and a LORAN-C receiver. The compass was a magnetic type manufactured by Aanderra with an accuracy of $\pm 2^\circ\text{C}$. The barometer was a precision pressure sensor (model AIR-DB-2A) from AIRCO with an accuracy of ± 0.5 mb over the range of -25°C to $+50^\circ\text{C}$ and 800 mb to 1060 mb. The current meter was a Savonius-rotor current meter patterned after the EG&G vector-averaging meter and built at PMEL (Figure 5). Eight magnets were placed in the rotor and rotation was sensed with a magnetically sensitive diode. Magnets also coupled the vane position to a compass mounted in the current meter housing. The current speed was estimated by counting the number of rotor rotations over a 20-minute period. The current meter was held 2 m below the bottom of the ice by a rigid aluminum pole clamped to the side of the GOES transmitter box. The LORAN-C receiver was a SI-TEX-KODEN model 787 with a relative time delay accuracy of 0.1 μs . See Reynolds et al. (1985) for a discussion of the relative errors between LORAN and ARGOS positioning. The GOES stations were powered by two 80-amp-hour car batteries which held their charge adequately through the experiment (Figure 6).

2.3 Deployment

Flight operations are detailed in Table 2. The distributions of the ARGOS buoys near the time of the deployments are given in Figures 7 and 8. The buoys in the eastern array (Figure 8) were not simultaneously deployed, while the six ARGOS buoys in Anadyr Strait were deployed on the same flight (Figure 7). It was not feasible to put ARGOS buoys off the south shore of St. Lawrence Island, since there was no significant ice south of the island during the entire deployment window.

Table 3 gives details about the deployment of the GOES stations. GOES-A and GOES-B were co-located with ARGOS 2326 and 2335 on the eastern end of St. Lawrence Island. GOES-C and GOES-D were established on the south shore of St. Lawrence Island on 6 February (GMT) and 22 February, respectively. Table 4 gives approximate deployment positions and times and transmission failure date and times for the ARGOS buoys.

Problems with the deployment fell into three categories: some equipment failures, the weather, and logistics related to weather. Because there were persistent southerly winds during January and into the first week of February, there was very little ice in the Bering Sea due to transport northward through the Bering Strait into the Chukchi Sea. Norton Sound retained some ice and there was some ice on the north side of St. Lawrence Island and along the Siberian Peninsula. This was confirmed by microwave images of the surface (Cavalieri, 1985) and from our own observations from the helicopter on 5 February. Had we properly interpreted the microwave map on the morning of 5 February, we would not have flown to St. Lawrence Island to deploy the shore meteorological stations that day because of the amount of open water. We were able to begin work on 19 February after about 10 days of cold, northerly winds which brought some ice back from the Chukchi Sea and produced enough young ice over the rest of the area to act as a safety net.

ARGOS 2325 transmitter failed in Seattle and was sent back to Synergetics for repairs after which it appeared to work properly. ARGOS 2330, however, failed in Nome, was returned to Synergetics for repair, and was not deployed. All of the other ARGOS transmitters worked satisfactorily. GOES-D was originally deployed on the same day (6 Feb) as GOES-C, but the GOES transmitter on D failed, so we recovered the station, replaced a fuse, and redeployed the station on 22 February. The anemometer vane did not work on GOES-C after 14 February and the current meter vane did not work on GOES-B, which were not recoverable. One LORAN-C unit failed and one has not been fully deciphered at this time. The other GOES transmitters worked satisfactorily.

The carrier for the deployment was a UH-1H helicopter maintained and operated by NOAA's Office of Aircraft Operations. Additionally, people and equipment were transported between Nome and Savoonga by commercial carrier (Ryan Air) to optimize helicopter flight hours and to minimize payloads.

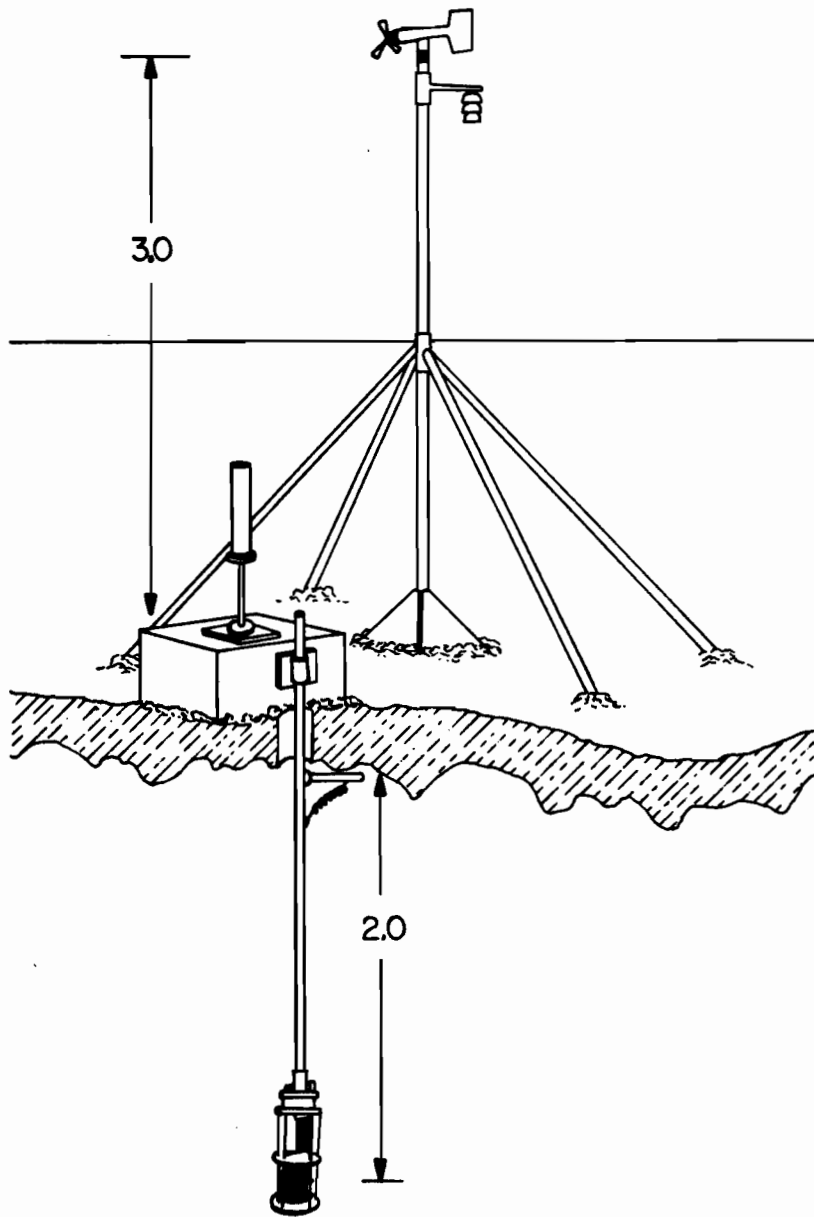


Figure 4.--Schematic of PMEL GOES ice station.

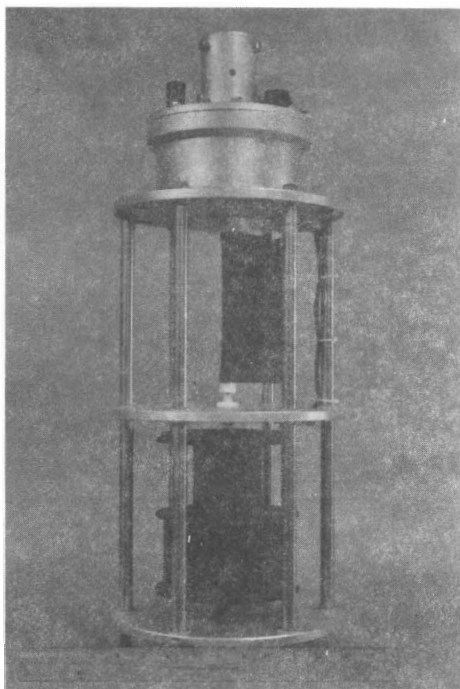


Figure 5.--Current meter developed by PMEL for under-ice measurements.

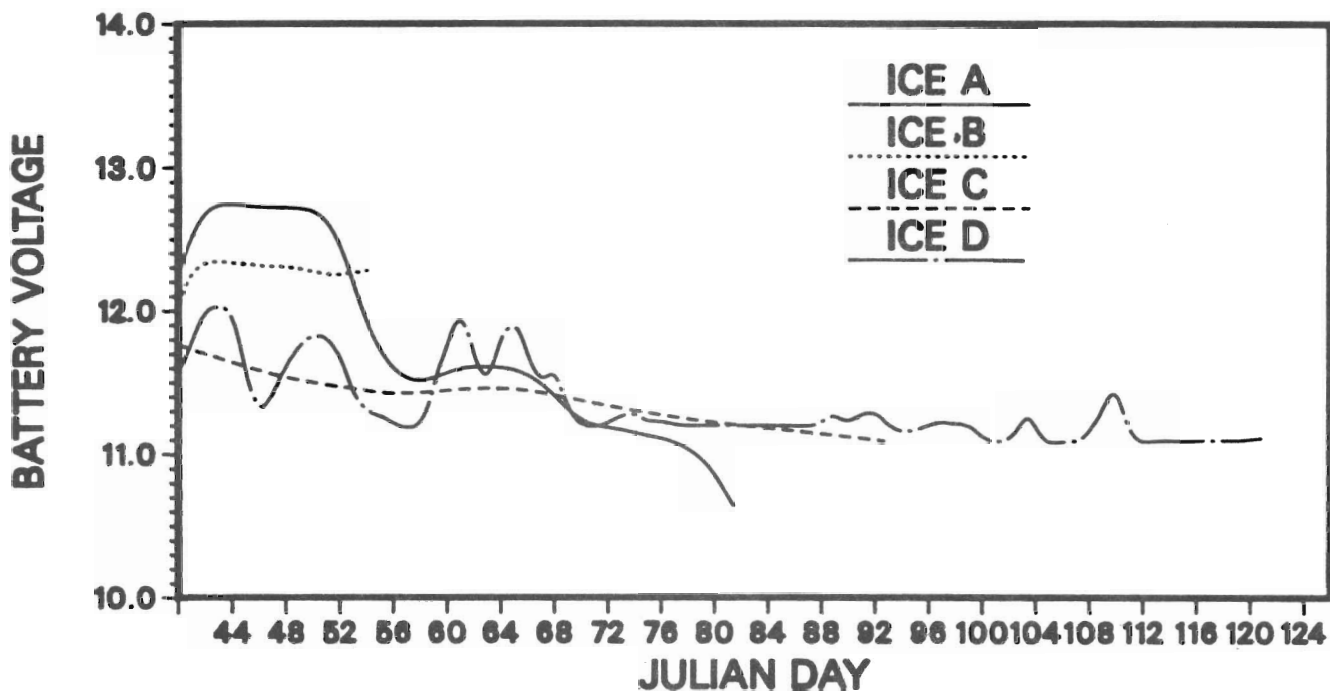


Figure 6.--Plot of battery voltage with time for the four GOES stations.

Argos Platform Positions for Julian Day 51

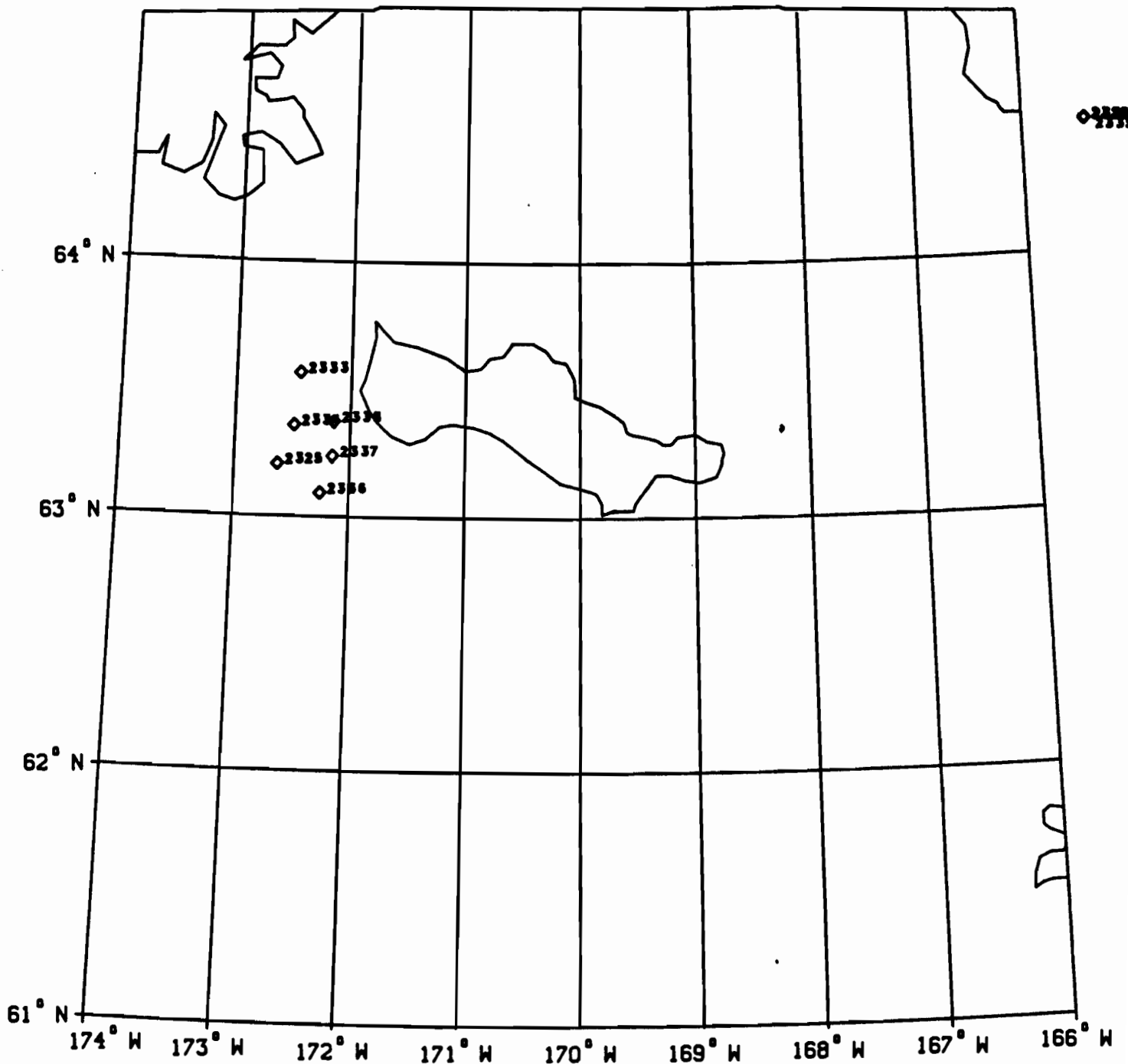


Figure 7.--ARGOS buoy positions on 20 February 1985, one day after the deployment of the western array. For an idea of the velocities toward the south, 2333 was deployed west and slightly north of Northwest Cape on St. Lawrence Island.

Argos Platform Positions for Julian Day 55

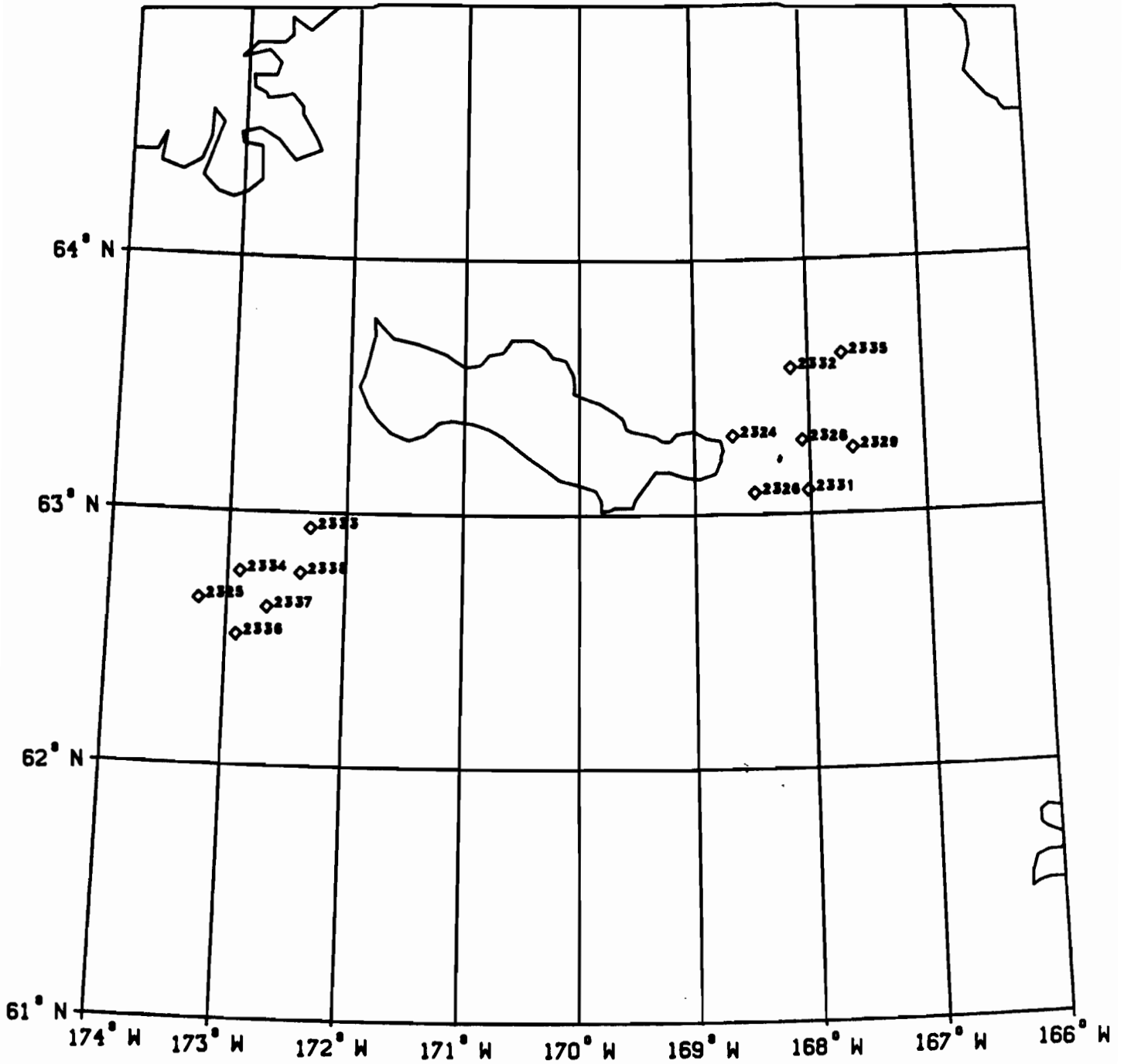


Figure 8.--ARGOS buoy positions on 24 February 1985, one day after the final deployment of the eastern array. Buoy 2327 had already been crushed and so is not represented.

Table 2.--Flight operations

Local Date	Mission Type	Personnel ¹	Departure	Return	Flight hours ²
5 Feb 1985	a) Ice Reconnaissance to Savoonga	Pease Reynolds	21:00	22:40	1:40
	b) Deploy GOES island stations	Reynolds Gologergren	23:30	02:00	1:00
	c) Return to Nome from Savoonga	Pease, Moen Reynolds	02:30	04:15	1:45
6 Feb	Check Out RDF and Ice Reconnaissance	Moen Campbell	23:00	00:00	1:00
12 Feb	Ice Reconnaissance and Coring	Pease	23:45	01:45	1:45
15 Feb	Ice Reconnaissance and Test	Pease	01:25	02:30	1:05
19 Feb	a) Ice Reconnaissance to Savoonga	Pease Reynolds	20:10	21:40	1:30
	b) ARCO ARGOS Deployment	Pease	22:30	00:50	2:20
	c) Get Siknik GOES and Return to Nome	Pease Reynolds	01:30	03:45	2:00
21 Feb	Deploy South Line of APEX Array	Pease Reynolds	19:45	23:50	3:00
22 Feb	a) Deploy Middle Line of APEX Array	Pease	19:30	21:30	2:00
	b) Return Siknik GOES and Return to Nome	Pease Reynolds	22:25	01:00	2:15
23 Feb	Deploy North Line of APEX Array	Pease Reynolds	20:50	00:30	2:40

¹ In two instances, people flew to Savoonga via Ryan Air's scheduled morning flight and are therefore only shown returning to Nome via helicopter.

² Flight hours are approximate and do not include time on station.

Table 3.--GOES Station deployment information.

Station Ident	Station Type ¹	Latitude (N)	Longitude (W)	Begin-Date (GMT)	Time (GMT)	End-Date (GMT)	Comments
A-1CA8	Ice	63°30'	168°16'	21 Feb 85	22:00	13 Mar 85	ARGOS 2326 Wind and air temp failed on 4 March
B-5FA2	Ice	63°40'	167°42'	23 Feb 85	23:00	30 Mar 85	ARGOS 2335 Current vane failed on deployment
C-5170	Shore	63°24'	171°18'	06 Feb 85	00:00	2 Apr 85	Powooiliak Camp Wind vane failed on 14 February
D-64EA	Shore	63°09'	170°15'	22 Feb 85	23:00	5 May 85	Siknik Point

¹ Shore stations transmitted wind speed and direction, air temperature, and battery voltage. Ice stations transmitted wind speed and direction, air temperature, current speed and direction, water temperature, sea-level pressure, LORAN-C rates, and battery voltage.

Table 4.--ARGOS Buoy deployment information.

Buoy Number	Buoy Type ¹	Latitude (N)	Longitude (W)	Begin-Date (GMT)	Time (GMT)	Array (E/W)	End-Date (GMT)	Time (GMT)
2324	PRL-T	63°30'	168°42'	21 Feb 85	22:25	east	24 Feb 85	04:47
2325	Syn-T	63°26'	172°19'	19 Feb 85	23:40	west	19 Mar 85	01:33
2326	PRL-T	63°30'	168°16'	21 Feb 85	21:30	east	4 Mar 85	08:16
								GOES A
2327	Syn-T	63°32'	168°30'	22 Feb 85	21:00	east	23 Feb 85	19:45
2328	Syn-T	63°33'	168°00'	22 Feb 85	20:45	east	23 May 85	18:20
2329	Syn-T	63°32'	167°32'	22 Feb 85	20:30	east	16 Apr 85	15:28
2330	Syn-T							never transmitted
2331	PRL-T	63°30'	167°45'	21 Feb 85	20:45	east	17 May 85	01:58
2332	Syn-T	63°40'	168°10'	23 Feb 85	23:00	east	4 Jun 85	15:05
2333	PRL-T	63°49'	172°14'	19 Feb 85	23:05	west	18 Mar 85	03:24
2334	PRL-N	63°36'	172°14'	19 Feb 85	23:25	west	26 Mar 85	15:53
2335	PRL-N	63°40'	167°42'	23 Feb 85	22:00	east	16 Jun 85	13:01
								GOES B
2336	PRL-N	63°18'	172°06'	19 Feb 85	23:50	west	19 Mar 85	17:39
2337	PRL-N	63°28'	171°59'	20 Feb 85	00:05	west	25 Mar 85	00:22
2338	PRL-N	63°37'	171°55'	20 Feb 85	00:20	west	2 Apr 85	18:45

¹ PRL-T is a Polar Research Laboratory ADAP model 901 modified for us by PRL to transmit air temperature. Syn-T is a Synergetics ARGOS transmitter and antenna built into a wooden box at PMEL and fitted with air temperature. PRL-N is a PRL ADAP model 901, not fitted with air temperature.

3. ICE TRAJECTORIES AND REGIONAL CONDITIONS

From mid-January through the end of the first week in February, ice exited the Bering Sea northward through the Bering Strait, so the St. Lawrence Island polynya could not close, as would normally be expected during winter southerly winds. After that time and through the end of the deployment window, the polynya was open and producing new ice in a more classical pattern, although there was no first-year ice preceding the young ice downwind of the St. Lawrence Island polynya.

Plots of the ARGOS buoy trajectories for individual buoys which lasted any significant period of time are given in Figures 9-11. The data used for these plots and for the preliminary analyses were clean, but irregularly spaced in time data. A more complete description is given in Section 2.1.

Due to deformation on the east end of St. Lawrence Island, several ARGOS units presumably were crushed. The first was unit 2327, deployed due west of 2328 on 22 February (JD 53), and lost in a shear zone during southward drift on 23 February (JD 54). These shears were readily visible from the helicopter on the 23rd and for the rest of the deployment period. The second unit was 2324, deployed due west of 2326 on 21 February (JD 52), peeled off from the array by the island (Figure 8), and crushed near Northeast Cape on 24 February (JD 55). The remainder of the eastern array drifted southward until 28 February (JD 59) and then moved northward with southerly winds. Unit 2336 (Figure 10a) was lost in a shear zone on 4 March (JD 63). The accompanying GOES-A lost its anemometer tower at the same time, although the current meter, compass, and air pressure continued to transmit. At the time of the deployment, the ARGOS unit was next to one of the anemometer tower legs, on the opposite side of the tower as the GOES transmitter box. It is possible that the tower was taken down by a bear observed in the area, but it is unlikely, since both units went out nearly simultaneously and the site was near a major shear flaw.

After 7 March (JD 66) the buoys in both arrays drifted southward for a long period (Figures 9-11). The western array drifted toward the southwest (Figure 9) and all of the buoys melted out at the ice edge in the conveyor belt sense (Pease, 1980) between 18 March (JD 77) and 2 April (JD 92). The eastern array drifted toward the south (Figures 10, 11) and a fourth ARGOS unit (2329, Figure 11b) was lost in a shear zone near the western tip of Nunivak Island on 16 April (JD 106). The remaining four buoys reached their maximum extents on 1 May (JD 121) very near the ice edge. They then made a slow clockwise circle and melted out by the spring surface melt process between 17 May (JD 137) and 16 June (JD 167).

Deformation on the west end of St. Lawrence Island was much less extreme than on the east end. There was a large east/west polynya west of Northwest Cape on the day of the deployment. This polynya was between ARGOS 2333 and the rest of the array. As the array first drifted southward, it rotated clockwise by 30 to 40 degrees (Figure 9). The southward drift continued until 27 February (JD 58) and turned northward a full day before the eastern array (Figures 9, 10). Both arrays moved northward until 6 March (JD 65) and then turned southward again.

The ice floes used for the western array were thicker and initially more heavily ridged than floes used for the eastern array. The initial western array thicknesses, based on freeboard and sail height scaling, were 1-2 m for undeformed ice and 4-20 m for ridges. The initial eastern array thicknesses based on freeboard scaling and coring, were 0.2 m to 1 m for undeformed ice. In particular, the floe for GOES-A (ARGOS 2326) was 0.60 m thick with 0.08 m of snow and the floe for GOES-B (ARGOS 2335) was 0.75 m thick with 0.15 m of snow. Another interesting floe, marked with ARGOS 2327, was thin first-year ice with striking salt flowers of order 2.0 cm diameter, spaced on about 2.5 cm centers.

The trajectories of the floes from the eastern array from this experiment contrast sharply with the trajectories of the floes from east of St. Lawrence Island during the winter of 1982 (Reynolds and Pease, 1984). In 1982 the deployment was made one to three weeks earlier. Those buoys deployed before the end of the first week in February in 1982, moved north through Bering Strait, while those deployed the third week in February stayed in the vicinity. In 1985 buoys from the same general area moved southward toward the ice edge. Weather conditions in the two years were quite different, but these findings suggest that we may not know the sign of the annual ice transport, let alone the magnitude.

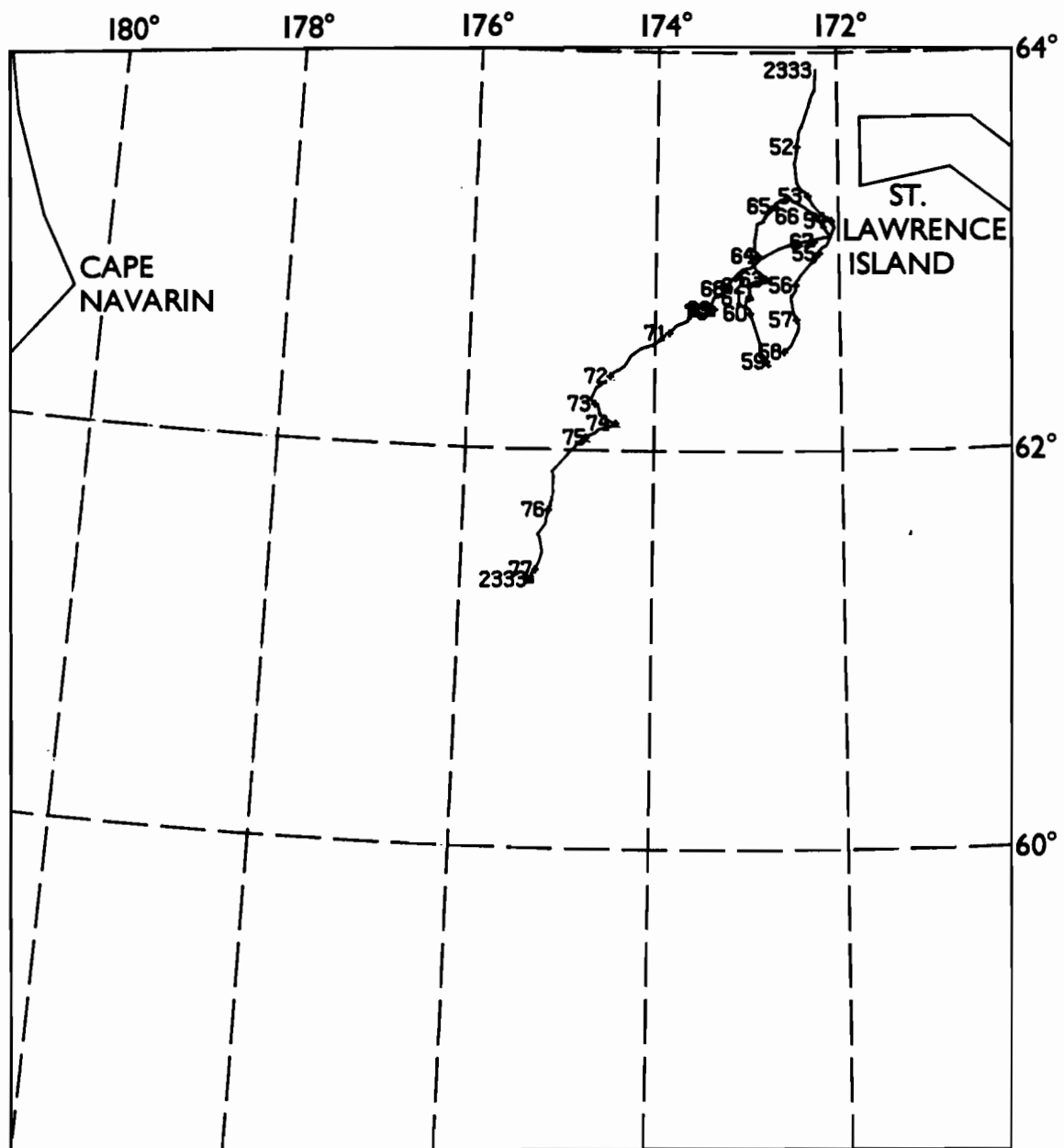


Figure 9a.--ARGOS buoy 2333 drift from the west end of St. Lawrence Island toward the southwest. Tick marks occur every 24 hours and labels are Julian days at 00 GMT.

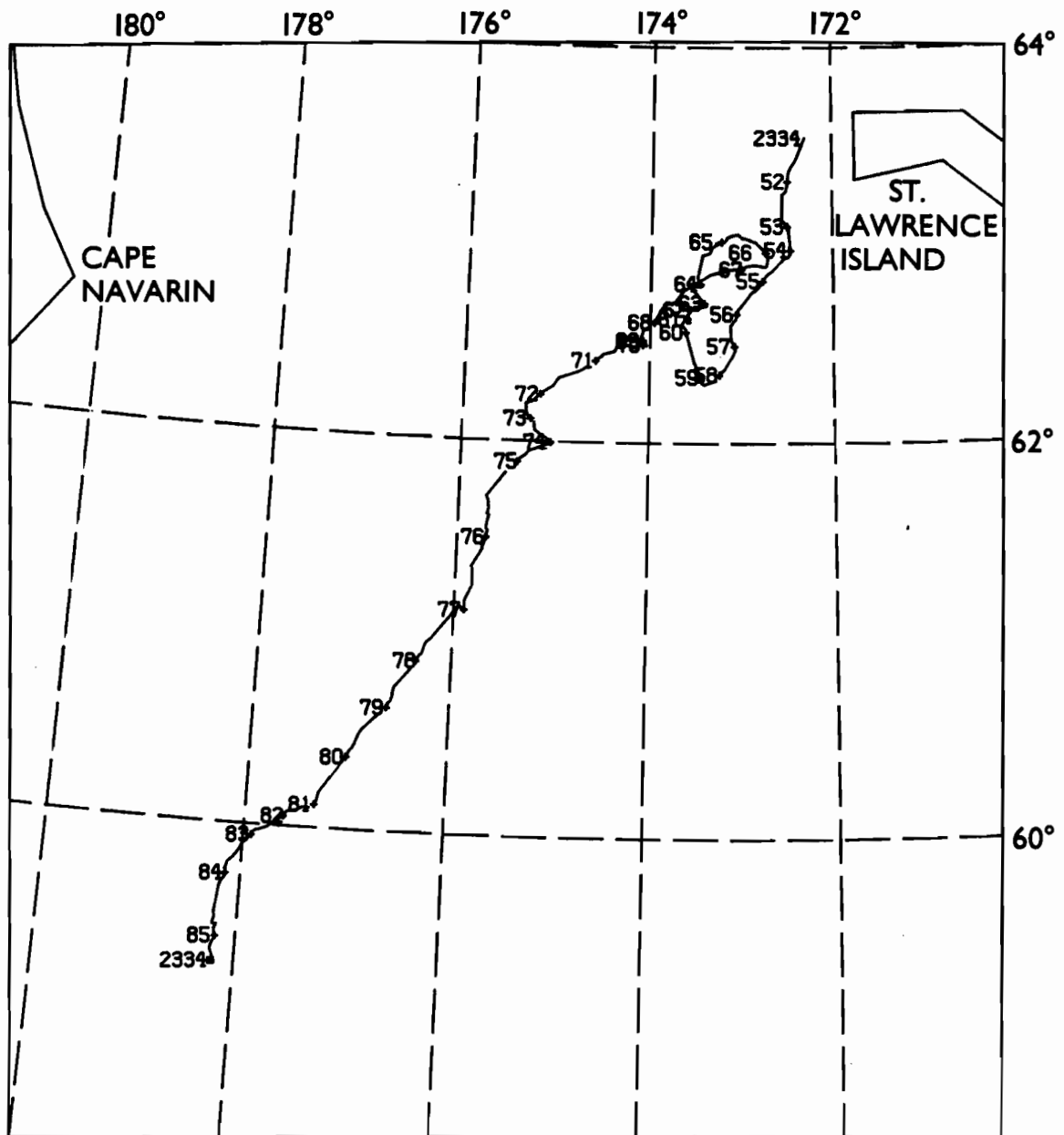


Figure 9b.--ARGOS buoy 2334 drift from the west end of St. Lawrence Island toward the southwest. Tick marks occur every 24 hours and labels are Julian days at 00 GMT.

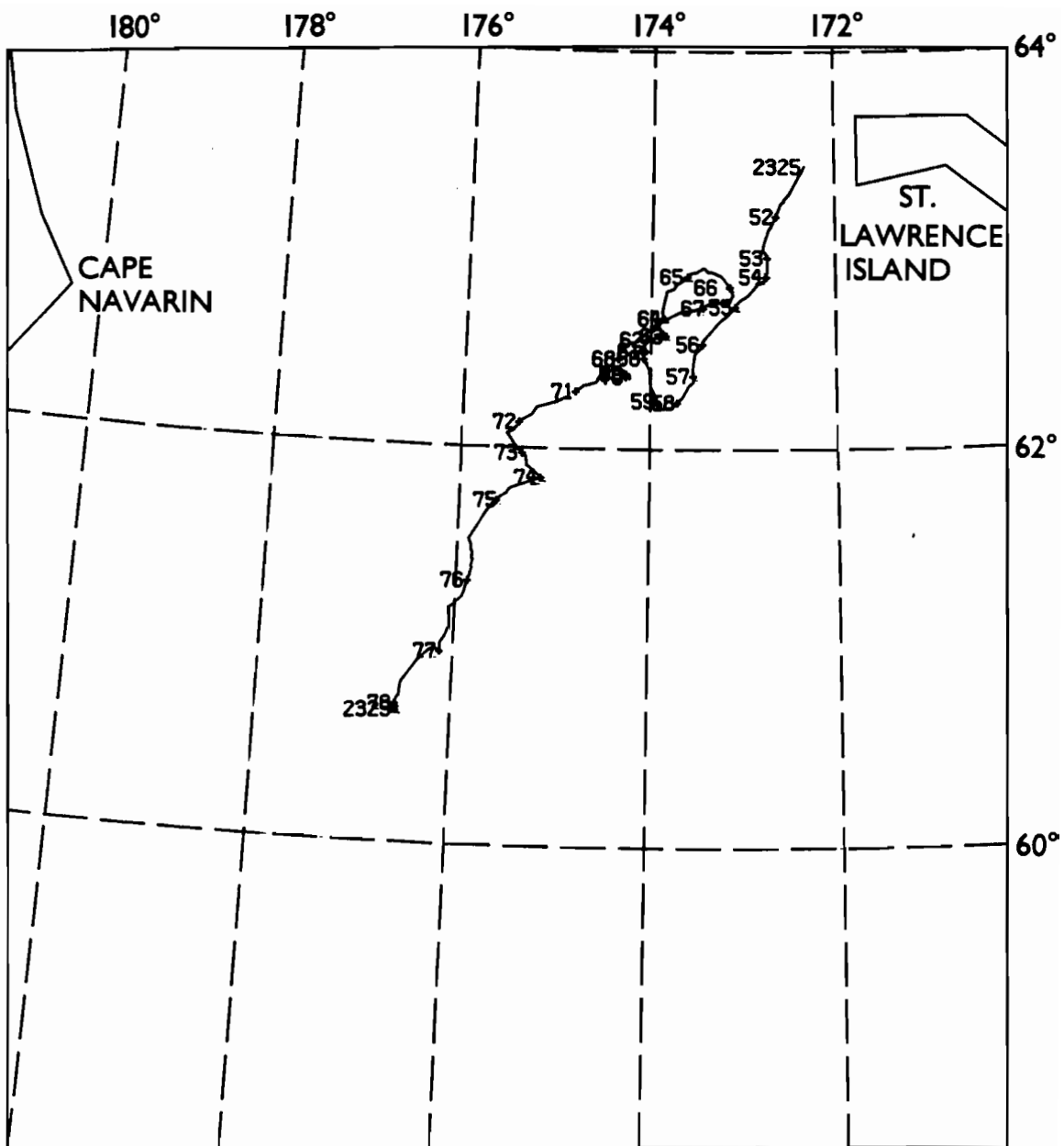


Figure 9c.--ARGOS buoy 2325 drift from the west end of St. Lawrence Island toward the southwest. Tick marks occur every 24 hours and labels are Julian days at 00 GMT.

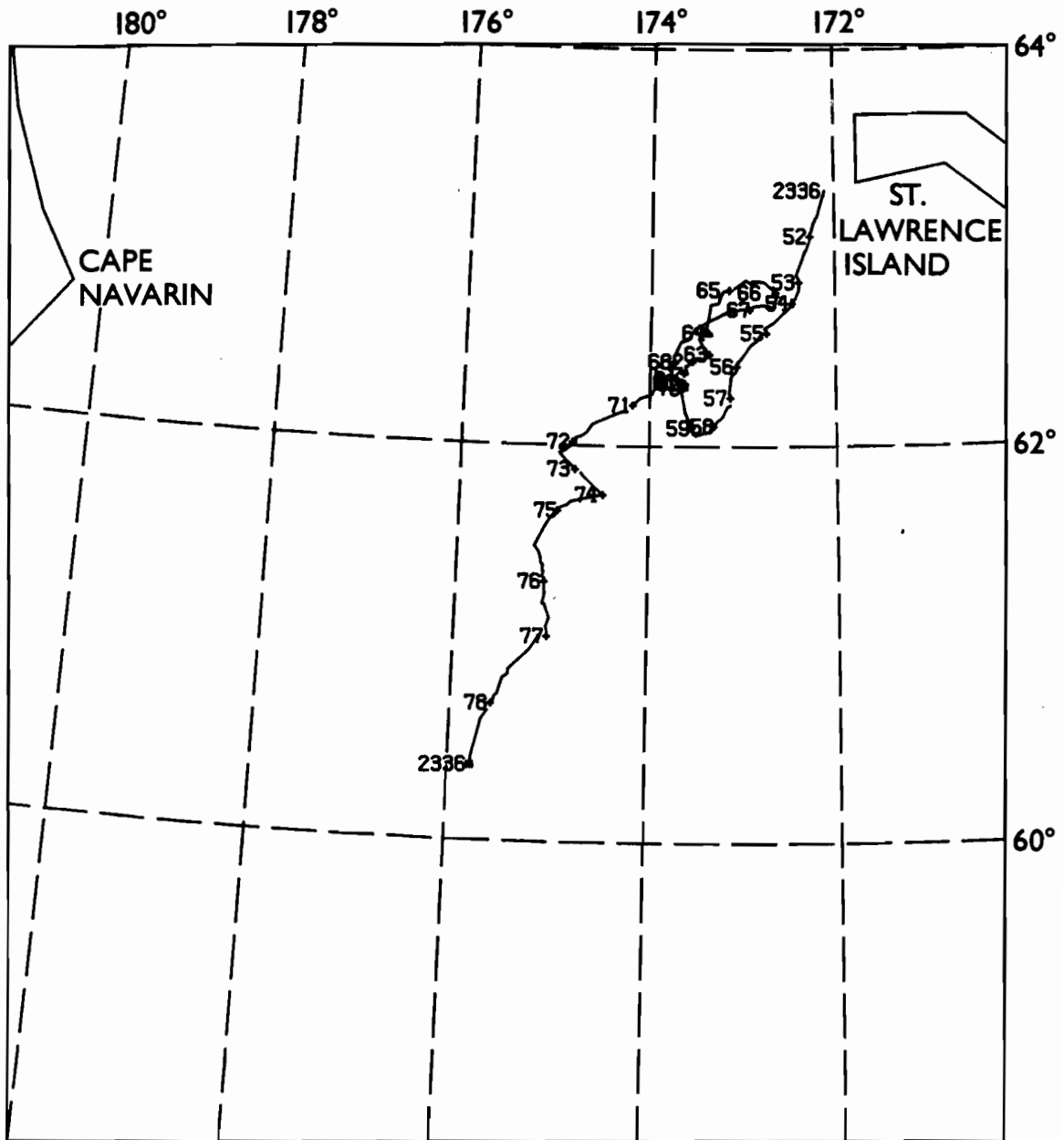


Figure 9d.--ARGOS buoy 2336 drift from the west end of St. Lawrence Island toward the southwest. Tick marks occur every 24 hours and labels are Julian days at 00 GMT.

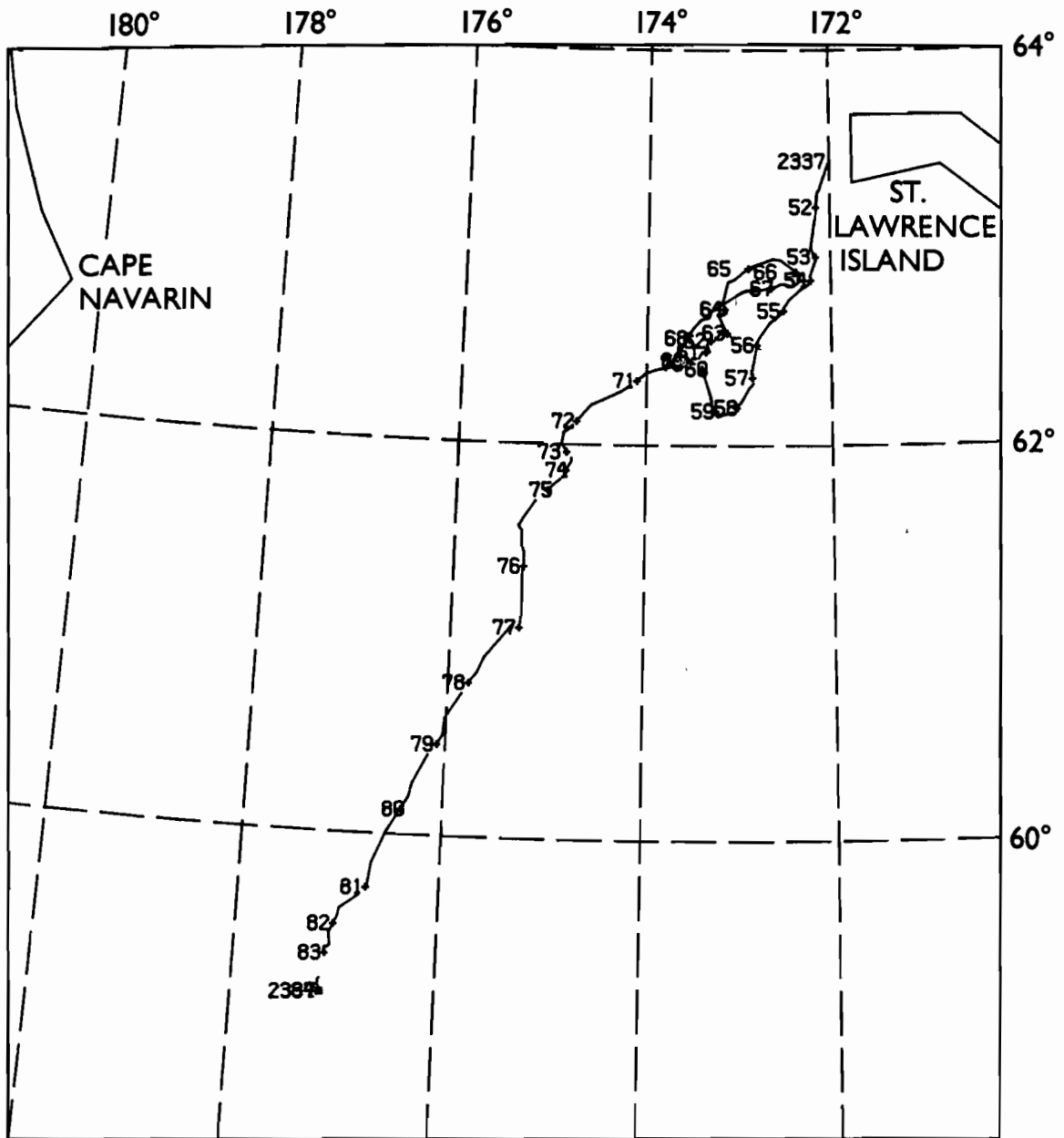


Figure 9e.--ARGOS buoy 2337 drift, from the west end of St. Lawrence Island toward the southwest. Tick marks occur every 24 hours and labels are Julian days at 00 GMT.

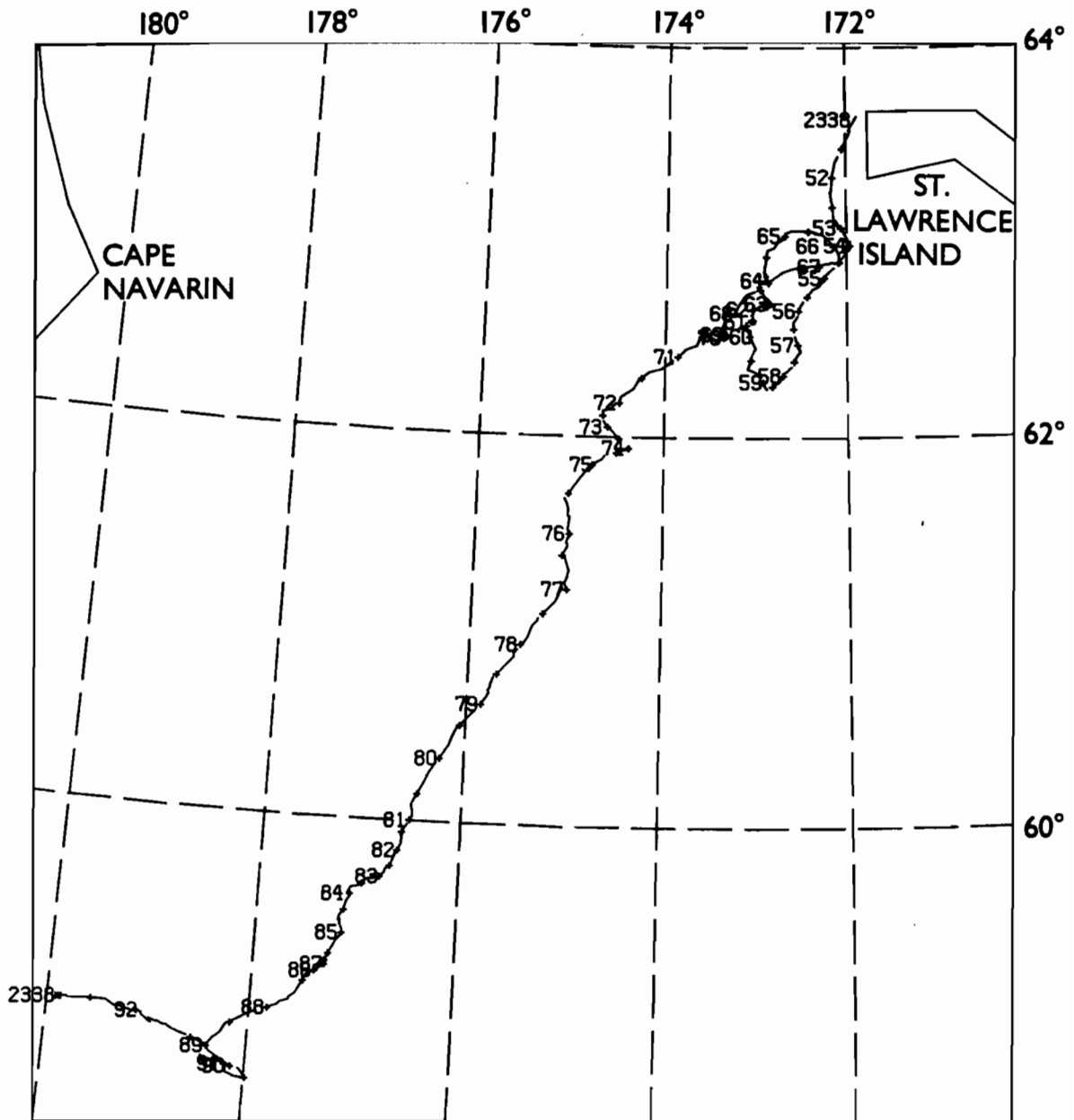


Figure 9f.--ARGOS buoy 2338 drift from the west end of St. Lawrence Island toward the southwest. Tick marks occur every 24 hours and labels are Julian days at 00 GMT.

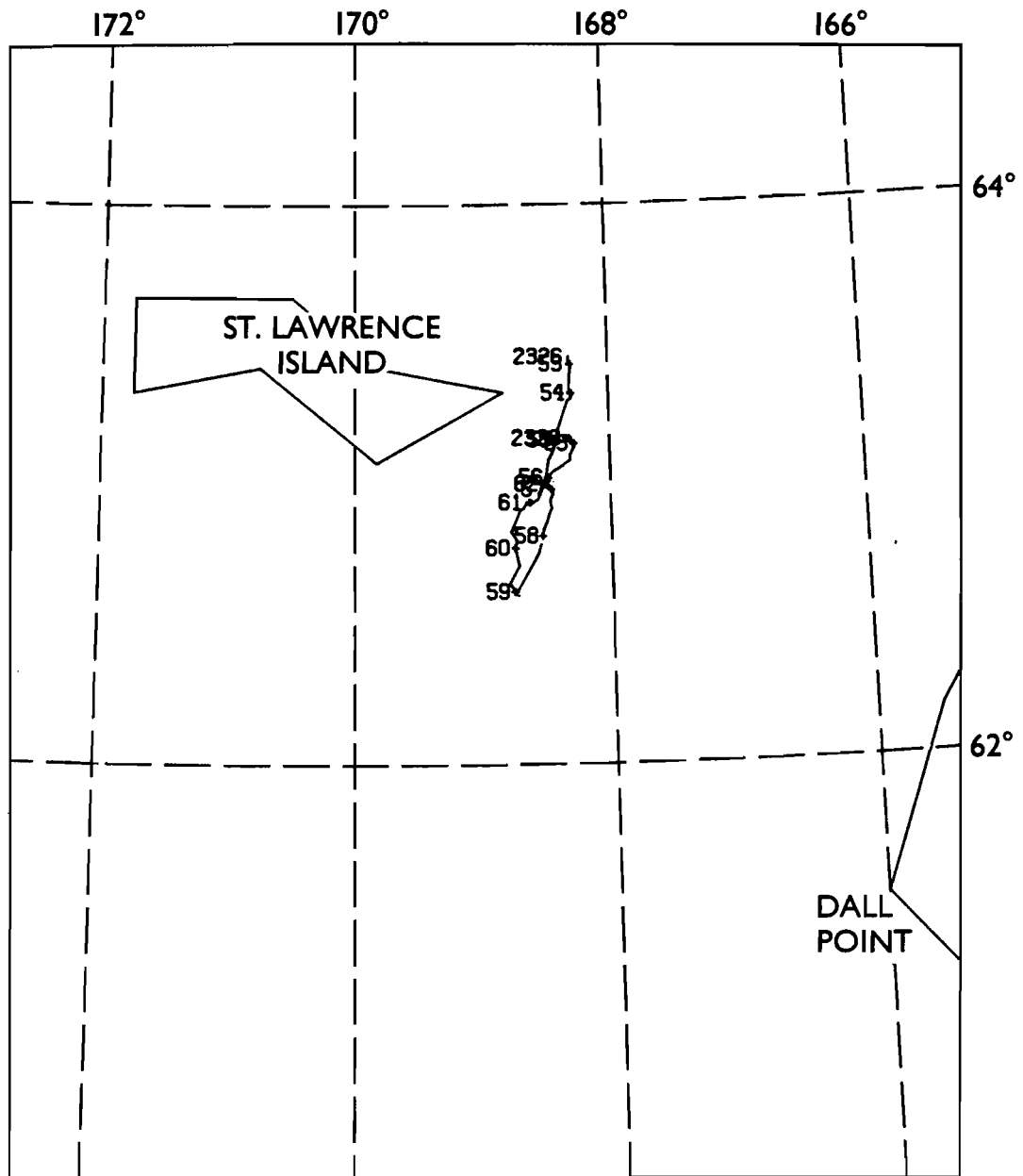


Figure 10a.--ARGOS buoy 2326 drift from the east end of St. Lawrence Island toward the south through 31 March (JD 90). Tick marks occur every 24 hours and labels are Julian days at 00 GMT.

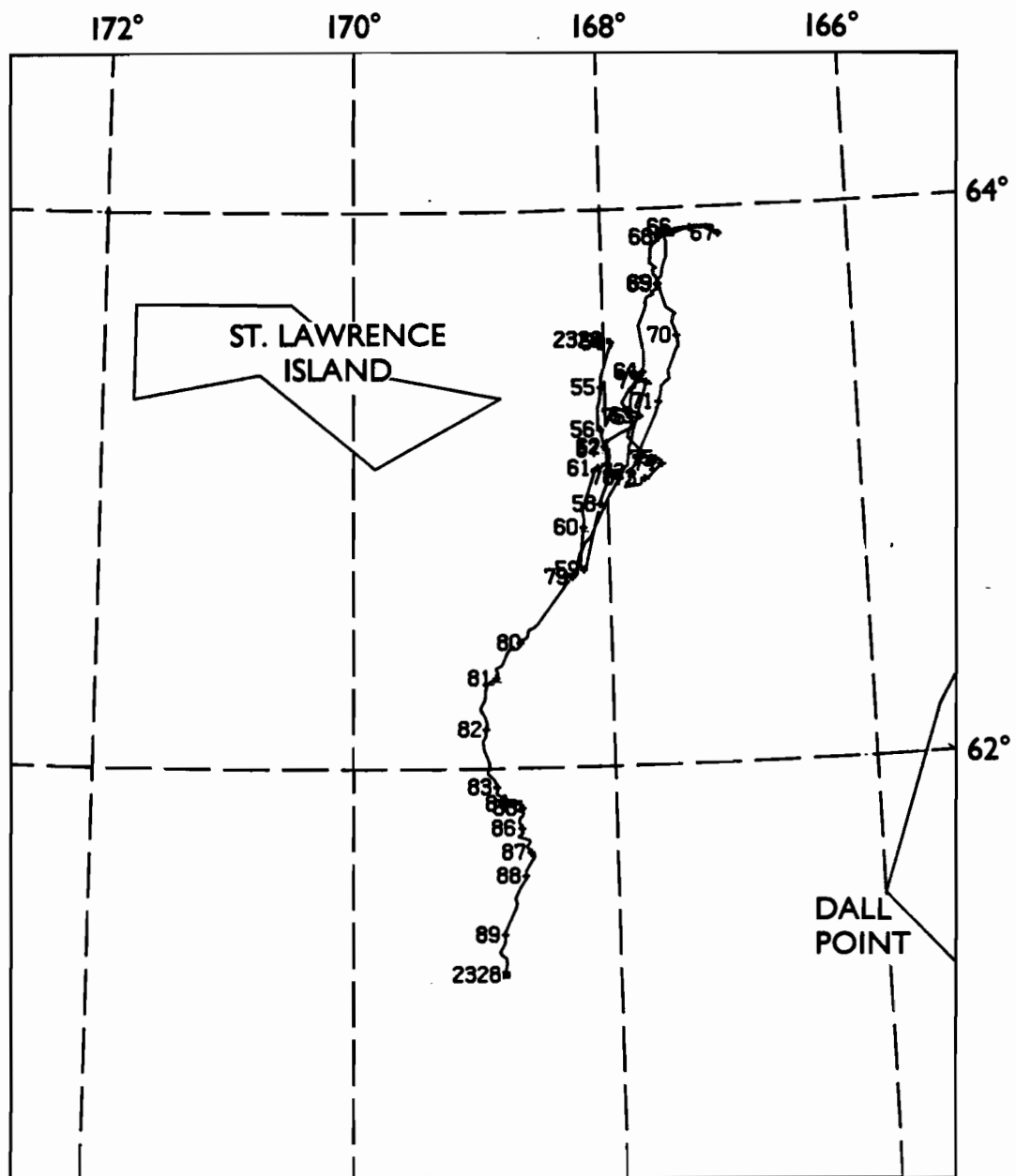


Figure 10b.--ARGOS buoy 2328 drift from the east end of St. Lawrence Island toward the south through 31 March (JD 90). Tick marks occur every 24 hours and labels are Julian days at 00 GMT.

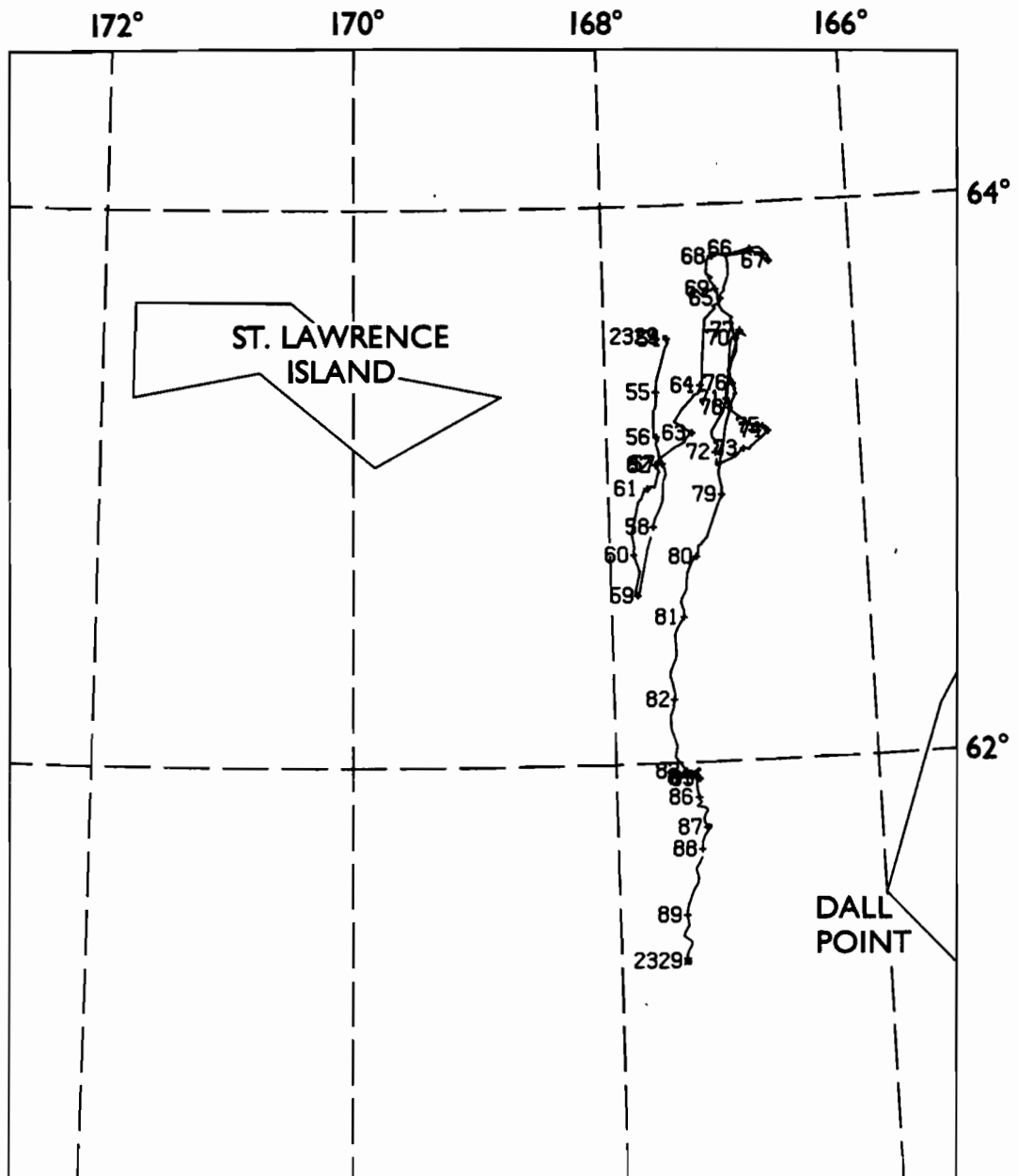


Figure 10c.--ARGOS buoy 2329 drift from the east end of St. Lawrence Island toward the south through 31 March (JD 90). Tick marks occur every 24 hours and labels are Julian days at 00 GMT.

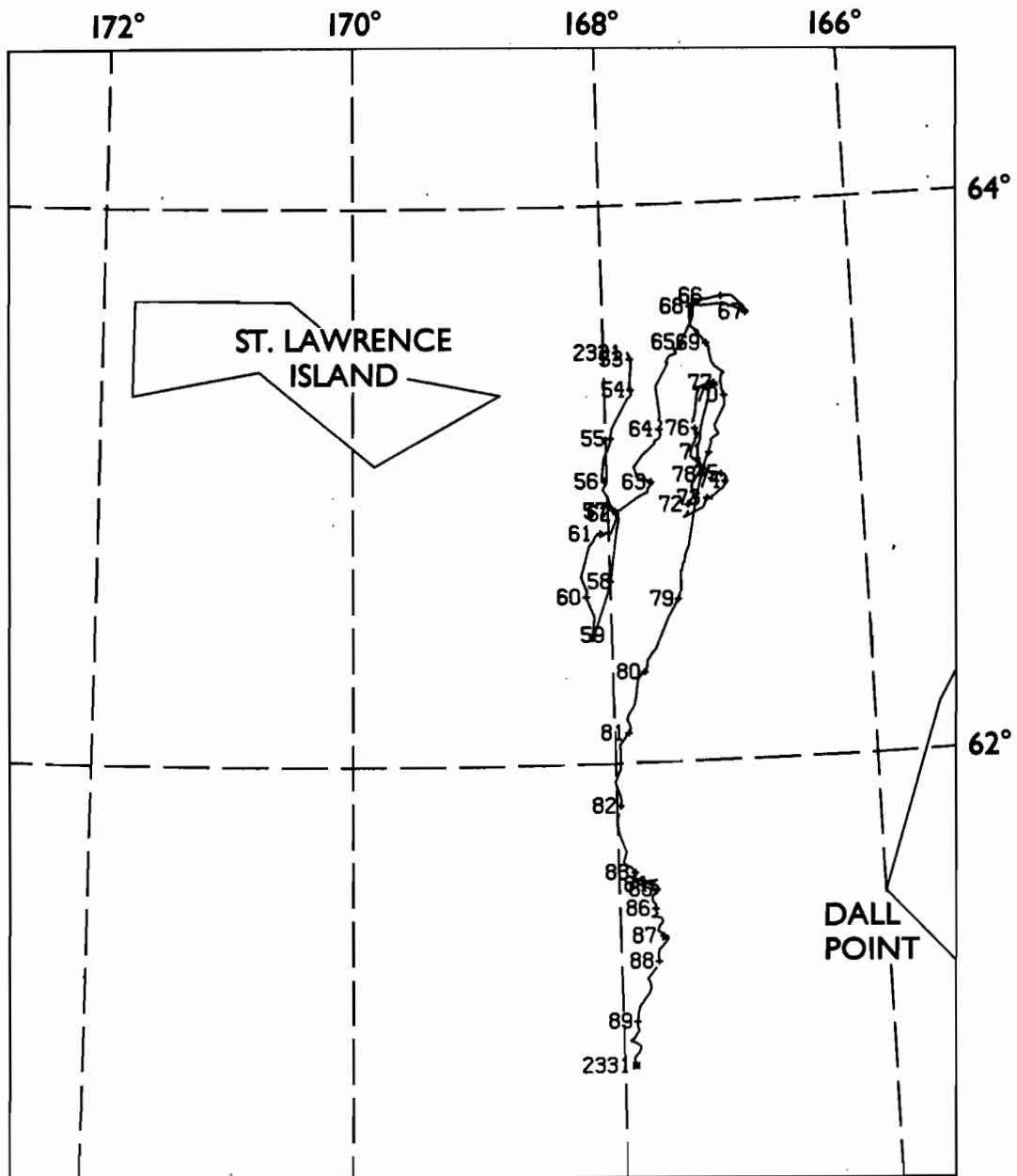


Figure 10d.--ARGOS buoy 2331 drift from the east end of St. Lawrence Island toward the south through 31 March (JD 90). Tick marks occur every 24 hours and labels are Julian days at 00 GMT.

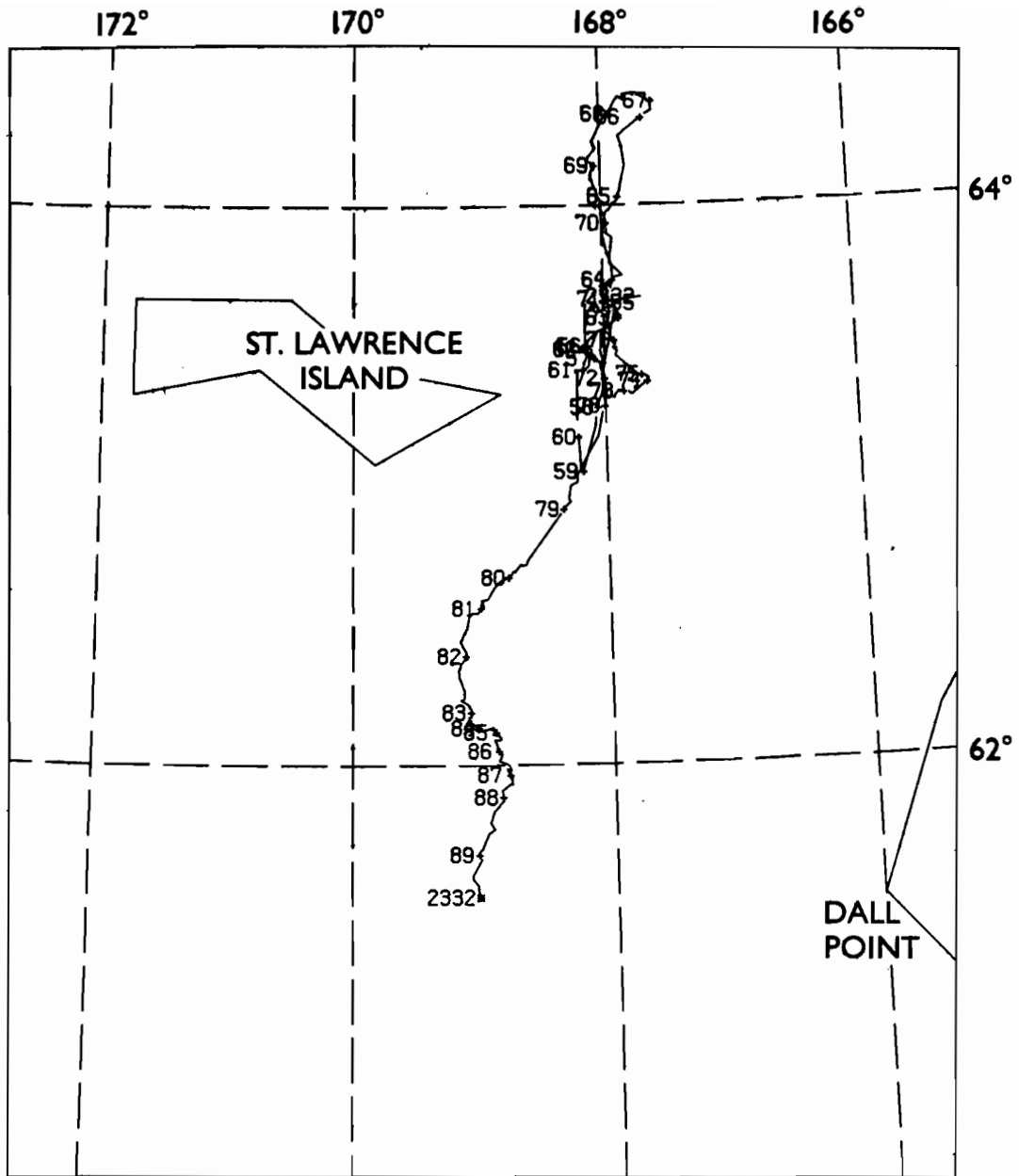


Figure 10e.--ARGOS buoy 2332 drift from the east end of St. Lawrence Island toward the south through 31 March (JD 90). Tick marks occur every 24 hours and labels are Julian days at 00 GMT.

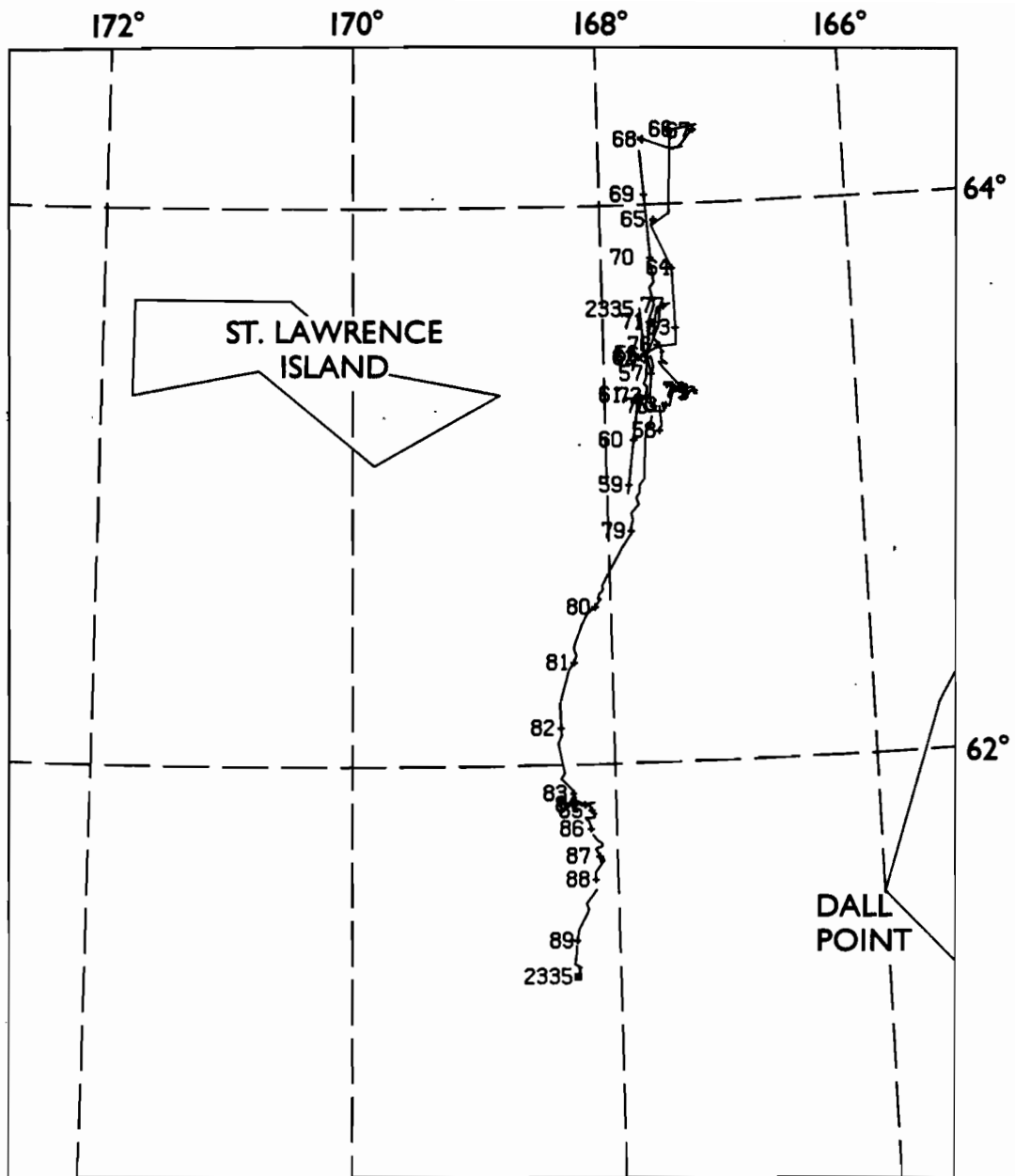


Figure 10f.--ARGOS buoy 2335 drift from the east end of St. Lawrence Island toward the south through 31 March (JD 90). Tick marks occur every 24 hours and labels are Julian days at 00 GMT.

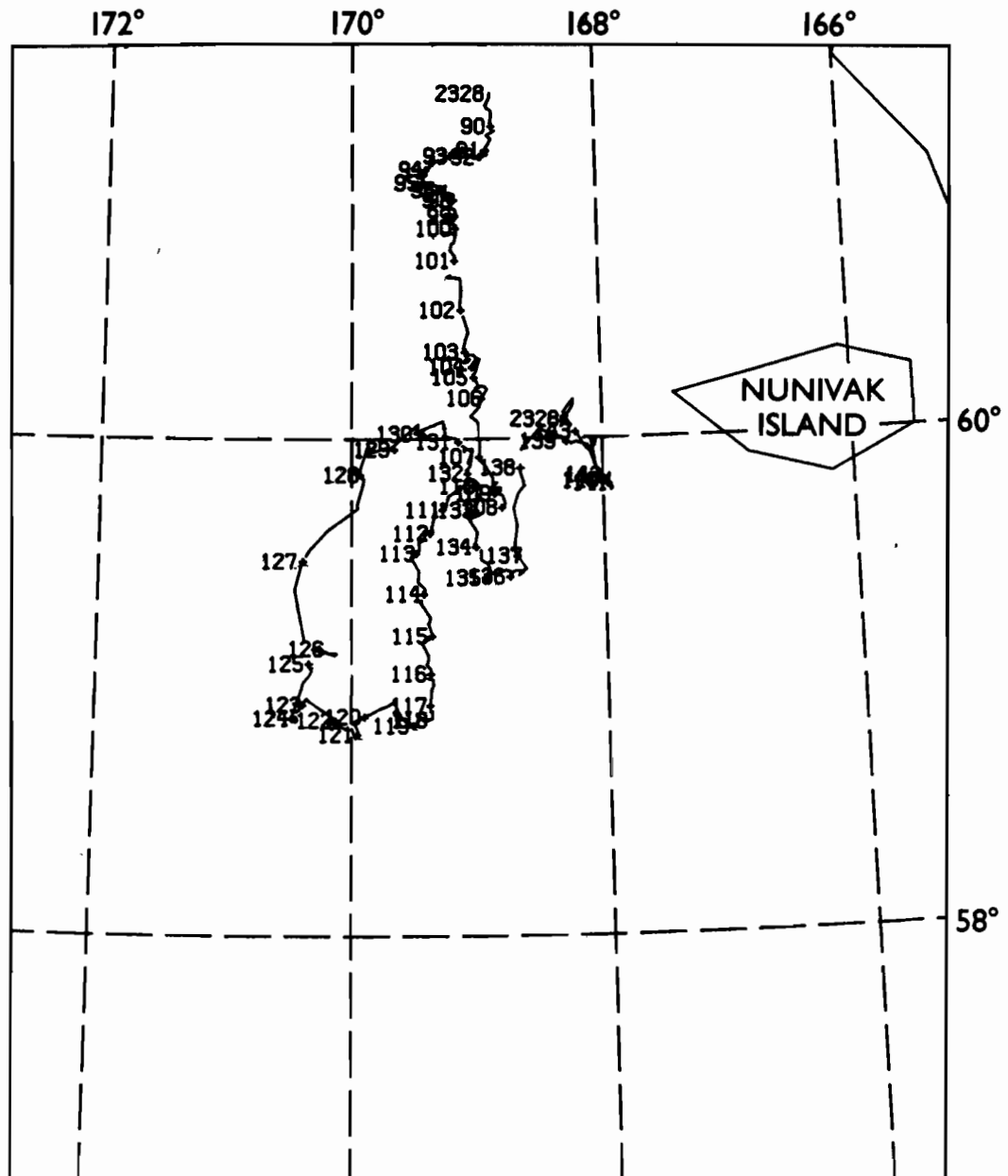


Figure 11a.--ARGOS buoy 2328 drift from the east end of St. Lawrence Island toward the south from 31 March (JD 90). Tick marks occur every 24 hours and labels are Julian days at 00 GMT.

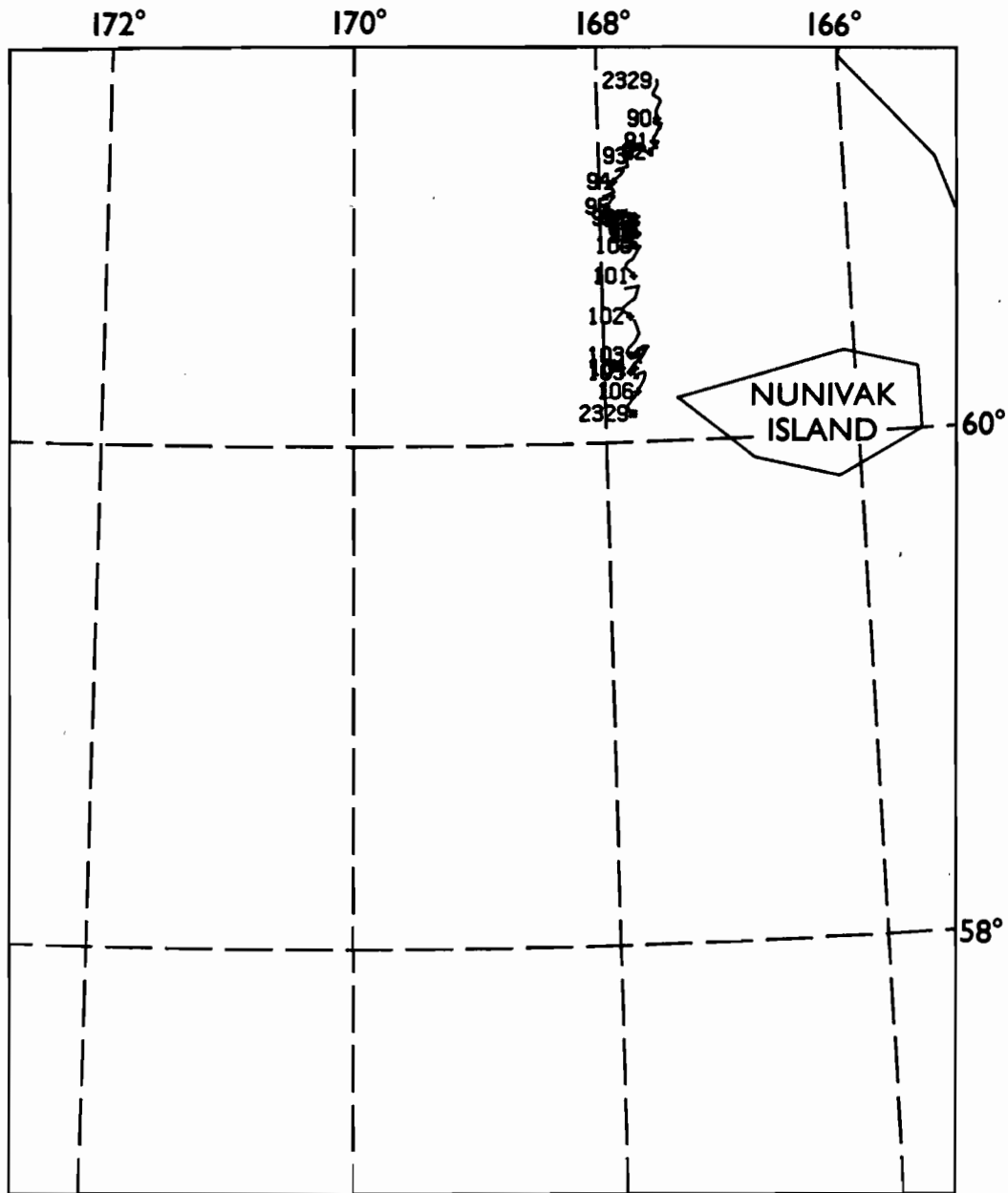


Figure 11b.--ARGOS buoy 2329 drift from the east end of St. Lawrence Island toward the south from 31 March (JD 90). Tick marks occur every 24 hours and labels are Julian days at 00 GMT.

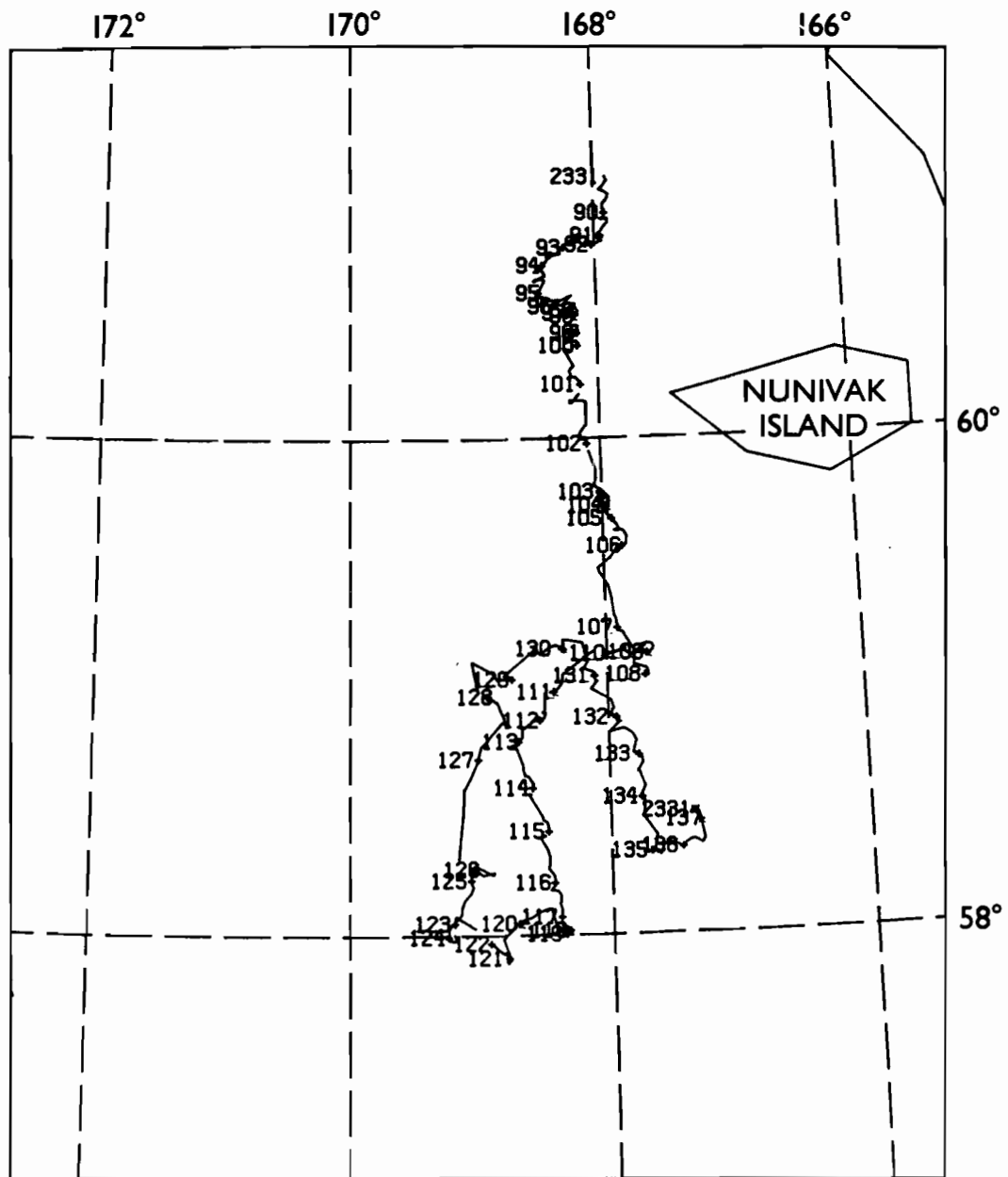


Figure 11c.--ARGOS buoy 2331 drift from the east end of St. Lawrence Island toward the south from 31 March (JD 90). Tick marks occur every 24 hours and labels are Julian days at 00 GMT.

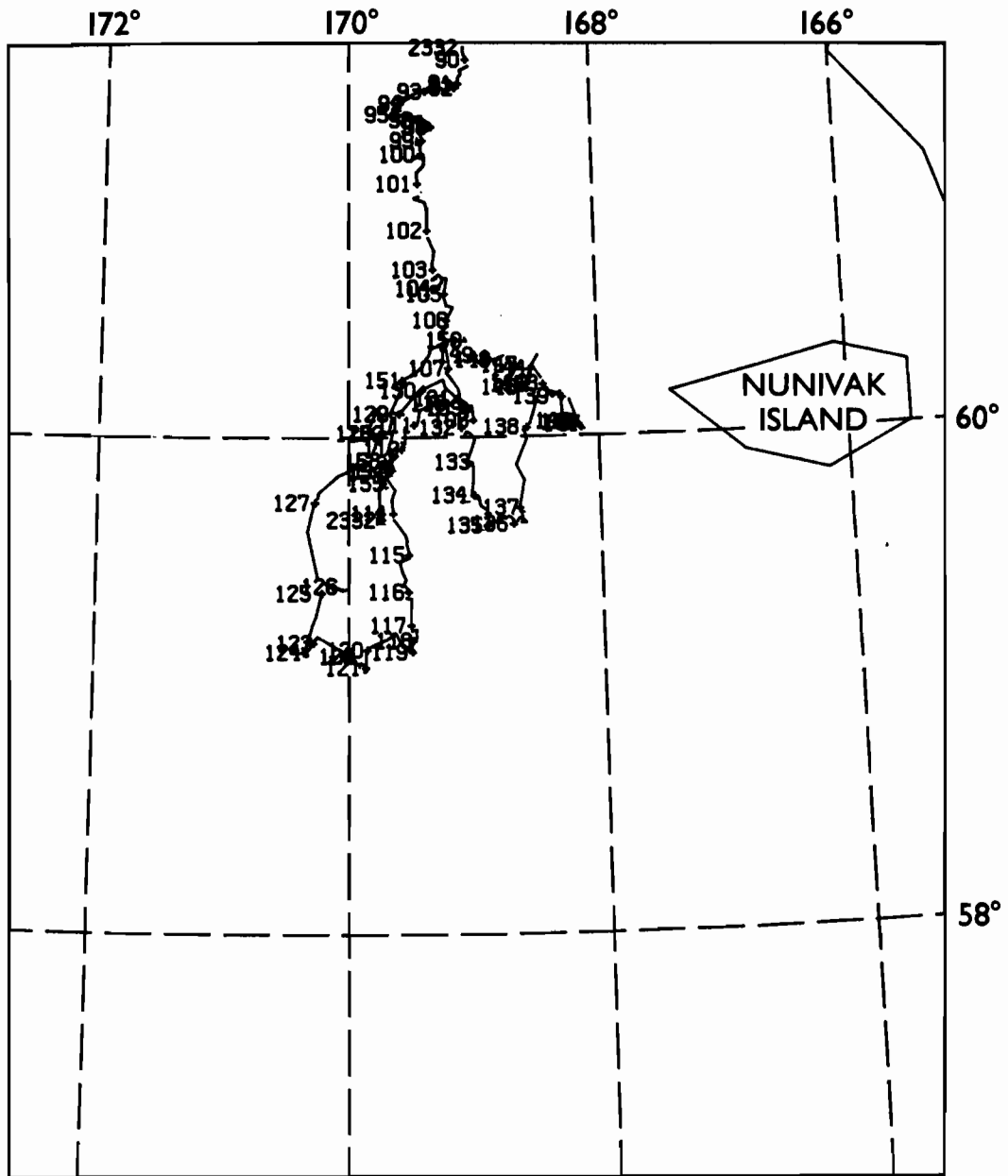


Figure 11d.--ARGOS buoy 2332 drift from the east end of St. Lawrence Island toward the south from 31 March (JD 90). Tick marks occur every 24 hours and labels are Julian days at 00 GMT.

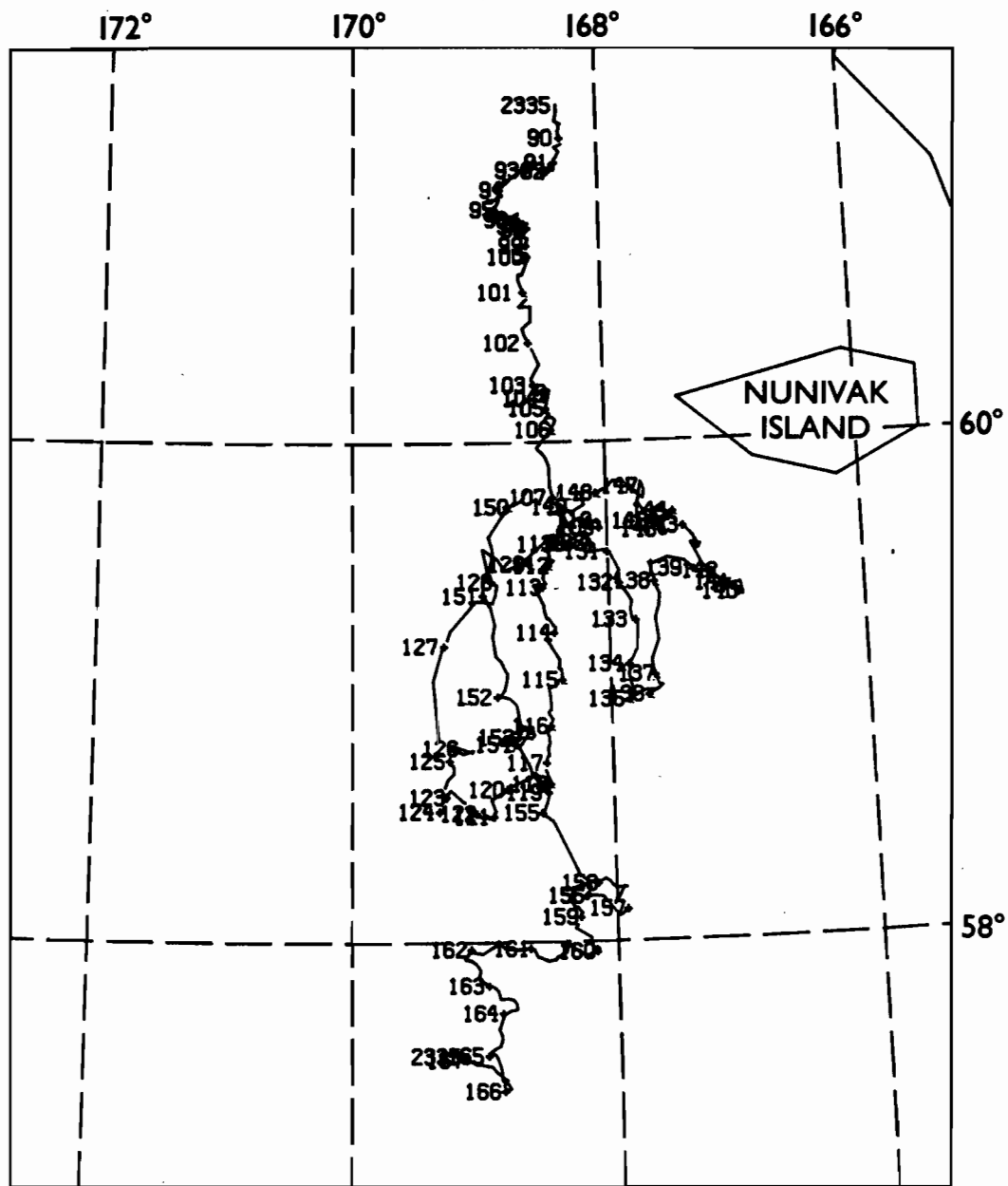


Figure 11e.--ARGOS buoy 2335 drift from the east end of St. Lawrence Island toward the south from 31 March (JD 90). Tick marks occur every 24 hours and labels are Julian days at 00 GMT.

4. METEOROLOGY

4.1 Regional Meteorology

During the period between mid-February and mid-April, the Bering Sea was affected by predominantly northerly to northeasterly winds advecting cold continental air from the Alaska mainland or Arctic southward through the Bering Strait. The track of cyclones across the North Pacific remained south of the Bering Sea throughout the 60-day period except for a significant northward shift of the track into the Bering Sea during the first part of March. Machine plots of surface air temperature, sea-level pressure, and surface wind vectors for every 12 hours from 15 February through 15 April are presented in Appendices A and B.

From mid to late February, the Bering Sea was dominated by a strong high over eastern Siberia interacting with traveling cyclones moving from the northwest Pacific to the Gulf of Alaska. Northwesterly to northeasterly winds occasionally to 35 knots and surface air temperatures in the -14°C to -30°C range prevailed over most of the Bering Sea between 15 and 24 February (Figures 12a,b). After the 24th, temperatures became more moderate over the southern Bering Sea as a 990 mb low pressure system moved into Bristol Bay. By the 26th (Figure 12c), a secondary, weak, northeast trending track of low pressure developed over the western Bering Sea, while high pressure with associated temperatures as low as -34°C moved eastward from the eastern Bering Sea over Alaska. The building high over Alaska commensurate with falling pressures over the Bering Sea caused southerly winds to 30 knots and warmer temperatures ranging from $+2^{\circ}\text{C}$ over the southern Bering to -10°C in the St. Lawrence Island vicinity on 28 February.

On 1 March, a low pressure center moved northeastward from the Gulf of Anadyr to the Chukchi Sea with an adjoining cold front sweeping eastward across the northern Bering Sea. The front (Figure 12d) ushered in a three day period of westerly winds to 20 knots and surface air temperatures down to -22°C over the northern Bering Sea and to -12°C south of 60°N latitude.

A series of three intense storms marched east-northeastward across the Bering Sea between 4 and 13 March (Figures 12e,f) with each successive low pressure system tracking at a more southerly latitude than the previous one. The first storm entered the western Bering Sea on 4 March and exited via eastern Siberia in 5 March. A warm front associated with this system moved swiftly northward through the eastern Bering Sea conveying above freezing temperatures as far as St. Lawrence Island by the night of 4 March. An occluded front followed, clearing the eastern Bering Sea by 5 March and bringing moderate westerly winds and surface air temperatures from -10°C to -15°C in its wake.

The second storm in the series crossed the Bering Sea between 6 and 8 March (Figure 12e), shifting the winds to northeasterly at 35 knots over the northeastern Bering Sea by the morning of 8 March. Temperatures remained around -10°C in the vicinity of St. Lawrence Island, as the storm moved south of the area and abruptly weakened in Norton Sound on 9 March, losing energy to a developing system south of the Alaska Peninsula.

The third and most intense storm of this series entered the western Bering Sea early on 10 March and rapidly deepened to 959 mb by afternoon. The low pressure center moved north of St. Paul Island by the afternoon of 11 March, causing northeasterly winds to 35 knots over the northern Bering Sea. The system then drifted northward and became stationary over Norton Sound between 12 and 15 March (Figure 12f), producing a light westerly to northwesterly flow and temperatures ranging from -18°C to -27°C over the northern Bering Sea.

During the third week of March, the intensity of storms increased in the west-to-east track south of the Aleutian Islands, while pressures increased over eastern Siberia. A 968 mb low pressure center moved from south of the Alaska Peninsula on 16 March to Bristol Bay on 18 March bringing northeasterly gales to much of the Bering Sea (Figure 12g). The winds diminished thereafter, except for a brief increase to 40 knots over St. Lawrence Island on 20 March as the pressure gradient tightened between a low pressure trough along Alaska's west coast and the Siberian high pressure system. The large Gulf of Alaska low pressure system dominated the weather over the region during the following four days (Figure 12h), producing northerly winds of 15 to 20 knots and temperatures ranging from -8°C to -24°C .

High pressure moved from the northwest Pacific to eastern Siberia between 24 and 27 March, resulting in light, mostly northwesterly winds and temperature minimums of -28°C over the northern Bering Sea. Winds switched to northeasterly and increased to 25 knots across the area, as a 980 mb low pressure center moved eastward south of the Aleutians to the Gulf of Alaska between 28 and 31 March (Figure 12i).

During the period between 28 March and 3 April (Figure 12j), the storm track temporarily shifted northward across the southern Bering Sea. This produced northeasterly winds to 30 knots and brought the -24°C surface isotherm as far south as St. Lawrence Island by 2 April. The weather improved after 3 April, as a ridge of high pressure built northward and strengthened over the Bering Sea and eastern Siberia during the following 8 days. Cyclone activity was confined to the Gulf of Alaska and the extreme southwestern Bering Sea. During the period from 4 to 12 April, the area experienced northwesterly to northeasterly winds up to 15 knots with surface air temperature minimums around -24°C in the northern Bering Sea.

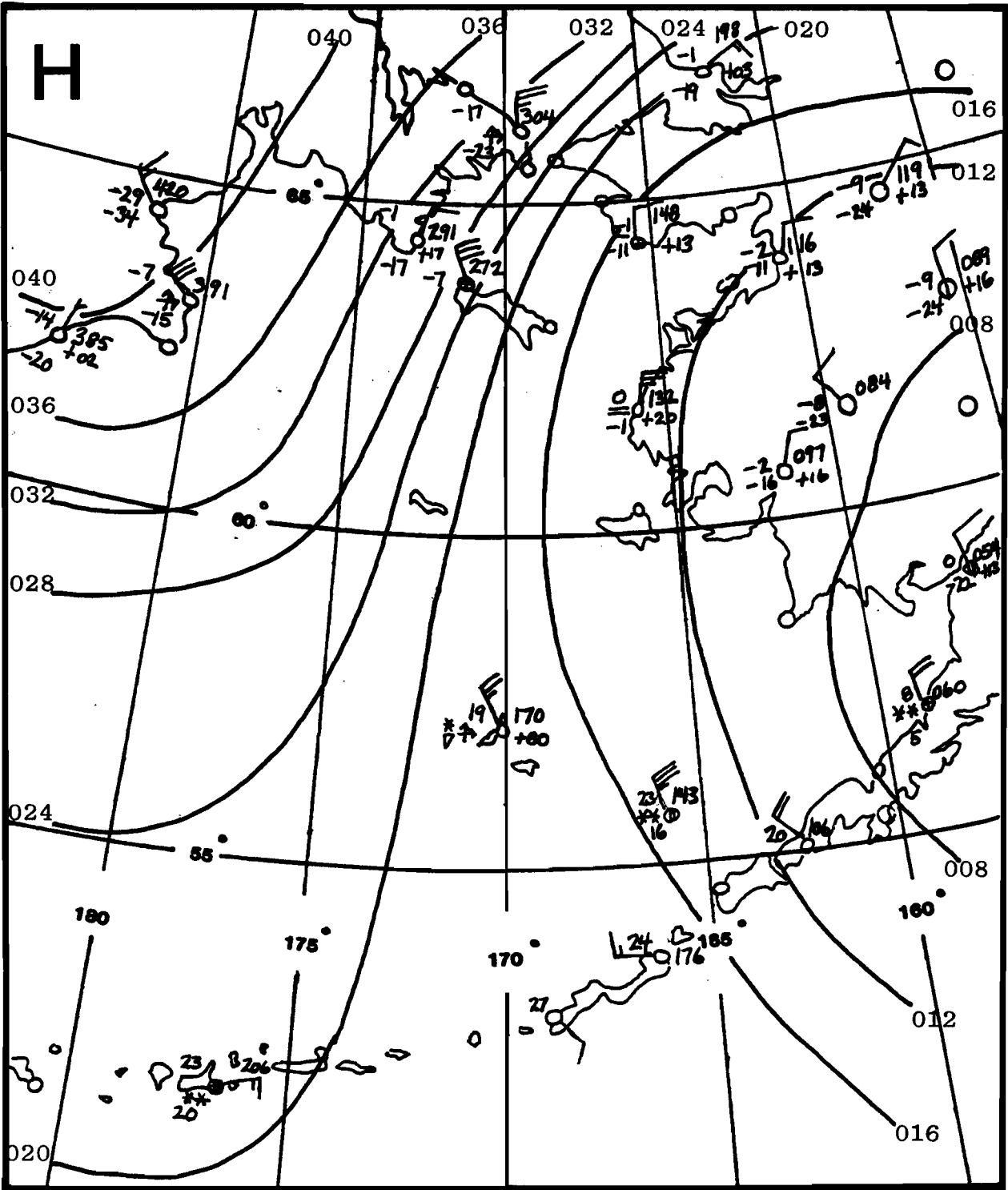
The high pressure weakened rapidly on 13 April as the region came under the influence of a storm moving eastward along the axis of the Aleutian Islands. The Bering Sea continued under the influence of this storm through 15 April with temperatures generally in the -8°C to -20°C range and winds northwesterly to northeasterly at 15 to 20 knots.

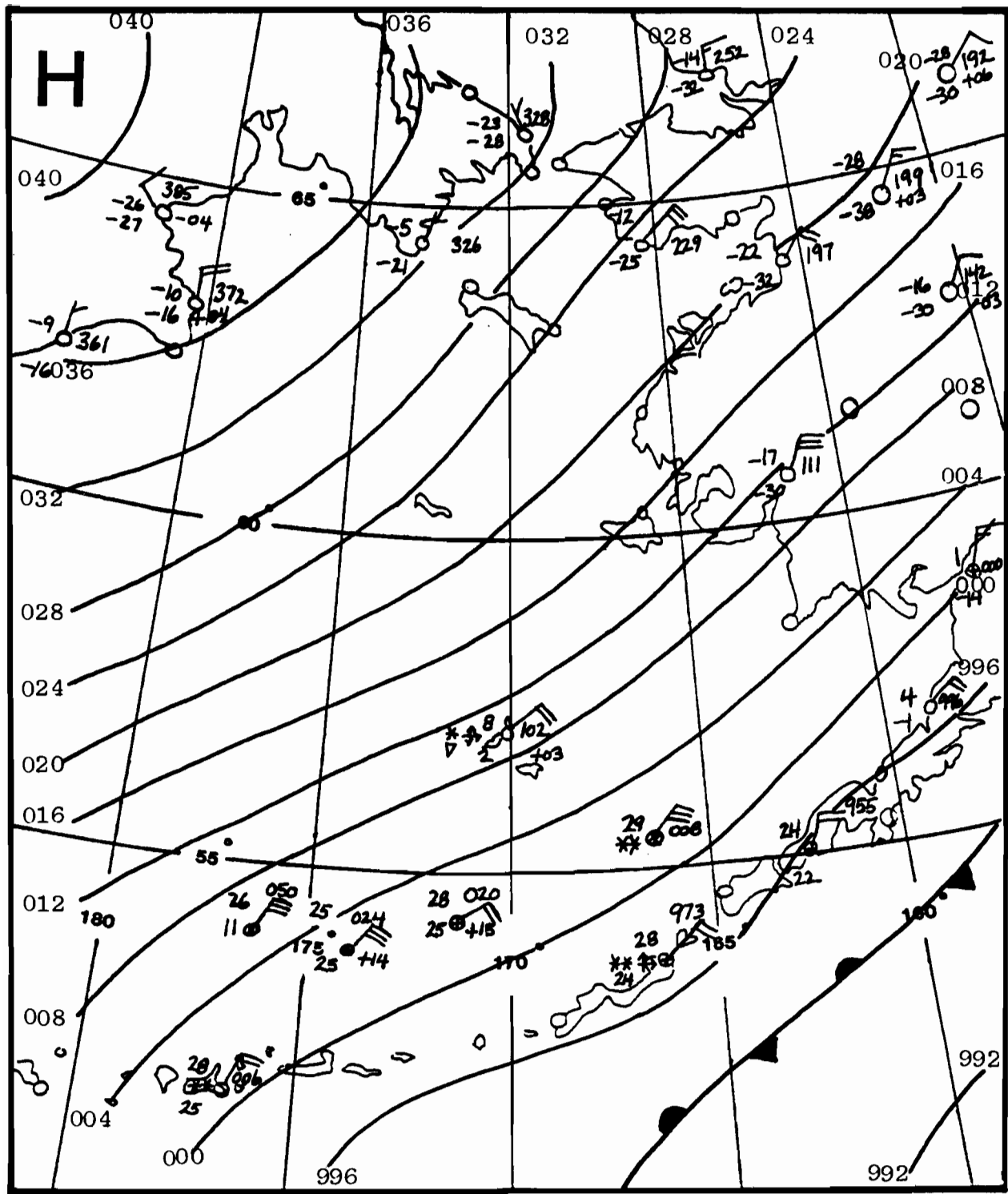
Further analysis of Alaska sea-level charts shows that from 16 April through 18 April a low pressure center over the southwest Bering Sea brought southerly winds over the eastern Bering. A strong mid-Pacific high pressure system kept the low from moving east along the Aleutian Islands. A new tight low formed southeast of Japan, moved northeast, and merged with the weakening Bering low on 18 April. This larger system and the Pacific high migrated eastward over several days, shifting winds to northerly by 20 April. By 21 April a small low pressure center formed in the southwestern Bering Sea and the larger low moved into the central Gulf of Alaska with a slight ridge over

the eastern Bering. These moved east slowly with the small low deepening and the large low filling slightly. By 23 April the small low reached the Alaska Peninsula and a broad weak high formed over the southwest Bering Sea bringing northerly to northeasterly winds over the eastern Bering. On 25 April a new deeper low pressure system moved eastward, south of the Aleutians and merged with the small low over Kodiak Island. The high in the southwest held, forming an effective bridge with the Siberian high pressure system through 28 April. The southern high pressure system moved eastward very slowly. A small low formed in southwest Bering Sea on 29 April, passed between the two high pressure centers, and merged with the old low over Bristol Bay. Weak northerly winds persisted, but by 1 May a weak ridge pushed up over the eastern Bering Sea, changing winds to easterly and southerly over the eastern Bering and increasing air temperatures to 0°C.

On 5 and 6 May a low from the southwest Bering Sea moved northward across western St. Lawrence Island, through Bering Strait, and up the Alaska coast over the Chukchi Sea. A new 972 mb low pressure center formed south of the central Aleutian Islands on 6 May and followed the same path as the previous low through 8 May. A third system with central pressure of 972 mb formed on 7 May over the central Aleutian Islands and passed north to St. Lawrence Island by 9 May. This last system turned east at the island and slowly filled as it drifted eastward and then southward. On 11 May it reached Dall Point with a central pressure of 1003 mb. Behind the low, the winds shifted to northerly again.

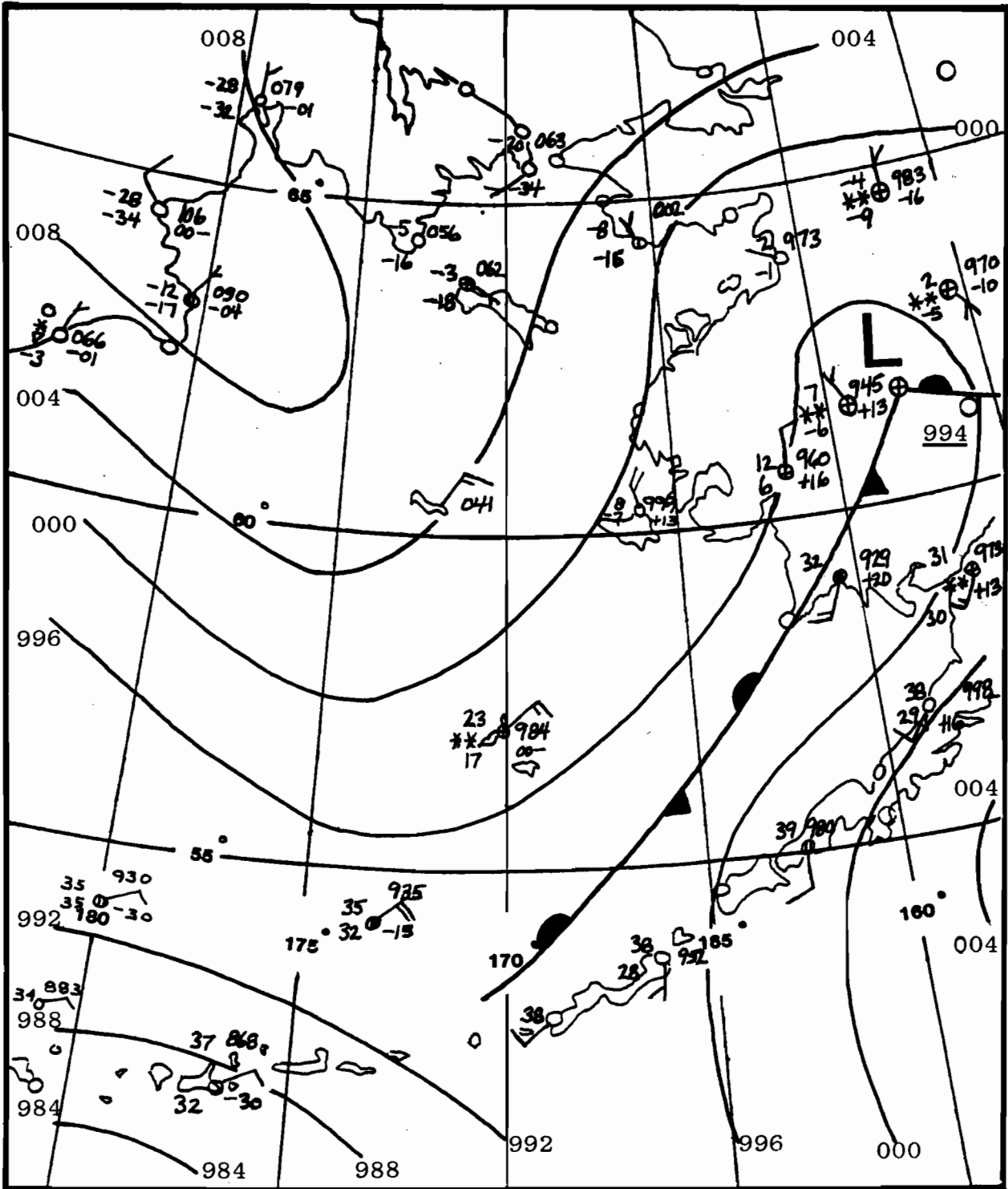
On 15 and 16 May, a large ridge of high pressure formed over the central Pacific bringing westerly to southwesterly winds over the eastern Bering Sea. This regime persisted through late May.





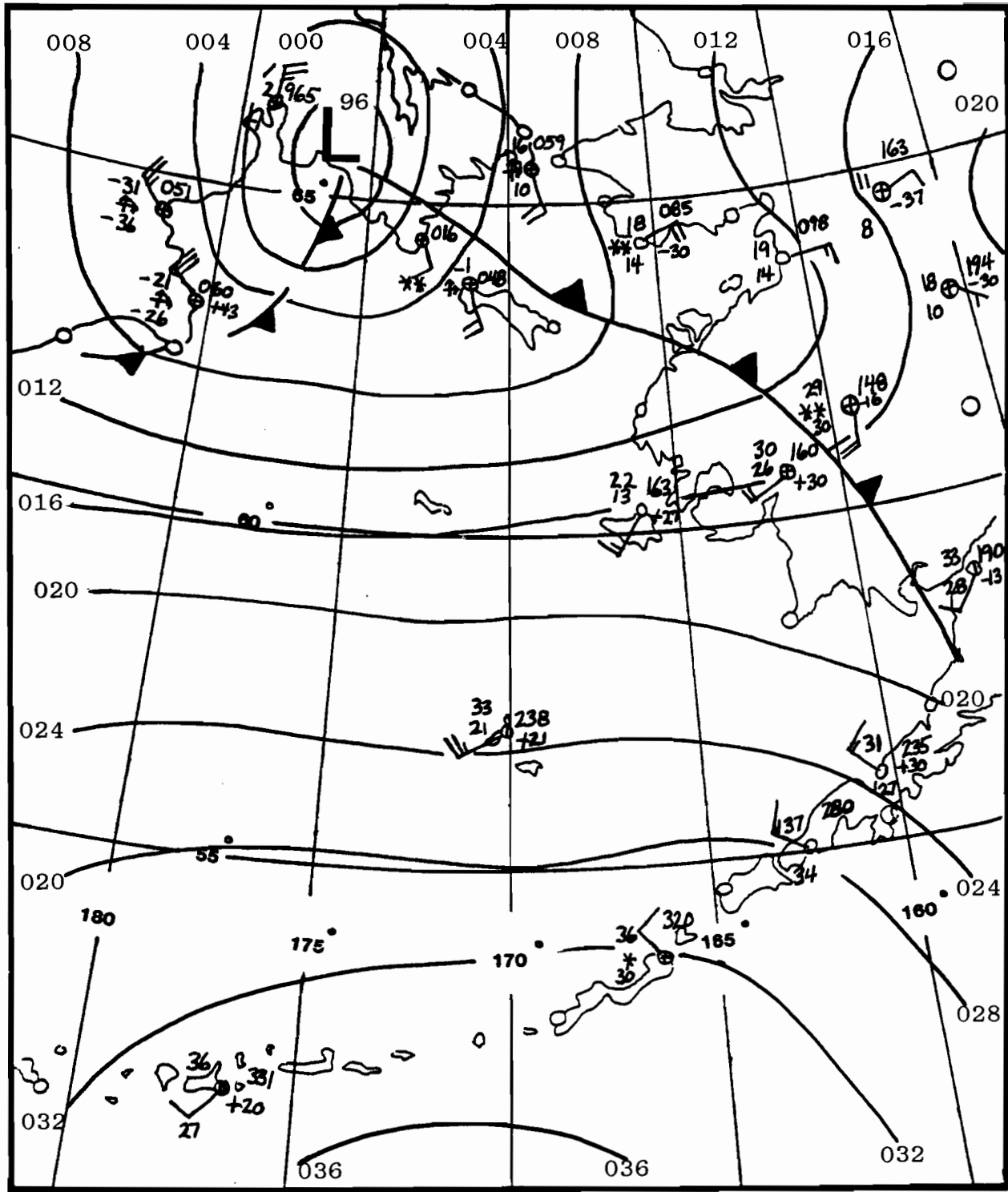
0000 GMT 21 FEB 1985

Figure 12b.--Sea-level pressure analysis for 00 GMT on 21 February 1985 (JD 52).



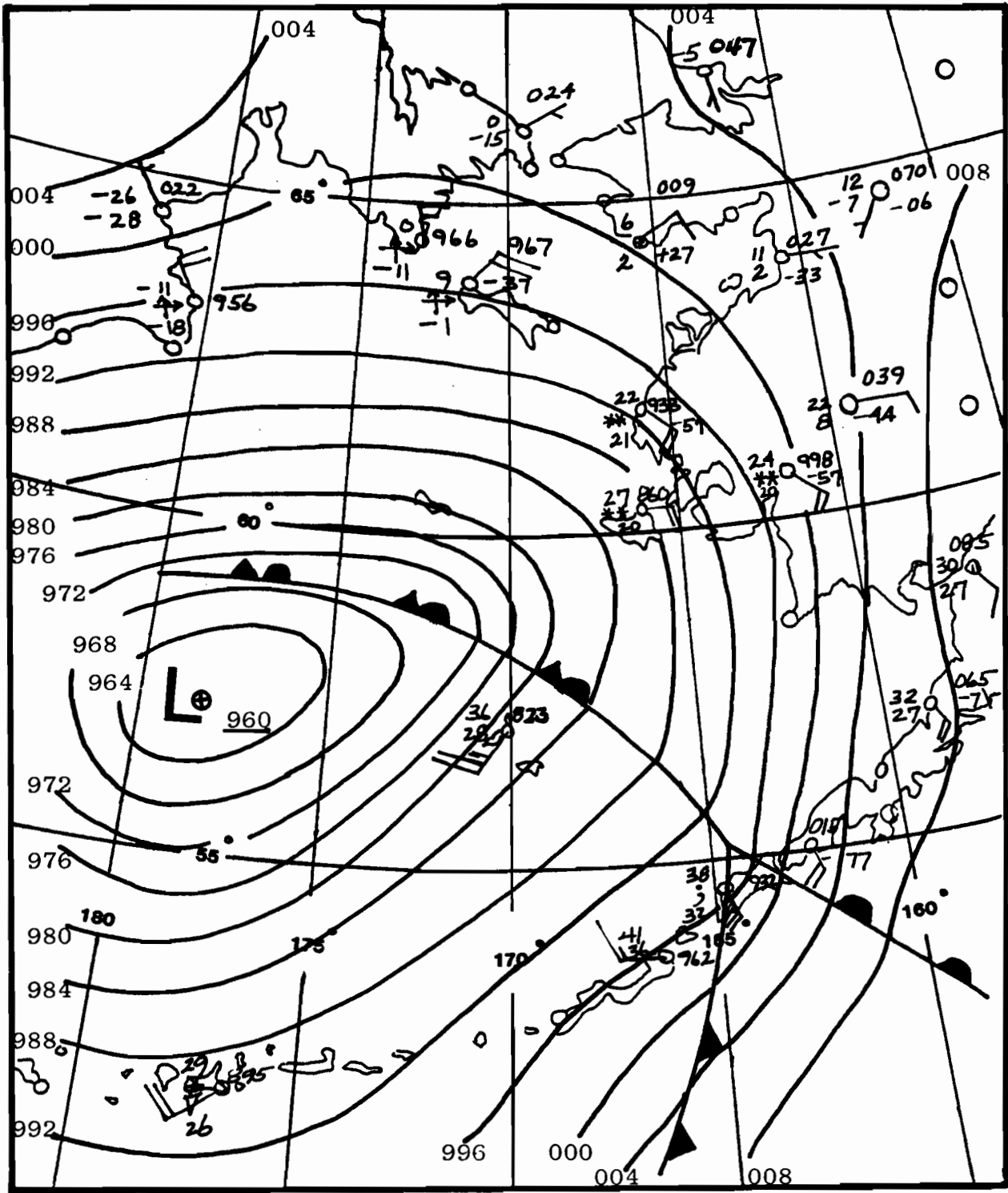
0000 GMT 26 FEB 1985

Figure 12c.--Sea-level pressure analysis for 00 GMT on 26 February 1985 (JD 57).



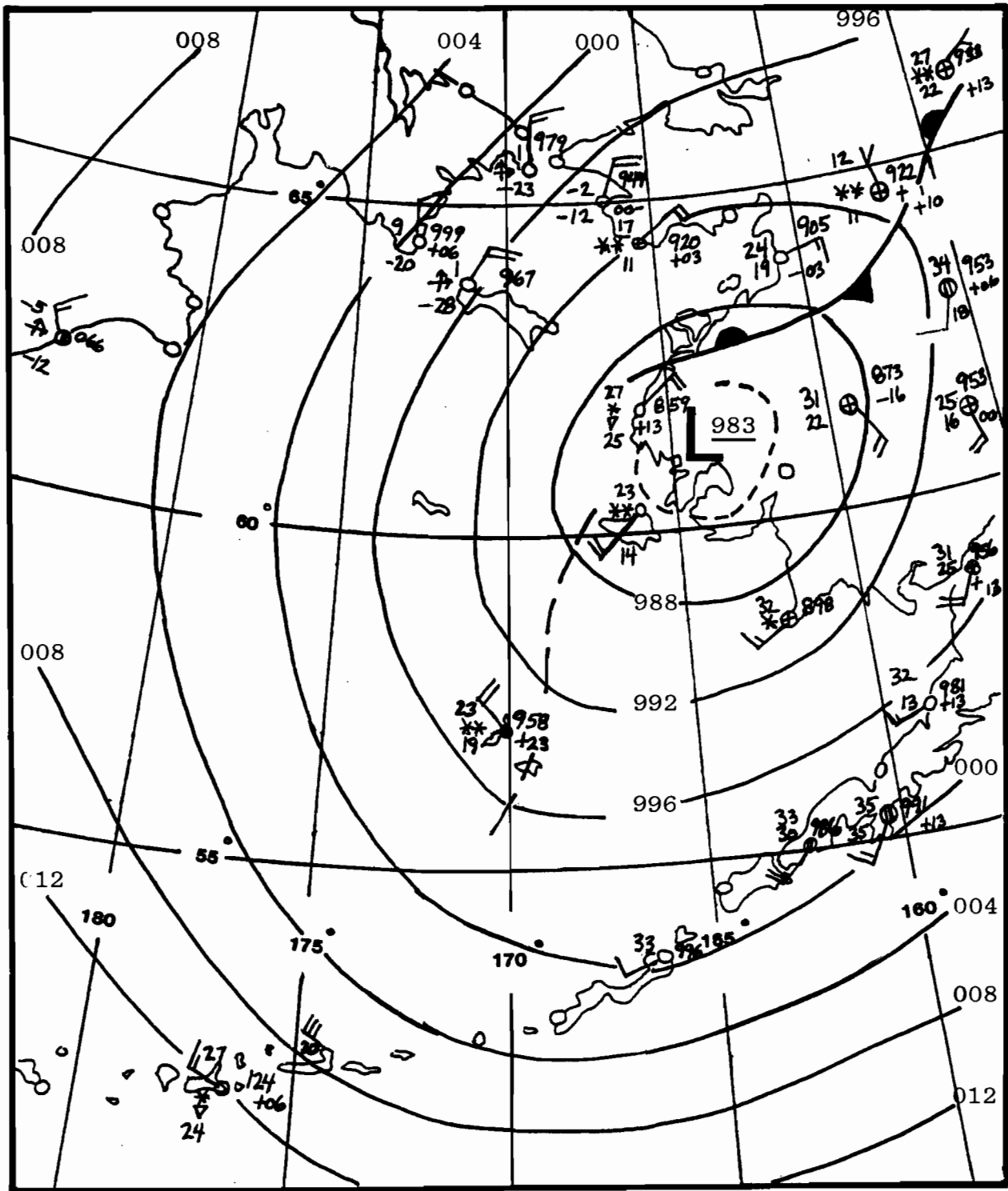
0000 GMT 03 MAR 1985

Figure 12d.--Sea-level pressure analysis for 00 GMT on 3 March 1985 (JD 62).



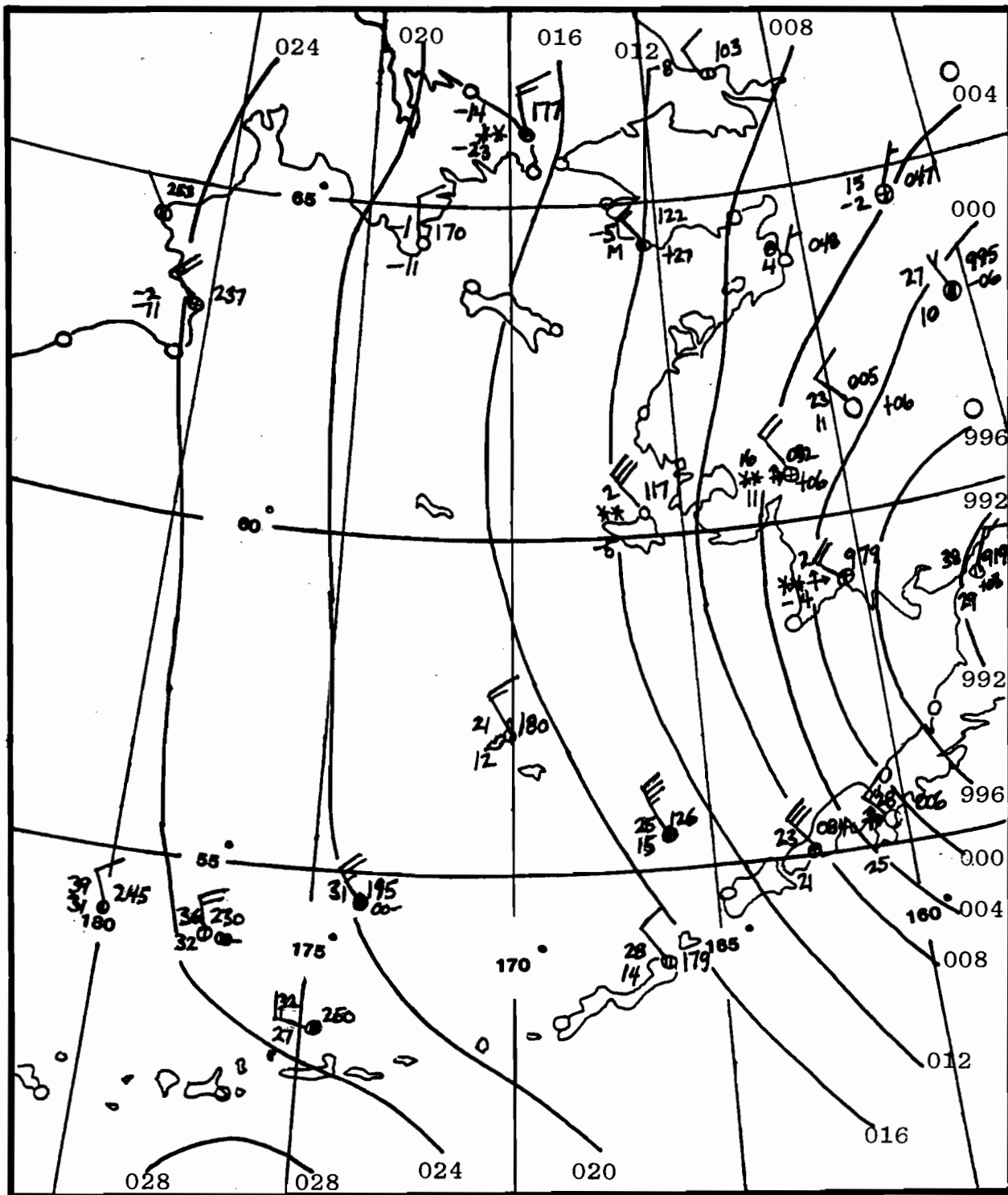
0000 GMT 08 MAR 1985

Figure 12e.--Sea-level pressure analysis for 00 GMT on 8 March 1985 (JD 67).



0000 GMT 13 MAR 1985

Figure 12f.--Sea-level pressure analysis for 00 GMT on 13 March 1985 (JD 72).



0000 GMT 23 MAR 1985

Figure 12h.--Sea-level pressure analysis for 00 GMT on 23 March 1985 (JD 82).

4.2 Meteorology Station Results

The GOES meteorological data for all four stations are given in Appendix C for the full run of each station and are summarized in Figures 13 through 16 for a comparison period from just before 00 GMT on 24 February until just after 00 GMT on 4 March 1985. Station C had three breaks in transmission and the vane failed after 14 February, but the wind speed, gust, and air temperature worked until the station was taken down. All of the other atmospheric sensors worked throughout the comparison period. All four stations tracked the same synoptic events with minor variations in timing. Stations A and B are more highly correlated in all variables because of their proximity, but the magnitude of the wind speed was about 10% lower at station A than at the other three sites probably due to locally rougher ice conditions. Also note that floes A and B rotated 45 degrees cyclonically (counter-clockwise) during the last week in February and back again in the first week in March. B continued with rotations of about this scale through the end of March, apparently related to the large-scale changes in wind and current direction.

The other notable characteristic of the meteorological data was the difference between the air temperatures at the two stations on St. Lawrence Island and the two drifting ice stations to the southeast. The temperatures over the ice were 3 to 5°C warmer during periods of extreme cold-air advection and were 1 to 3°C colder during warm-air advection events. Diurnal variations in temperature of several degrees Centigrade were common to all sites. This is more apparent in the full-scale plots in the appendix than in the stretch-scale plots in Figures 13 to 16. The diurnal signal became larger as spring progressed, especially at the island station D.

St. Lawrence Island has four mountain groups between 400 and 700 m high (Figure 1b), separated by relatively flat plains near sea level. When the wind blows from the east or west the island offers a high, narrow cross-section, but when the wind blows from the north or south, the island presents a broad cross-section varying markedly in height. There is some indication that the winds at Powoiliak Camp (GOES-C) were somewhat affected by the Roovoot Range when the wind blew from the west or northwest, compared to the winds at Siknik Cape (GOES-D) which is very exposed. The difference in weather regimes along the length of the island can be large, however. Also since there is typically a strong, capping inversion in the atmosphere in winter of 200 to 600 m, the effects of the island's mountains should be felt over the polynya.

TIME SERIES PLOT FOR APEX ICE STATION A
 23 FEB 85 TO 4 MAR 85 INTERVAL= 30.0 MINS

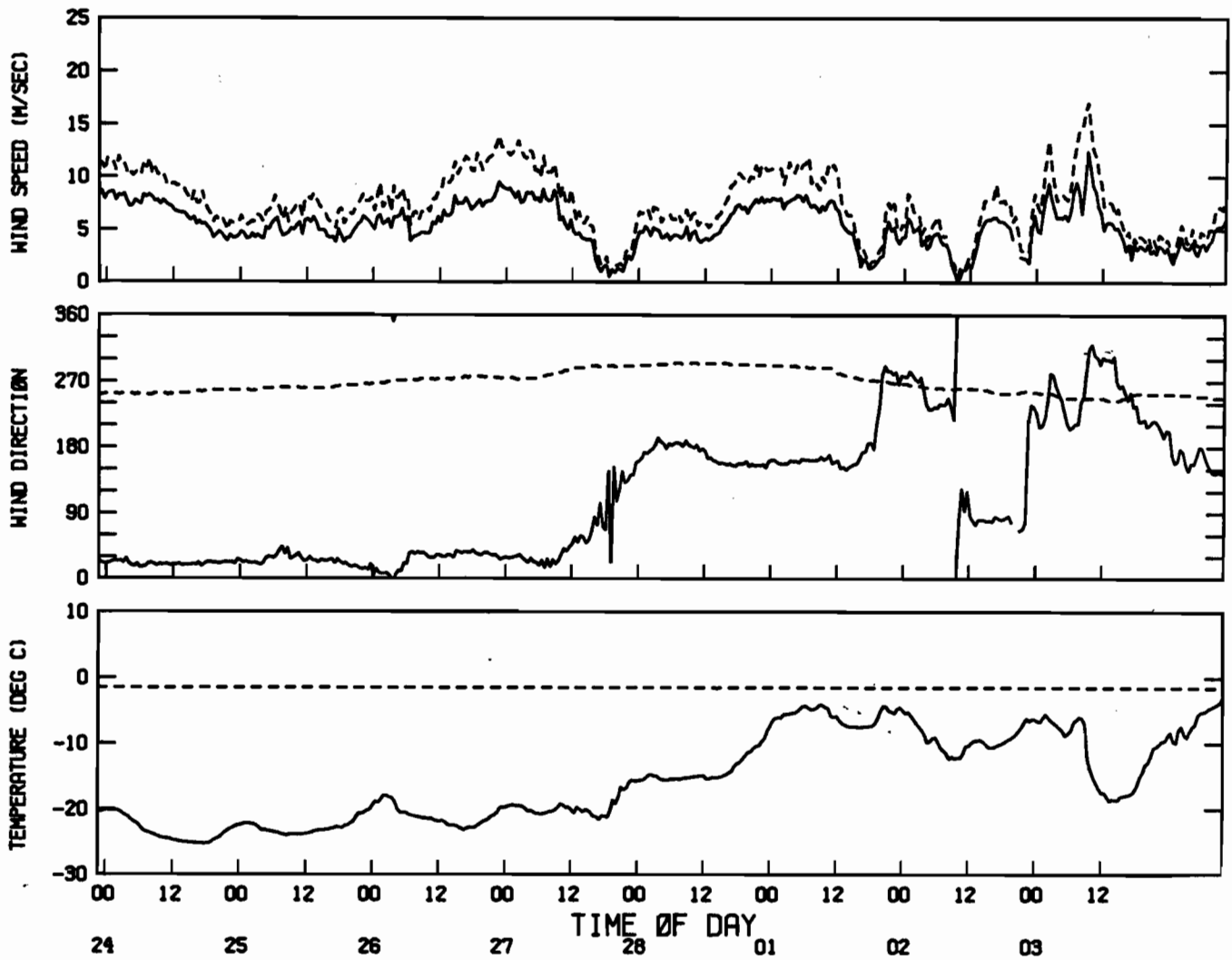


Figure 13a.--Meteorological time series plot for GOES station A accompanying ARGOS Buoy 2326. The dashed line in the top panel is the maximum gust and the solid line is the mean speed. The dashed line in the center panel is the floe compass and the solid line is the wind direction. The dashed line in the lower panel is the water temperature and the solid line is the air temperature.

TIME SERIES PLOT FOR APEX ICE STATION A
 23 FEB 85 TO 4 MAR 85 INTERVAL= 30.0 MINS

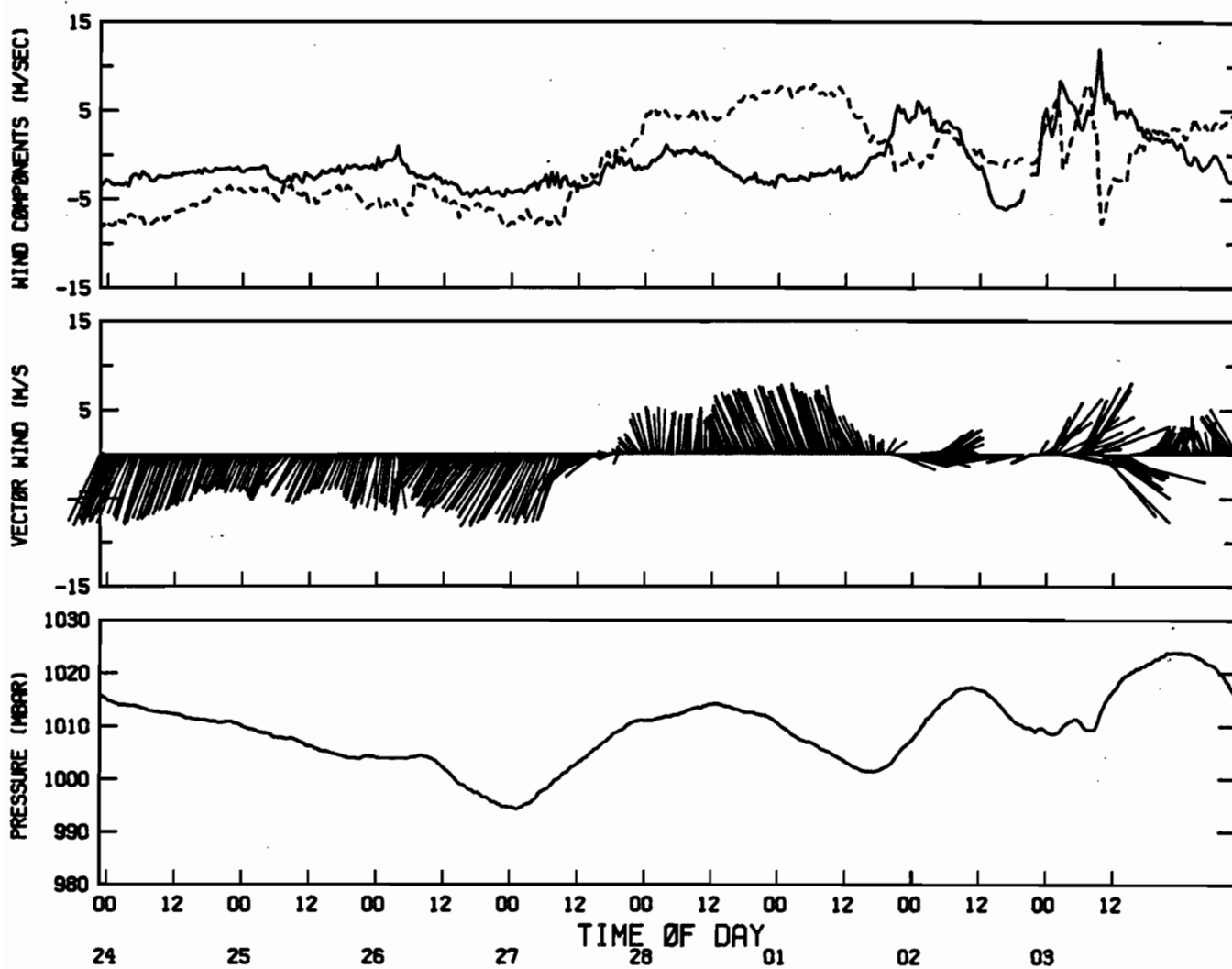


Figure 13b.--Meteorological time series plot for GOES station A accompanying ARGOS Buoy 2326. The dashed line in the top panel is the v-component and the solid line is the u-component of the vector-mean wind. The vectors are plotted in the center panel in the oceanographic convention. The lower panel gives measured sea-level pressure.

TIME SERIES PLOT FOR APEX ICE STATION B
 23 FEB 85 TO 4 MAR 85 INTERVAL= 30.0 MINS

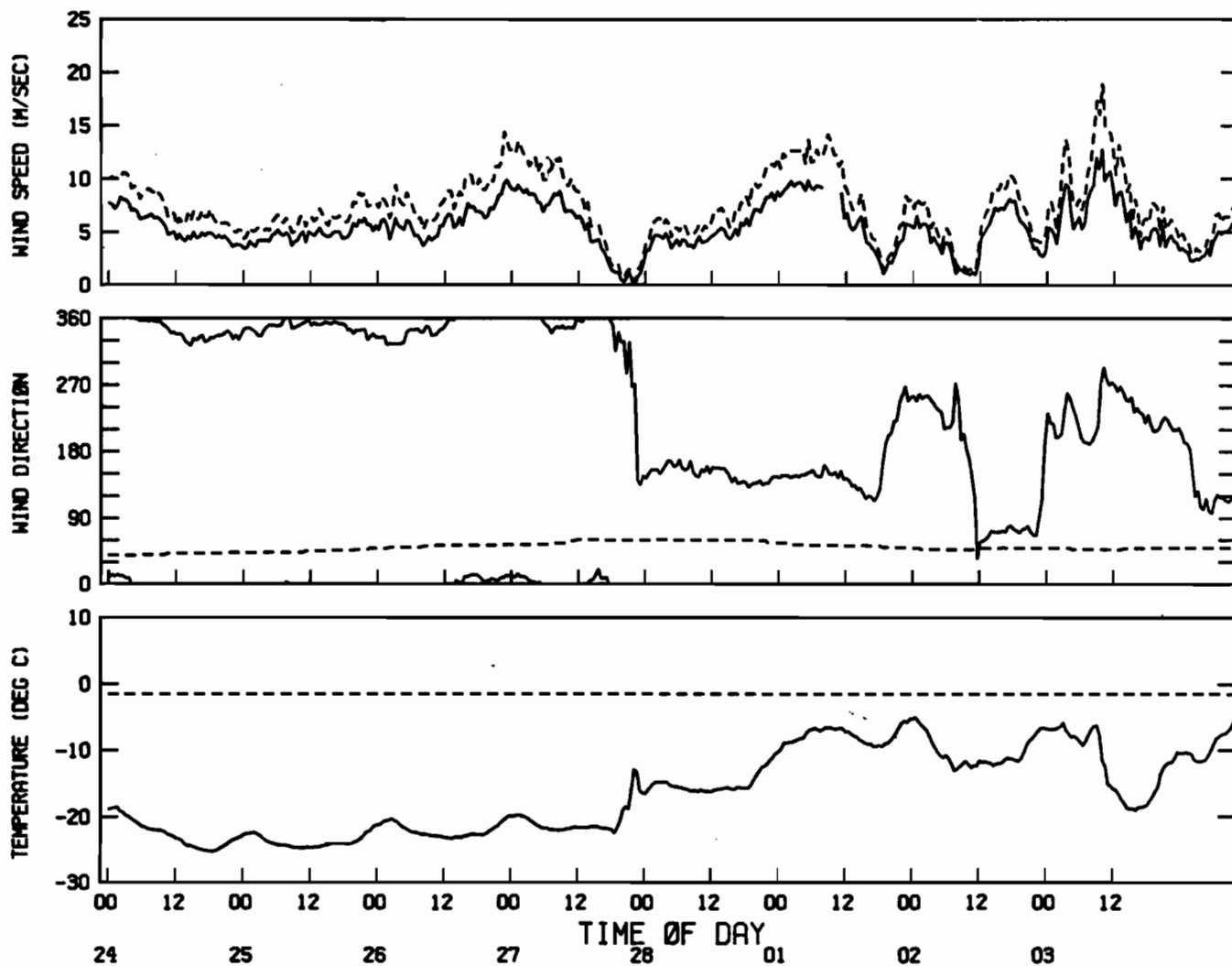


Figure 14a.--Meteorological time series plot for GOES station B accompanying ARGOS Buoy 2335. The dashed line in the top panel is the maximum gust and the solid line is the mean speed. The dashed line in the center panel is the floe compass and the solid line is the wind direction. The dashed line in the lower panel is the water temperature and the solid line is the air temperature.

TIME SERIES PLOT FOR APEX ICE STATION B
 23 FEB 85 TO 4 MAR 85 INTERVAL= 30.0 MINS

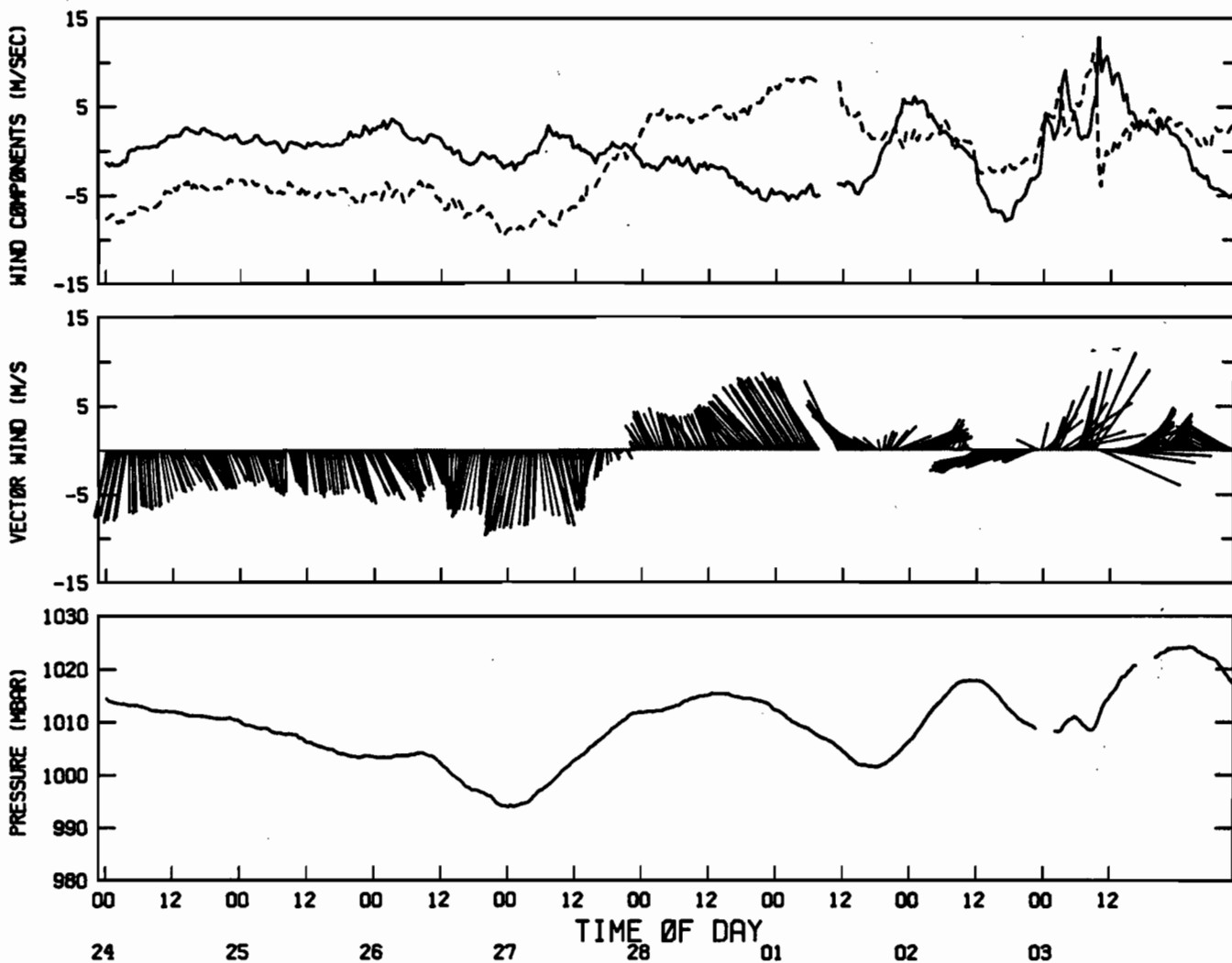


Figure 14b.--Meteorological time series plot for GOES station B accompanying ARGOS Buoy 2335. The dashed line in the top panel is the v-component and the solid line is the u-component of the vector-mean wind. The vectors are plotted in the center panel in the oceanographic convention. The lower panel gives measured sea-level pressure.

TIME SERIES PLOT FOR APEX ICE STATION C
 23 FEB 85 TO 4 MAR 85 INTERVAL= 30.0 MINS

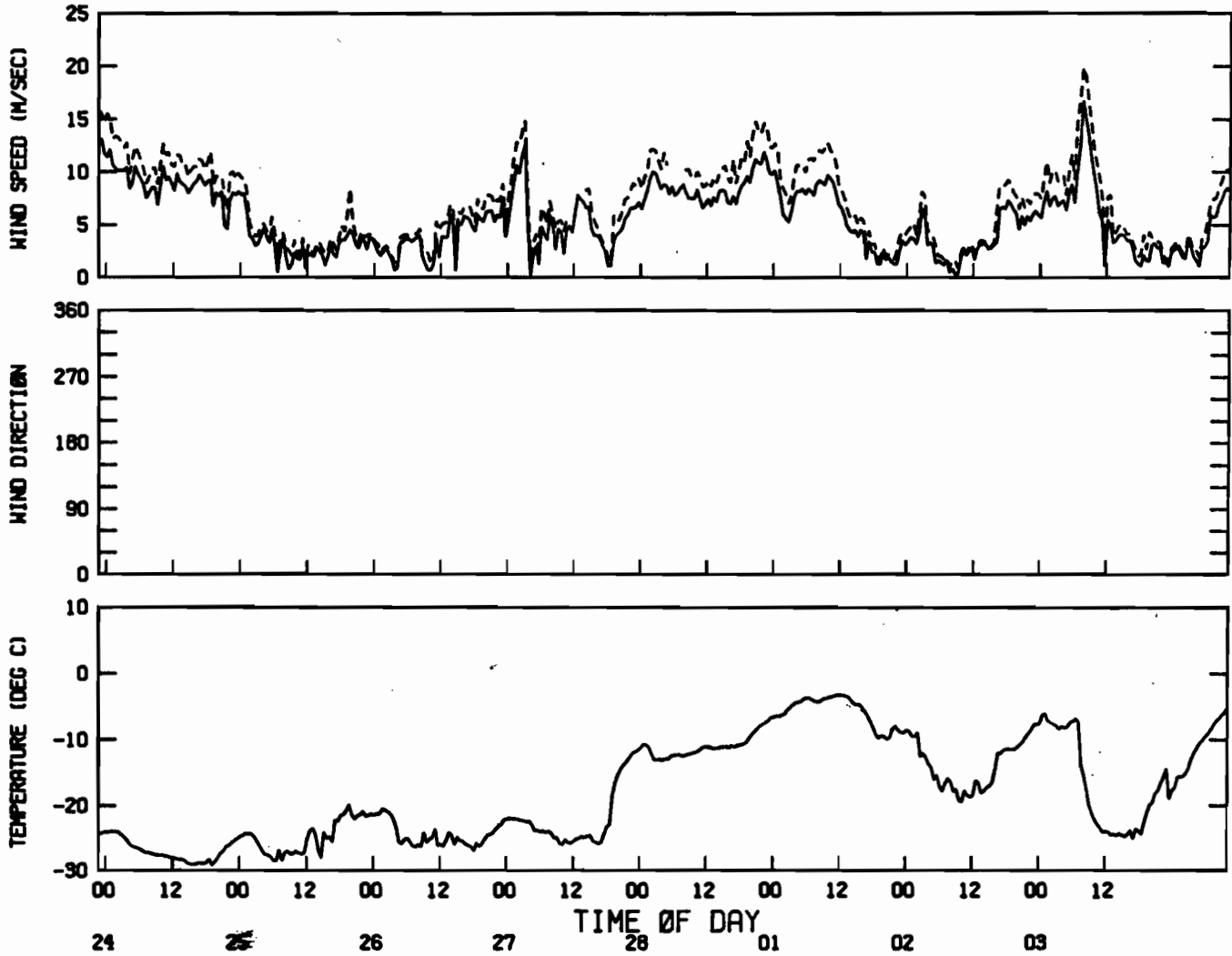


Figure 15.--Meteorological time series plot for GOES station C located on southwest St. Lawrence Island. The dashed line in the top panel is the maximum gust and the solid line is the mean speed. The wind vane did not function on this station. In the lower panel the solid line is the air temperature.

TIME SERIES PLOT FOR APEX ICE STATION D
 23 FEB 85 TO 4 MAR 85 INTERVAL= 30.0 MINS

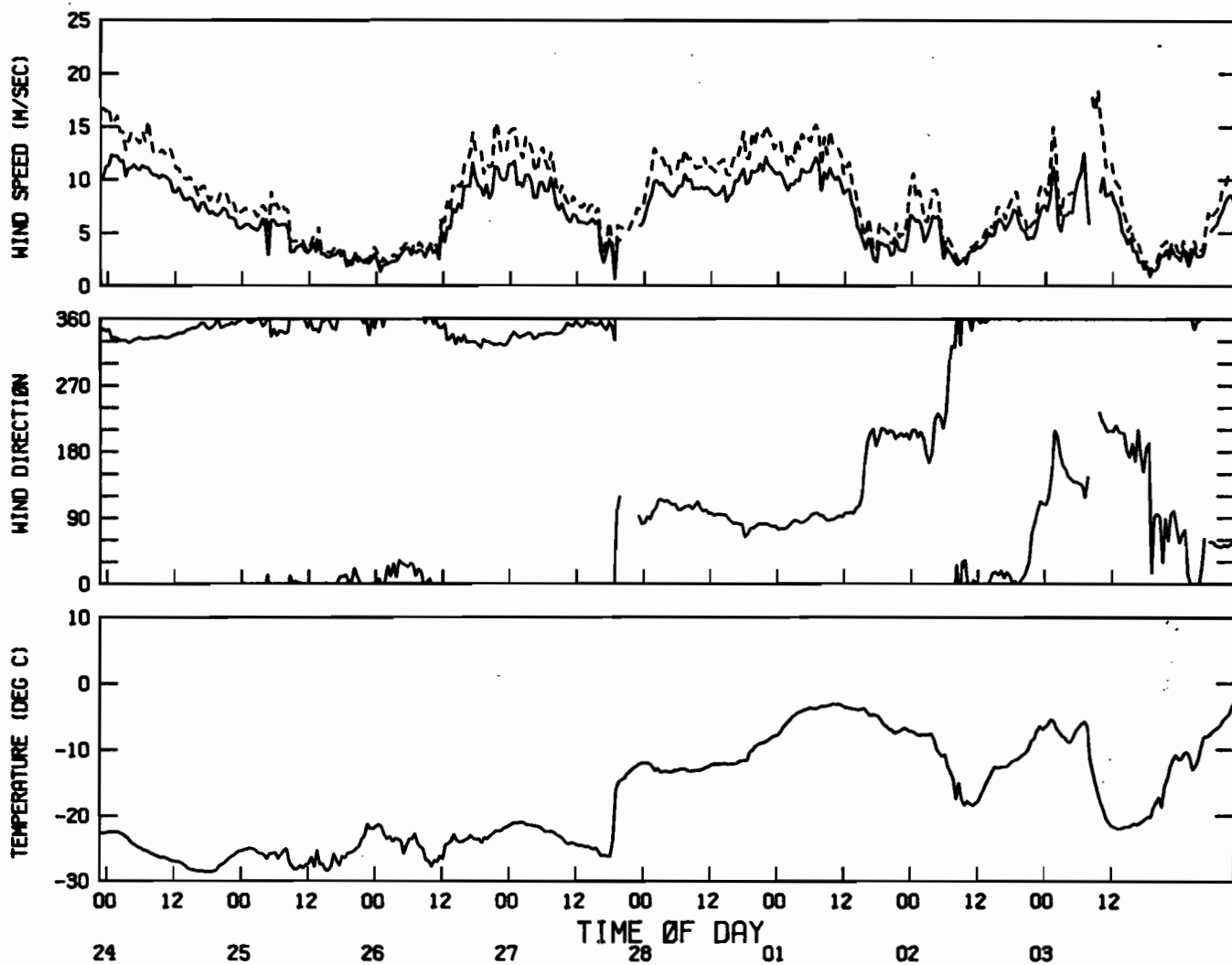


Figure 16a.--Meteorological time series plot for GOES station D on south central St. Lawrence Island. The dashed line in the top panel is the maximum gust and the solid line is the mean speed. In the center panel the solid line is the wind direction. In the lower panel the solid line is the air temperature.

TIME SERIES PLOT FOR APEX ICE STATION D
 23 FEB 85 TO 4 MAR 85 INTERVAL= 30.0 MINS

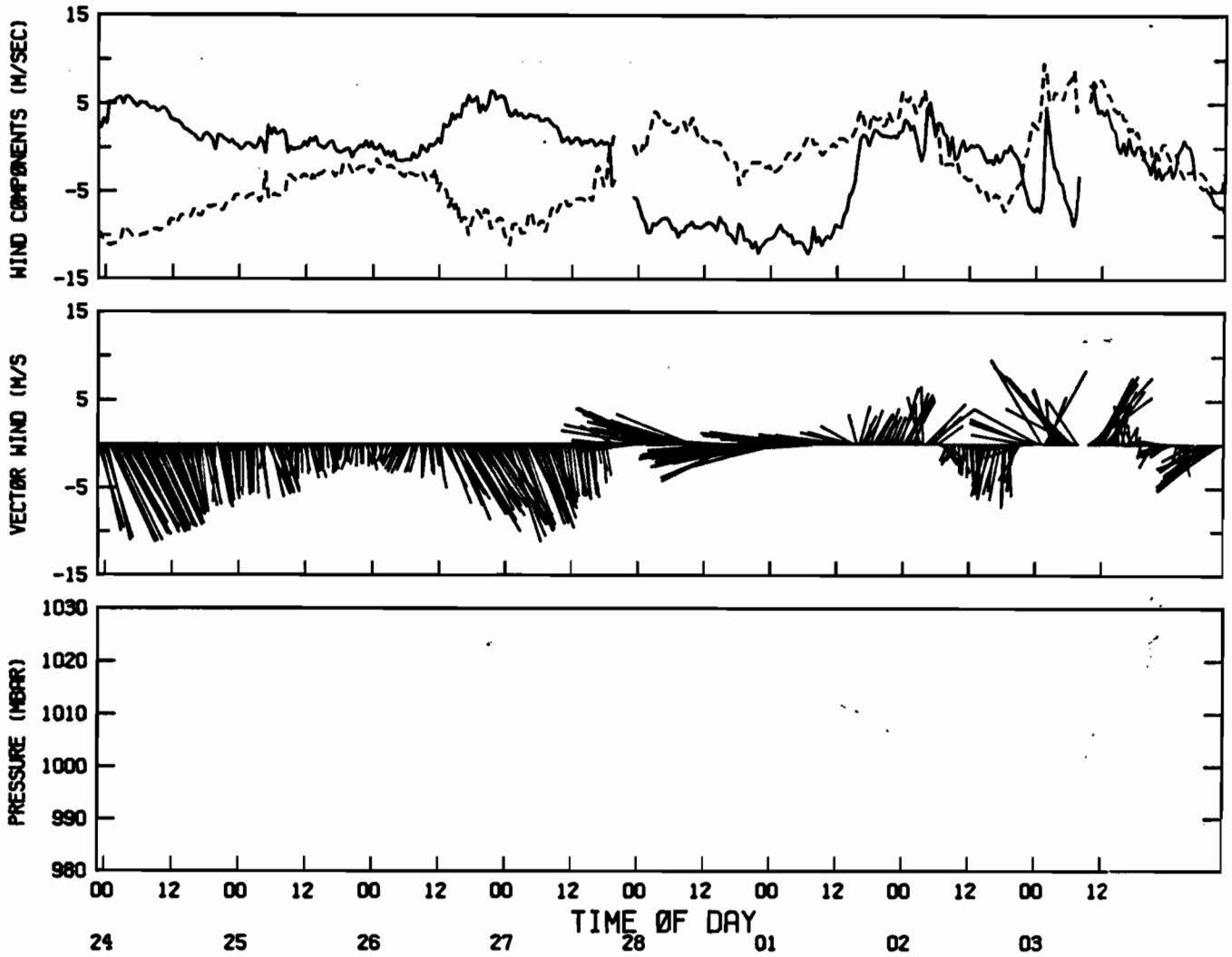


Figure 16b.--Meteorological time series plot for GOES station D on south central St. Lawrence Island. The dashed line in the top panel is the v-component and the solid line is the u-component of the vector-mean wind. The vectors are plotted in the center panel in the oceanographic convention. Pressure was not measured at this station.

5. OCEANOGRAPHY

5.1 Regional Oceanography

The regional oceanography will be discussed in detail in a later report, but there are some comments which can be made in the context of the meteorological conditions and ice drift observations during the winter and spring of 1985. Throughout November, December, and January, the currents in the three straits (Shpanberg, Anadyr, and Bering) were generally northward with infrequent reversals. Beginning the first of February, however, there were frequent and prolonged current reversals, which extended until the first of May. After this time the currents reverted to northward again in the northern Bering Sea. From the ice drift, there was an indication that the reversals in Anadyr Strait did not last as long as reversals in Shpanberg Strait. In subjectively comparing 1985 to the annual transport cycle for Bering Strait (Figure 10 in Aagaard *et al.*, 1985), northward transport was probably above normal in January, below or at normal in February, and below normal in March and April, but with the overall minimum transport in February per the normal annual cycle.

5.2 Oceanography Station Results

Relative current velocities and water temperatures measured 2 m below the bottom of the ice for the two drifting GOES stations are given in Appendix D for the full run of each station and are summarized in Figures 17 and 18 for a comparison period from just before 00 GMT on 24 February until just after 00 GMT on 4 March 1985. The vane on the current meter on station B must have frozen during the deployment, and since water temperatures remained at the freezing point throughout the experiment, did not thaw. All other oceanographic sensors seemed to function properly until the transmitters failed in the spring. The current meter on station A lasted 9 days longer than the anemometer.

Both stations seemed to track the same synoptic events, even periods of zero relative current associated with periods of winds below 3 m/s, such as late on 27 February and midday on 2 March. Rotations in relative current direction also are related to very low wind speeds. One interesting observation is that the ice speeds seem better correlated with the wind gust speeds than the mean wind speeds. This point bears further investigation. Another observation is that there are high frequency signals in the relative current that are not apparently wind related. Reynolds *et al.* (1985) noted similar high frequency relative current variations during MIZEX-West in the southern Bering Sea during 1983. These variations may be caused by ice floe interactions. In general, tidal and other long-period oceanic variations do not appear in the relative current record because the ice and current are nearly perfectly coupled at frequencies less than 4 cycles/day (Pease *et al.*, 1983; Reynolds *et al.*, 1985).

The relative current direction for ice station A was typically 150° to the right of the wind direction, although there were some isolated rotation events related to low wind speeds during which this relationship did not hold. This result is similar to results obtained for other first-year ice floes in 1981 (Pease *et al.*, 1983) and in 1983 (Reynolds *et al.*, 1985). The

rotation events were similar to those observed for a floe near Bering Strait in 1980 (Pease and Salo, 1981) which also occurred during light wind periods that accompanied a change in the weather regime. The relative-current rotations appear to represent the lag between the response of the ice to the wind and the response of the water to the wind and ice. The response time appears to be longer than an hour but shorter than a day for a variety of conditions.

TIME SERIES PLOT FOR APEX ICE STATION A
 23 FEB 85 TO 4 MAR 85 INTERVAL= 30.0 MINS

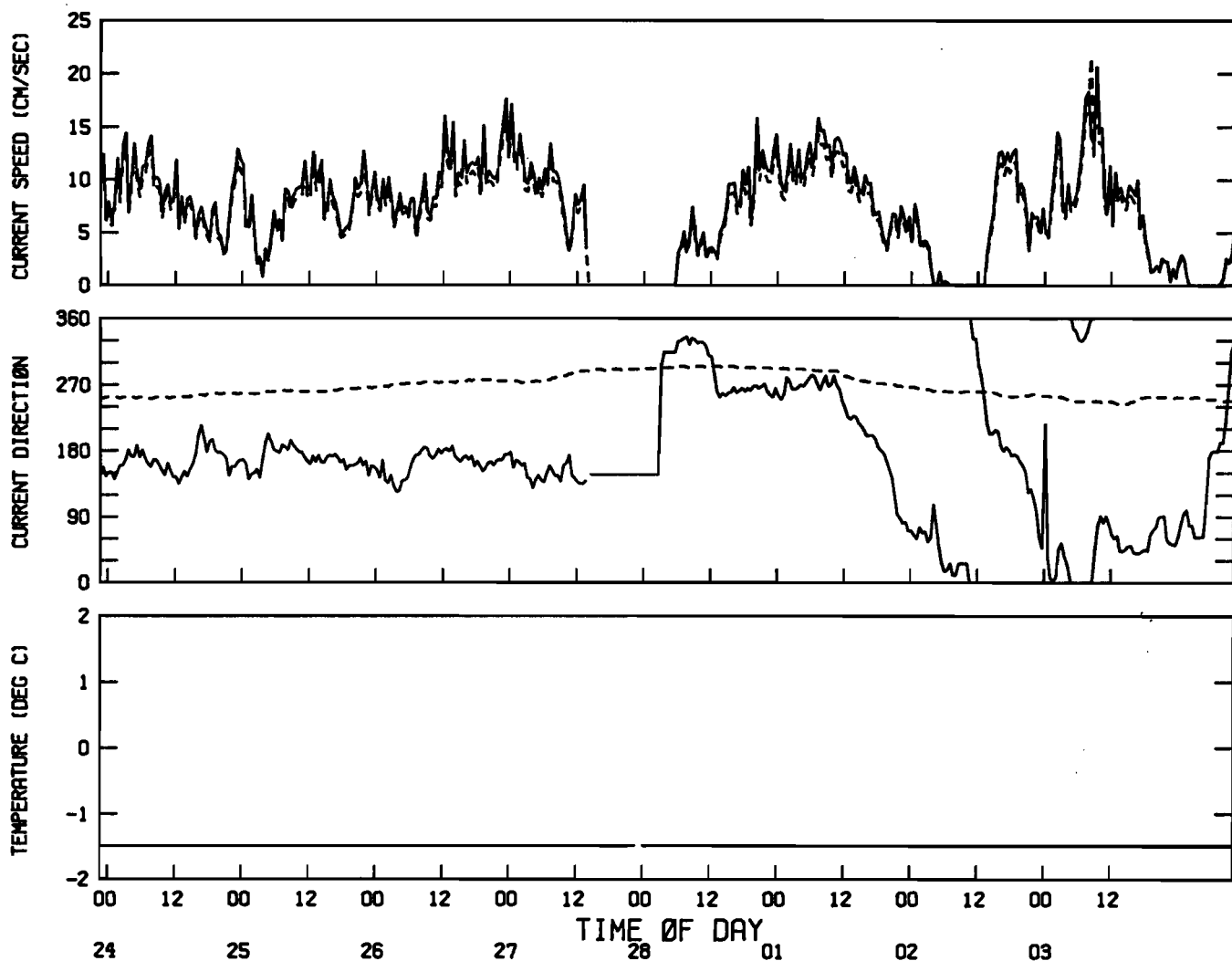


Figure 17a.--Oceanographic time series plot for GOES station A accompanying ARGOS Buoy 2326. The solid line in the top panel is the vector-mean speed, while the dashed line is the mean speed calculated directly from the number of turns of the rotor. The dashed line in the center panel is the floe compass and the solid line is the current direction. The solid line in the lower panel is the water temperature.

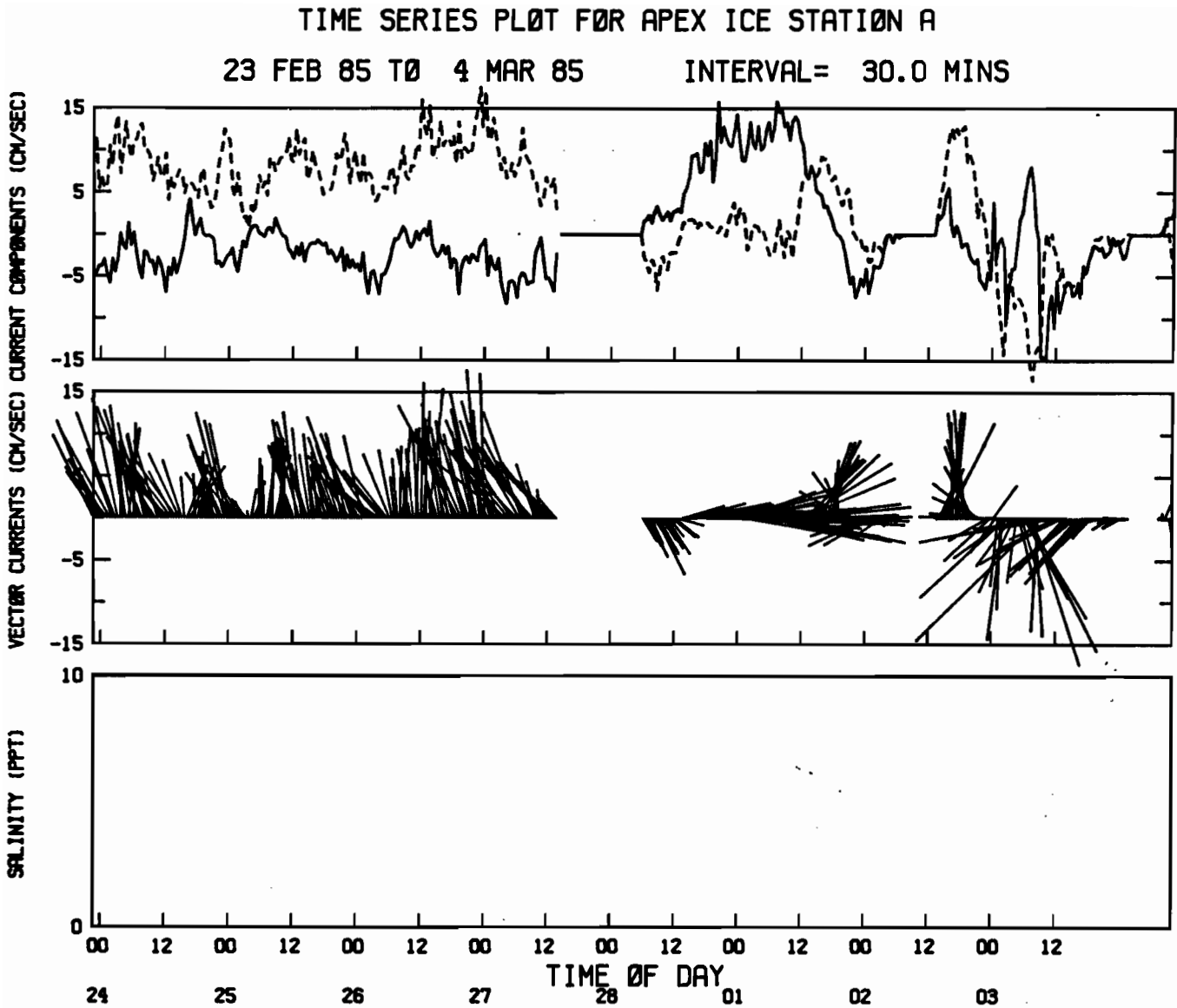


Figure 17b.--Oceanographic time series plot for GOES station A accompanying ARGOS Buoy 2326. The dashed line in the top panel is the v-component and the solid line is the u-component of the vector-mean current. The vectors are plotted in the center panel in the oceanographic convention. Salinity was not measured at this station.

TIME SERIES PLOT FOR APEX ICE STATION B
 23 FEB 85 TO 4 MAR 85 INTERVAL= 30.0 MINS

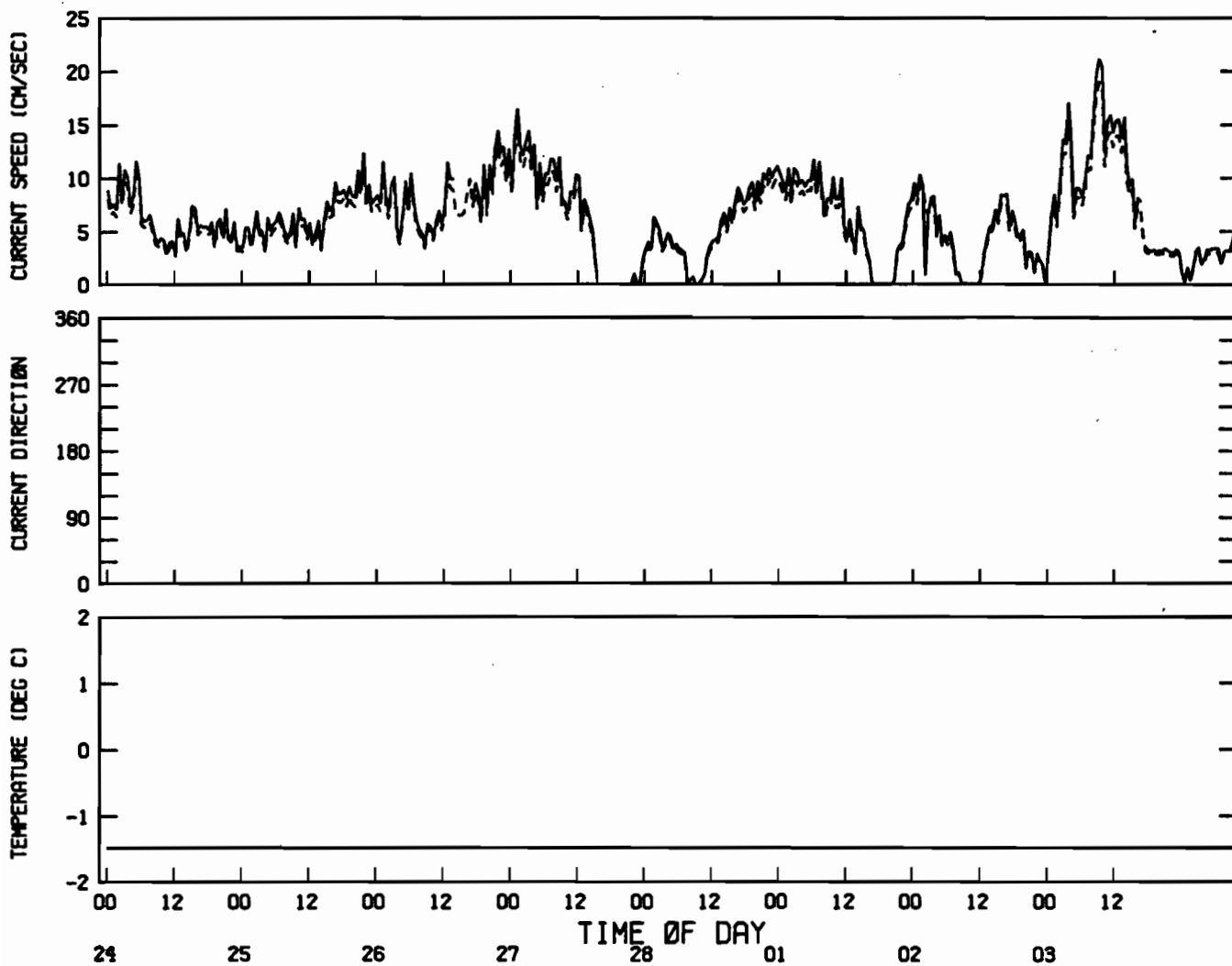


Figure 18.--Oceanographic time series plot for GOES station B accompanying ARGOS Buoy 2335. The solid line in the top panel is the vector-mean speed, while the dashed line is the mean speed calculated directly from the number of turns of the rotor. The dashed line in the center panel is the floe compass and the solid line is the current direction. The solid line in the lower panel is the water temperature.

6. SUMMARY

Ice drifted toward the south and west across most of the Bering Sea shelf from mid-February until the beginning of May 1985 due to a prolonged period of northerly winds. Although the overall maximum was not extreme, the ice season was very late. The conveyor belt process was in evidence, especially south and west of St. Lawrence Island, where six ARGOS buoys drifted toward the ice edge and melted out between 18 March and 2 April. Southeast of St. Lawrence four ARGOS buoys (which survived ridging and shearing events which four other buoys did not) were approaching the ice edge at the onset of spring weather in May. All of these four melted out with the change in radiation balance.

The net drift pattern of sea ice from the northern Bering Sea was quite different in 1985 than had been observed in a similar experiment in 1982. In 1982 there was a net drift of ice from the northern Bering Sea toward the Chukchi Sea, while in 1985 there was a net drift of ice from the northern Bering Sea toward the south in a conveyor sense. This contrast points out the enormous interannual variations in ice transport in this area and suggests that it is possible that the winter net ice direction may change through the Bering Strait from year to year.

Several open questions were presented by this preliminary data analysis.

1. How are the Lagrangian currents measured from the ice related to the Eulerian current measurements over the region?
2. Over what frequencies are the relative currents related to ice motions?
3. Are wind gusts better correlated with ice motion than the mean wind?
4. What are the average annual and seasonal ice transports in the vicinity of Bering Strait?

7. ACKNOWLEDGMENTS

This study is a contribution to the Marine Services Project of the Marine Services Division of the Pacific Marine Environmental Laboratory (PMEL) and was financed in part by the Office of Naval Research, Arctic Program, and by ARCO Resources Technology, Office of Operations and Production Research. Helicopter logistics were supported by NOAA's Office of Aircraft Operations (OAO).

Lt. Paul Moen (NOAA Corps) from PMEL, Bradley Gologergren and Elvin Noongwook from Savoonga, St. Lawrence Island, Lt. Miles Croom (NOAA Corps), pilot, and Russel Talley, mechanic from OAO, contributed to the sea ice and meteorology field operations. Grady Svaboda, Meteorologist-in-charge at NWSFO Nome, and Ronald Scheidt, NWS Marine Services Unit Anchorage, provided supporting information on environmental conditions. The Army National Guard unit at Nome provided hanger space and logistical support.

Allen Macklin oversaw the transfer of the ARGOS analysis package to the new computer system. Dr. R.D. Muench was both the principal investigator for SAIC and overall program co-ordinator for APEX. Dr. J.D. Schumacher was the PMEL focus for the current meter moorings. Dr. J.E. Overland reviewed the manuscript.

8. REFERENCES

- Aagaard, K., A.T. Roach, and J.D. Schumacher (1985): On the wind-driven variability of the flow through Bering Strait, *J. Geophys. Res.*, *90*, 7213-7222.
- Cavalieri, D.J. (1985): *The Arctic Polynya Experiment: Passive Microwave Satellite Observations, Data Report*, Laboratory for Oceans, Goddard Space Flight Center, NASA, Greenbelt, MD, 84 pp.
- Macklin, S.A., C.H. Pease, and R.M. Reynolds (1984): *Bering Air-Sea-Ice Study (BASICS) - February and March 1981*, NOAA Technical Memorandum ERL PMEL-52, NTIS PB84-196161, 104 pp.
- Macklin, S.A., R.L. Brown, J. Gray, R.W. Lindsay (1984): *METLIB-II - A Program Library for Calculating and Plotting Atmospheric and Oceanic Fields*, NOAA Technical Memorandum ERL PMEL-54, NTIS PB84-205434, 53 pp.
- McNutt, L. (1981): *Ice Conditions in the Eastern Bering Sea from NOAA and LANDSAT Imagery: Winter Conditions 1974, 1976, 1977, 1979*, NOAA Technical Memorandum ERL PMEL-24, NTIS PB81-220188, 179 pp.
- Muench, R.D. and K. Ahlnäs (1976): Ice movement and distribution in the Bering Sea from March to June 1974, *J. Geophys. Res.*, *81*, 4467-4476.
- Muench, R.D. and J.D. Schumacher (1985): The Bering Sea ice edge front, *J. Geophys. Res.*, *90*, 3185-3197.
- Overland, J.E., R.A. Brown, and C.D. Mobley (1980): *METLIB - A Program Library for Calculating and Plotting Marine Boundary Layer Wind Fields*, NOAA Technical Memorandum ERL PMEL-20, NTIS PB81-141038, 82 pp.
- Overland, J.E., and C.H. Pease (1982): Cyclone climatology of the Bering Sea and its relation to sea ice extent, *Mon. Weather Rev.*, *110*, 5-13.
- Pease, C.H. (1980): Eastern Bering Sea ice processes, *Mon. Weather Rev.*, *108*, 2015-2023.
- Pease, C.H., and S.A. Salo (1981): *Drift Characteristics of Northeastern Bering Sea Ice during 1980*, NOAA Technical Memorandum ERL PMEL-32, NTIS PB83-112466, 78 pp.
- Pease, C.H., S.A. Salo, and J.E. Overland (1983): Drag measurements for first-year sea ice over a shallow sea, *J. Geophys. Res.*, *88*, 2853-2862.
- Reynolds, M. (1983): A simple meteorological buoy with satellite telemetry, *Ocean Engineering*, *10*, 65-76.
- Reynolds, M., and C.H. Pease (1984): *Drift Characteristics of Northeastern Bering Sea Ice during 1982*, NOAA Technical Memorandum ERL PMEL-55, NTIS PB84-213982, 135 pp.

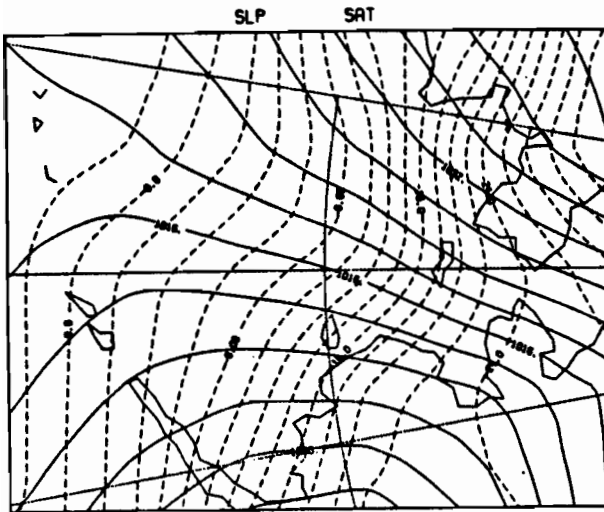
- Reynolds, M., C.H. Pease, and J.E. Overland (1985): Ice drift and regional meteorology in the southern Bering Sea: Results from MIZEX West, *J. Geophys. Res.*, 90, (in press).
- Salo, S.A., C.H. Pease, and R.W. Lindsay (1980): *Physical Environment of the Eastern Bering Sea March 1979*, NOAA Technical Memorandum ERL PMEL-21, NTIS PB81-148496, 119 pp.
- Salo, S.A., J.D. Schumacher, and L.K. Coachman (1983): *Winter Currents on the Eastern Bering Sea Shelf*, NOAA Technical Memorandum ERL PMEL-45, NTIS PB83-248823, 53 pp.
- Schumacher, J.D., K. Aagaard, C.H. Pease, and R.B. Tripp (1983): Effects of a shelf polynya on flow and water properties in the northern Bering Sea, *J. Geophys. Res.*, 88, 2723-2732.
- Thomas, D.R., and R.S. Pritchard (1981): *Norton Sound and Bering Sea Ice Motion: 1981*, Flow Research Report No. 209, Flow Industries, Kent, WA, 37 pp.
- World Meteorological Organization (1983): *Guide to Data Collection and Location Services using ARGOS, Marine Meteorology and Related Oceanographic Activities Report No. 10*, WMO, Geneva, 47 pp. + appendices.

Appendix A. METLIB Meteorological Data

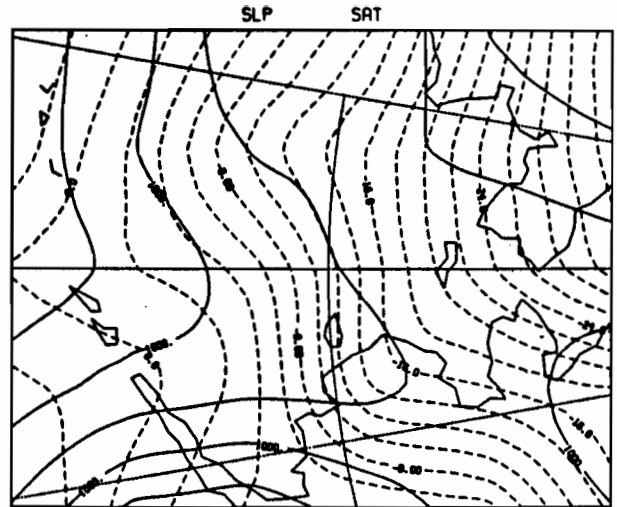
- Surface Air Temperature and Sea-level Pressure Fields.

The surface air temperature (SAT) was analyzed using late station reports and then hand-digitized onto a grid compatible with the NWS National Meteorological Center's Primitive Equation grid. The sea-level pressure (SLP) was reanalyzed for late data from the NWS Alaska Region's analysis and also hand digitized onto the same grid. A program library for interpolating and plotting marine meteorological variables called METLIB (Overland *et al.*, 1980; Macklin *et al.*, 1984) was used to interpolate the fields to one-quarter mesh, contour, and plot the fields.

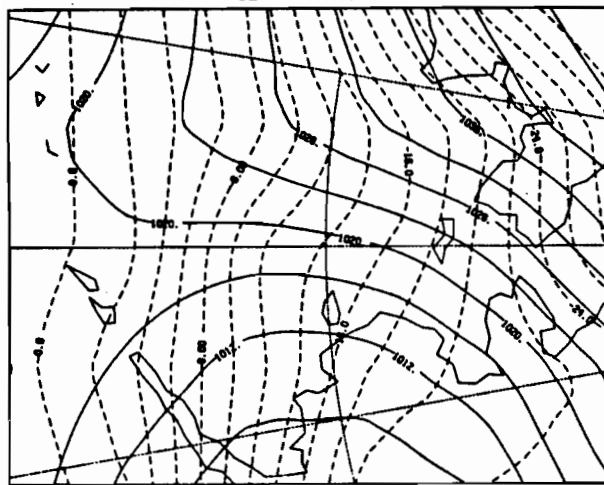
The following scalar plots represent the approximate pressure and temperature conditions for 00 GMT and 12 GMT from 00 GMT 15 February 1985 through 12 GMT 15 April 1985. Note that true north is toward the right, temperature is given in degrees centigrade and pressure is given in mb.



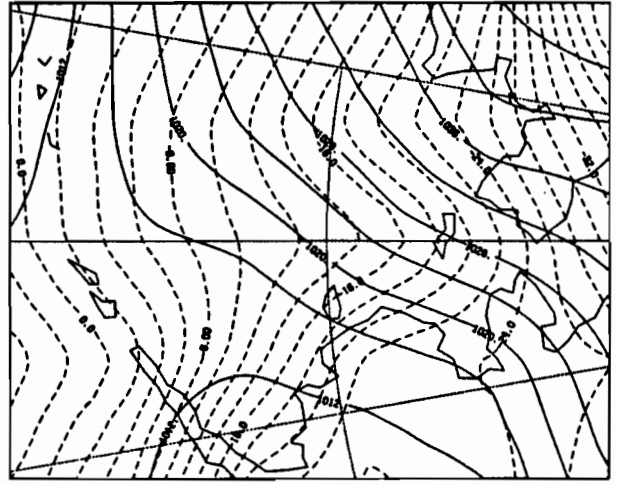
00Z 15 FEB 1985
1985-BERING SEA
SLP SAT



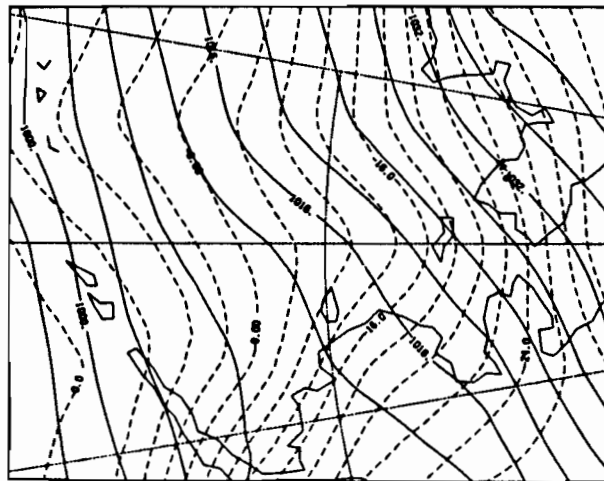
12Z 15 FEB 1985
1985-BERING SEA



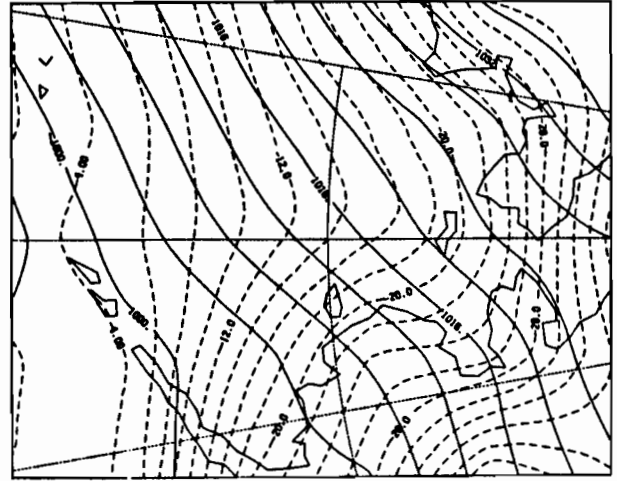
00Z 16 FEB 1985
1985-BERING SEA



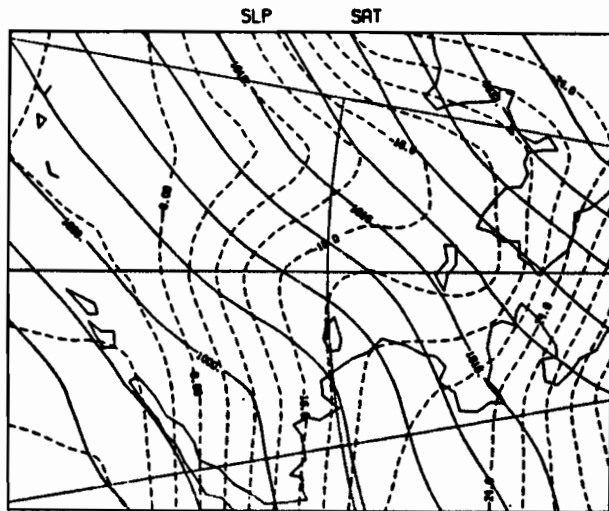
12Z 16 FEB 1985
1985-BERING SEA



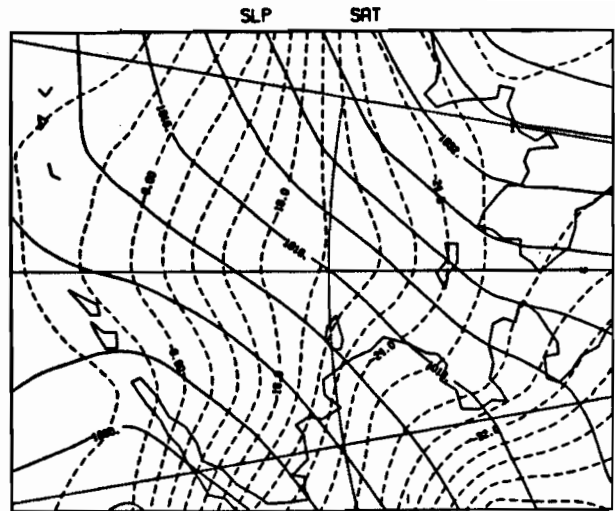
00Z 17 FEB 1985
1985-BERING SEA



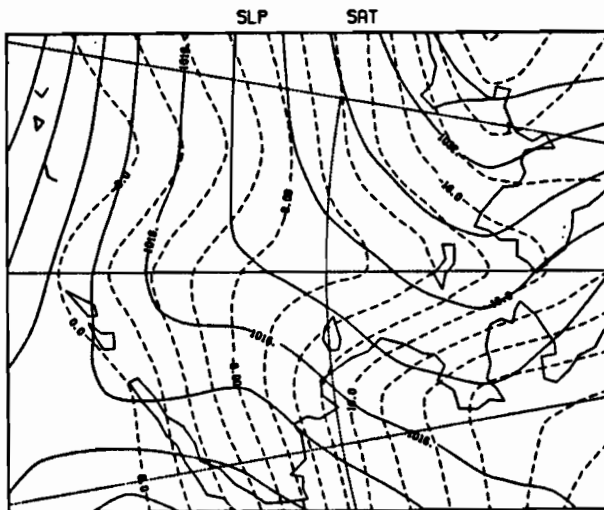
12Z 17 FEB 1985
1985-BERING SEA



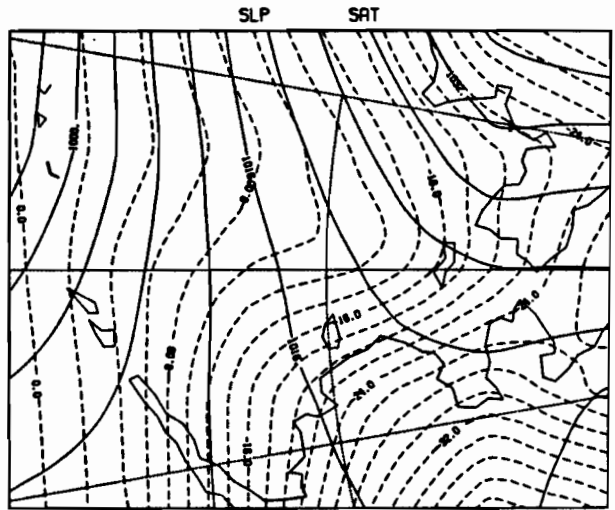
00Z 18 FEB 1985
1985-BERING SEA



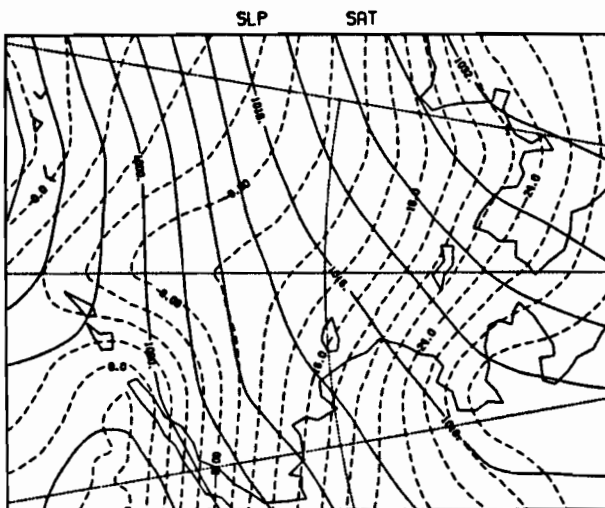
12Z 18 FEB 1985
1985-BERING SEA



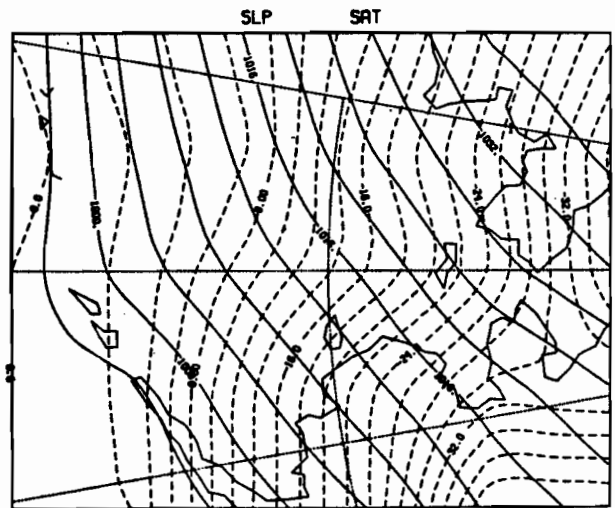
00Z 19 FEB 1985
1985-BERING SEA



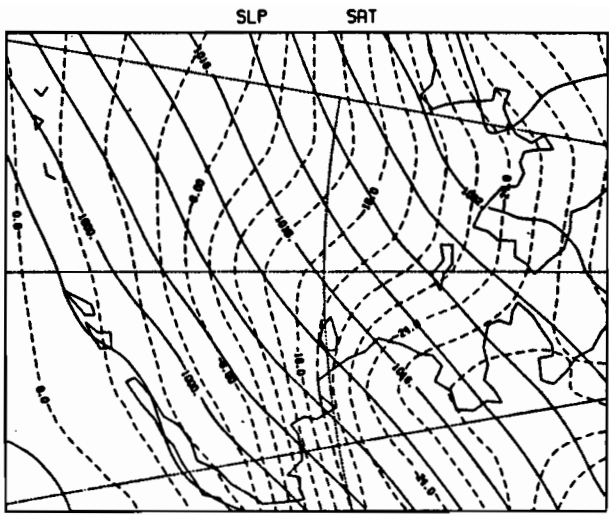
12Z 19 FEB 1985
1985-BERING SEA



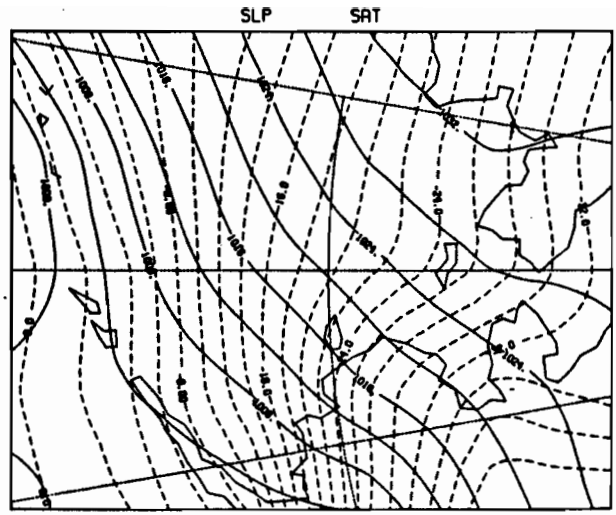
00Z 20 FEB 1985
1985-BERING SEA



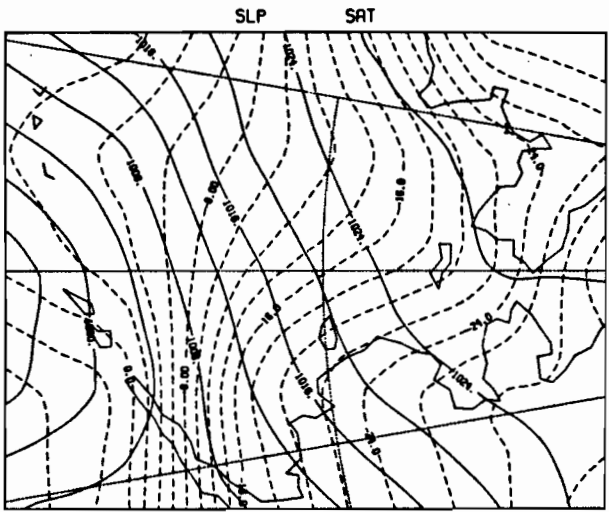
12Z 20 FEB 1985
1985-BERING SEA



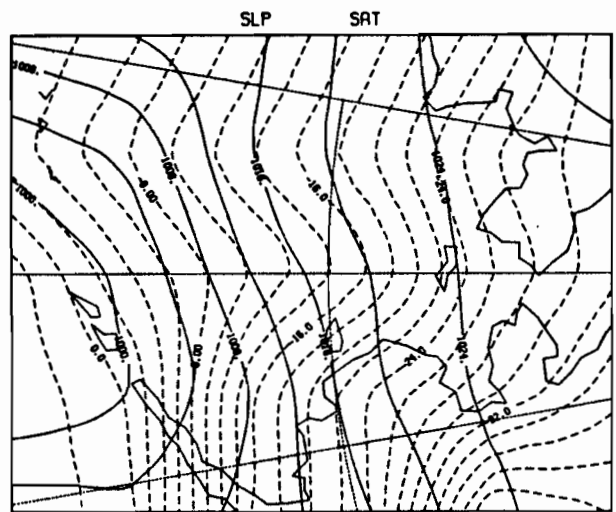
00Z 21 FEB 1985
1985-BERING SEA



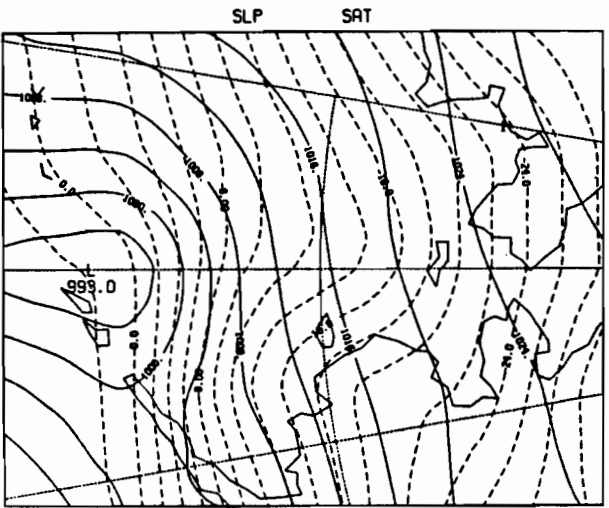
12Z 21 FEB 1985
1985-BERING SEA



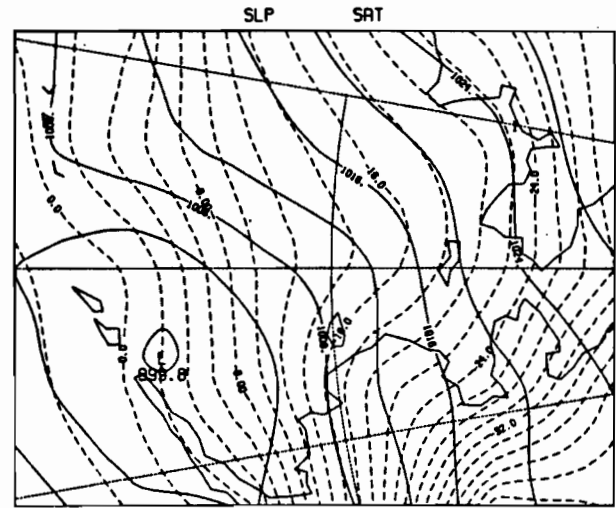
00Z 22 FEB 1985
1985-BERING SEA



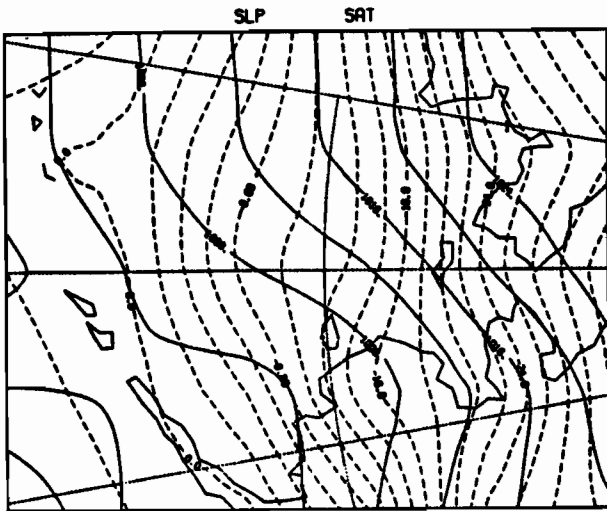
12Z 22 FEB 1985
1985-BERING SEA



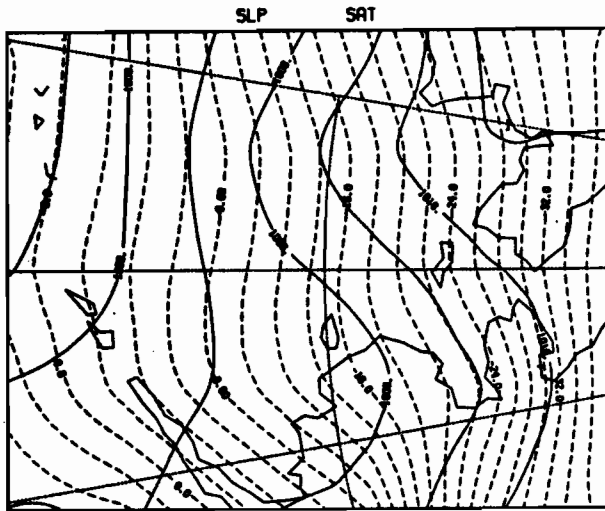
00Z 23 FEB 1985
1985-BERING SEA



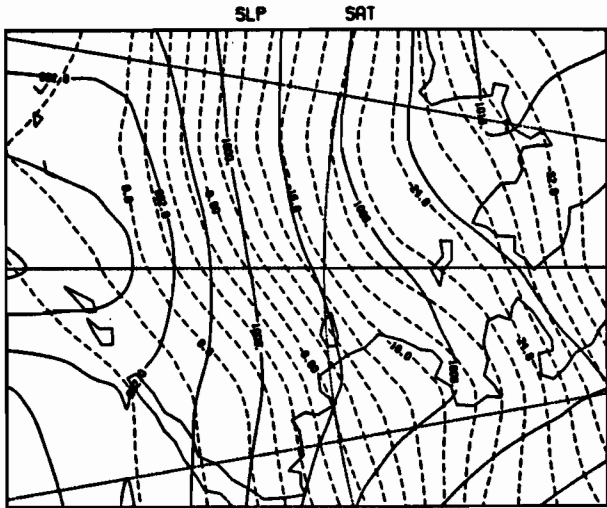
12Z 23 FEB 1985
1985-BERING SEA



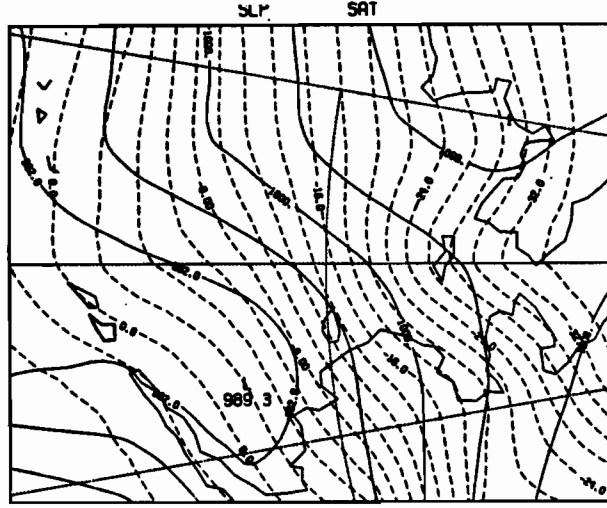
00Z 24 FEB 1985
1985-BERING SEA



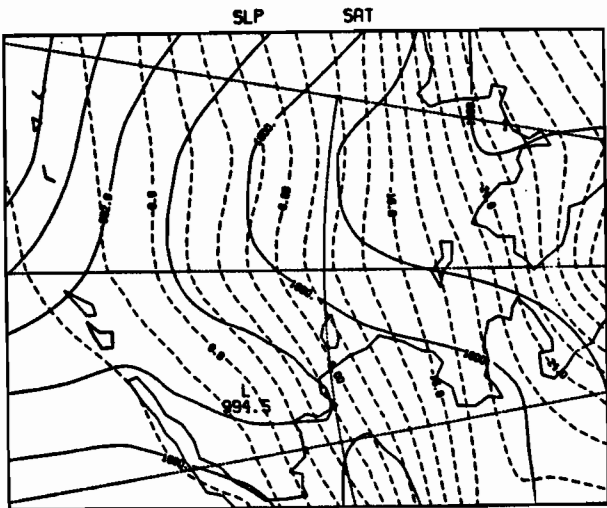
12Z 24 FEB 1985
1985-BERING SEA



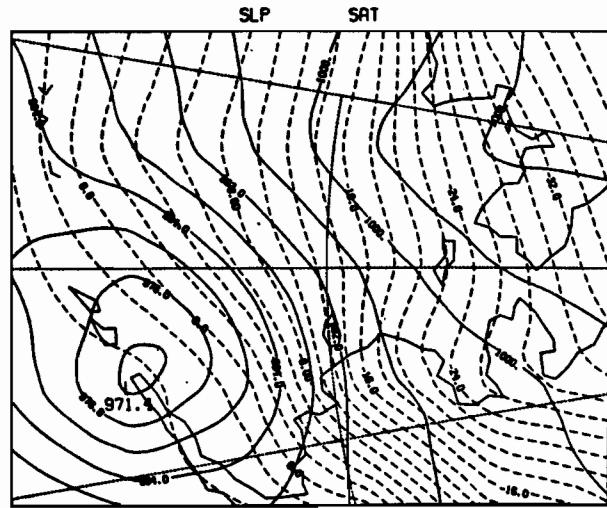
00Z 25 FEB 1985
1985-BERING SEA



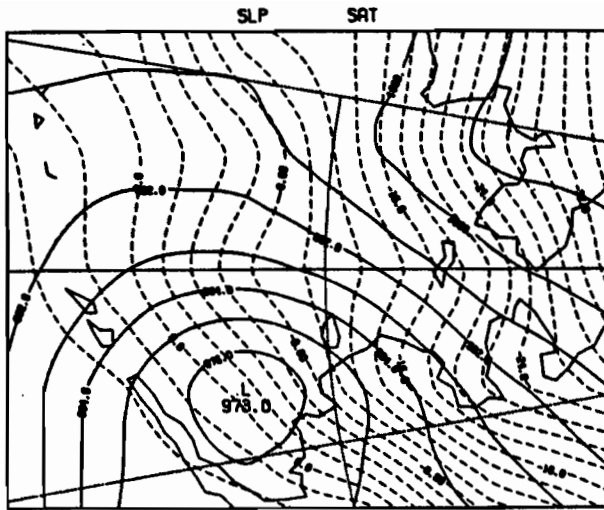
12Z 25 FEB 1985
1985-BERING SEA



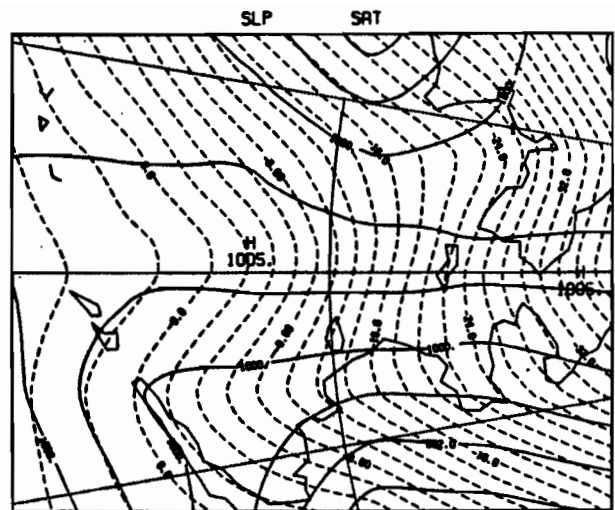
00Z 26 FEB 1985
1985-BERING SEA



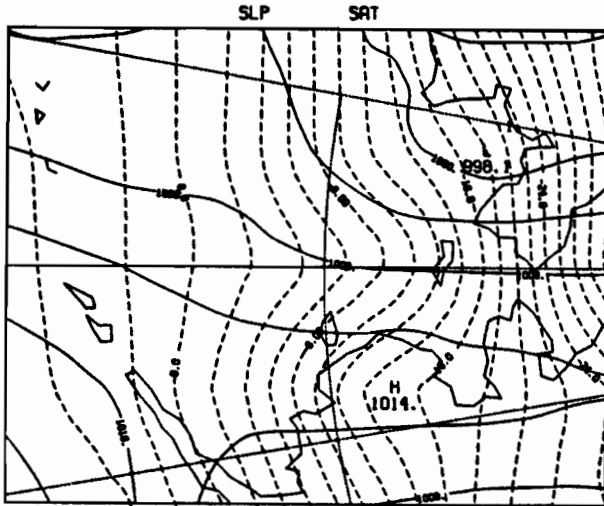
12Z 26 FEB 1985
1985-BERING SEA



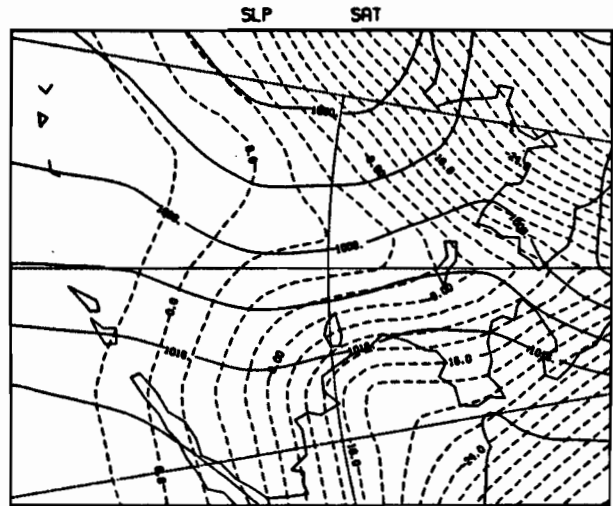
00Z 27 FEB 1985
1985-BERING SEA



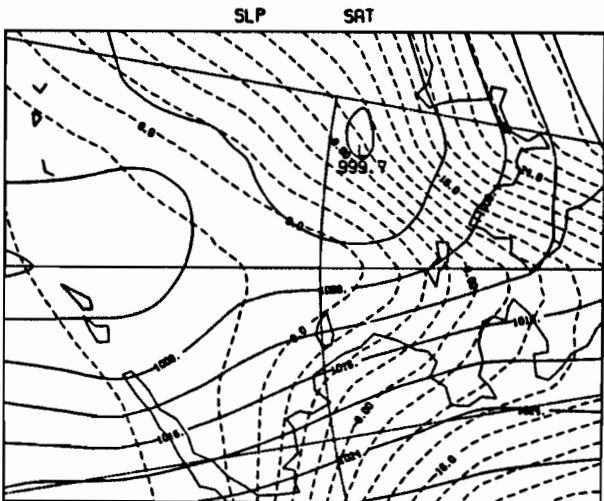
12Z 27 FEB 1985
1985-BERING SEA



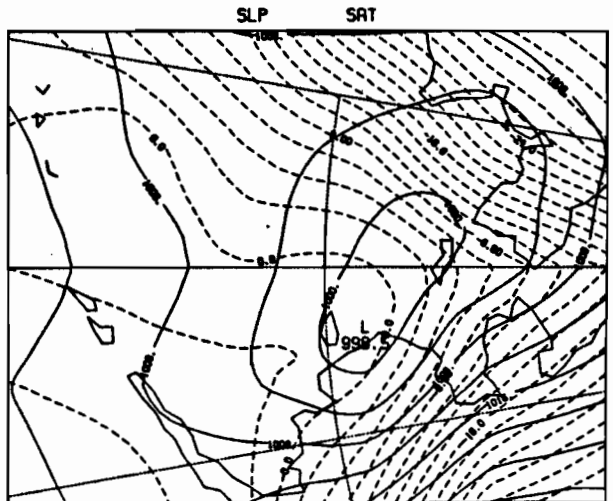
00Z 28 FEB 1985
1985-BERING SEA



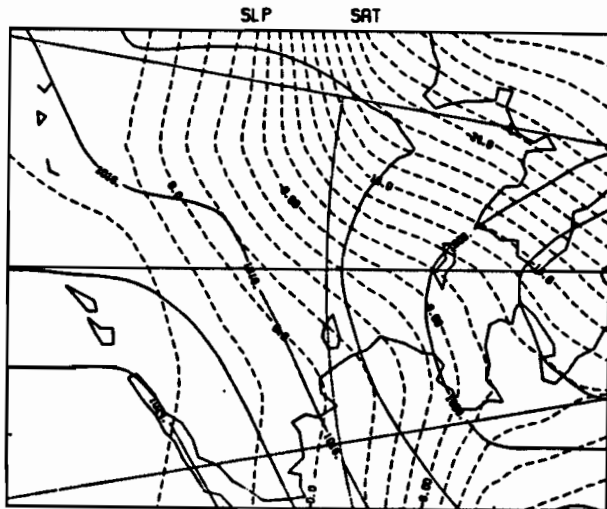
12Z 28 FEB 1985
1985-BERING SEA



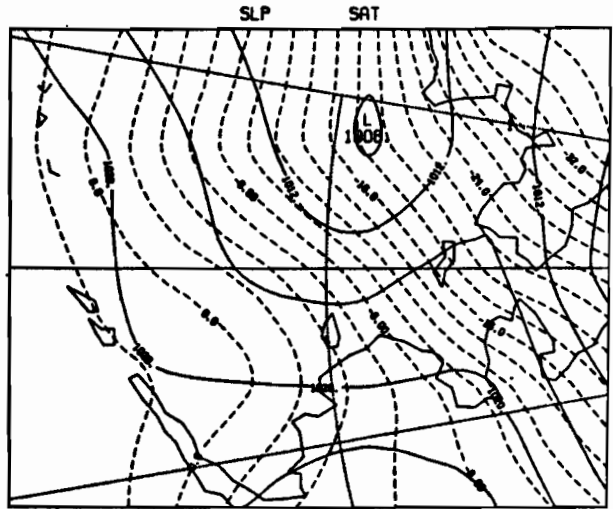
00Z 1 MAR 1985
1985-BERING SEA



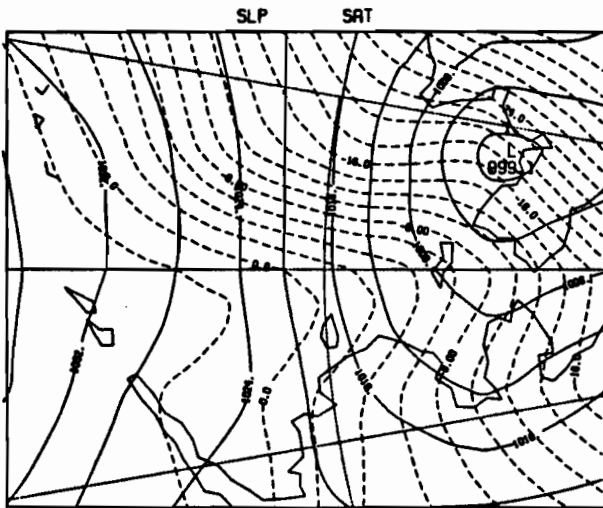
12Z 1 MAR 1985
1985-BERING SEA



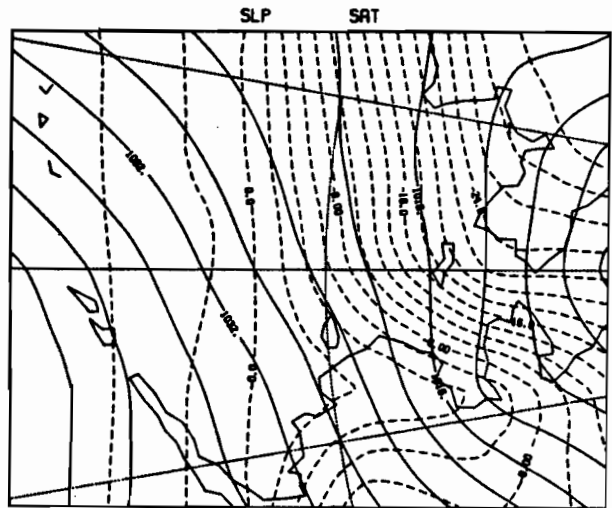
00Z 2 MAR 1985
1985-BERING SEA



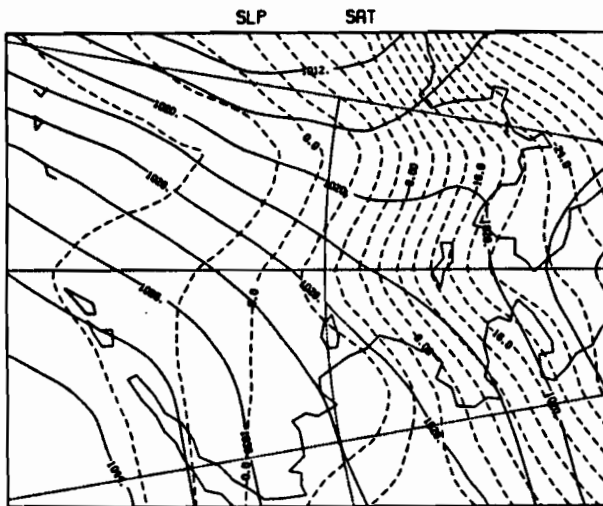
12Z 2 MAR 1985
1985-BERING SEA



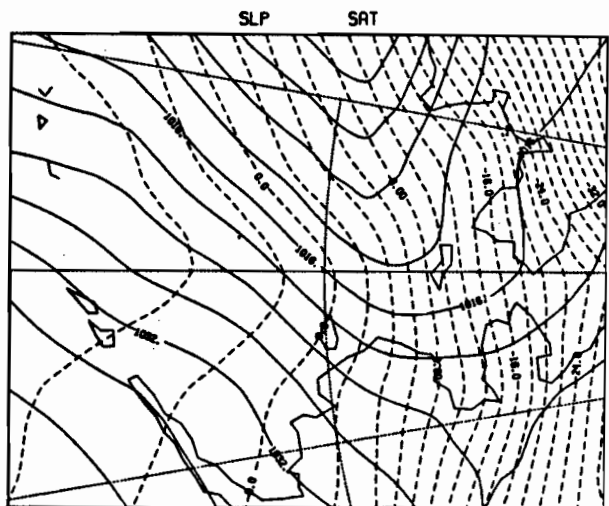
00Z 3 MAR 1985
1985-BERING SEA



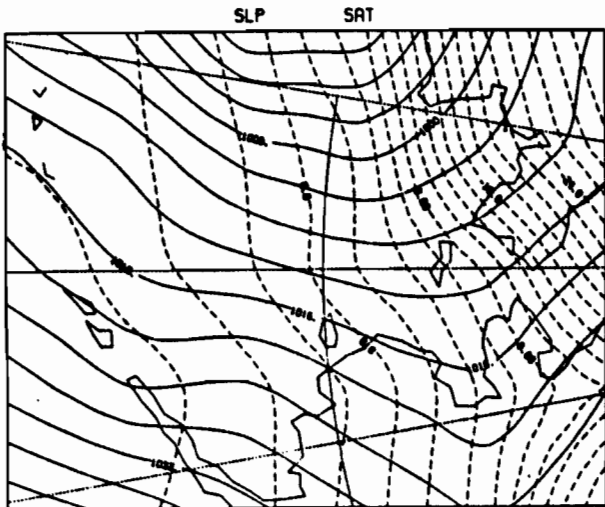
12Z 3 MAR 1985
1985-BERING SEA



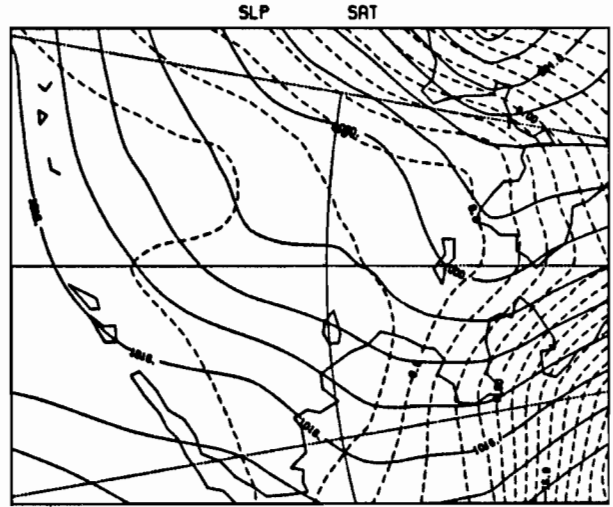
00Z 4 MAR 1985
1985-BERING SEA



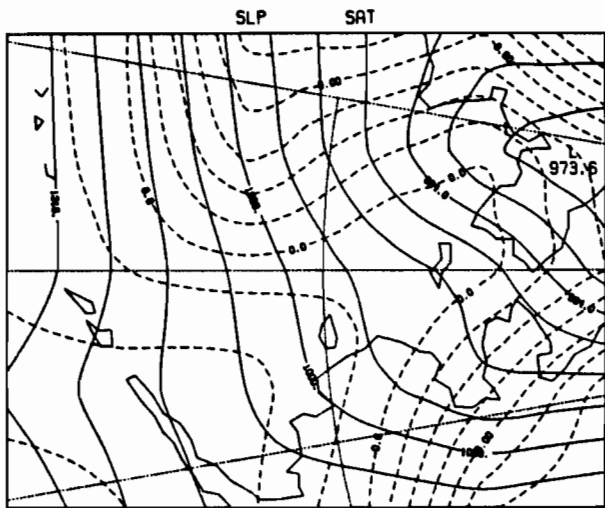
12Z 4 MAR 1985
1985-BERING SEA



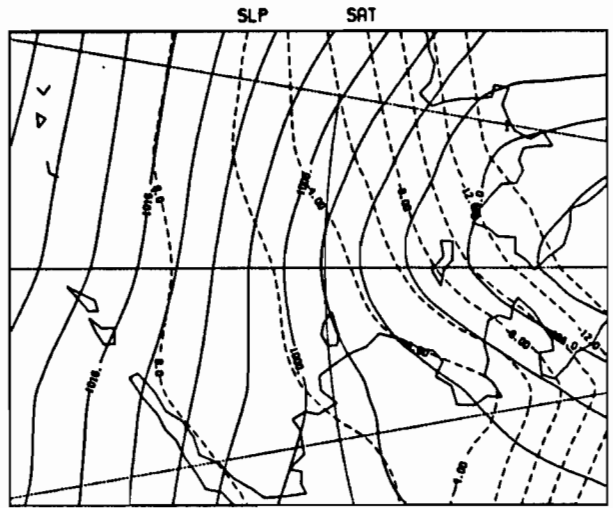
00Z 5 MAR 1985
1985-BERING SEA



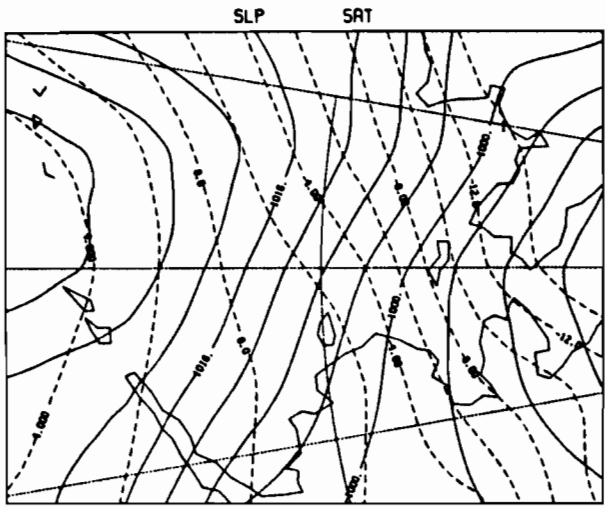
12Z 5 MAR 1985
1985-BERING SEA



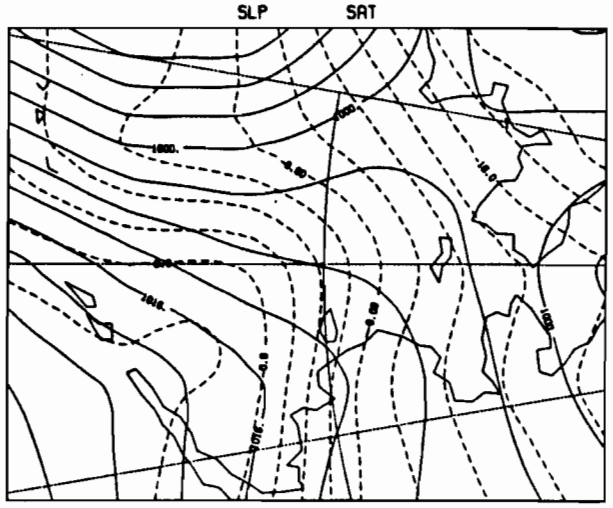
00Z 6 MAR 1985
1985-BERING SEA



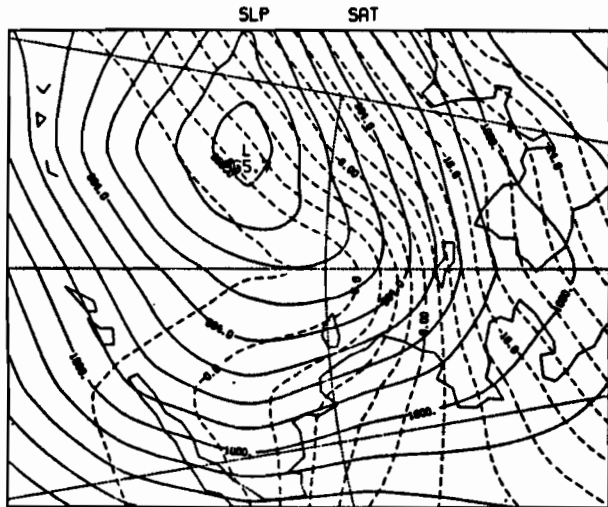
12Z 6 MAR 1985
1985-BERING SEA



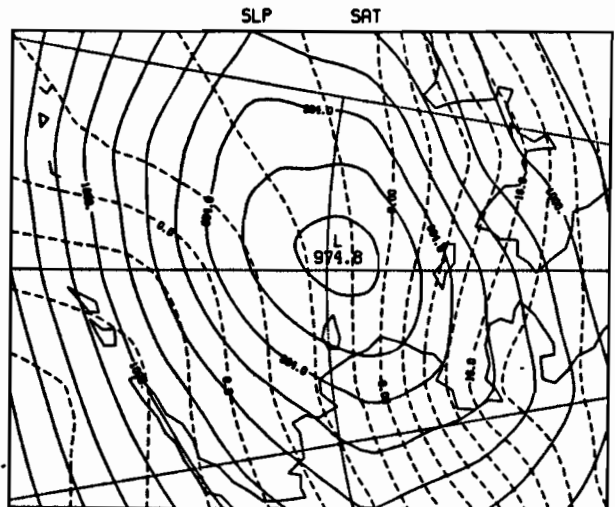
00Z 7 MAR 1985
1985-BERING SEA



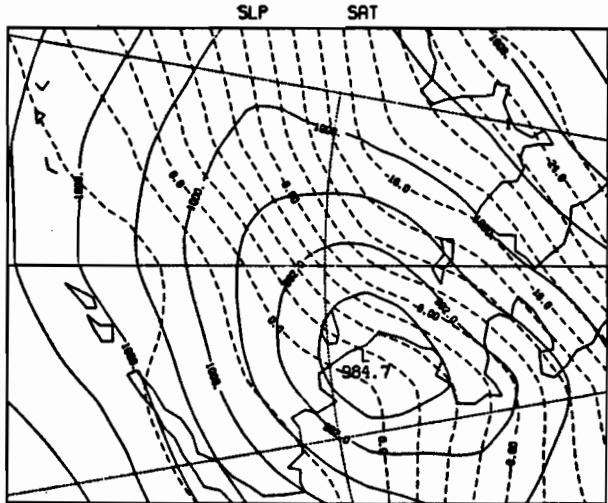
12Z 7 MAR 1985
1985-BERING SEA



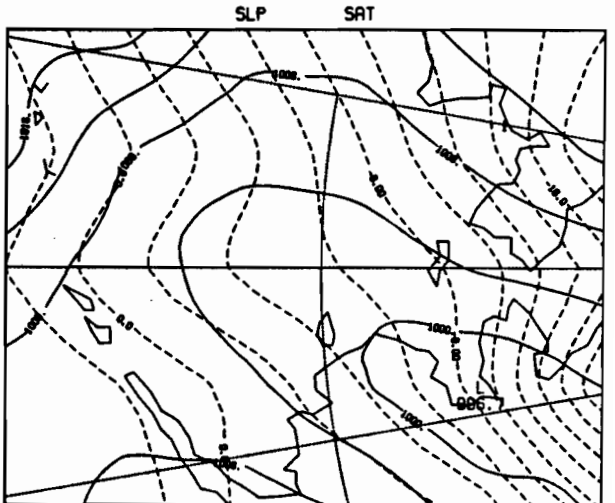
00Z 8 MAR 1985
1985-BERING SEA



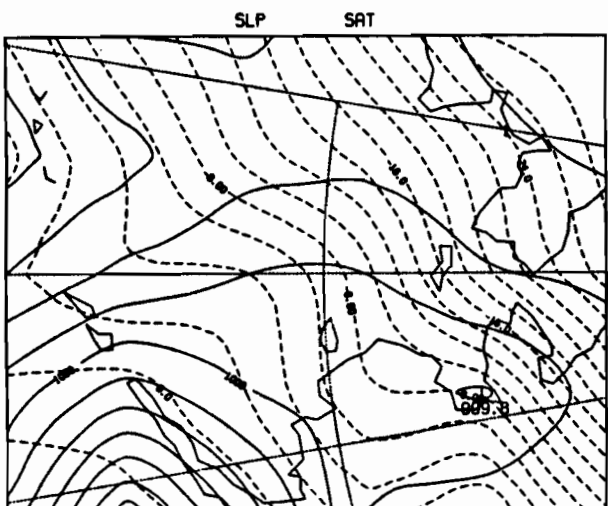
12Z 8 MAR 1985
1985-BERING SEA



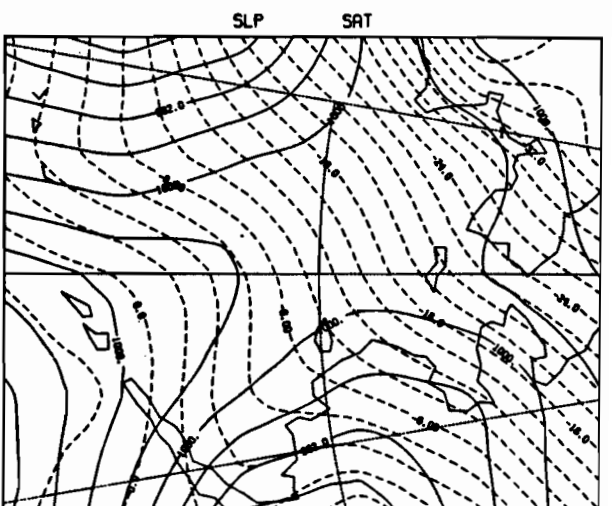
00Z 9 MAR 1985
1985-BERING SEA



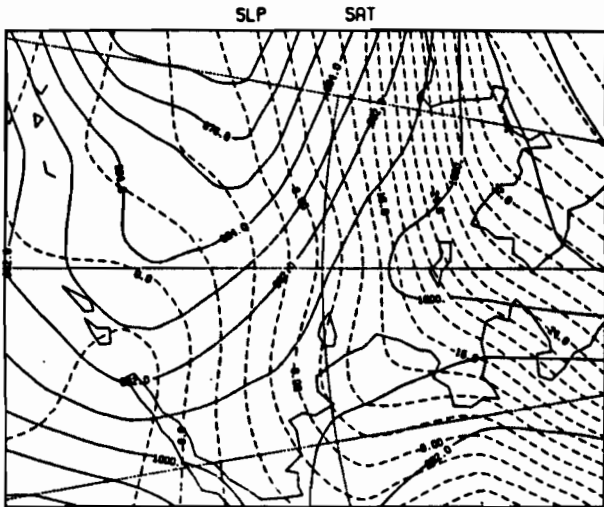
12Z 9 MAR 1985
1985-BERING SEA



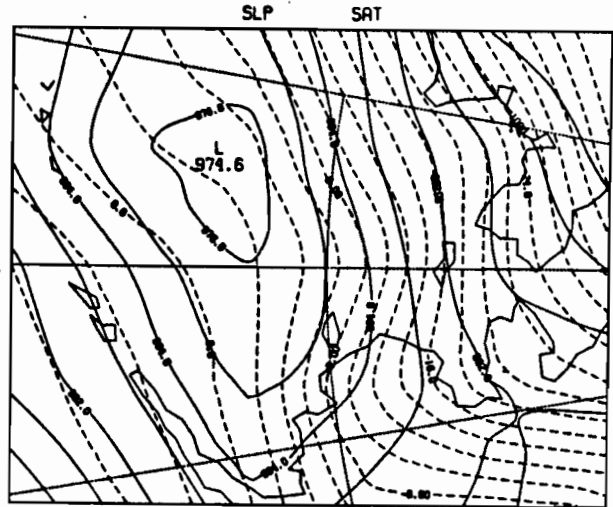
00Z 10 MAR 1985
1985-BERING SEA



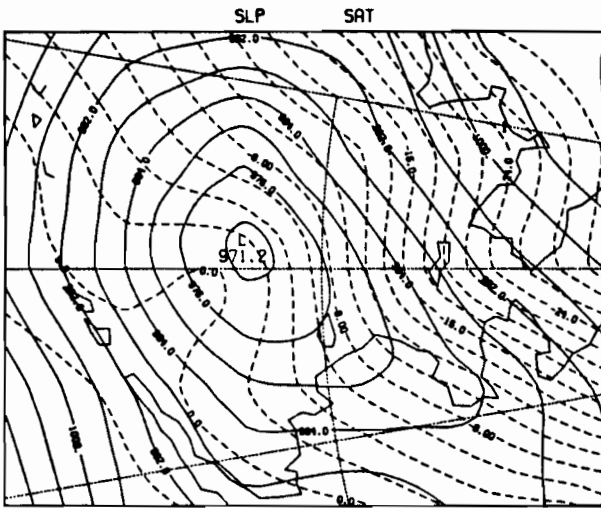
12Z 10 MAR 1985
1985-BERING SEA



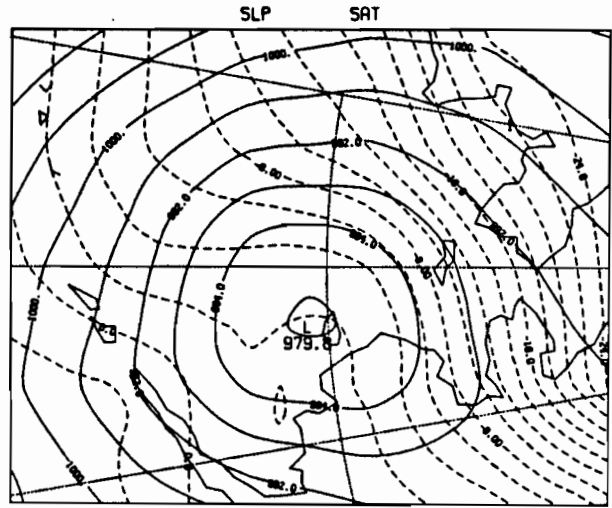
00Z 11 MAR 1985
1985-BERING SEA



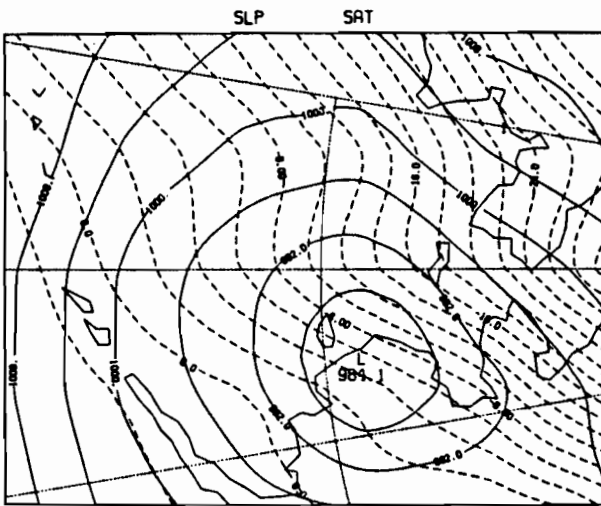
12Z 11 MAR 1985
1985-BERING SEA



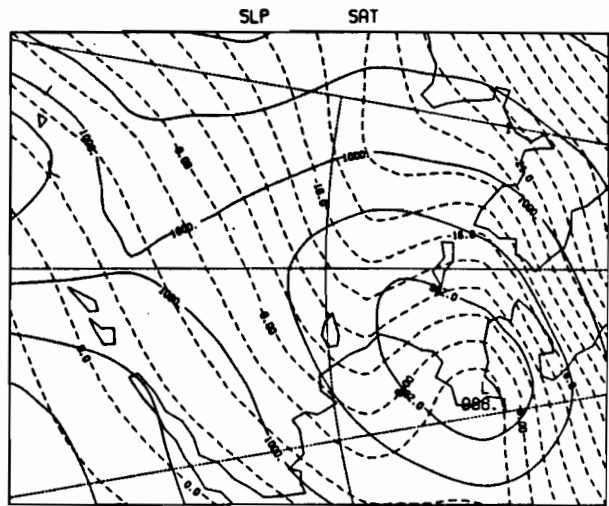
00Z 12 MAR 1985
1985-BERING SEA



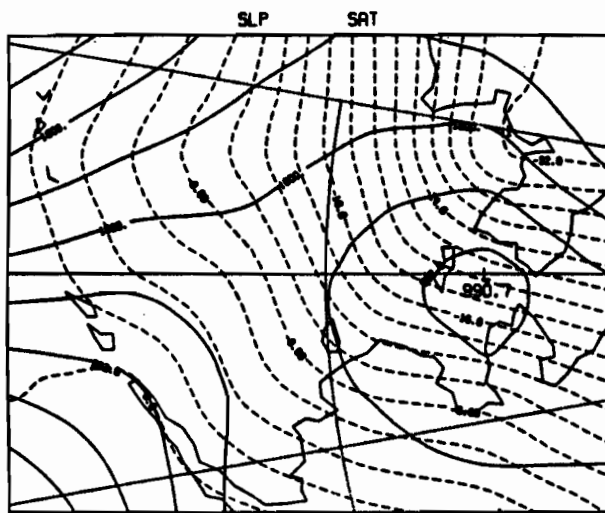
12Z 12 MAR 1985
1985-BERING SEA



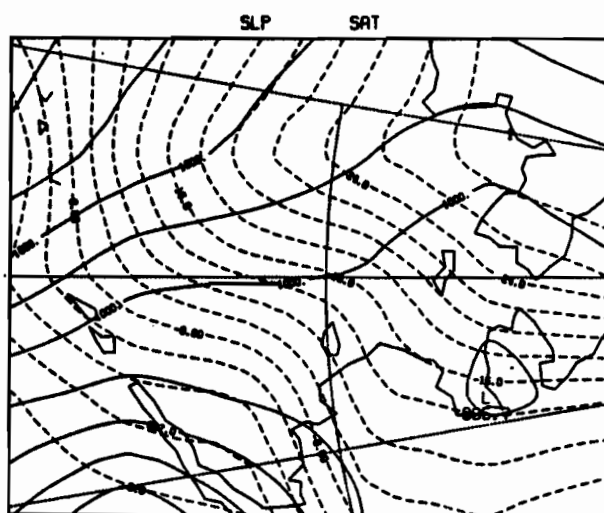
00Z 13 MAR 1985
1985-BERING SEA



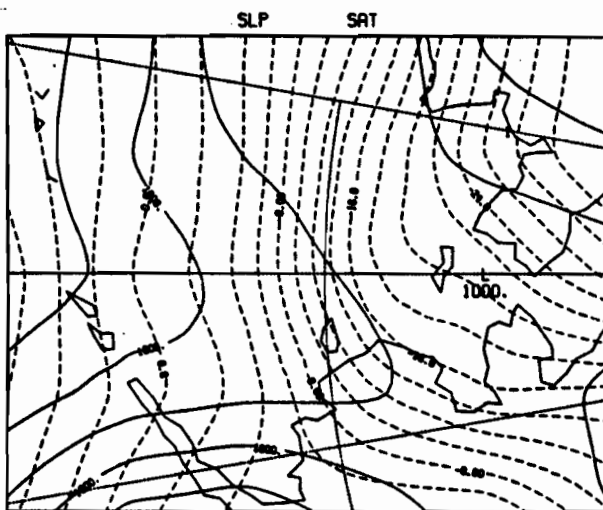
12Z 13 MAR 1985
1985-BERING SEA



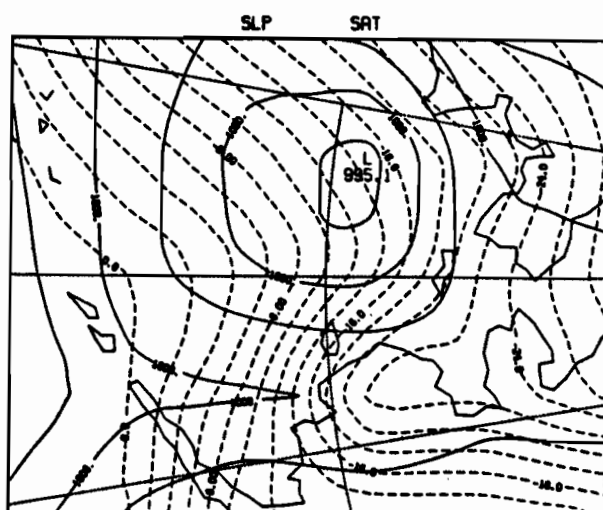
00Z 14 MAR 1985
1985-BERING SEA



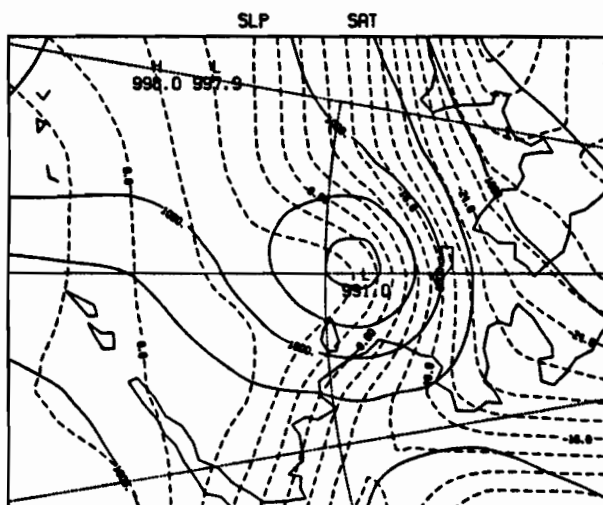
12Z 14 MAR 1985
1985-BERING SEA



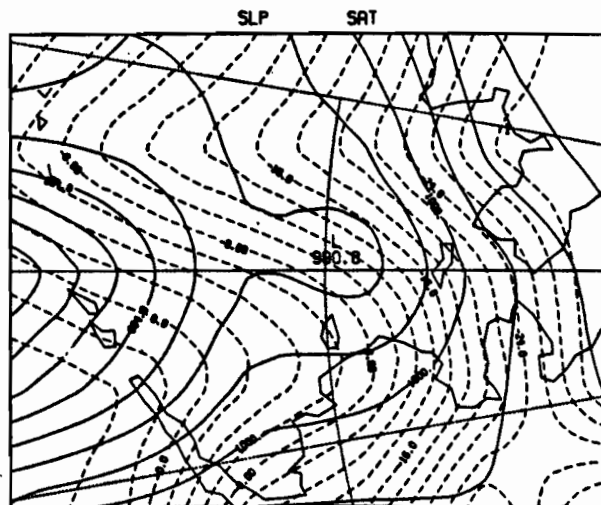
00Z 15 MAR 1985
1985-BERING SEA



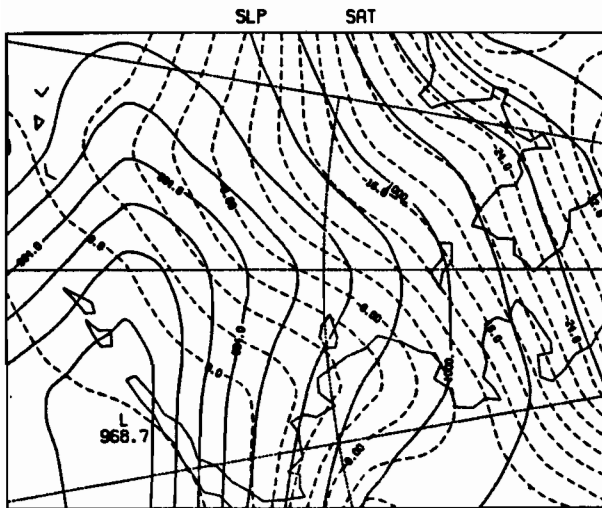
12Z 15 MAR 1985
1985-BERING SEA



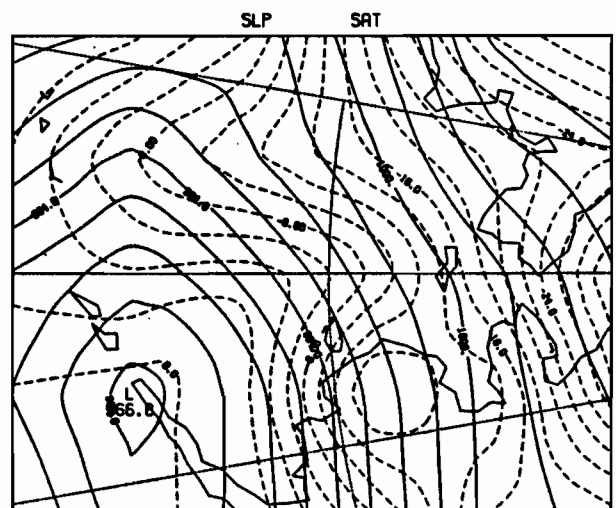
00Z 16 MAR 1985
1985-BERING SEA



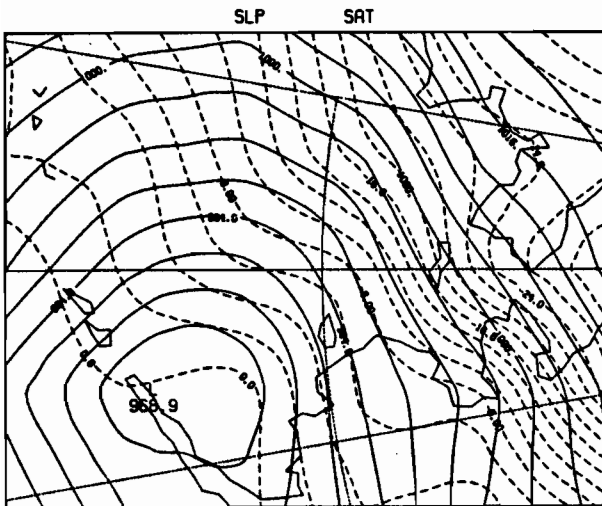
12Z 16 MAR 1985
1985-BERING SEA



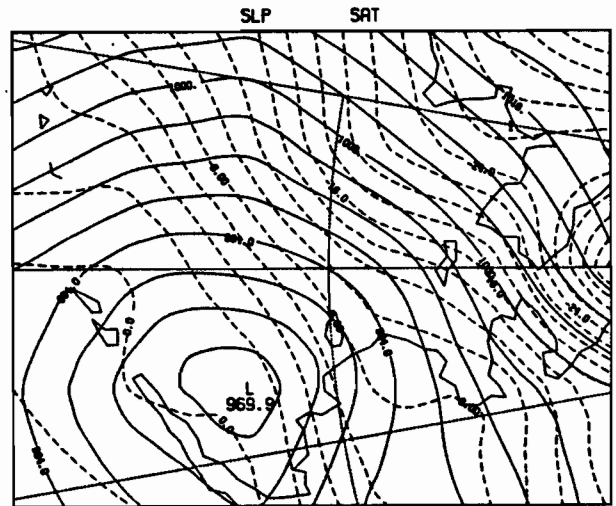
00Z 17 MAR 1985
1985-BERING SEA



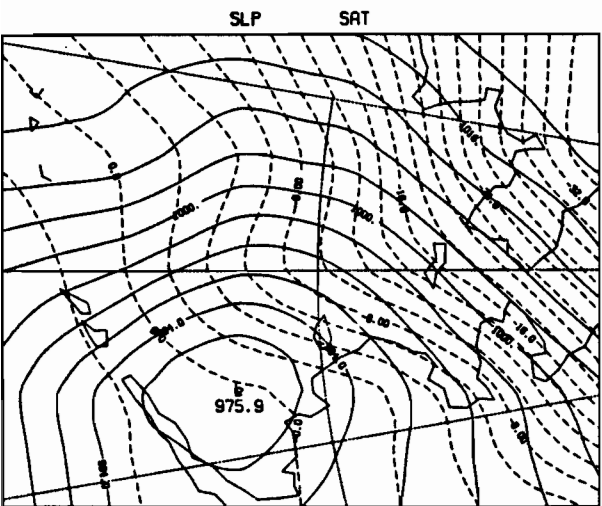
12Z 17 MAR 1985
1985-BERING SEA



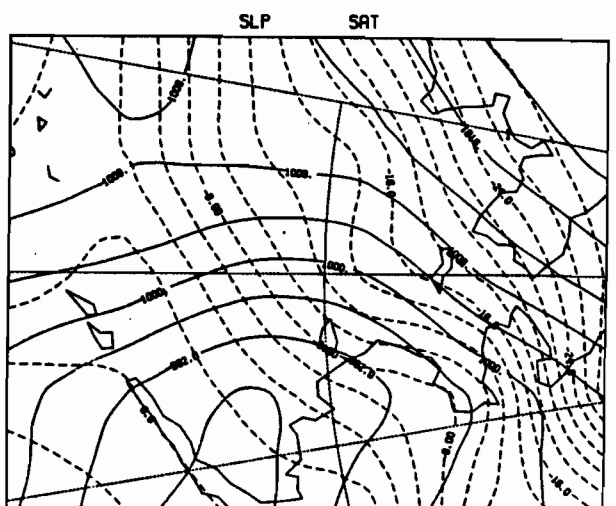
00Z 18 MAR 1985
1985-BERING SEA



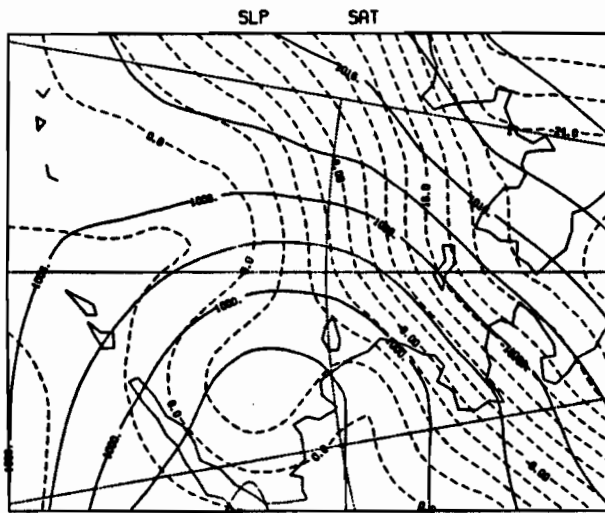
12Z 18 MAR 1985
1985-BERING SEA



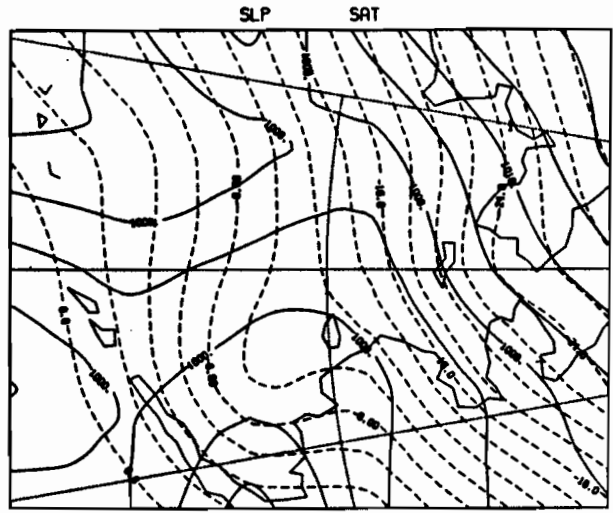
00Z 19 MAR 1985
1985-BERING SEA



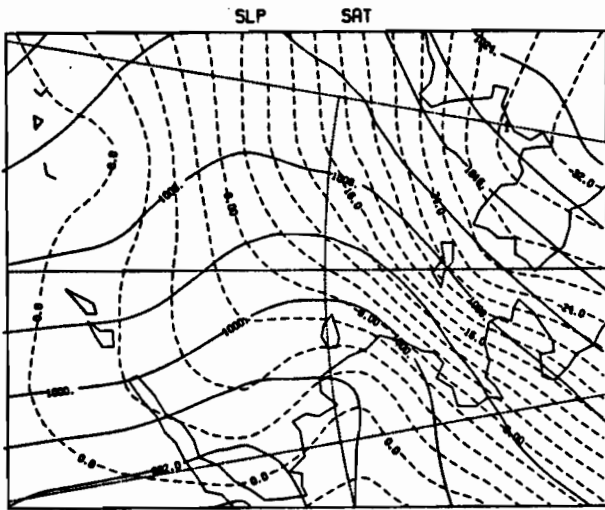
12Z 19 MAR 1985
1985-BERING SEA



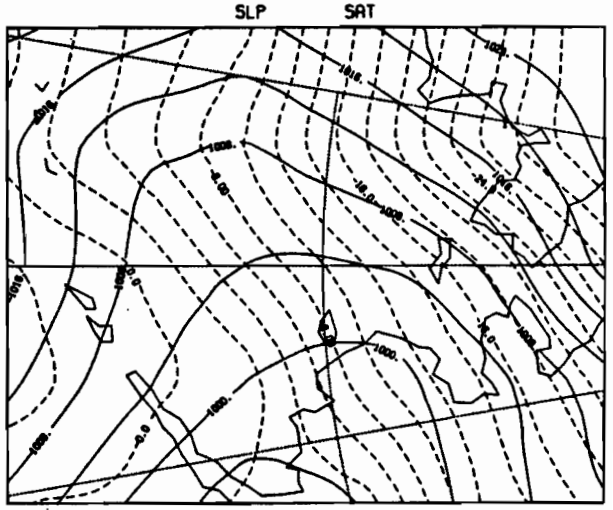
00Z 20 MAR 1985
1985-BERING SEA



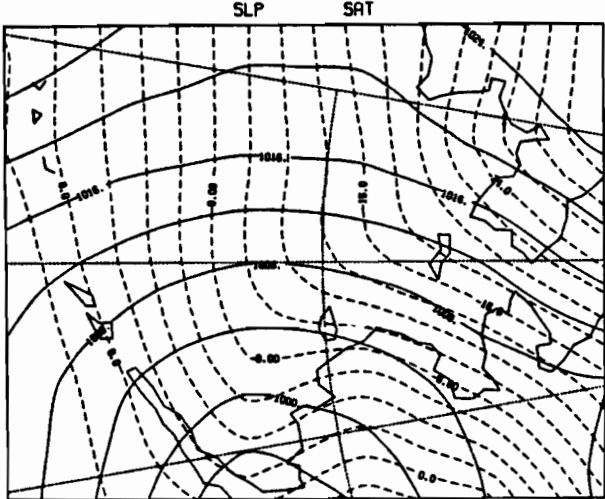
12Z 20 MAR 1985
1985-BERING SEA



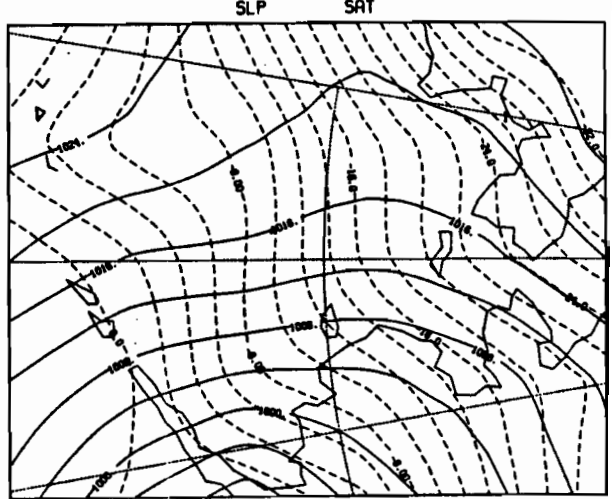
00Z 21 MAR 1985
1985-BERING SEA



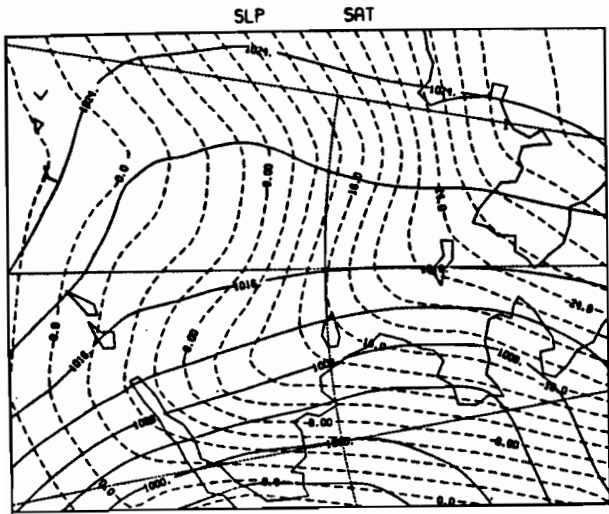
12Z 21 MAR 1985
1985-BERING SEA



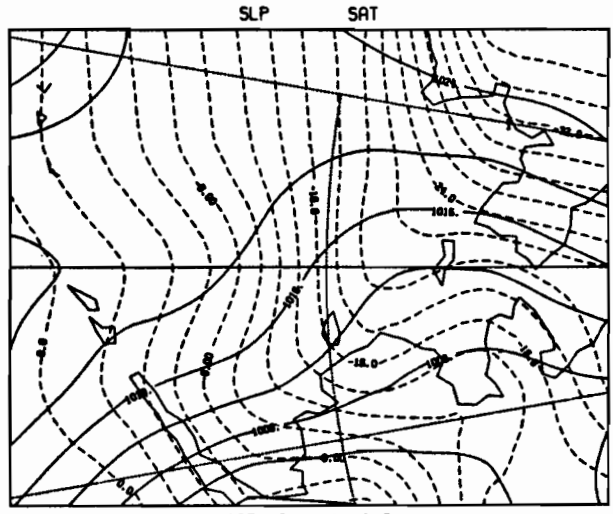
00Z 22 MAR 1985
1985-BERING SEA



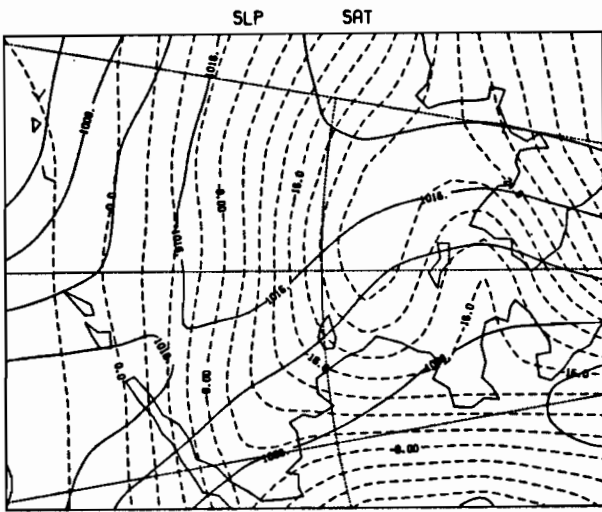
12Z 22 MAR 1985
1985-BERING SEA



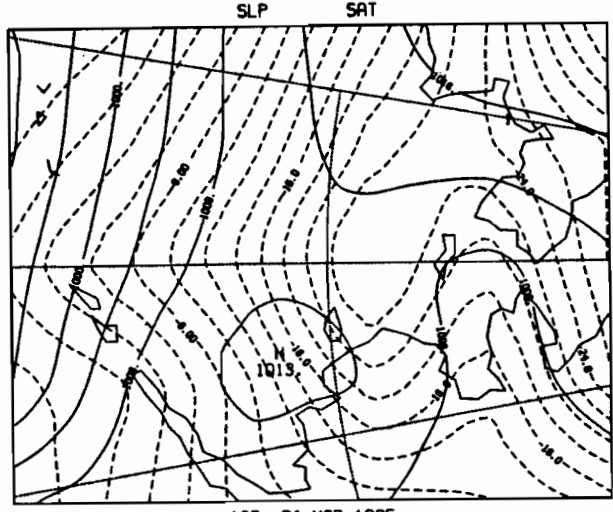
00Z 23 MAR 1985
1985-BERING SEA



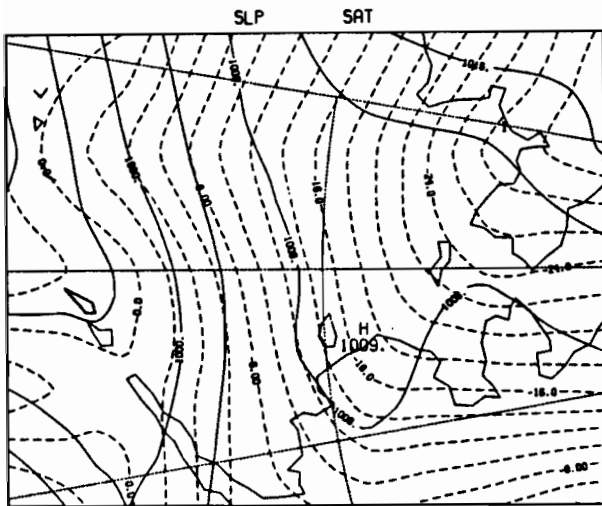
12Z 23 MAR 1985
1985-BERING SEA



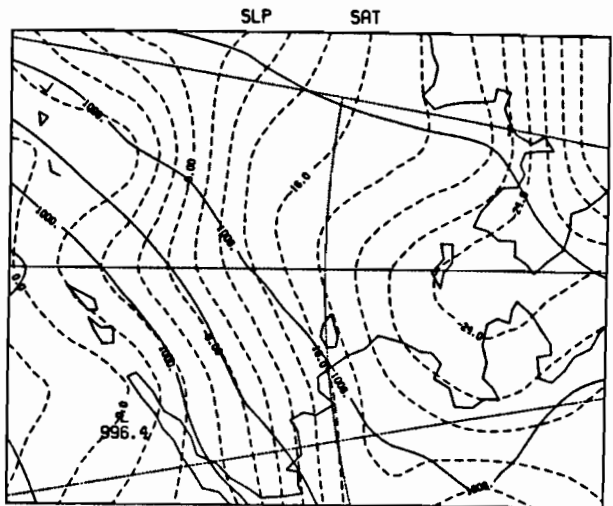
00Z 24 MAR 1985
1985-BERING SEA



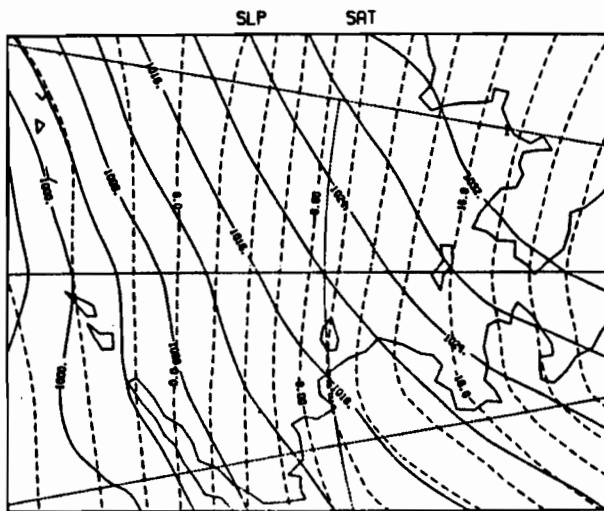
12Z 24 MAR 1985
1985-BERING SEA



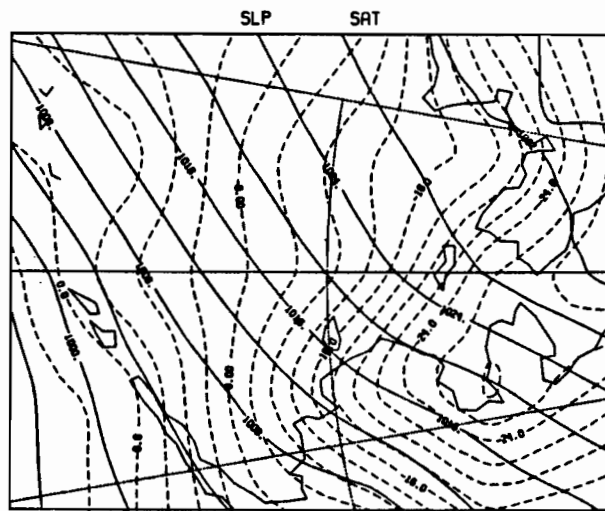
00Z 25 MAR 1985
1985-BERING SEA



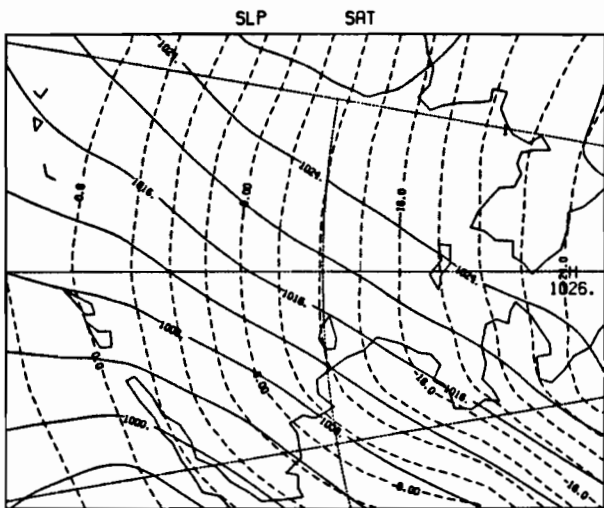
12Z 25 MAR 1985
1985-BERING SEA



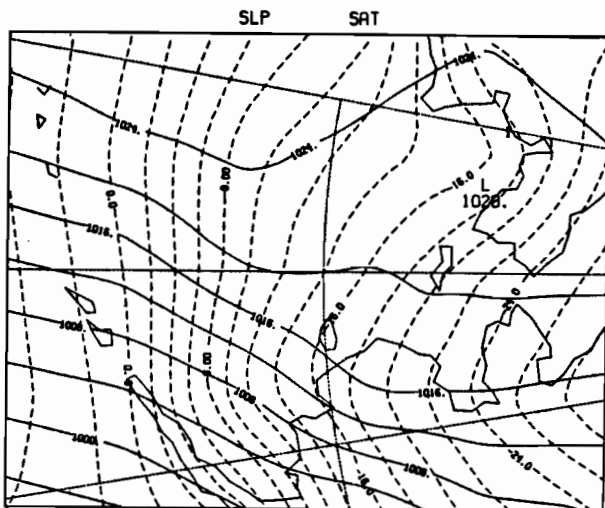
00Z 29 MAR 1985
1985-BERING SEA



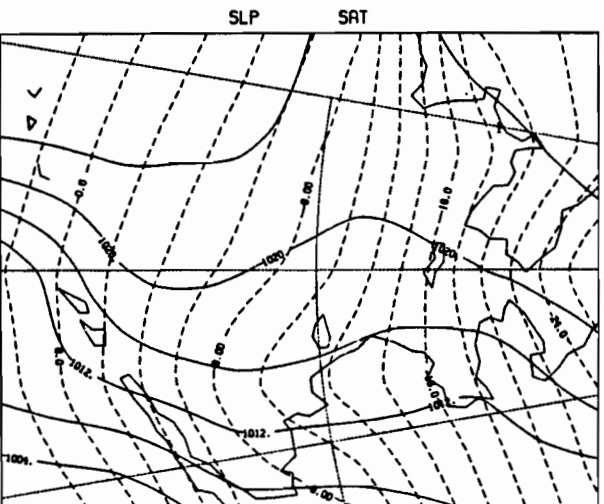
12Z 29 MAR 1985
1985-BERING SEA



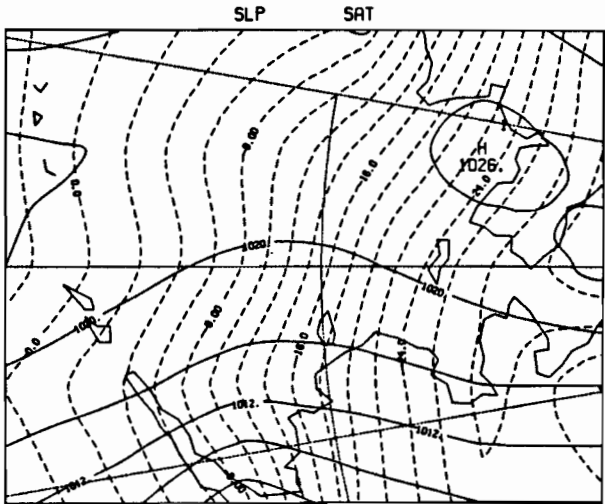
00Z 30 MAR 1985
1985-BERING SEA



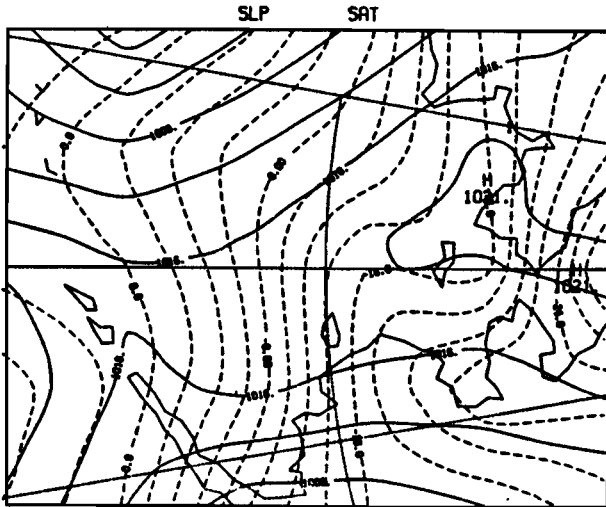
12Z 30 MAR 1985
1985-BERING SEA



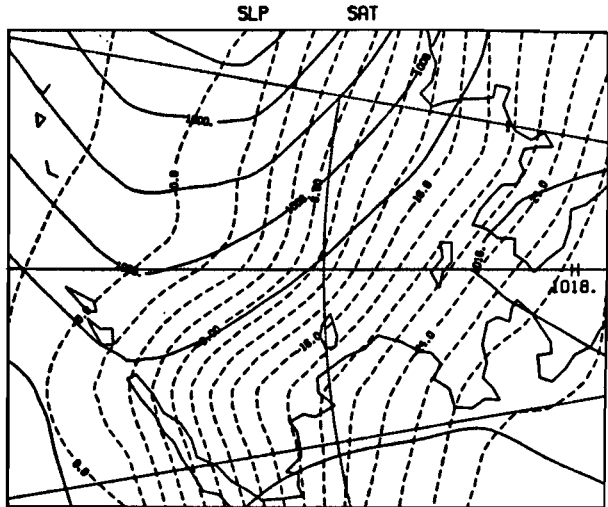
00Z 31 MAR 1985
1985-BERING SEA



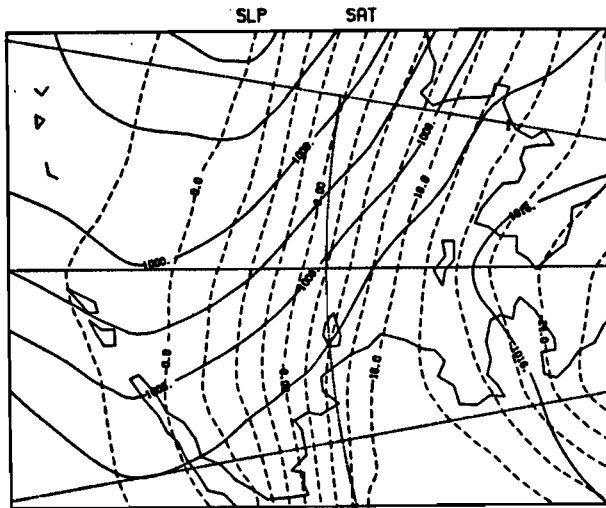
12Z 31 MAR 1985
1985-BERING SEA



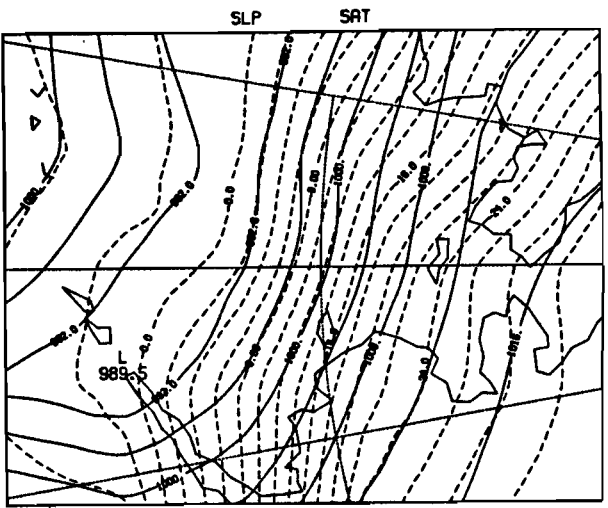
00Z 1 APR 1985
1985-BERING SEA



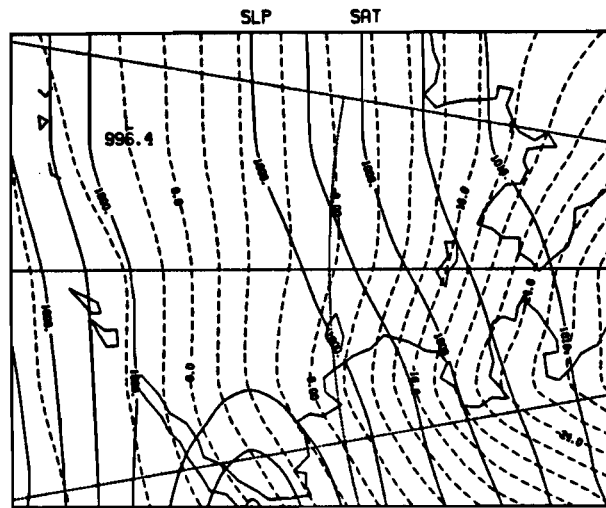
12Z 1 APR 1985
1985-BERING SEA



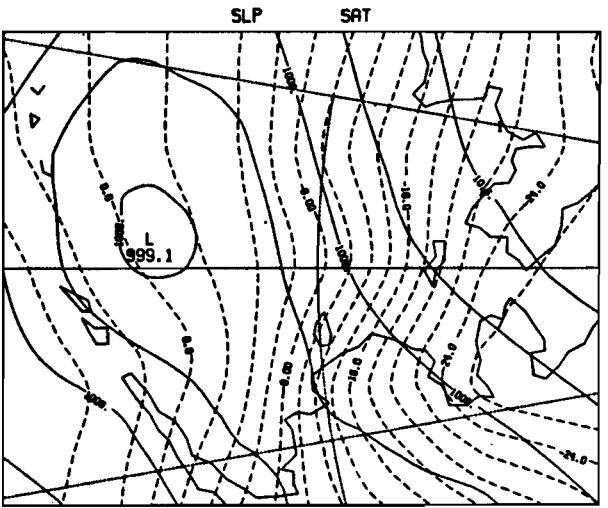
00Z 2 APR 1985
1985-BERING SEA



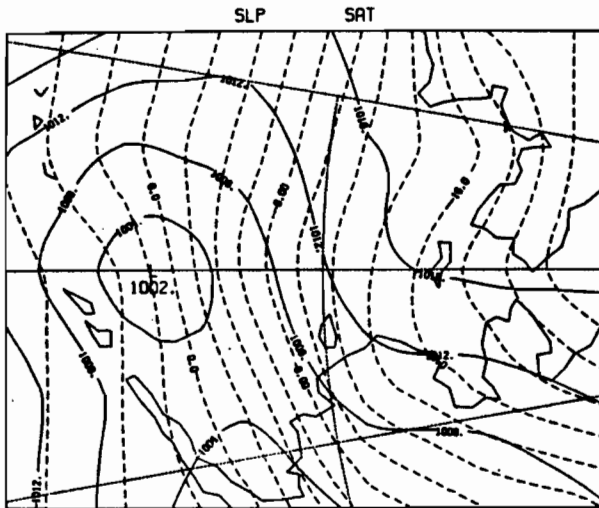
12Z 2 APR 1985
1985-BERING SEA



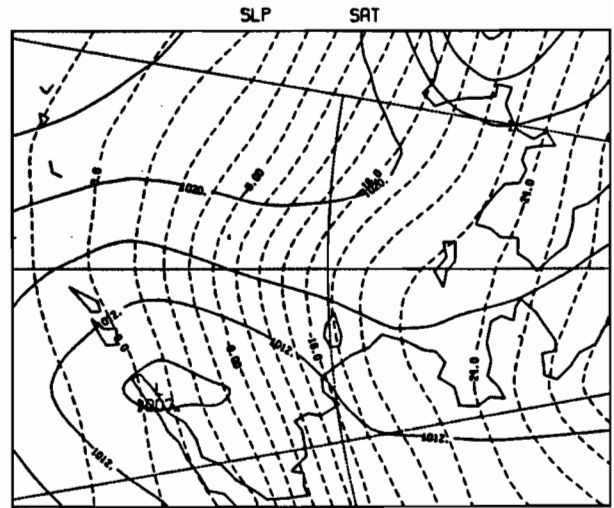
00Z 3 APR 1985
1985-BERING SEA



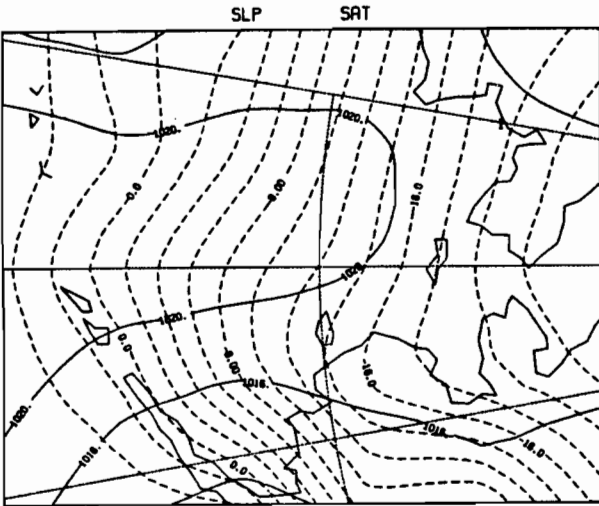
12Z 3 APR 1985
1985-BERING SEA



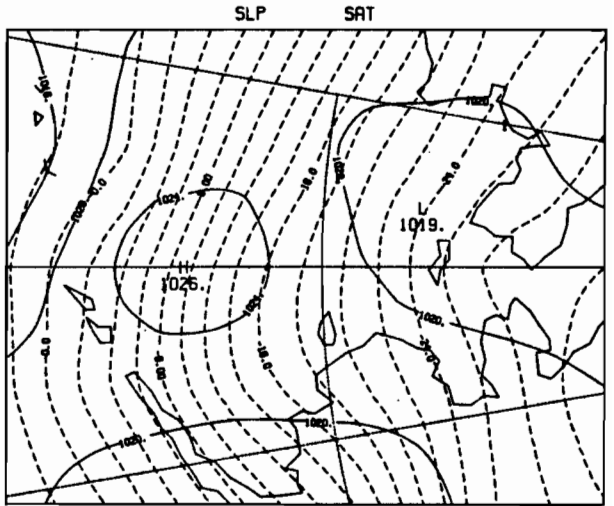
00Z 4 APR 1985
1985-BERING SEA



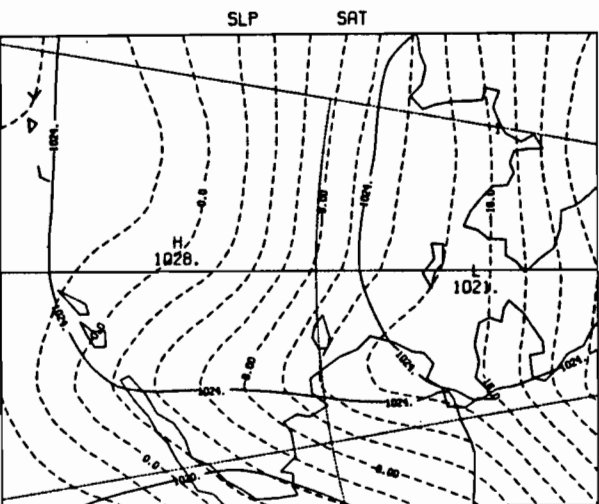
12Z 4 APR 1985
1985-BERING SEA



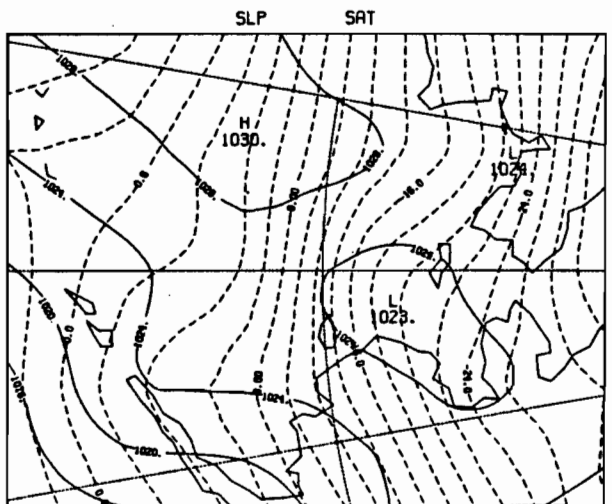
00Z 5 APR 1985
1985-BERING SEA



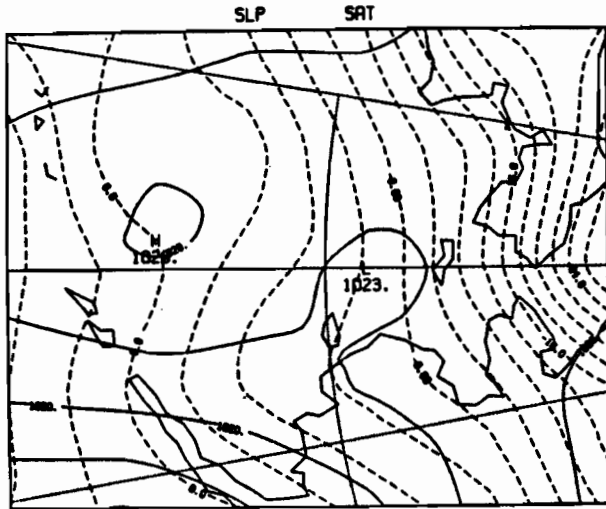
12Z 5 APR 1985
1985-BERING SEA



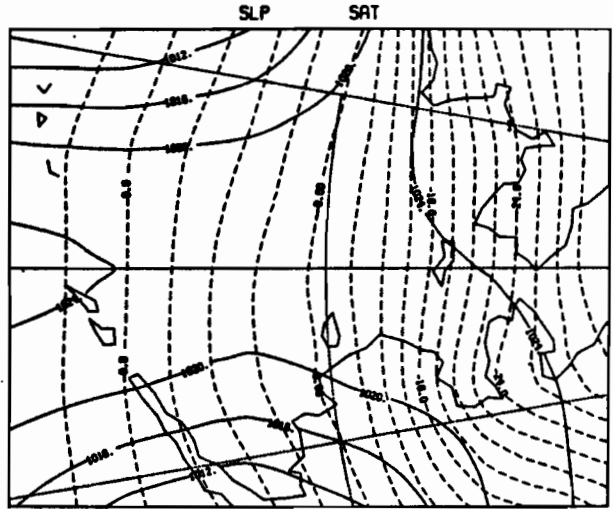
00Z 6 APR 1985
1985-BERING SEA



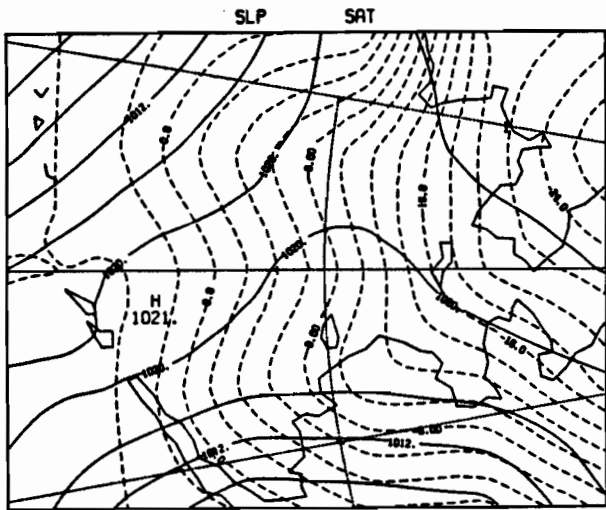
12Z 6 APR 1985
1985-BERING SEA



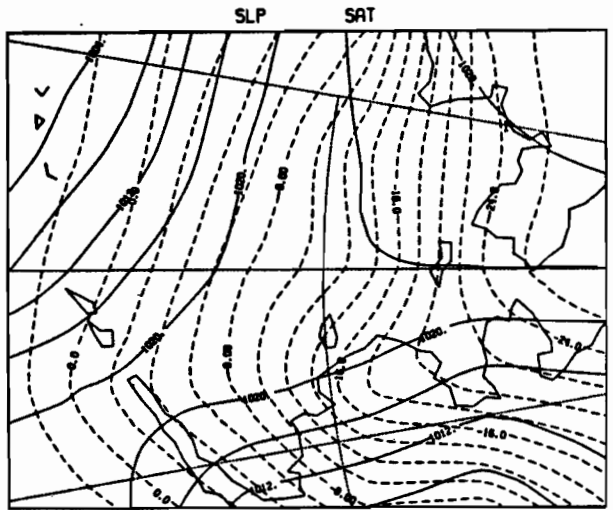
00Z 7 APR 1985
1985-BERING SEA



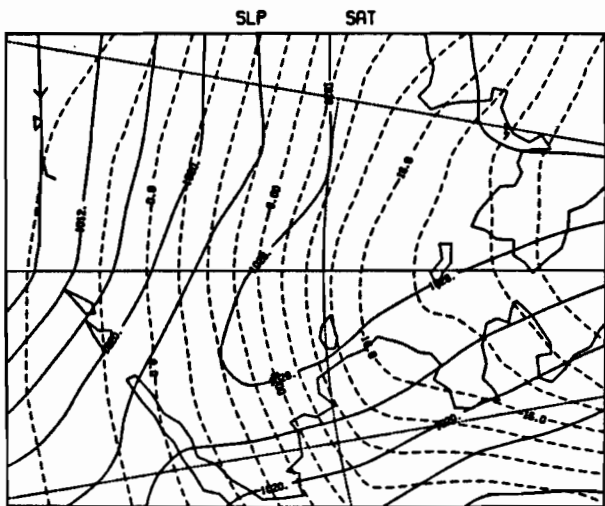
12Z 7 APR 1985
1985-BERING SEA



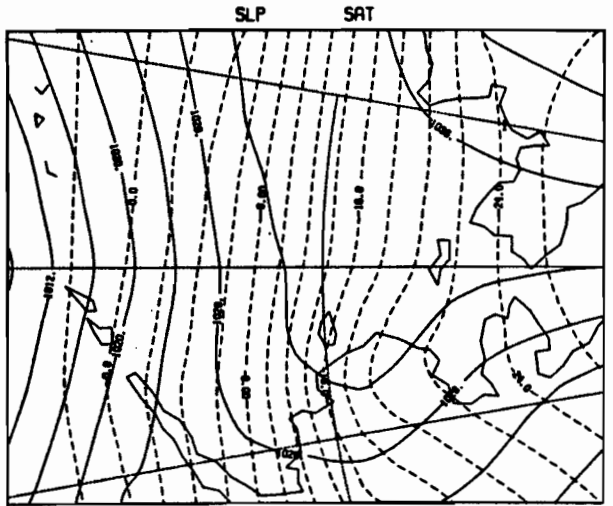
00Z 8 APR 1985
1985-BERING SEA



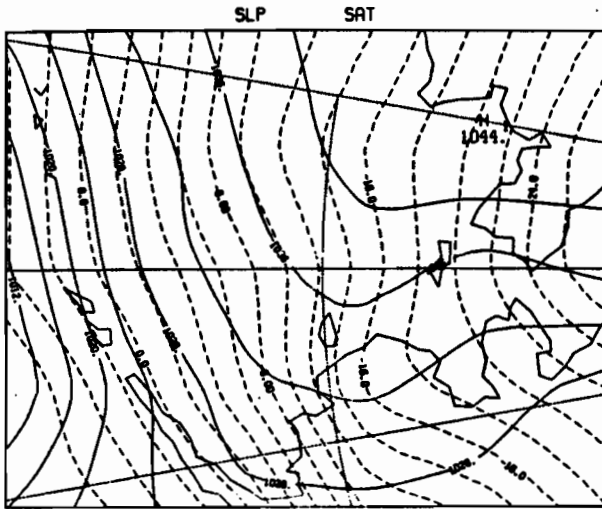
12Z 8 APR 1985
1985-BERING SEA



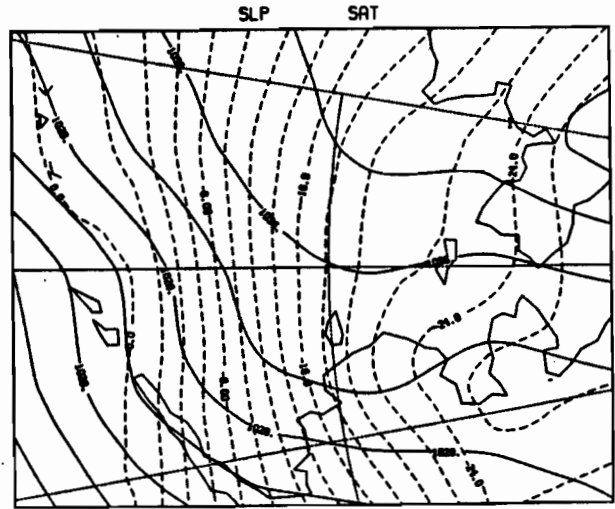
00Z 9 APR 1985
1985-BERING SEA



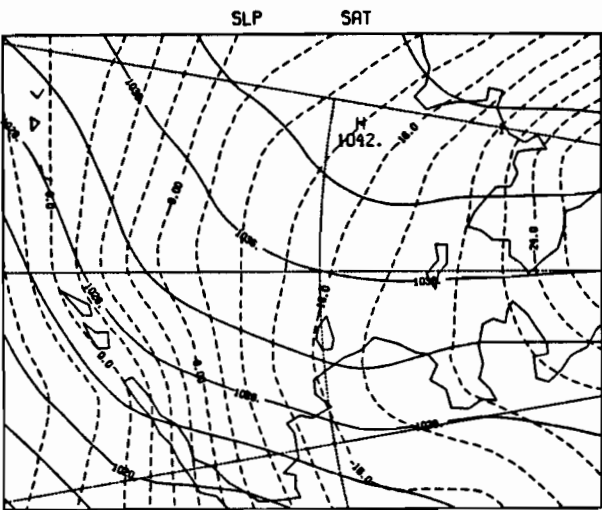
12Z 9 APR 1985
1985-BERING SEA



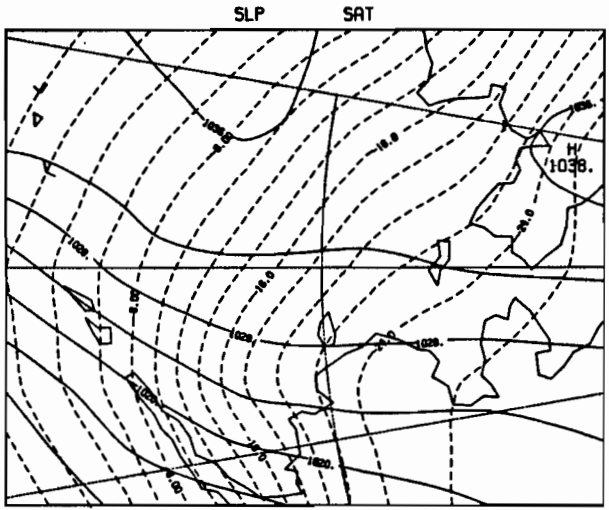
00Z 10 APR 1985
1985-BERING SEA



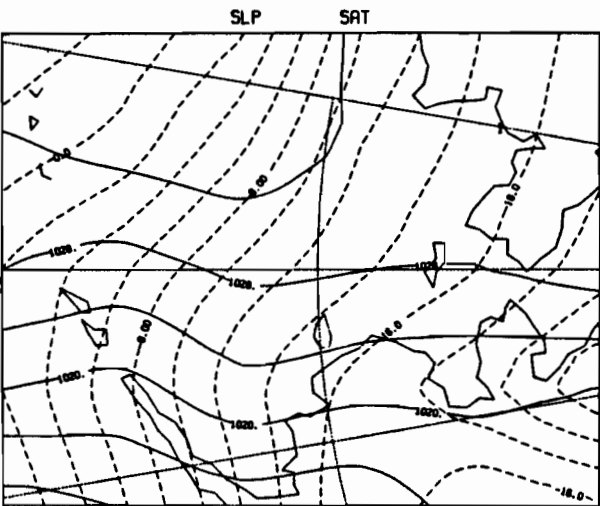
12Z 10 APR 1985
1985-BERING SEA



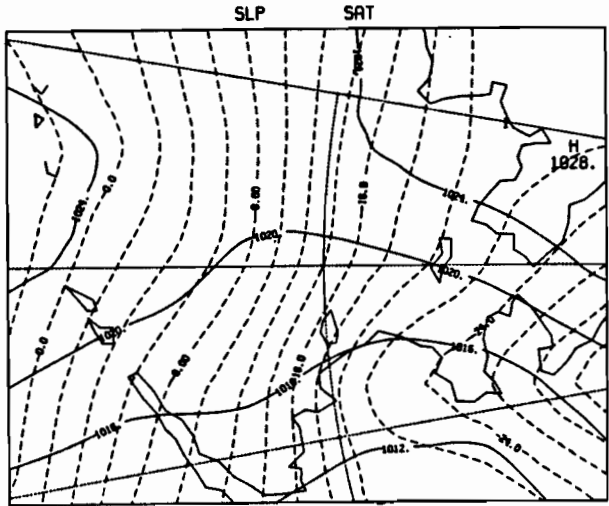
00Z 11 APR 1985
1985-BERING SEA



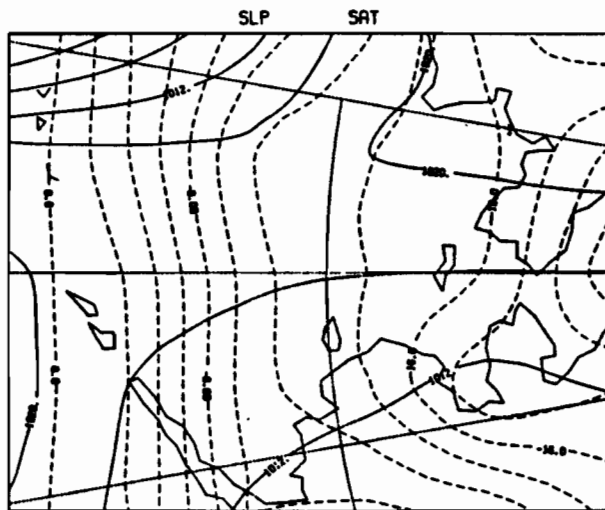
12Z 11 APR 1985
1985-BERING SEA



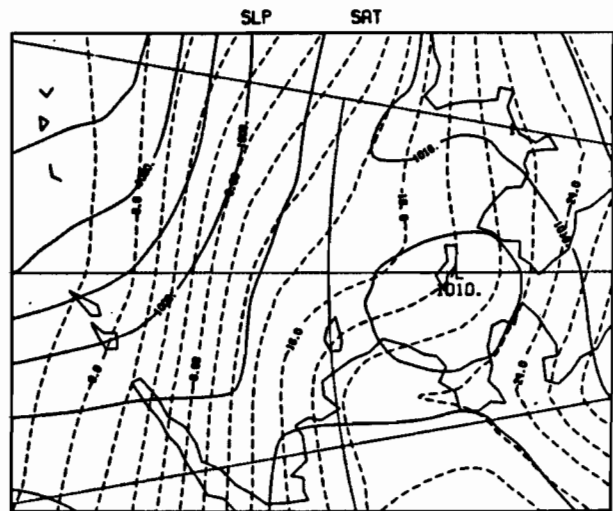
00Z 12 APR 1985
1985-BERING SEA



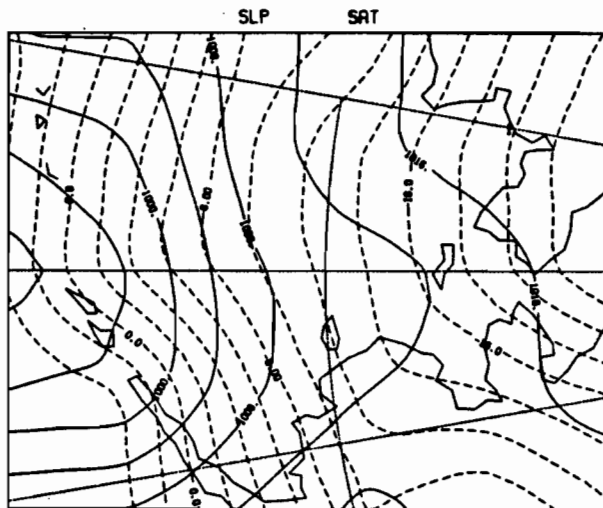
12Z 12 APR 1985
1985-BERING SEA



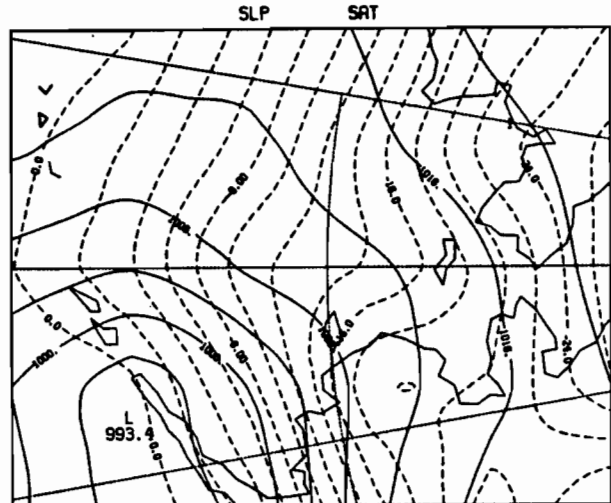
00Z 13 APR 1985
1985-BERING SEA



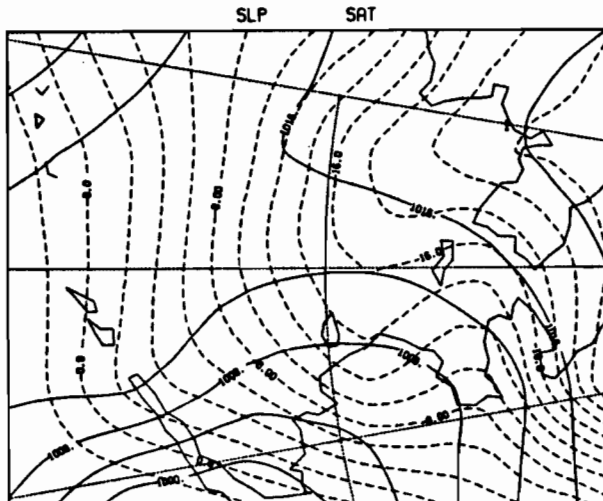
12Z 13 APR 1985
1985-BERING SEA



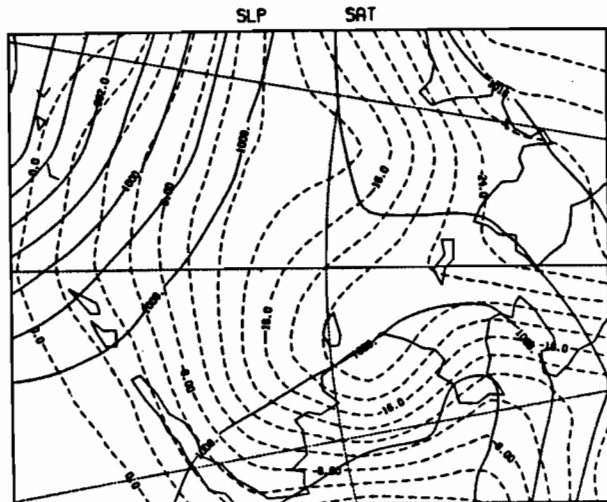
00Z 14 APR 1985
1985-BERING SEA



12Z 14 APR 1985
1985-BERING SEA



00Z 15 APR 1985
1985-BERING SEA



12Z 15 APR 1985
1985-BERING SEA

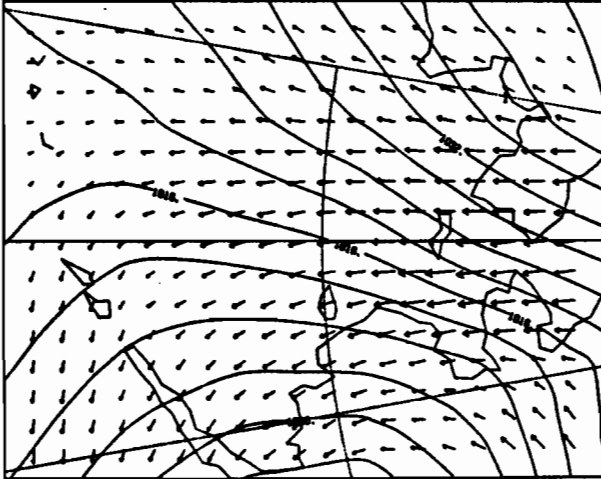
Appendix B. METLIB Meteorological Data

- Sea-level Pressure Fields and Surface Wind Vectors

The sea-level pressure (SLP) from the NWS Alaska Region was reanalyzed for late data and hand-digitized onto a grid compatible with the NWS National Meteorological Center's Primitive Equation grid. A program library for calculating and plotting marine boundary layer wind fields called METLIB (Overland *et al.*, 1980; Macklin *et al.*, 1984) was used to calculate gradient winds from pressures which had first been interpolated to one-quarter mesh. The gradient winds were then rotated counterclockwise (cyclonically) 30° and reduced in speed by 20% to approximate surface wind conditions (EMPR WINDS).

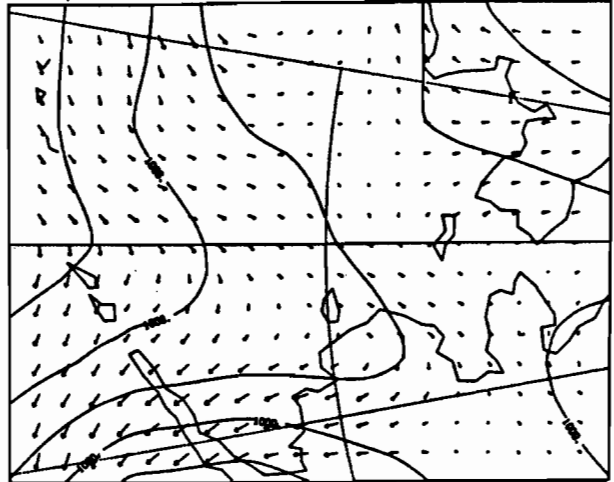
The following vector wind plots represent the approximate surface wind conditions for 00 GMT and 12 GMT from 00 GMT 15 February 1985 through 12 GMT 15 April 1985. The distance between grid points (tails of vectors) in the following plots is the vector length scale for 25 m/s wind speed. Wind speeds higher than this magnitude cannot be handled by the plotting package, resulting in occasional missing vectors with only a dot at the base. Note that true north is toward the right and pressure is given in mb.

SLP
EMPR WINDS



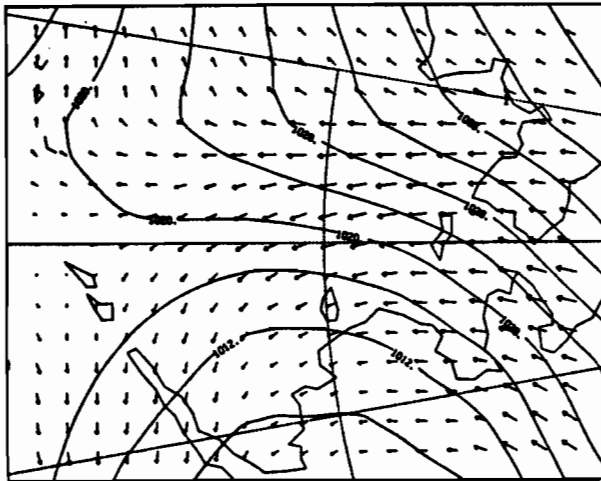
00Z 15 FEB 1985

SLP
EMPR WINDS



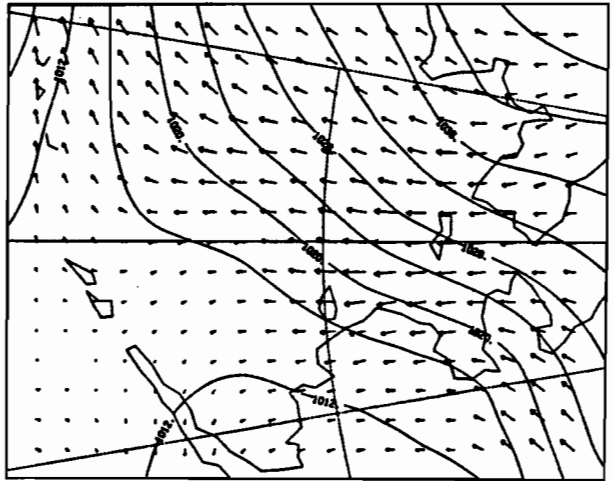
12Z 15 FEB 1985

SLP
EMPR WINDS



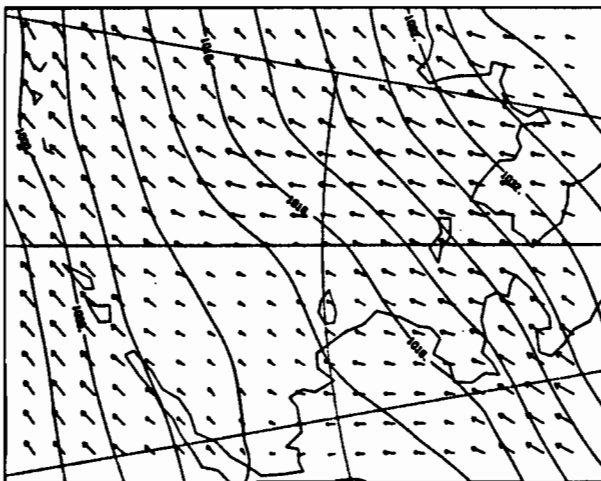
00Z 16 FEB 1985

SLP
EMPR WINDS



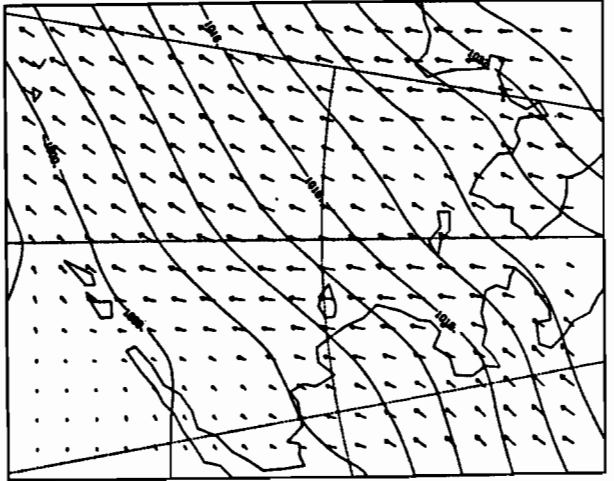
12Z 16 FEB 1985

SLP
EMPR WINDS



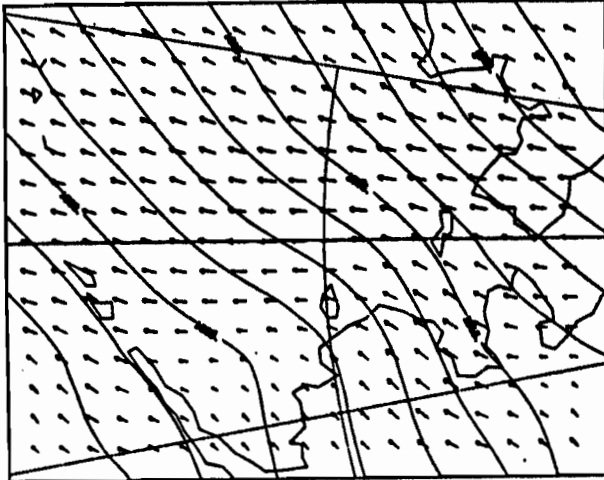
00Z 17 FEB 1985

SLP
EMPR WINDS



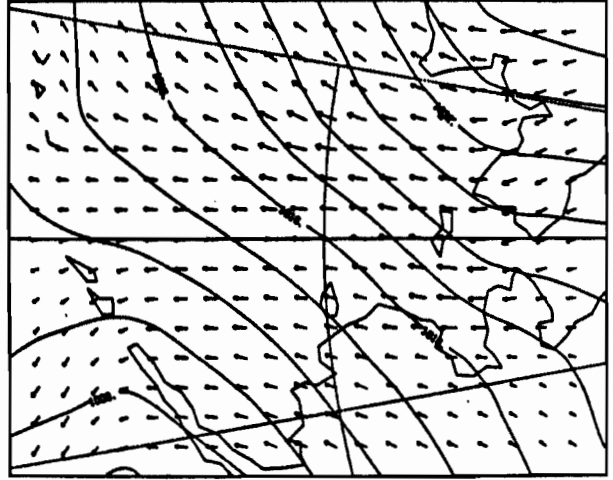
12Z 17 FEB 1985

SLP
EMPR WINDS



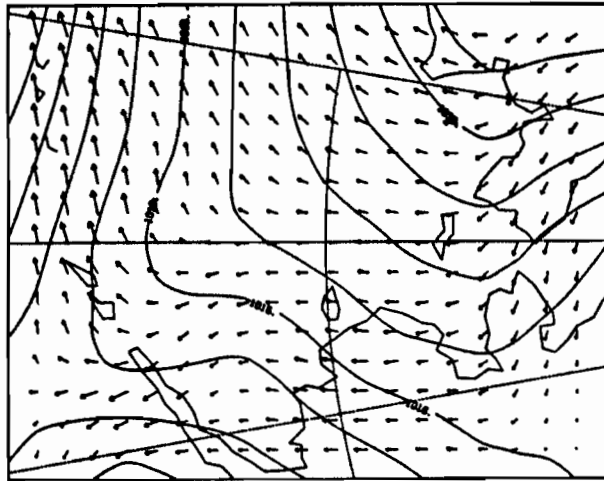
00Z 18 FEB 1985

SLP
EMPR WINDS



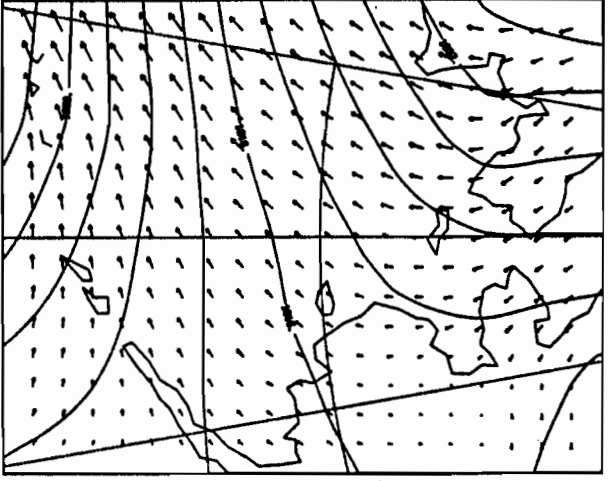
12Z 18 FEB 1985

SLP
EMPR WINDS



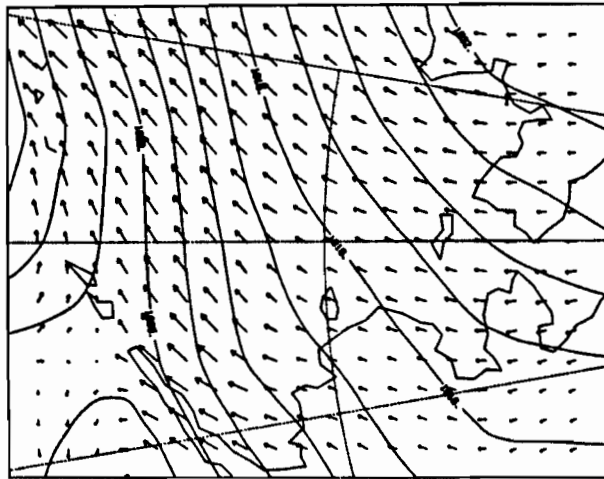
00Z 19 FEB 1985

SLP
EMPR WINDS



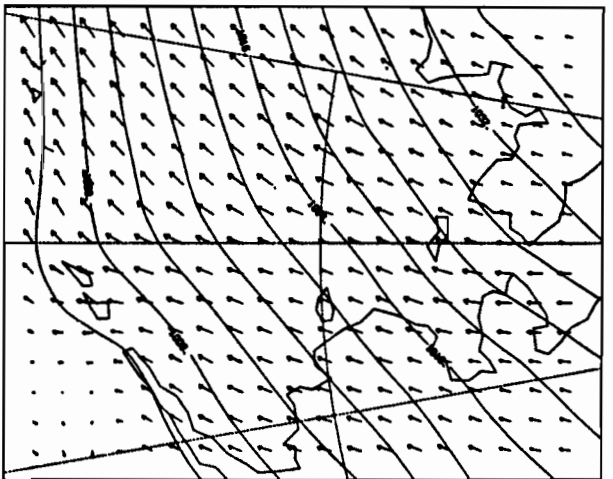
12Z 19 FEB 1985

SLP
EMPR WINDS

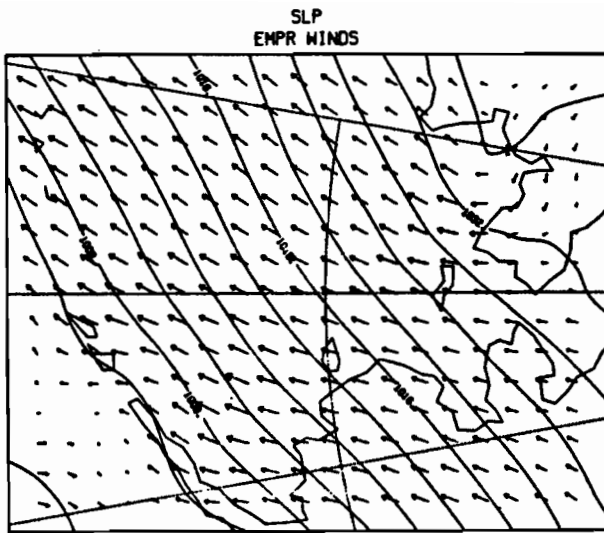


00Z 20 FEB 1985

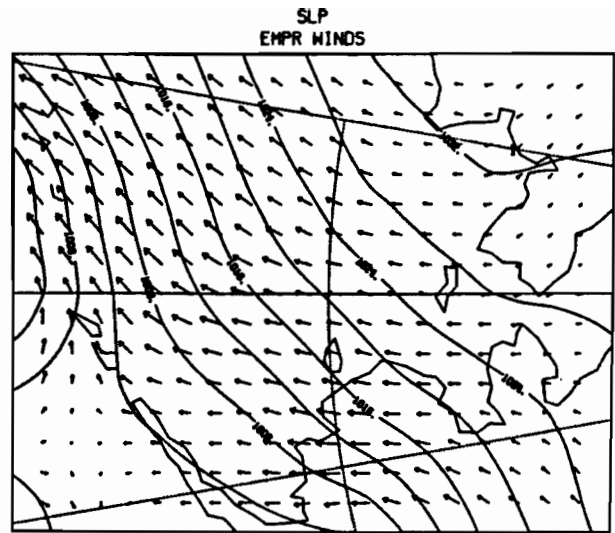
SLP
EMPR WINDS



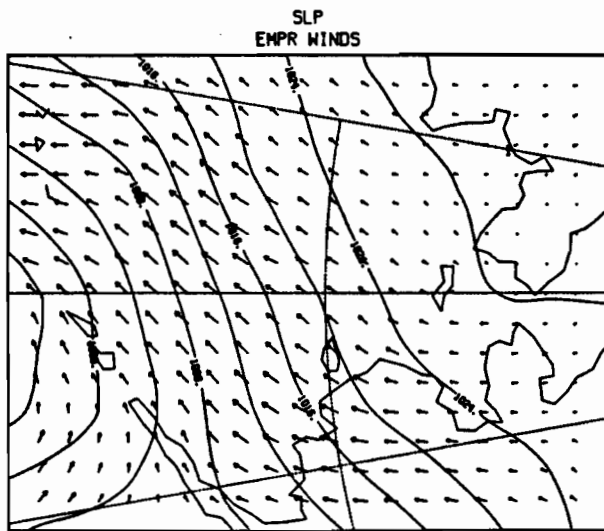
12Z 20 FEB 1985



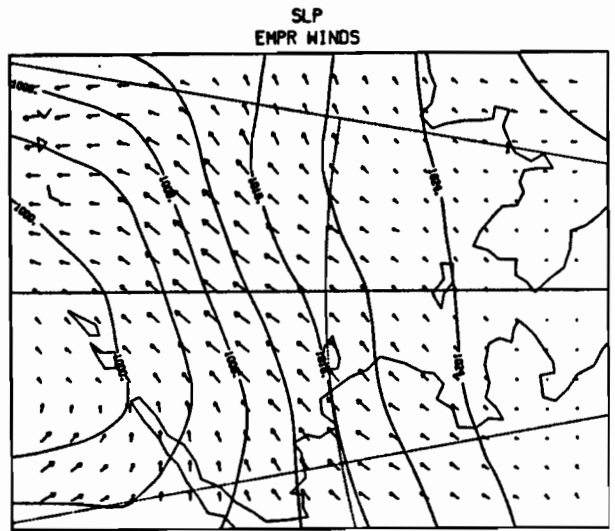
00Z 21 FEB 1985



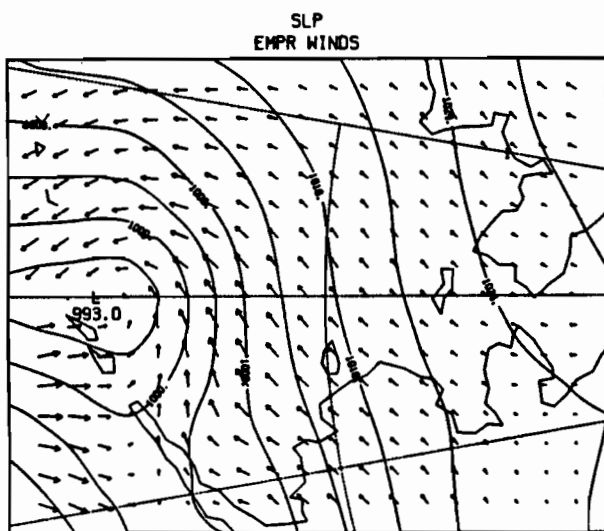
12Z 21 FEB 1985



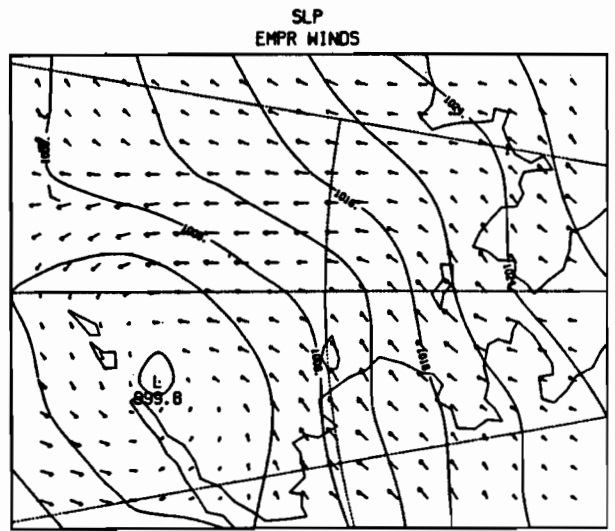
00Z 22 FEB 1985



12Z 22 FEB 1985

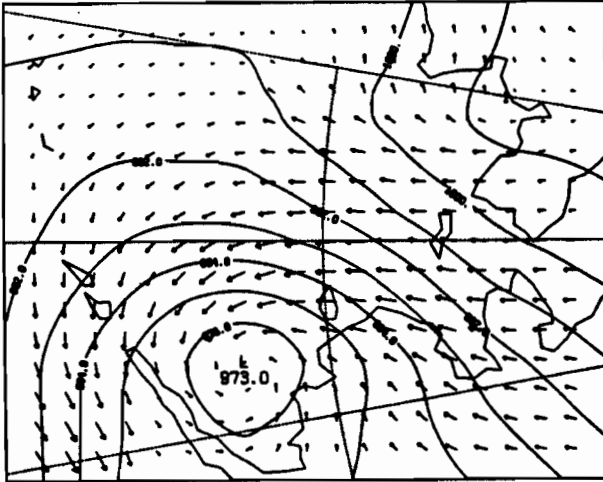


00Z 23 FEB 1985



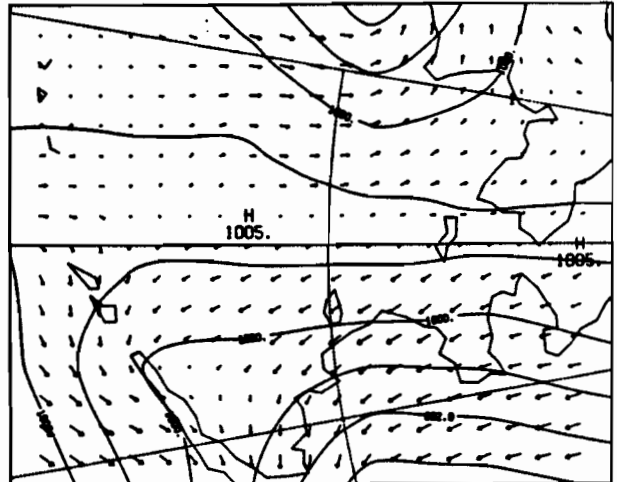
12Z 23 FEB 1985

SLP
EMPR WINDS



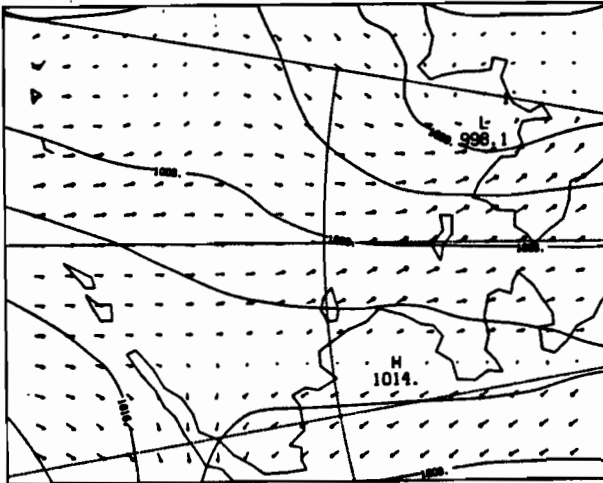
00Z 27 FEB 1985

SLP
EMPR WINDS



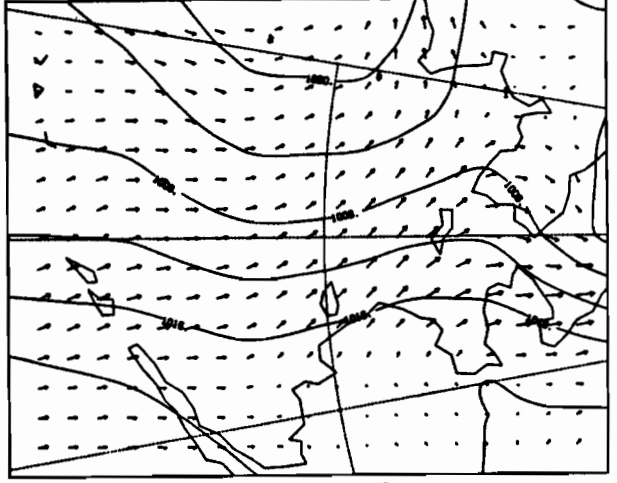
12Z 27 FEB 1985

SLP
EMPR WINDS



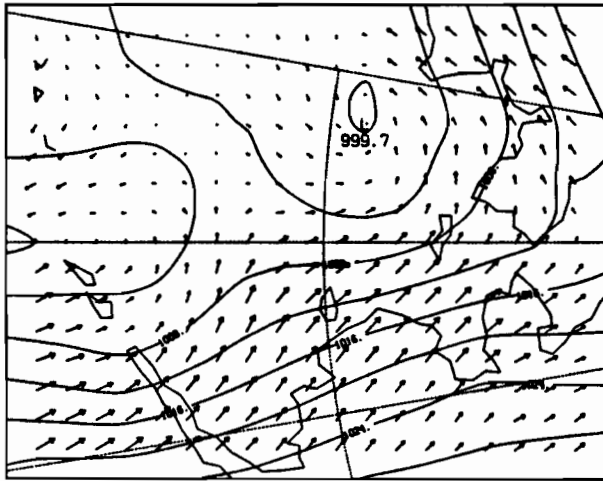
00Z 28 FEB 1985

SLP
EMPR WINDS



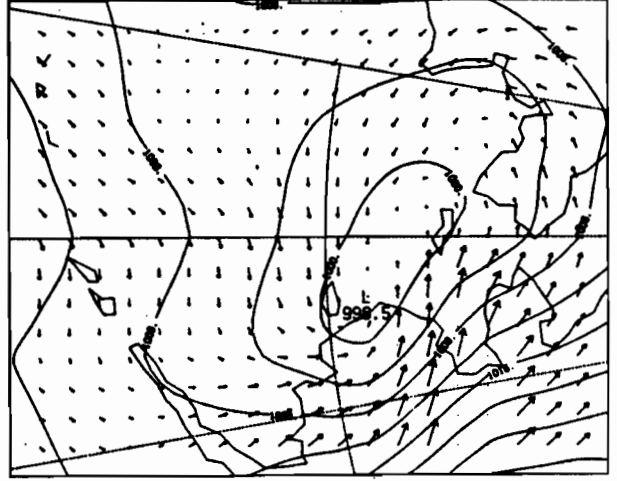
12Z 28 FEB 1985

SLP
EMPR WINDS



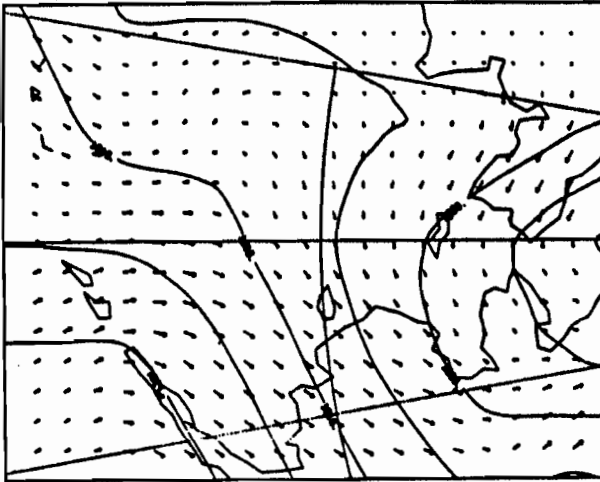
00Z 1 MAR 1985

SLP
EMPR WINDS



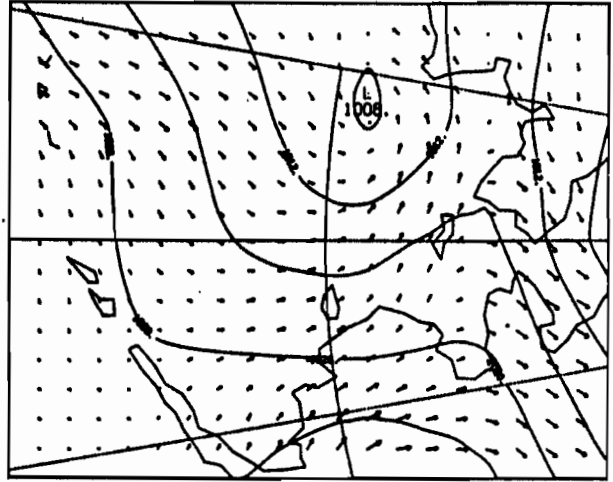
12Z 1 MAR 1985

SLP
EMPR WINDS



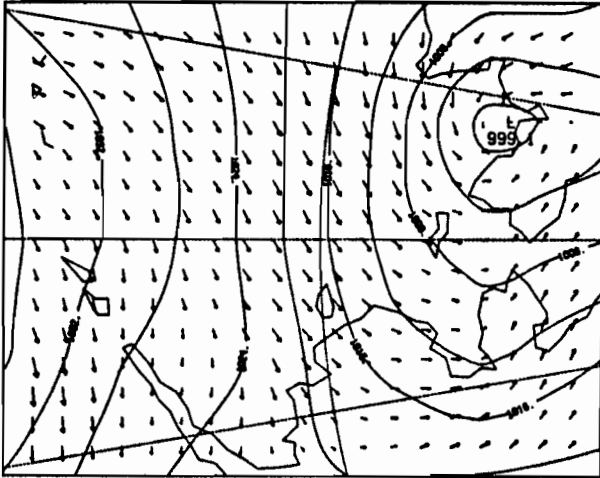
00Z 2 MAR 1985

SLP
EMPR WINDS



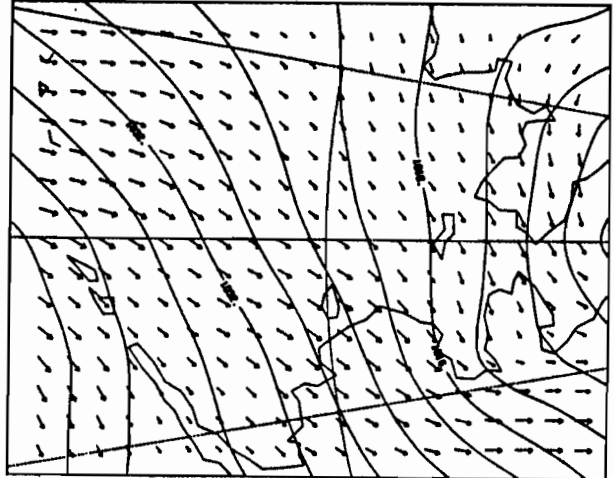
12Z 2 MAR 1985

SLP
EMPR WINDS



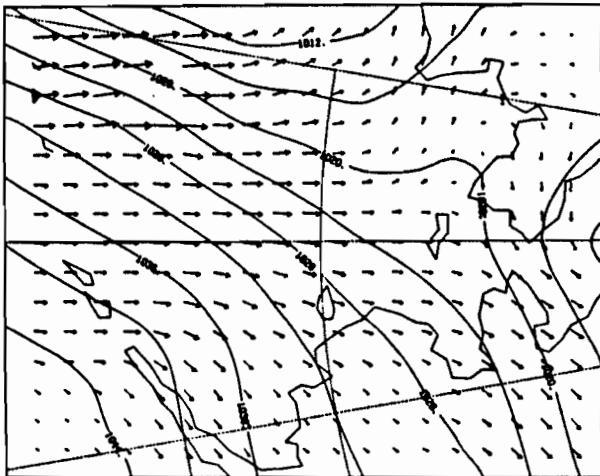
00Z 3 MAR 1985

SLP
EMPR WINDS



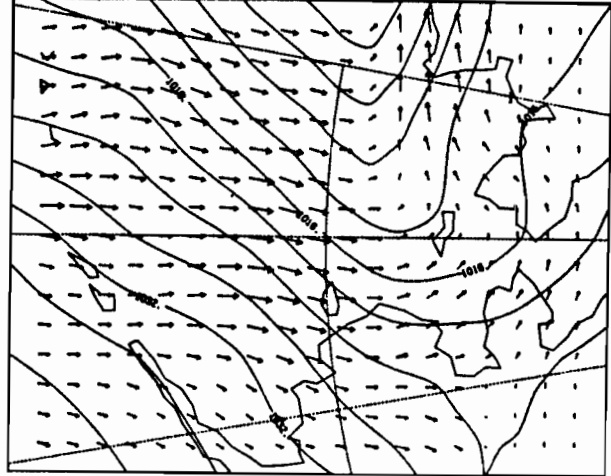
12Z 3 MAR 1985

SLP
EMPR WINDS



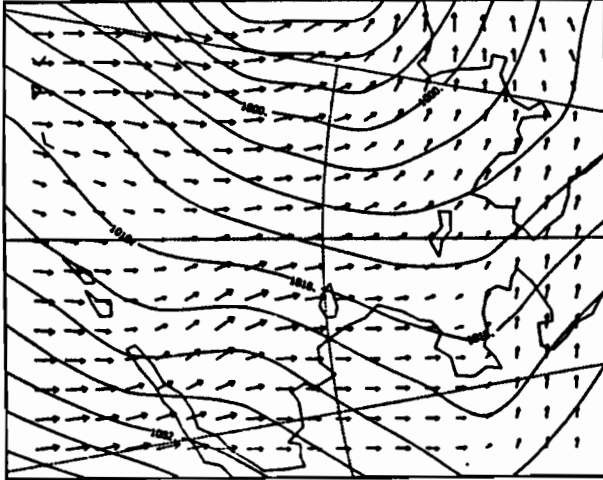
00Z 4 MAR 1985

SLP
EMPR WINDS



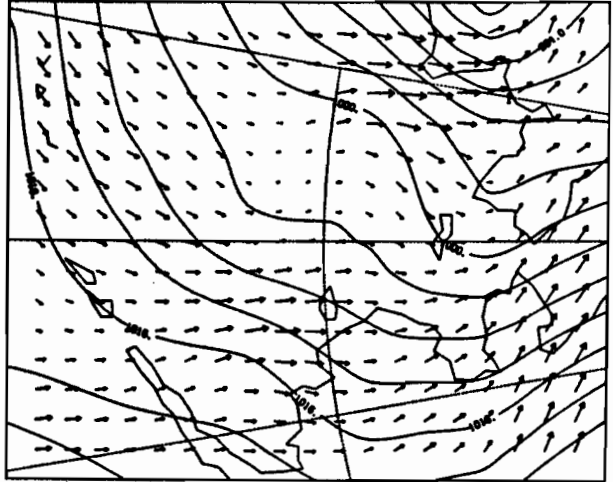
12Z 4 MAR 1985

SLP
EMPR WINDS



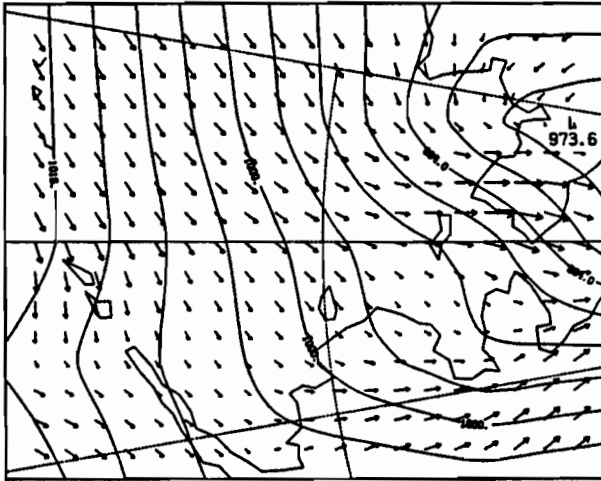
00Z 5 MAR 1985

SLP
EMPR WINDS



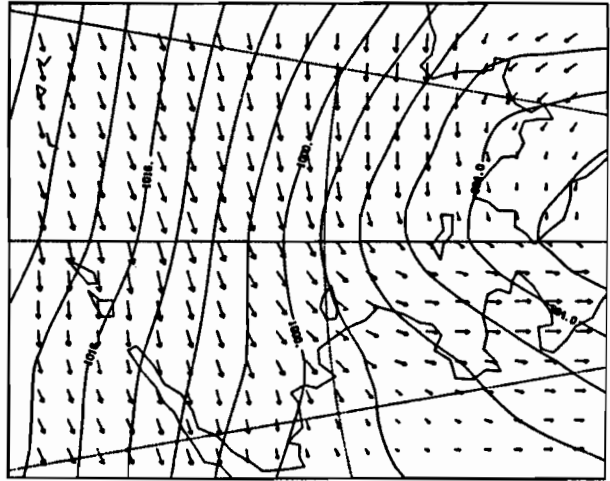
12Z 5 MAR 1985

SLP
EMPR WINDS



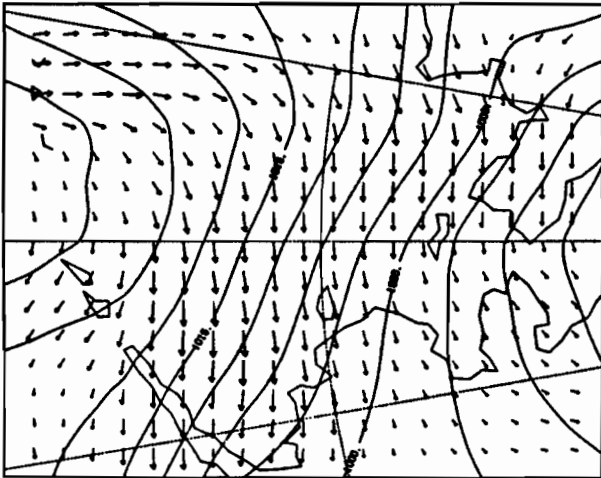
00Z 6 MAR 1985

SLP
EMPR WINDS



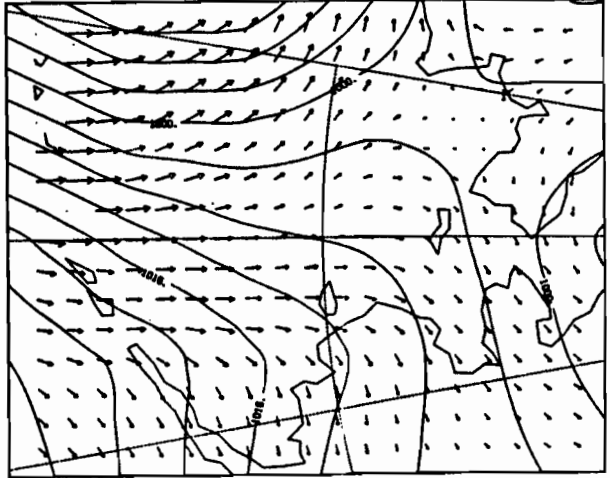
12Z 6 MAR 1985

SLP
EMPR WINDS



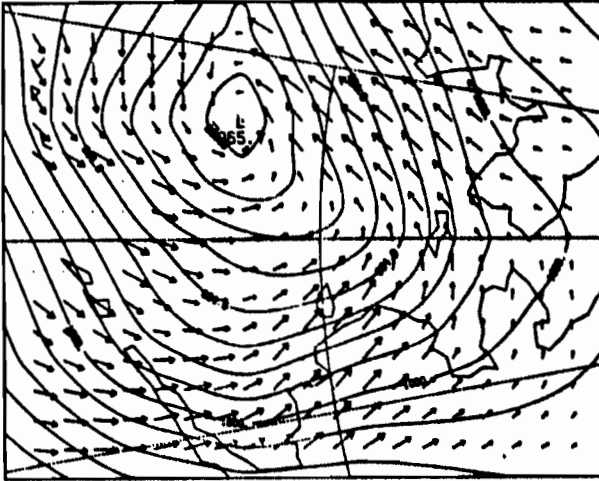
00Z 7 MAR 1985

SLP
EMPR WINDS



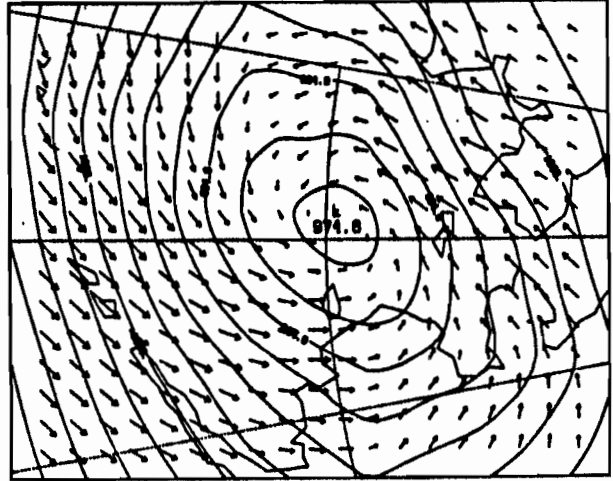
12Z 7 MAR 1985

SLP
EMPR WINDS



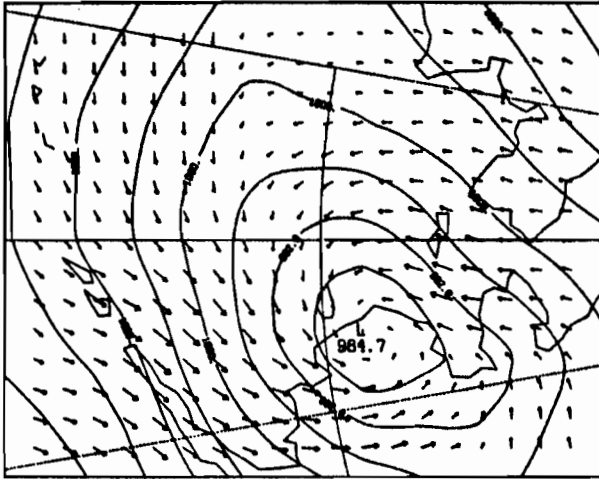
00Z 8 MAR 1985

SLP
EMPR WINDS



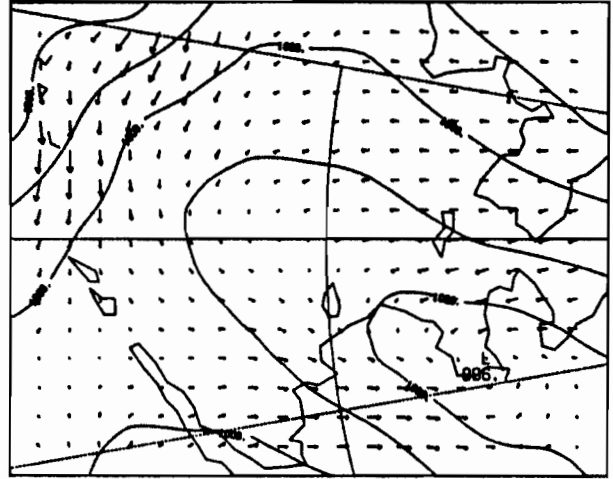
12Z 8 MAR 1985

SLP
EMPR WINDS



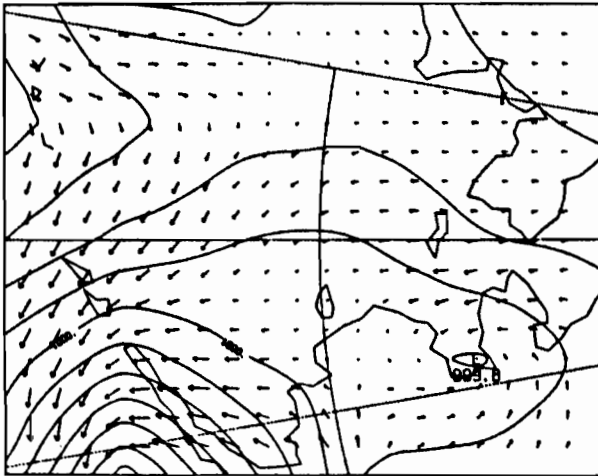
00Z 9 MAR 1985

SLP
EMPR WINDS



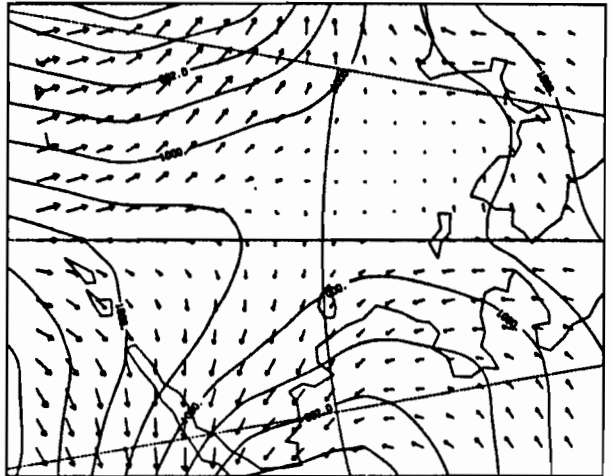
12Z 9 MAR 1985

SLP
EMPR WINDS



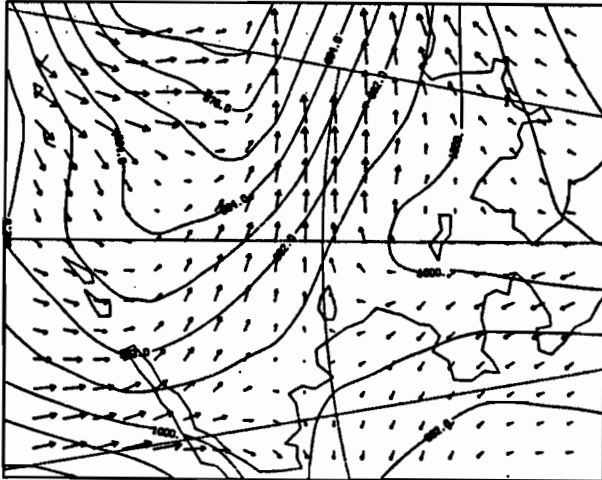
00Z 10 MAR 1985

SLP
EMPR WINDS



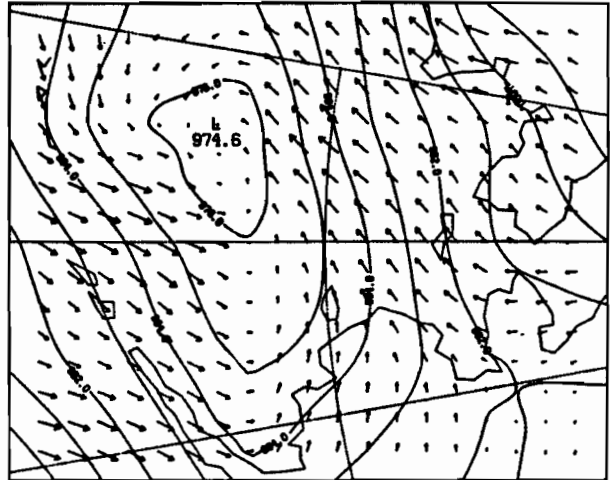
12Z 10 MAR 1985

SLP
EMPR WINDS



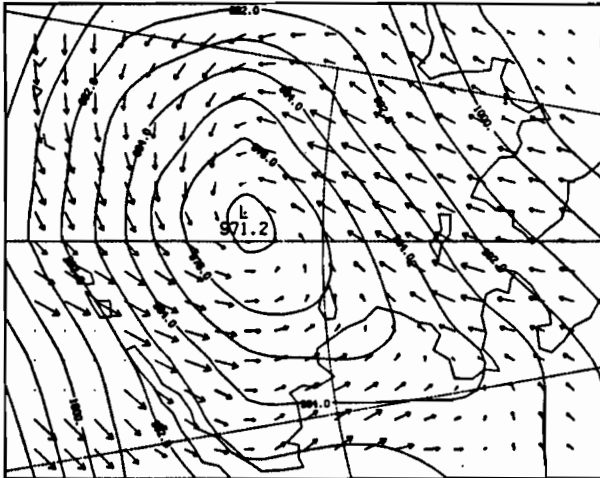
00Z 11 MAR 1985

SLP
EMPR WINDS



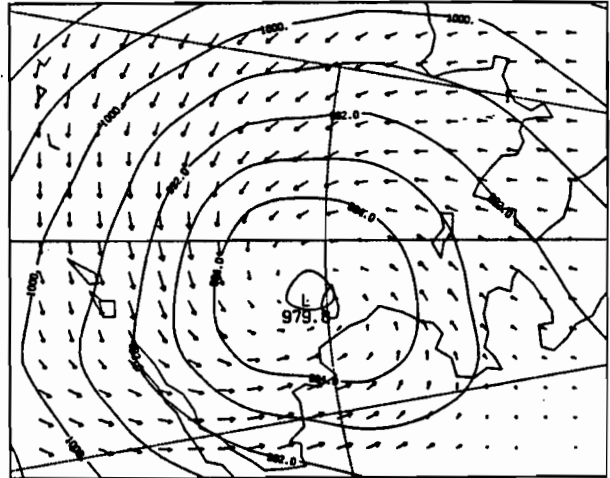
12Z 11 MAR 1985

SLP
EMPR WINDS



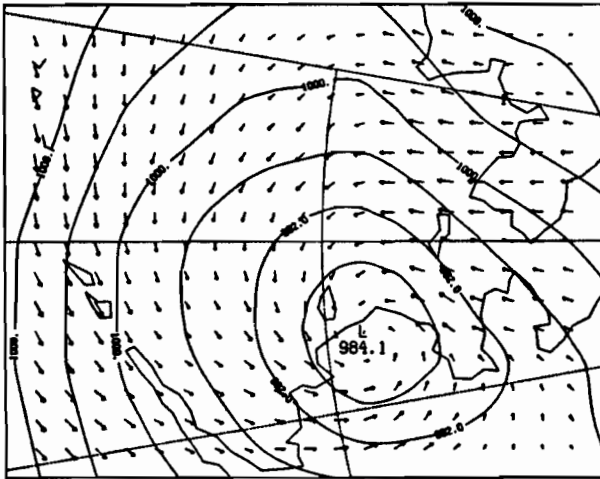
00Z 12 MAR 1985

SLP
EMPR WINDS



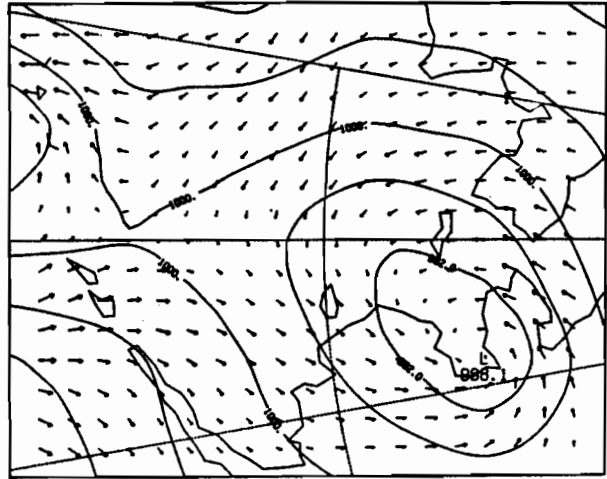
12Z 12 MAR 1985

SLP
EMPR WINDS



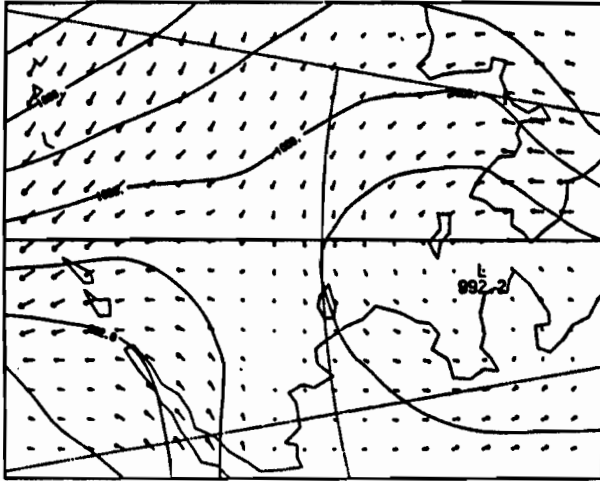
00Z 13 MAR 1985

SLP
EMPR WINDS



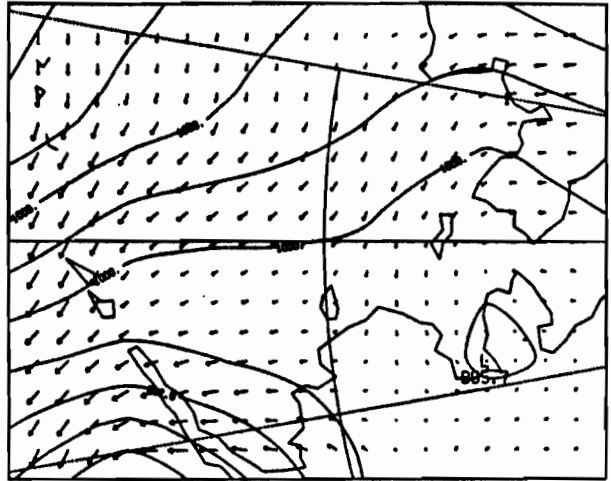
12Z 13 MAR 1985

SLP
EMPR WINDS



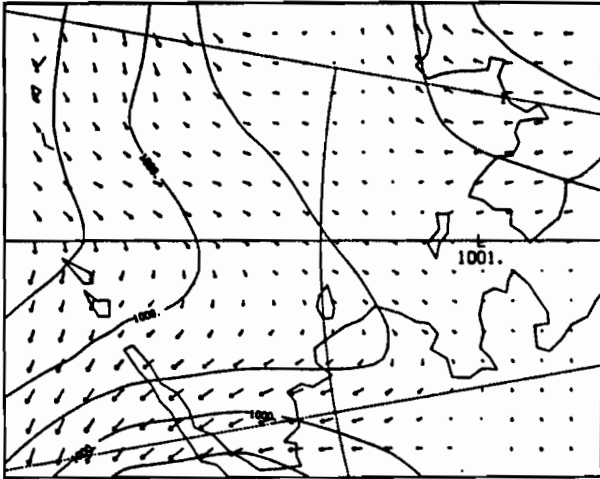
00Z 14 MAR 1985

SLP
EMPR WINDS



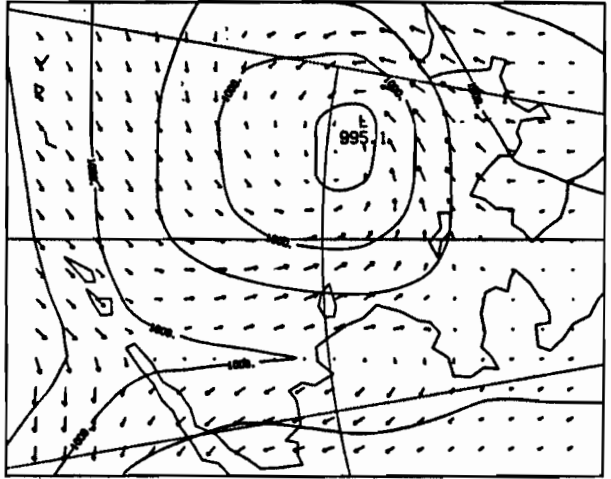
12Z 14 MAR 1985

SLP
EMPR WINDS



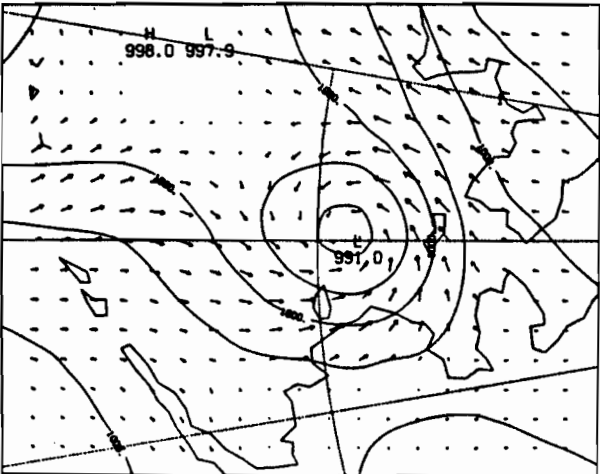
00Z 15 MAR 1985

SLP
EMPR WINDS



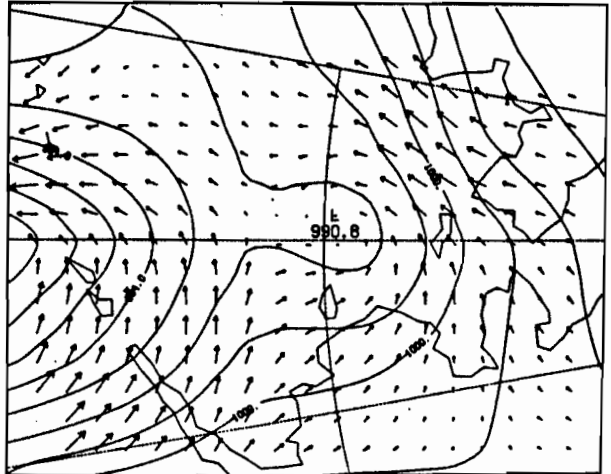
12Z 15 MAR 1985

SLP
EMPR WINDS



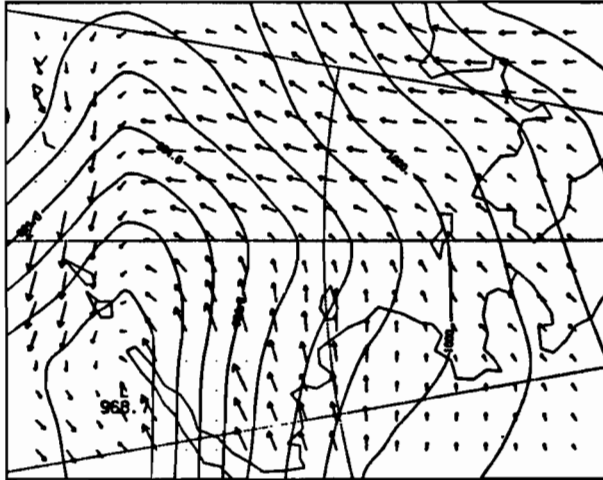
00Z 16 MAR 1985

SLP
EMPR WINDS



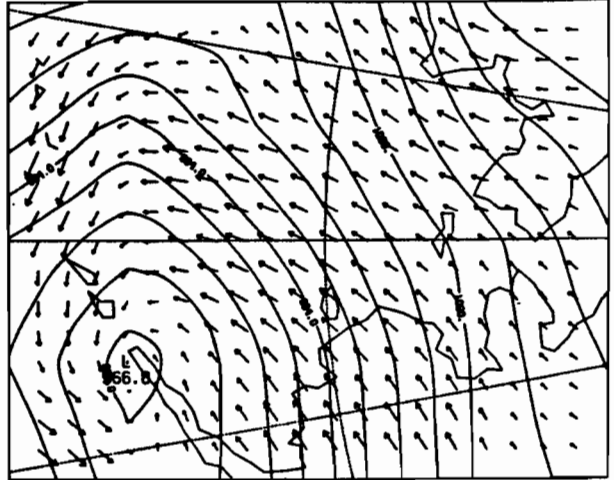
12Z 16 MAR 1985

SLP
EMPR WINDS



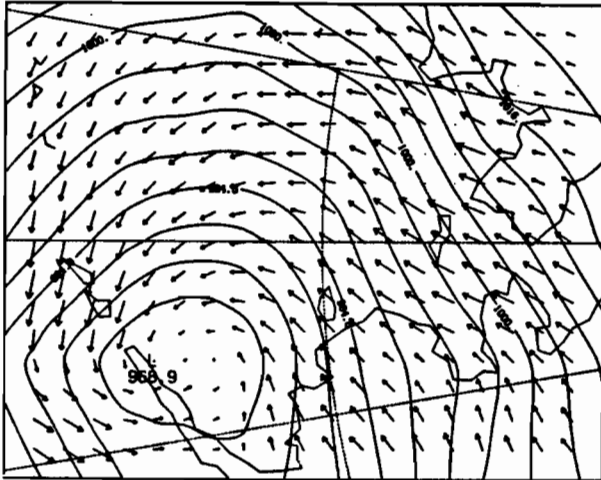
00Z 17 MAR 1985

SLP
EMPR WINDS



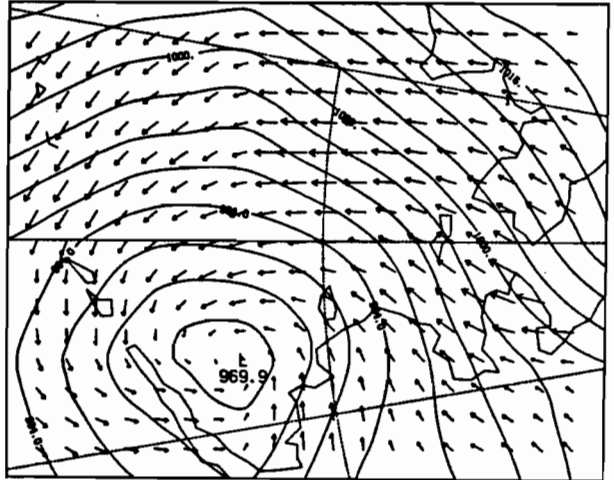
12Z 17 MAR 1985

SLP
EMPR WINDS



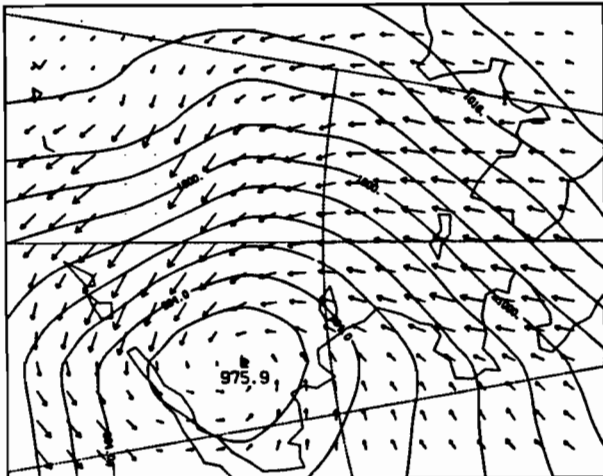
00Z 18 MAR 1985

SLP
EMPR WINDS



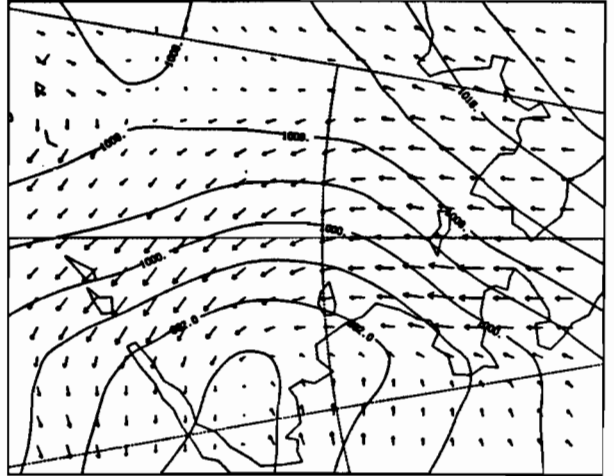
12Z 18 MAR 1985

SLP
EMPR WINDS



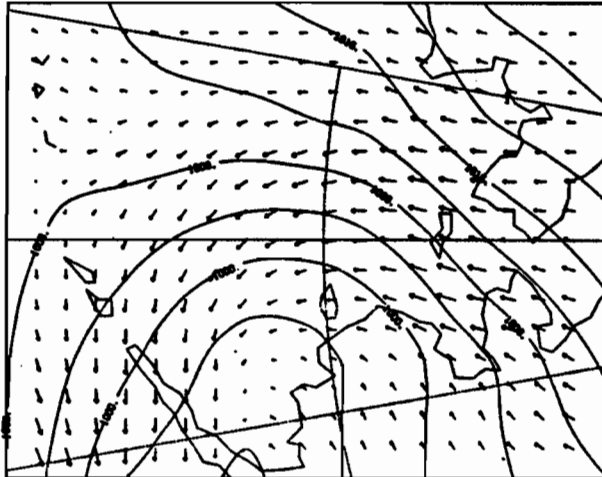
00Z 19 MAR 1985

SLP
EMPR WINDS



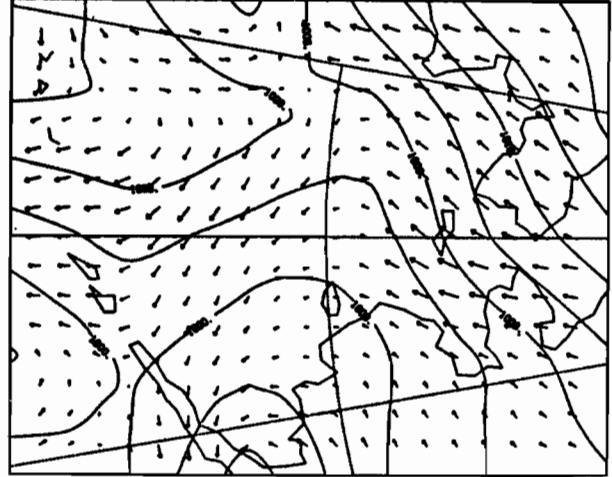
12Z 19 MAR 1985

SLP
EMPR WINDS



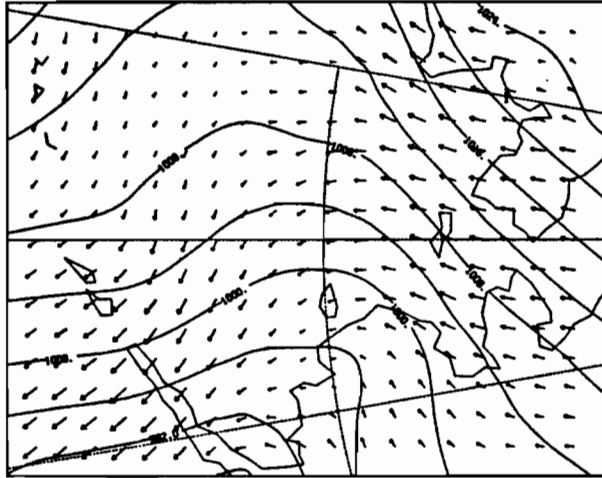
00Z 20 MAR 1985

SLP
EMPR WINDS



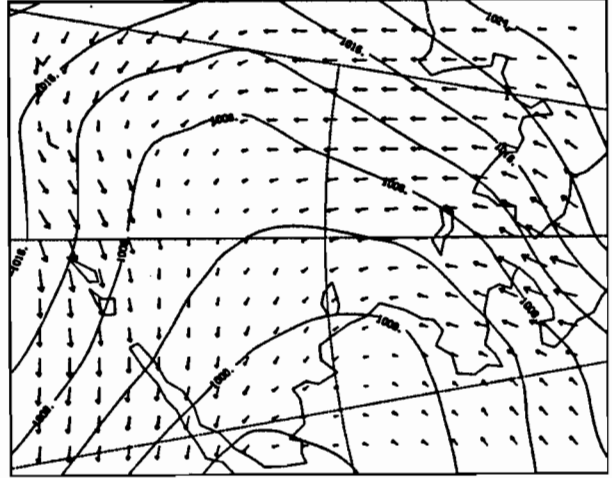
12Z 20 MAR 1985

SLP
EMPR WINDS



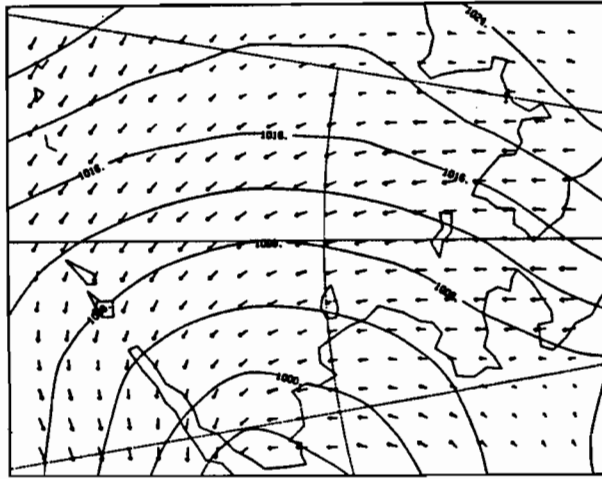
00Z 21 MAR 1985

SLP
EMPR WINDS



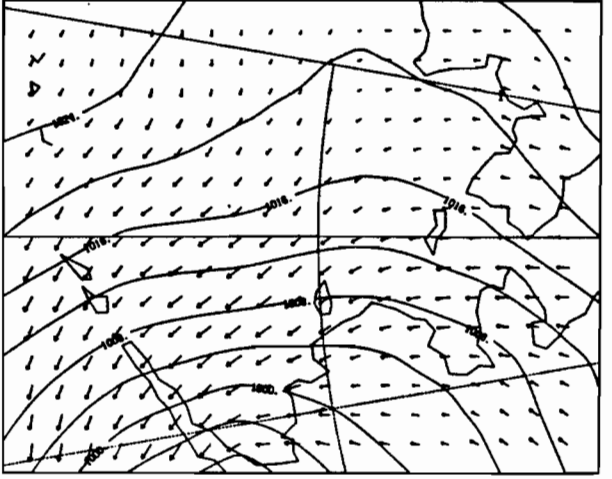
12Z 21 MAR 1985

SLP
EMPR WINDS



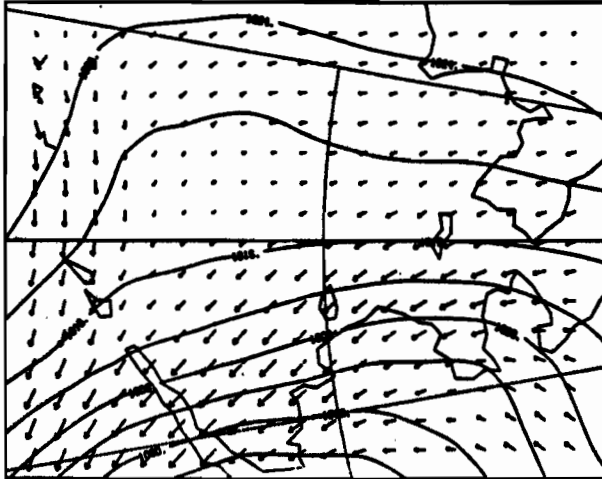
00Z 22 MAR 1985

SLP
EMPR WINDS



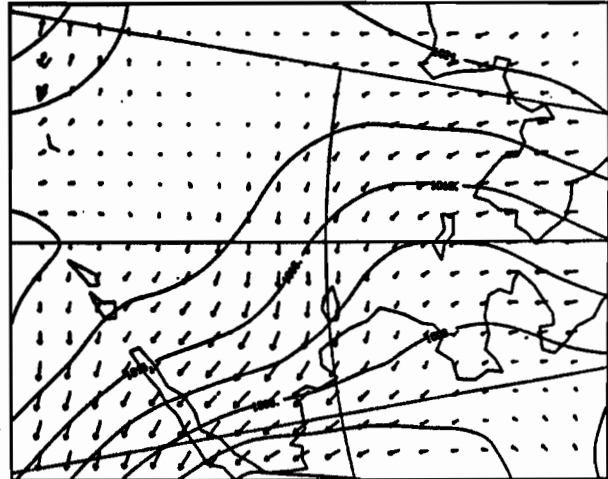
12Z 22 MAR 1985

SLP
EMPR WINDS



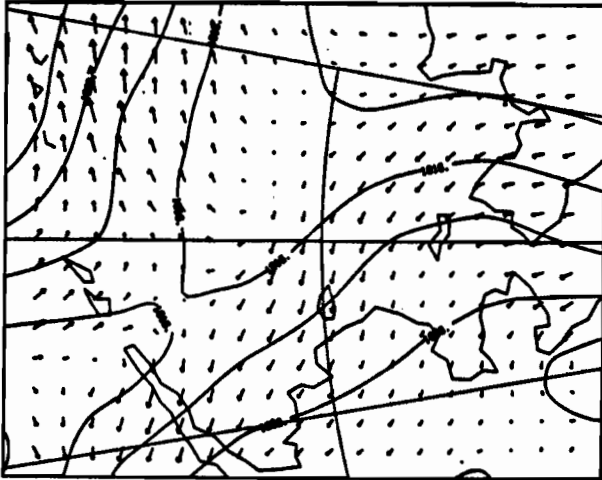
00Z 23 MAR 1985

SLP
EMPR WINDS



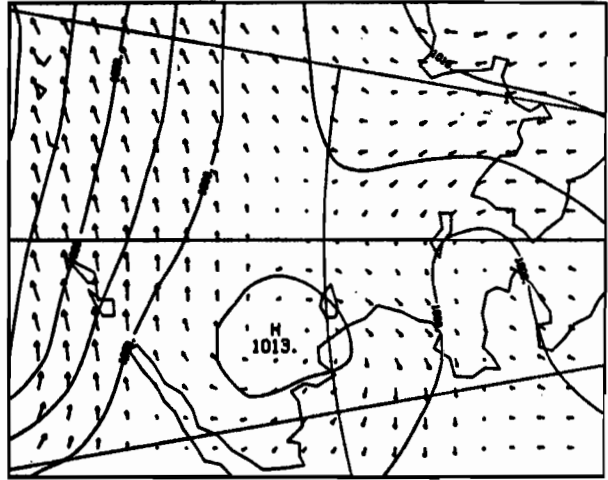
12Z 23 MAR 1985

SLP
EMPR WINDS



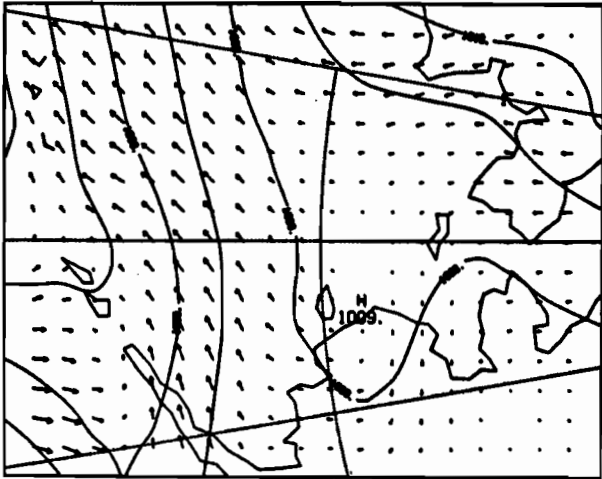
00Z 24 MAR 1985

SLP
EMPR WINDS



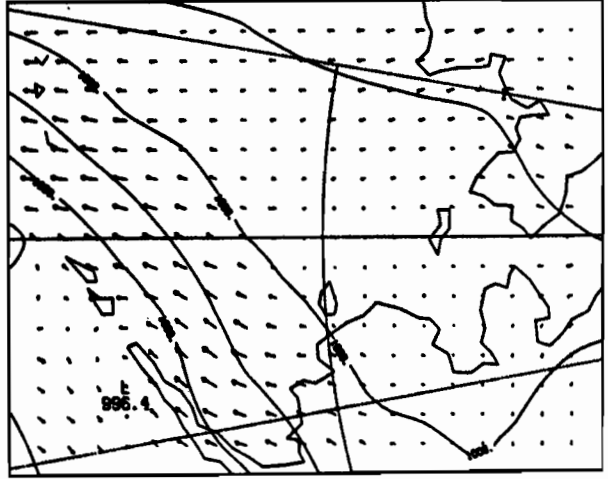
12Z 24 MAR 1985

SLP
EMPR WINDS



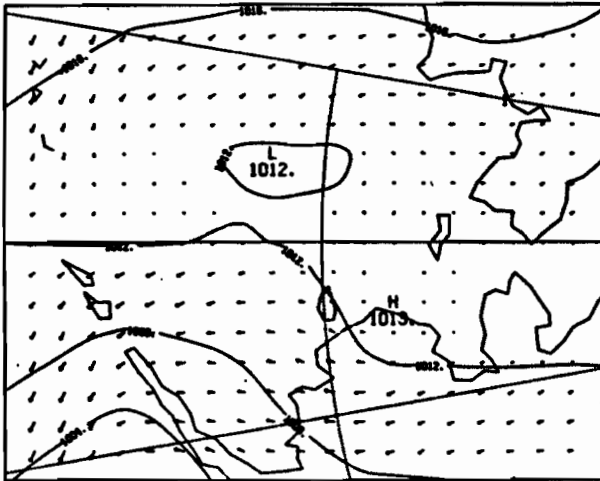
00Z 25 MAR 1985

SLP
EMPR WINDS



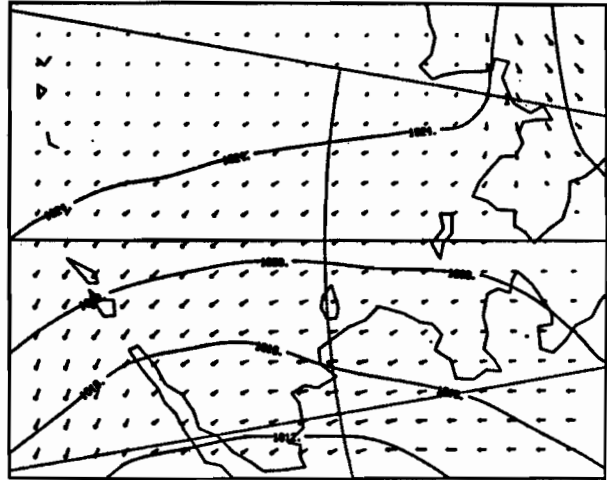
12Z 25 MAR 1985

SLP
EMPR WINDS



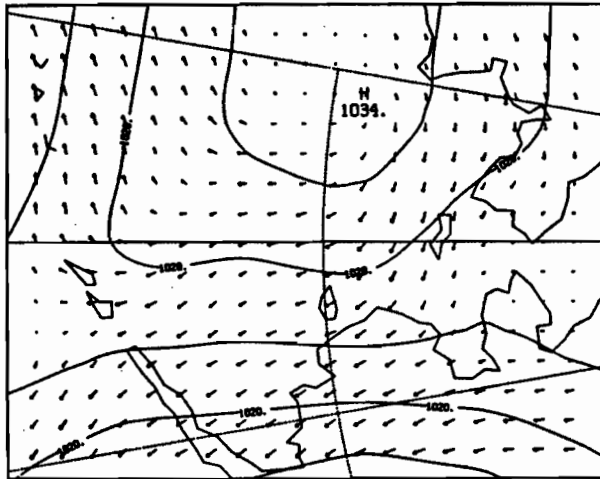
00Z 26 MAR 1985

SLP
EMPR WINDS



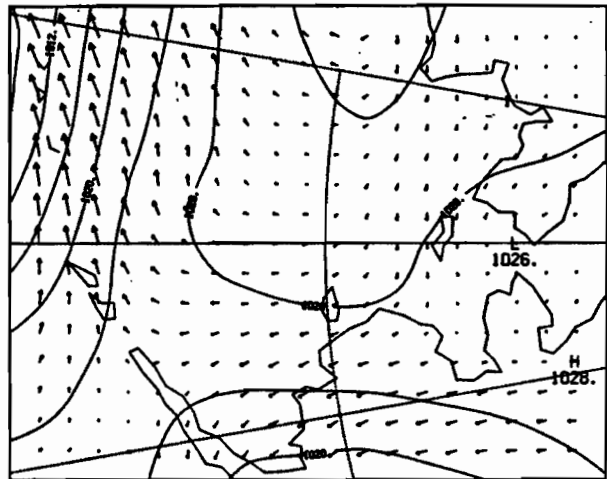
12Z 26 MAR 1985

SLP
EMPR WINDS

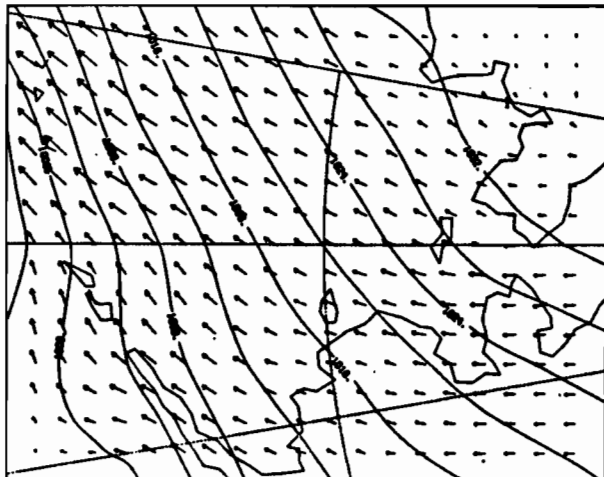


00Z 27 MAR 1985

SLP
EMPR WINDS

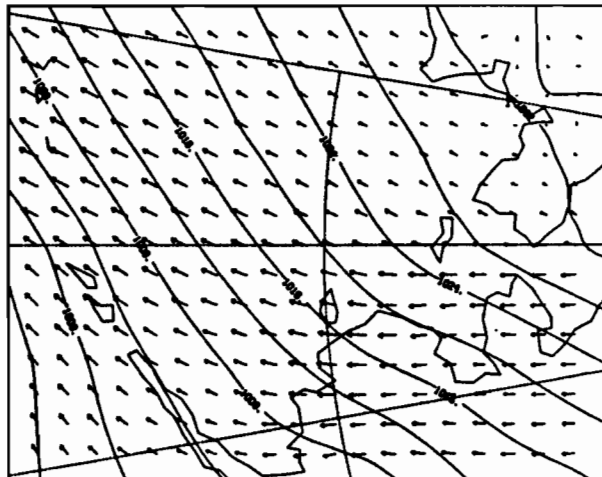


SLP
EMPR WINDS



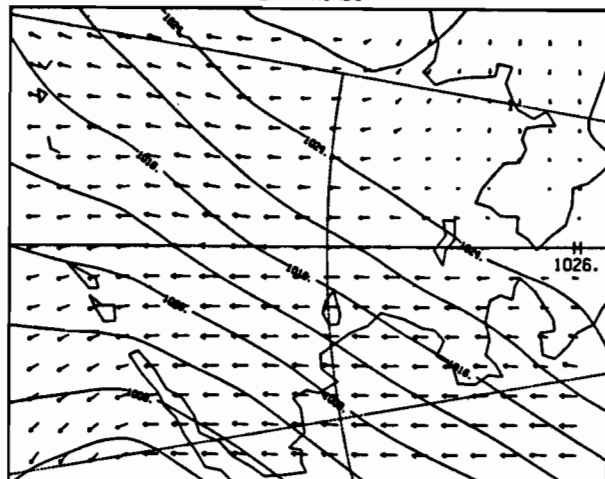
00Z 29 MAR 1985

SLP
EMPR WINDS



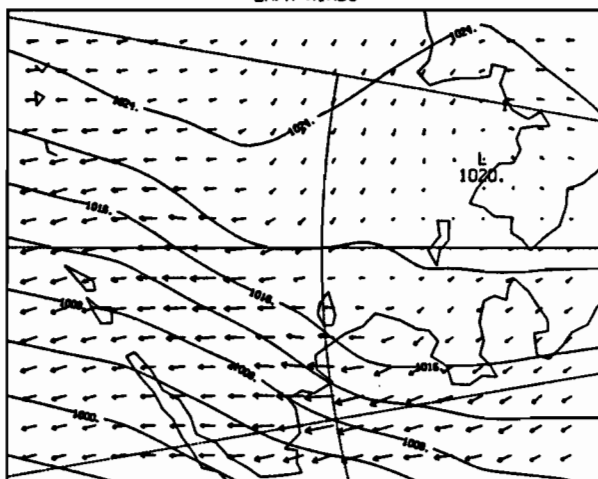
12Z 29 MAR 1985

SLP
EMPR WINDS



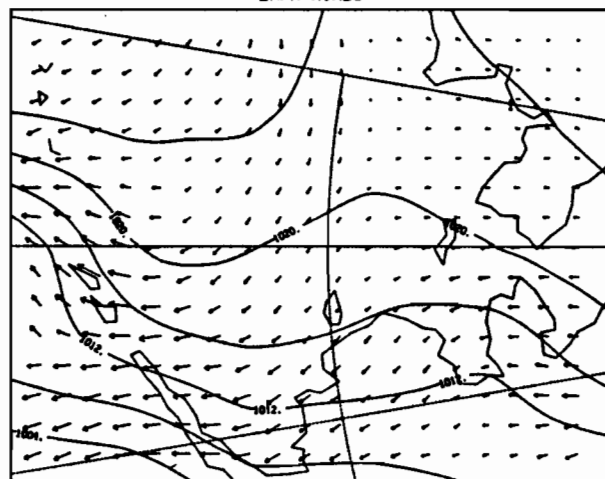
00Z 30 MAR 1985

SLP
EMPR WINDS



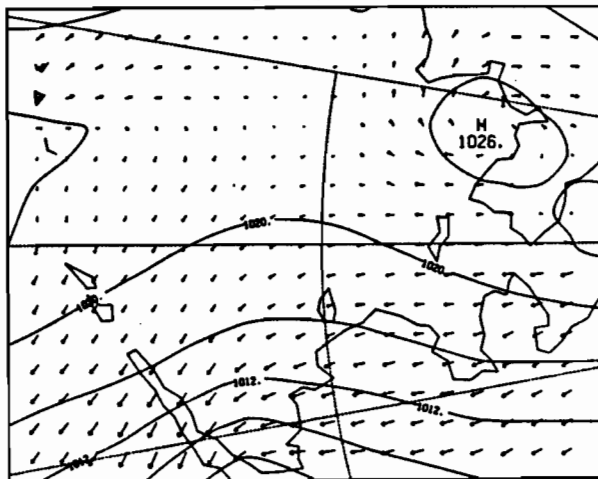
12Z 30 MAR 1985

SLP
EMPR WINDS

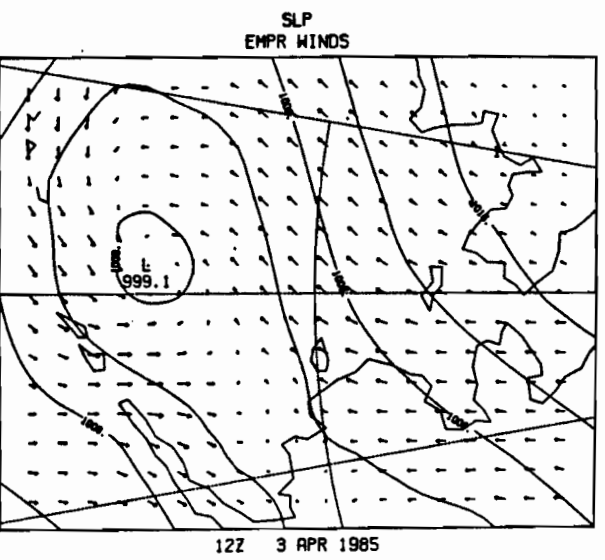
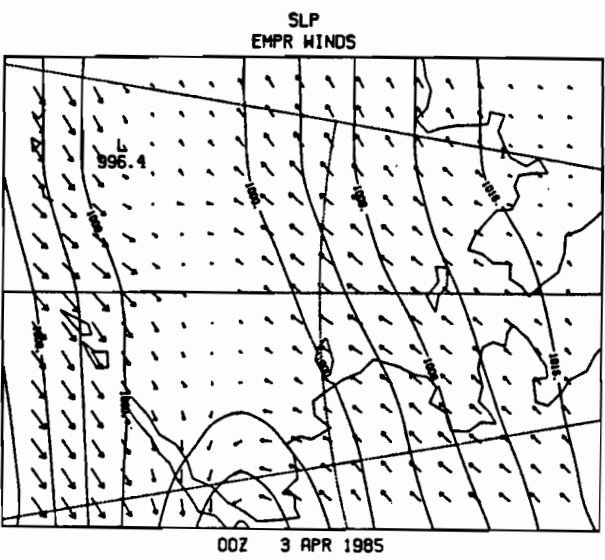
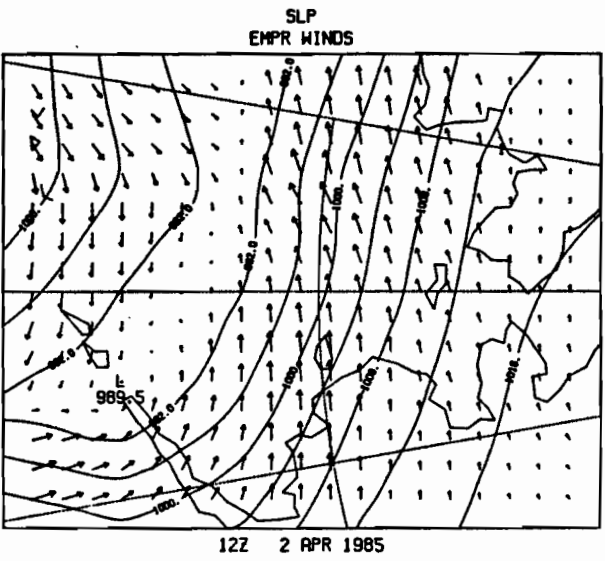
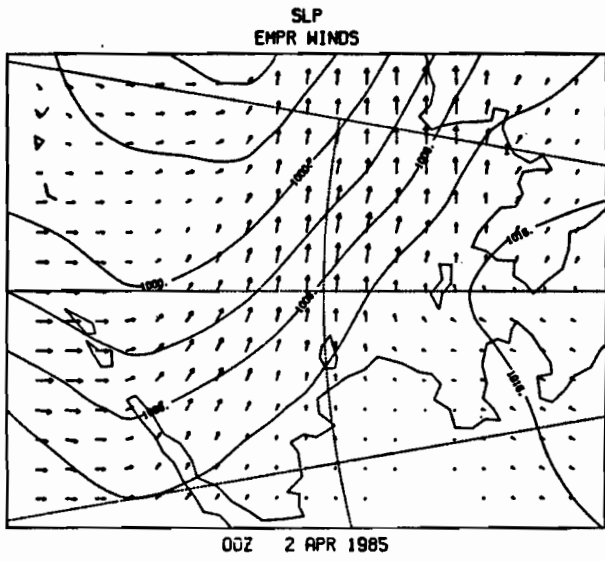
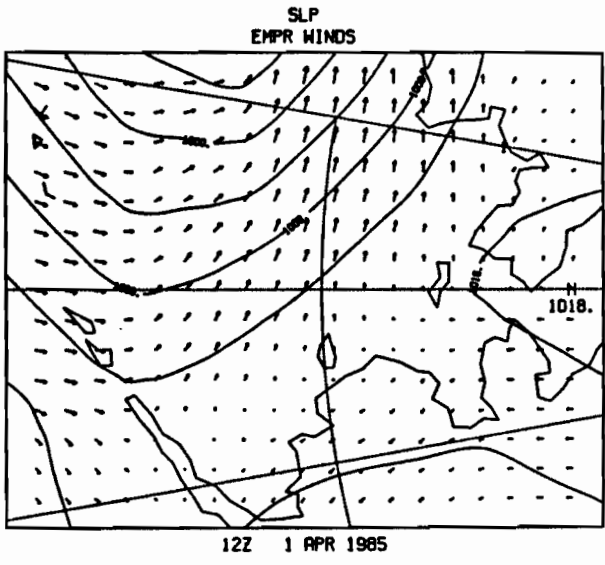
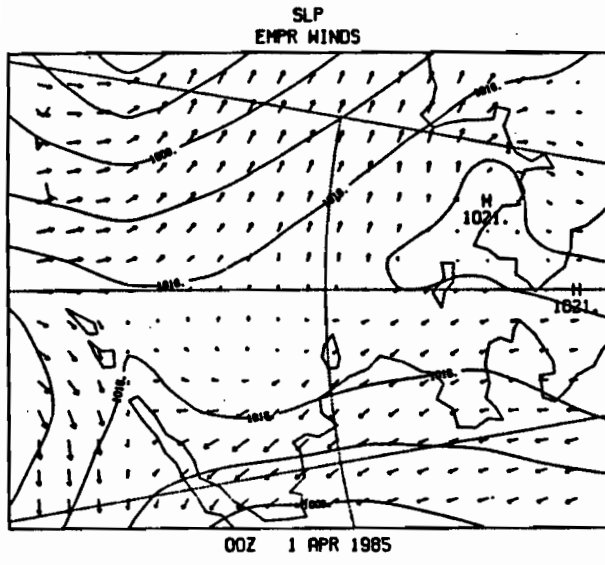


00Z 31 MAR 1985

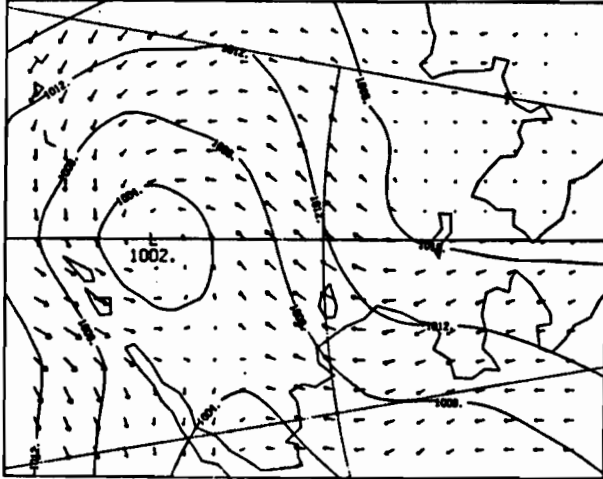
SLP
EMPR WINDS



12Z 31 MAR 1985

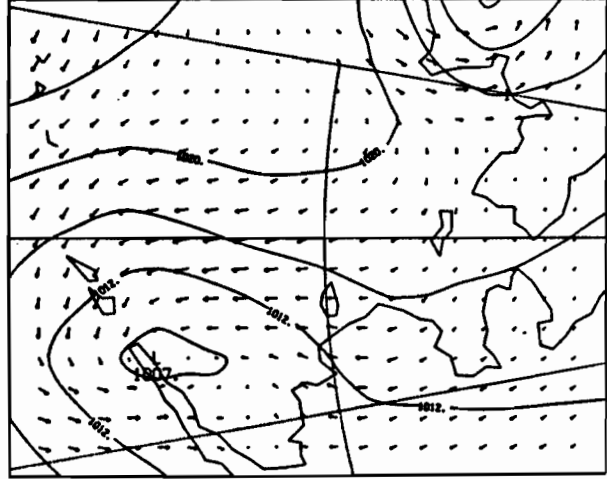


SLP
EMPR WINDS



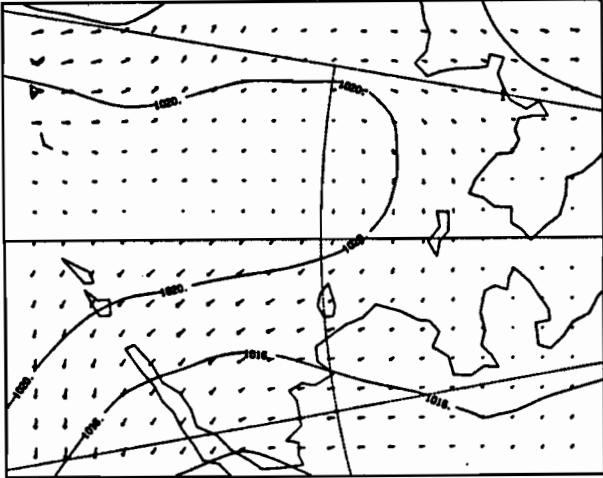
00Z 4 APR 1985

SLP
EMPR WINDS



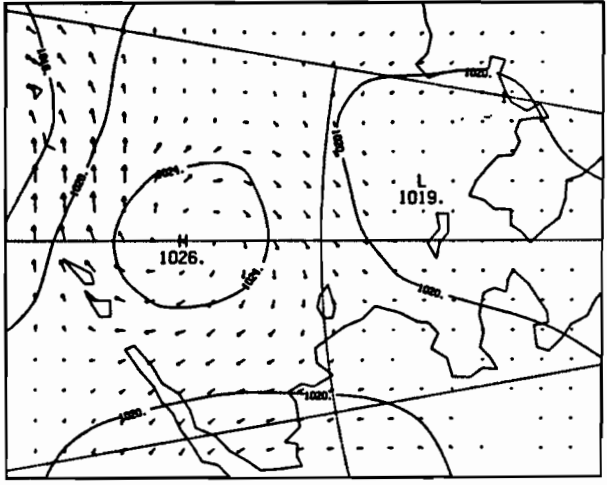
12Z 4 APR 1985

SLP
EMPR WINDS



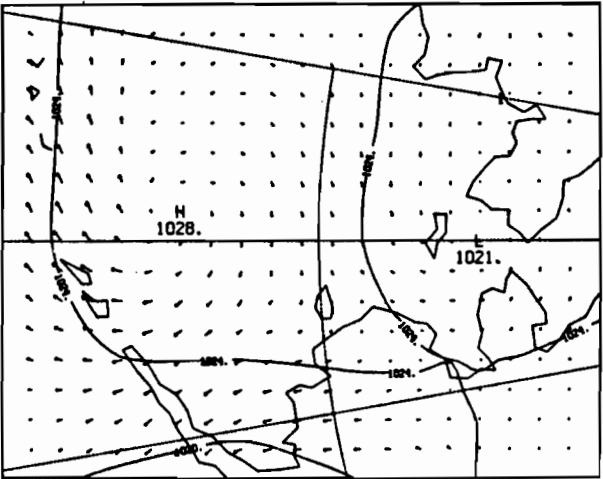
00Z 5 APR 1985

SLP
EMPR WINDS



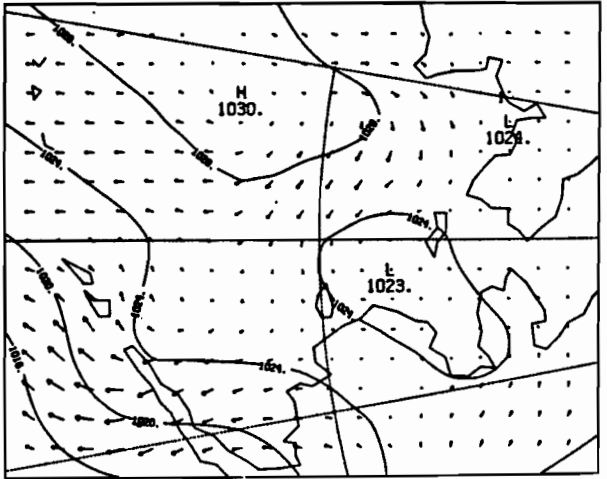
12Z 5 APR 1985

SLP
EMPR WINDS



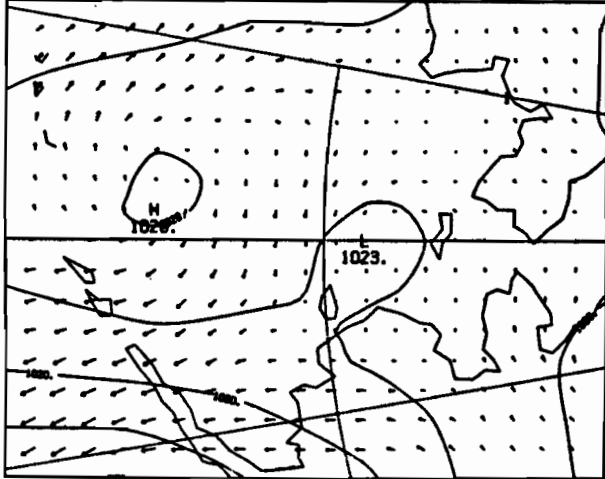
00Z 6 APR 1985

SLP
EMPR WINDS



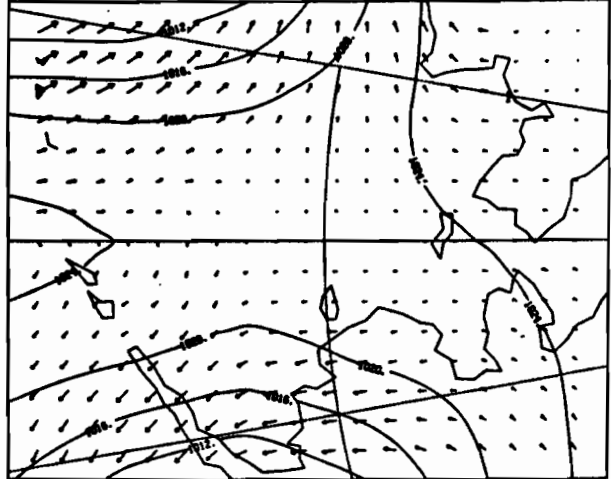
12Z 6 APR 1985

SLP
EMPR WINDS



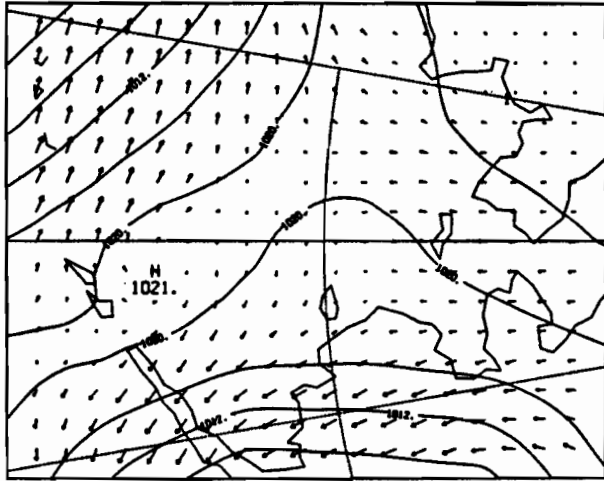
00Z 7 APR 1985

SLP
EMPR WINDS



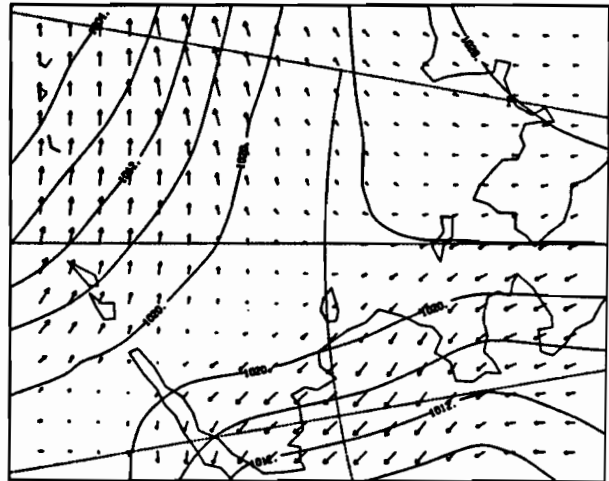
12Z 7 APR 1985

SLP
EMPR WINDS



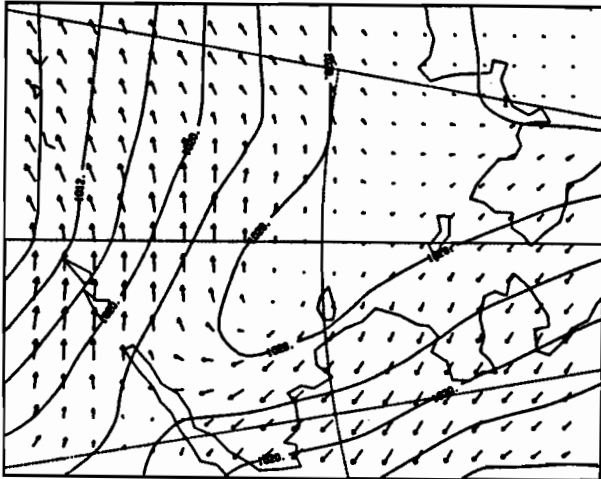
00Z 8 APR 1985

SLP
EMPR WINDS



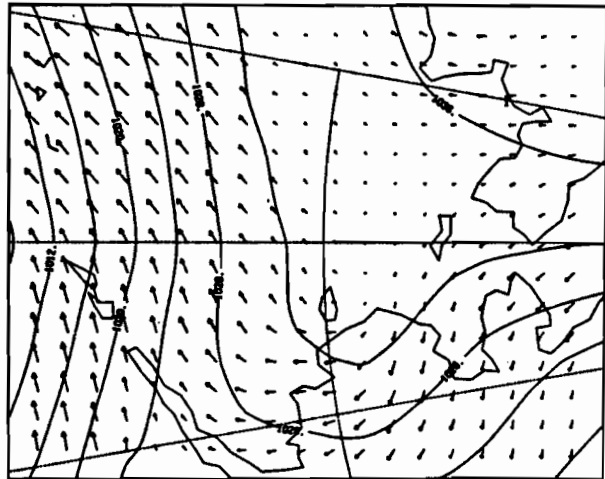
12Z 8 APR 1985

SLP
EMPR WINDS



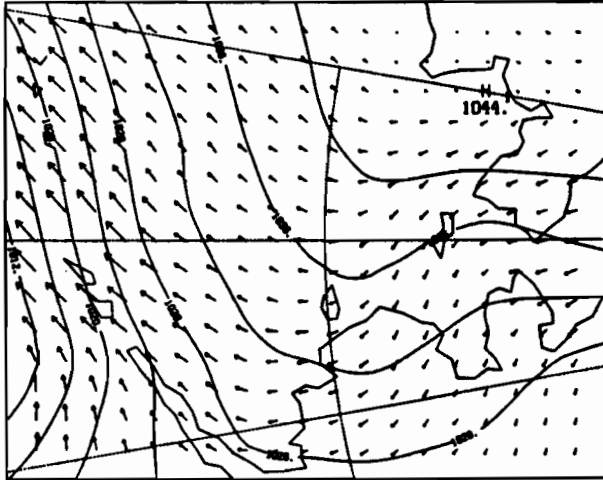
00Z 9 APR 1985

SLP
EMPR WINDS



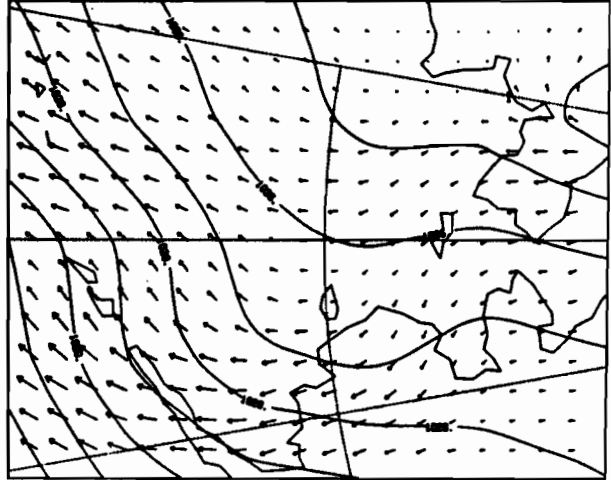
12Z 9 APR 1985
1985-BERING SEA

SLP
EMPR WINDS



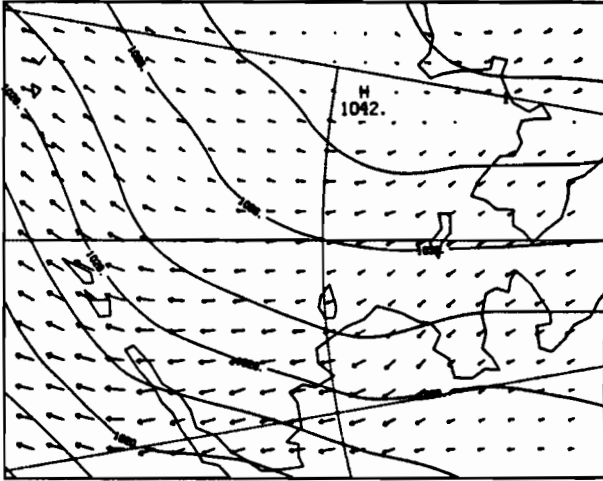
00Z 10 APR 1985

SLP
EMPR WINDS



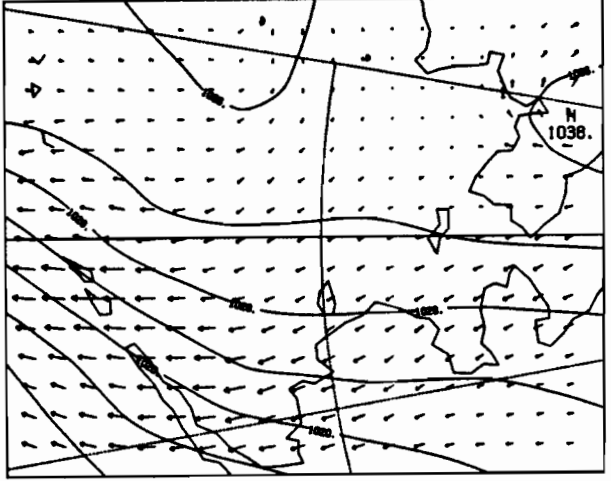
12Z 10 APR 1985

SLP
EMPR WINDS



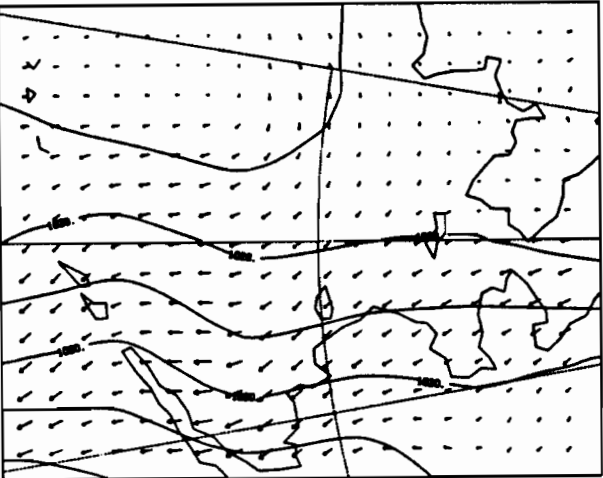
00Z 11 APR 1985

SLP
EMPR WINDS



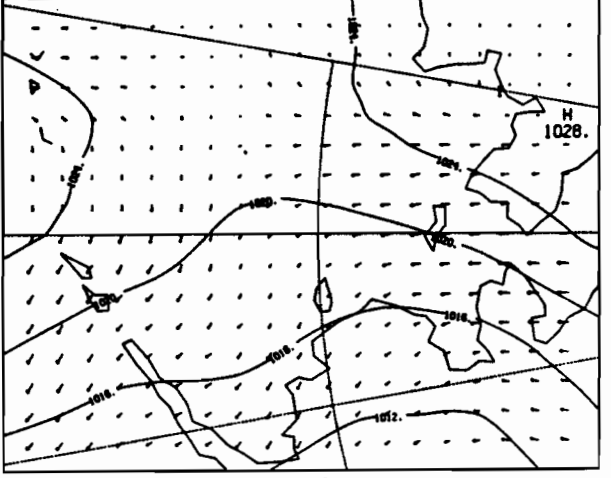
12Z 11 APR 1985

SLP
EMPR WINDS

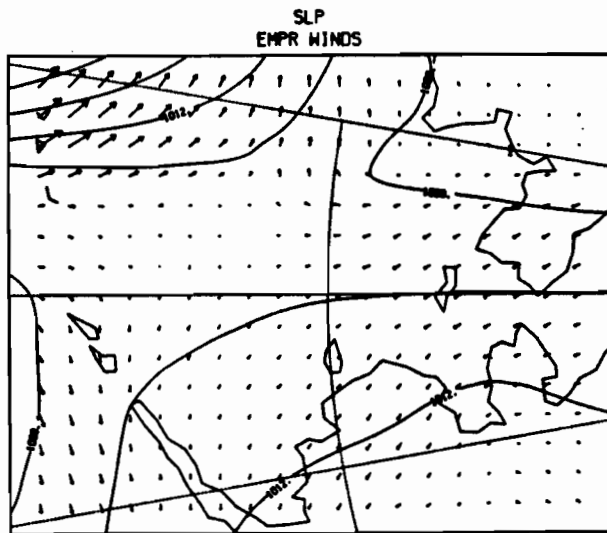


00Z 12 APR 1985

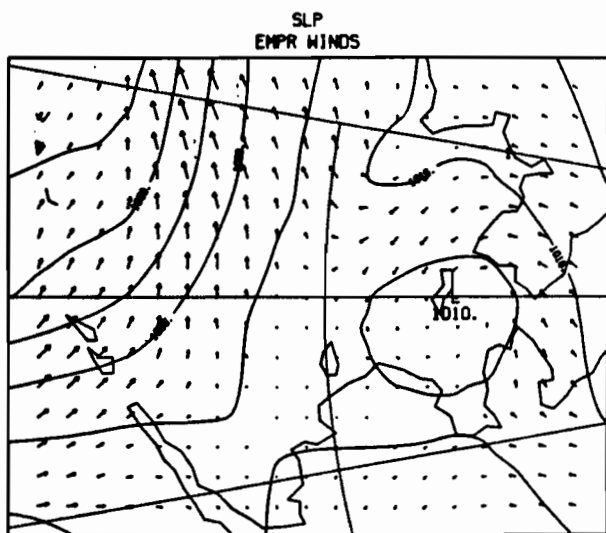
SLP
EMPR WINDS



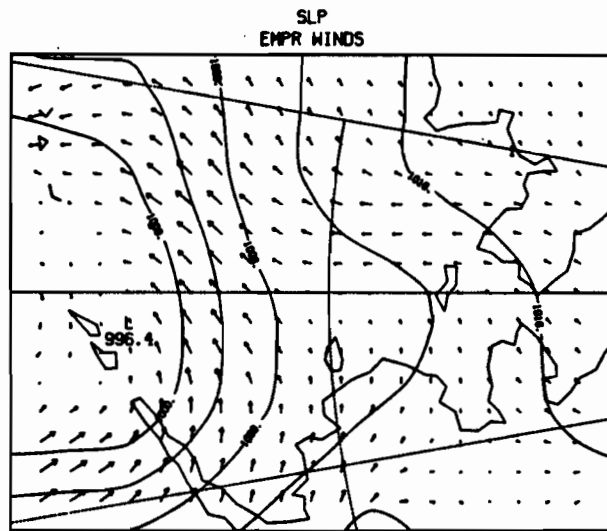
12Z 12 APR 1985



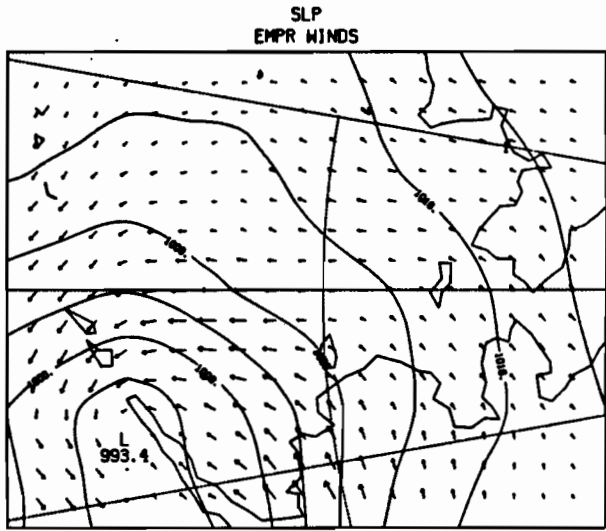
00Z 13 APR 1985



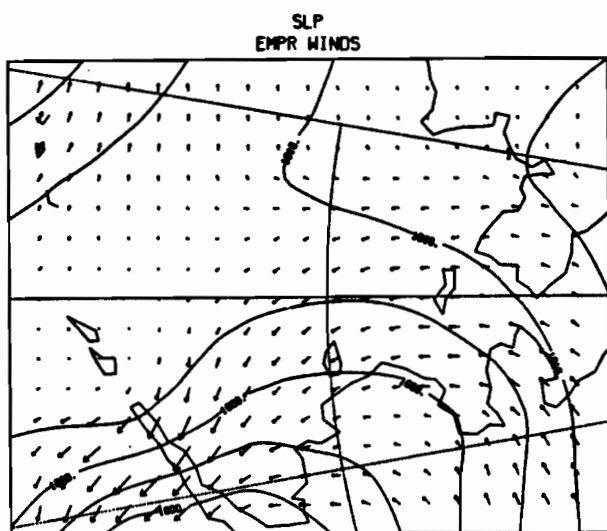
12Z 13 APR 1985



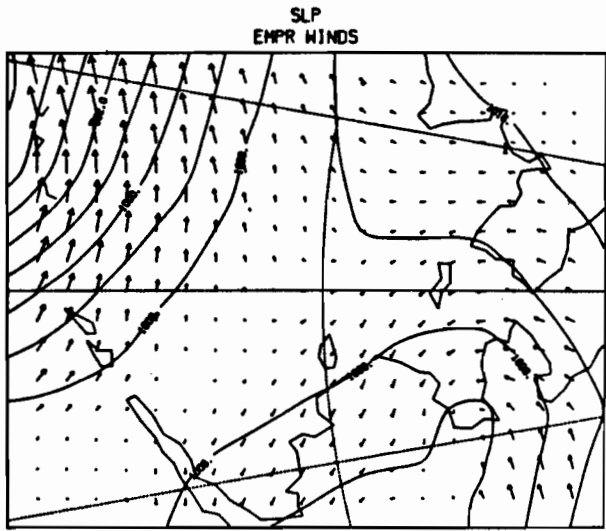
00Z 14 APR 1985



12Z 14 APR 1985



00Z 15 APR 1985

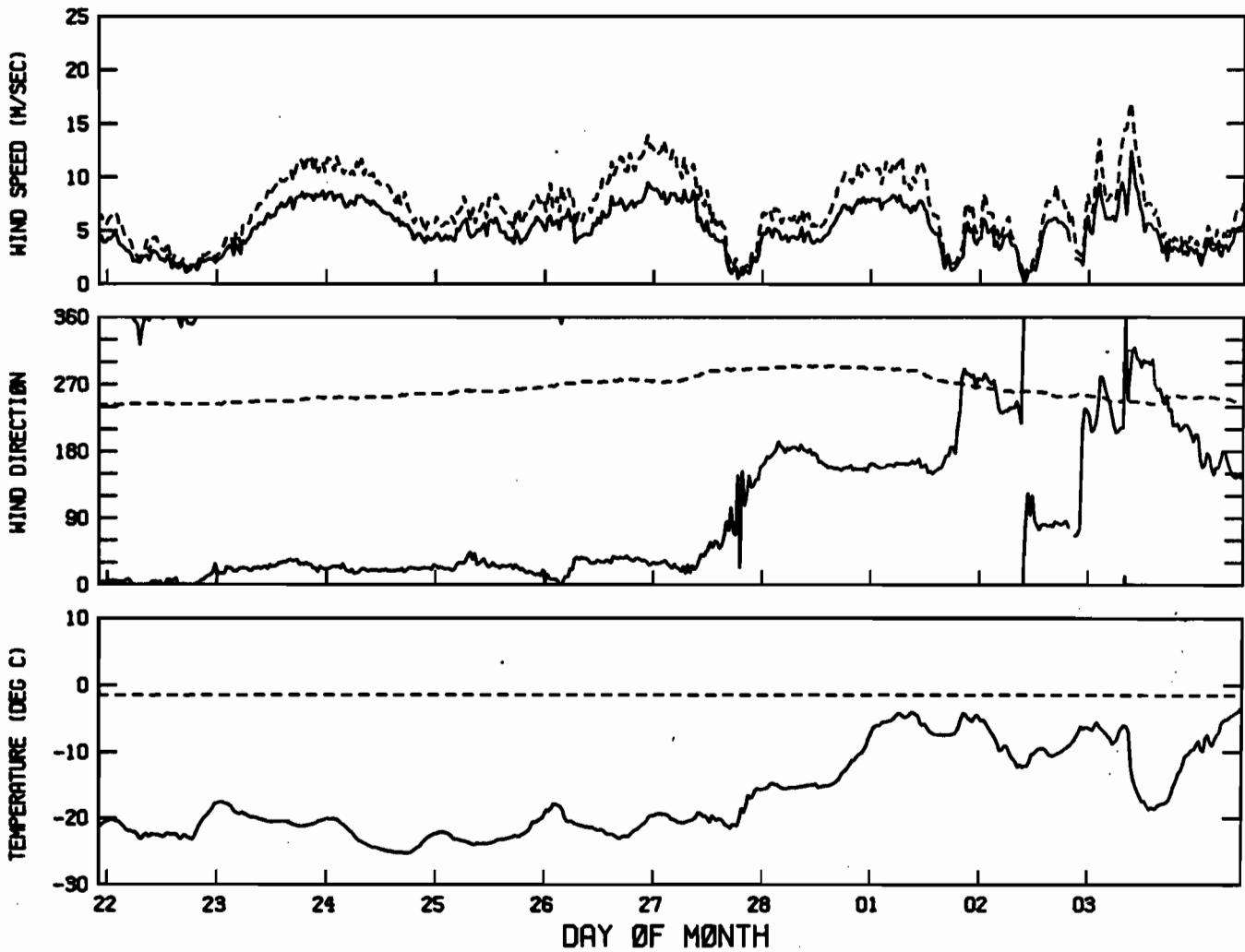


12Z 15 APR 1985

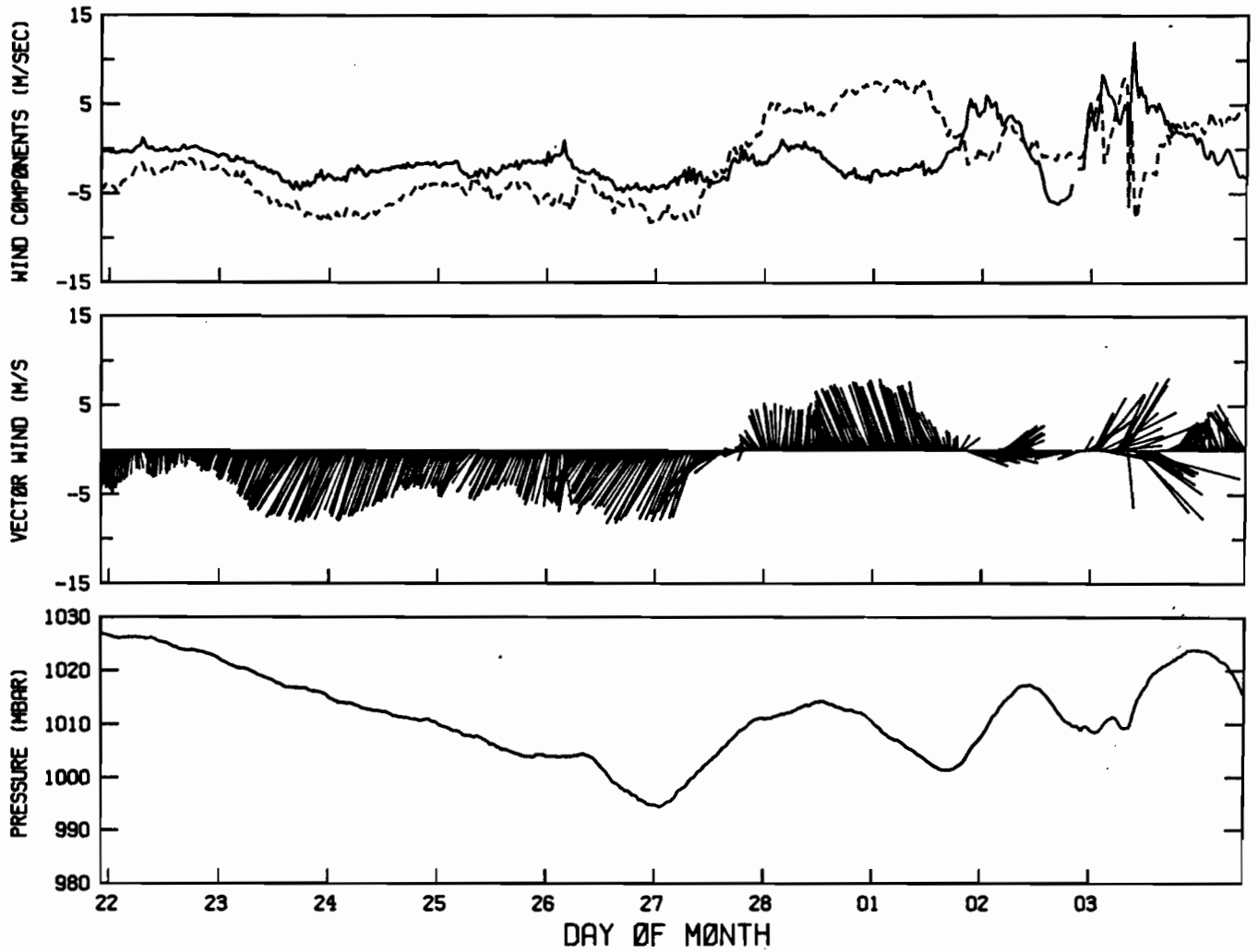
Appendix C. GOES Meteorological Data

Please see section 2.2 for a description of the GOES instrumentation and sampling.

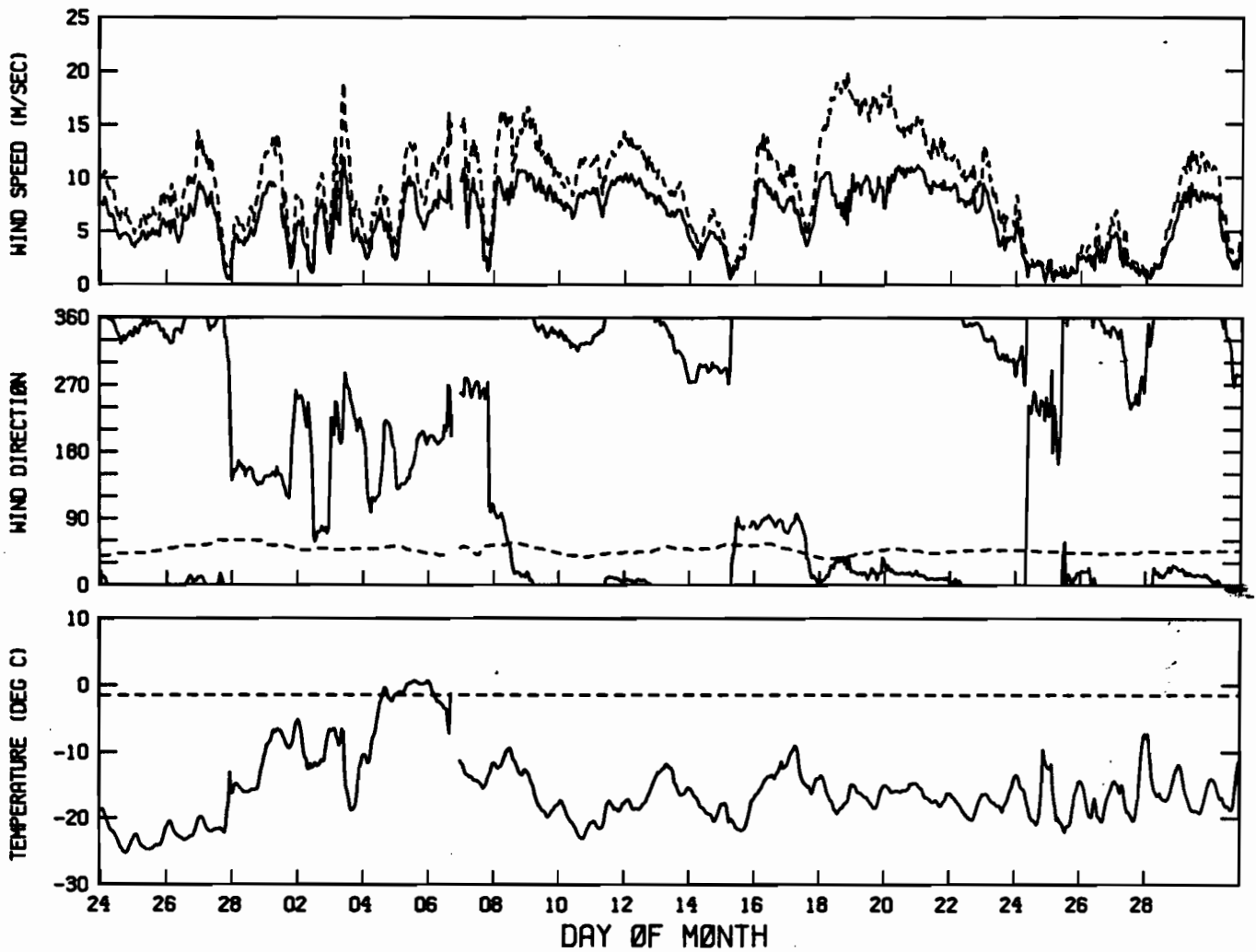
TIME SERIES PLOT FOR APEX ICE STATION A
21 FEB 85 TO 4 MAR 85 INTERVAL= 30.0 MINS



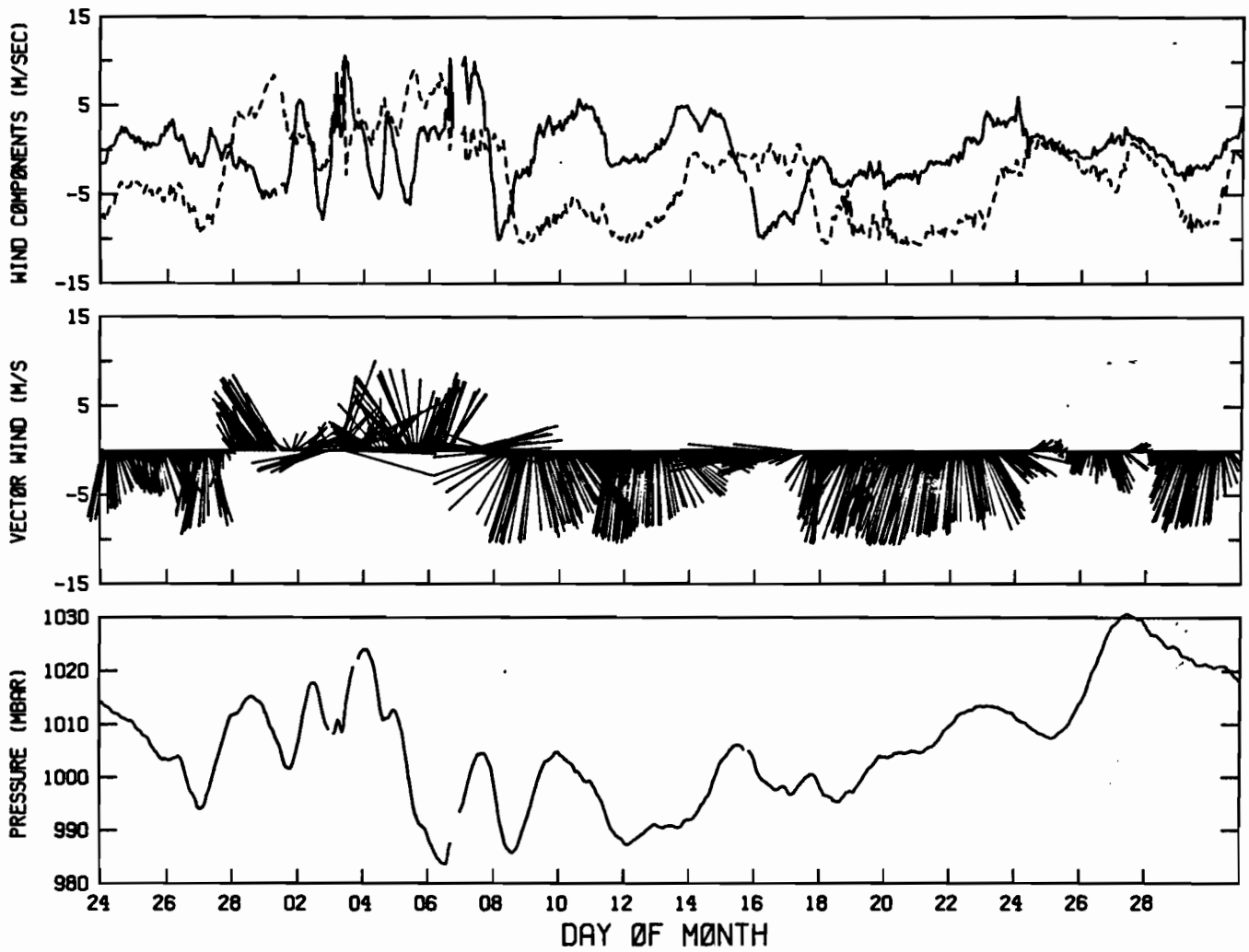
TIME SERIES PLOT FOR APEX ICE STATION A
21 FEB 85 TO 4 MAR 85 INTERVAL= 30.0 MINS



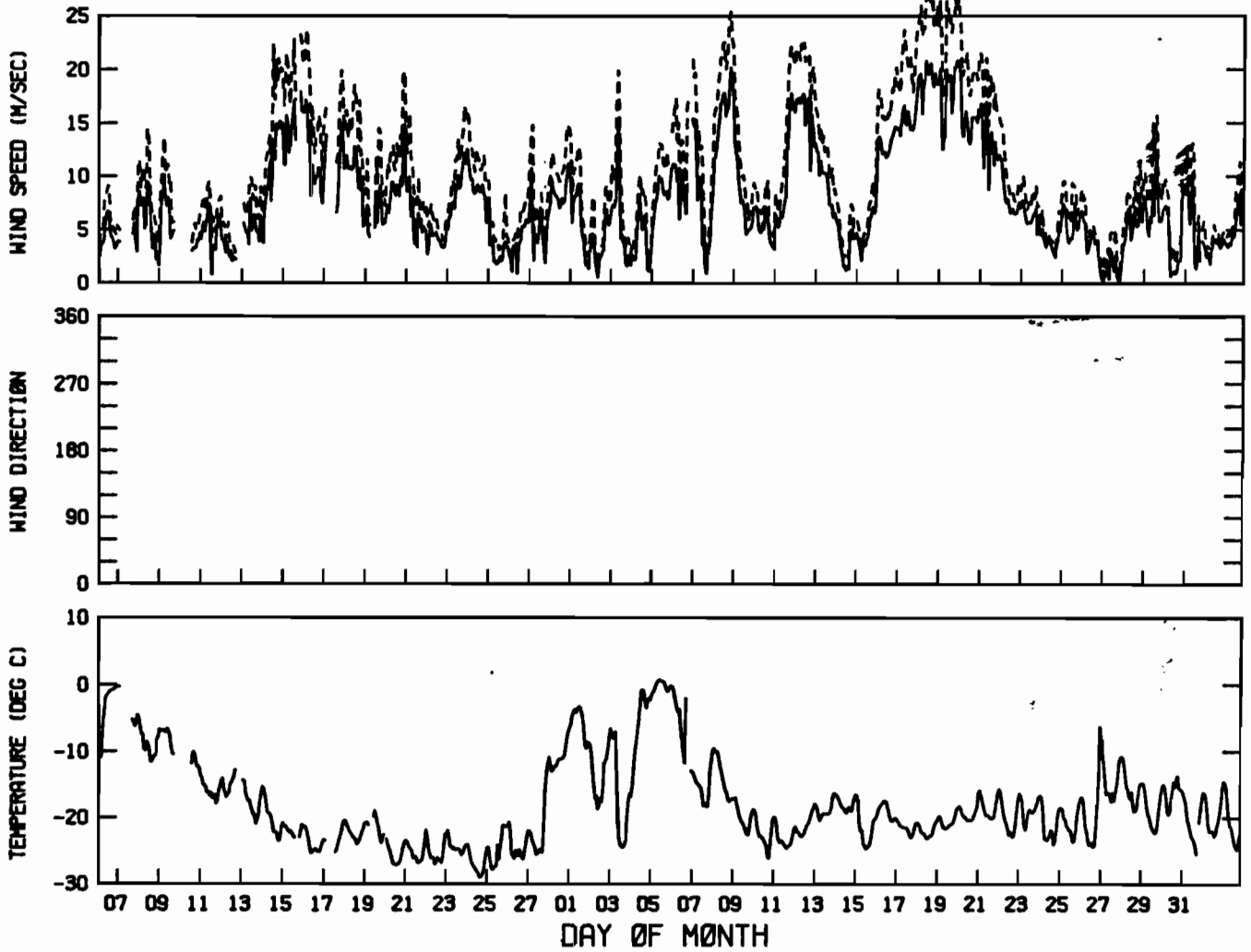
TIME SERIES PLOT FOR APEX ICE STATION B
23 FEB 85 TO 30 MAR 85 INTERVAL= 60.0 MINS



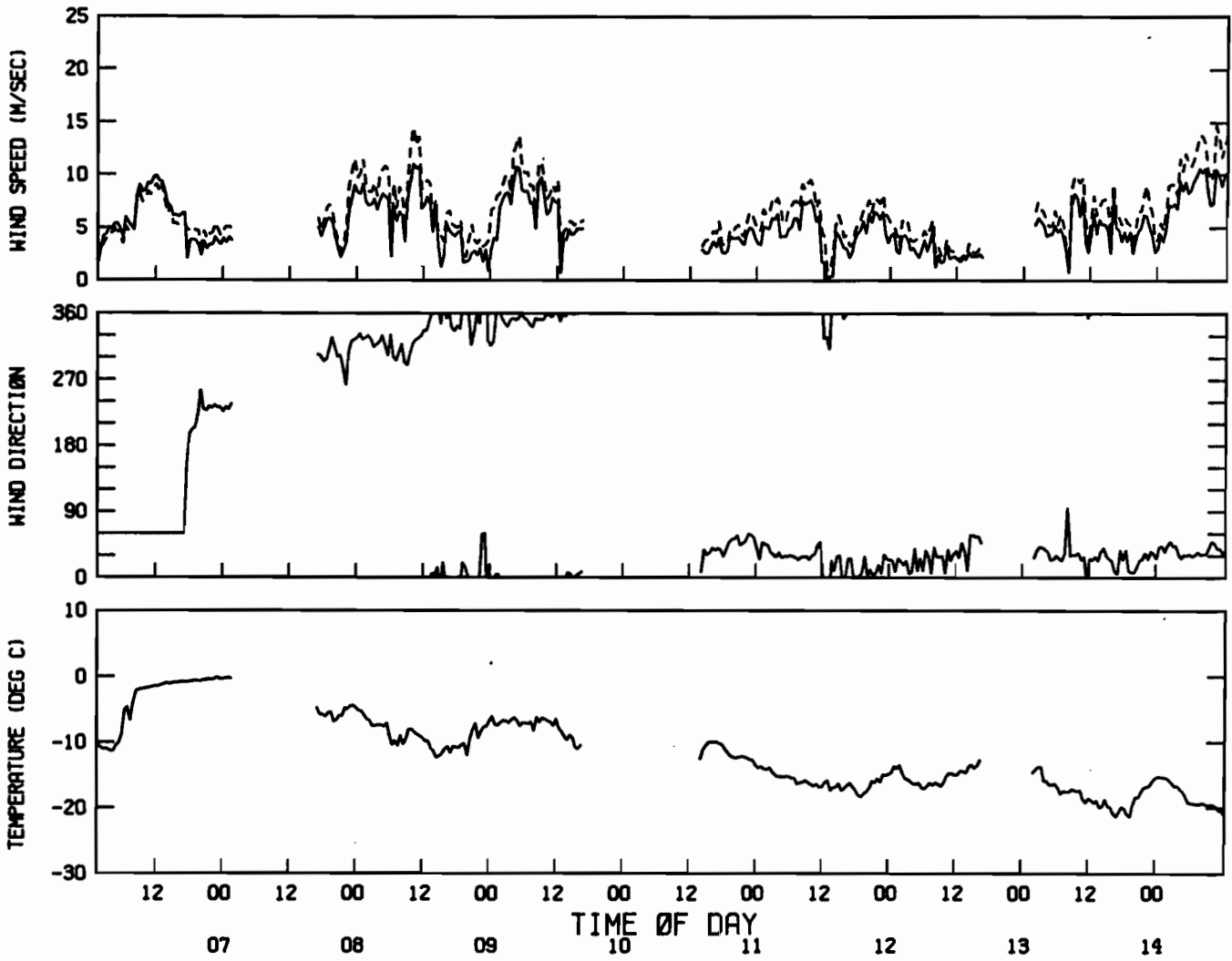
TIME SERIES PLOT FOR APEX ICE STATION B
23 FEB 85 TO 30 MAR 85 INTERVAL= 60.0 MINS



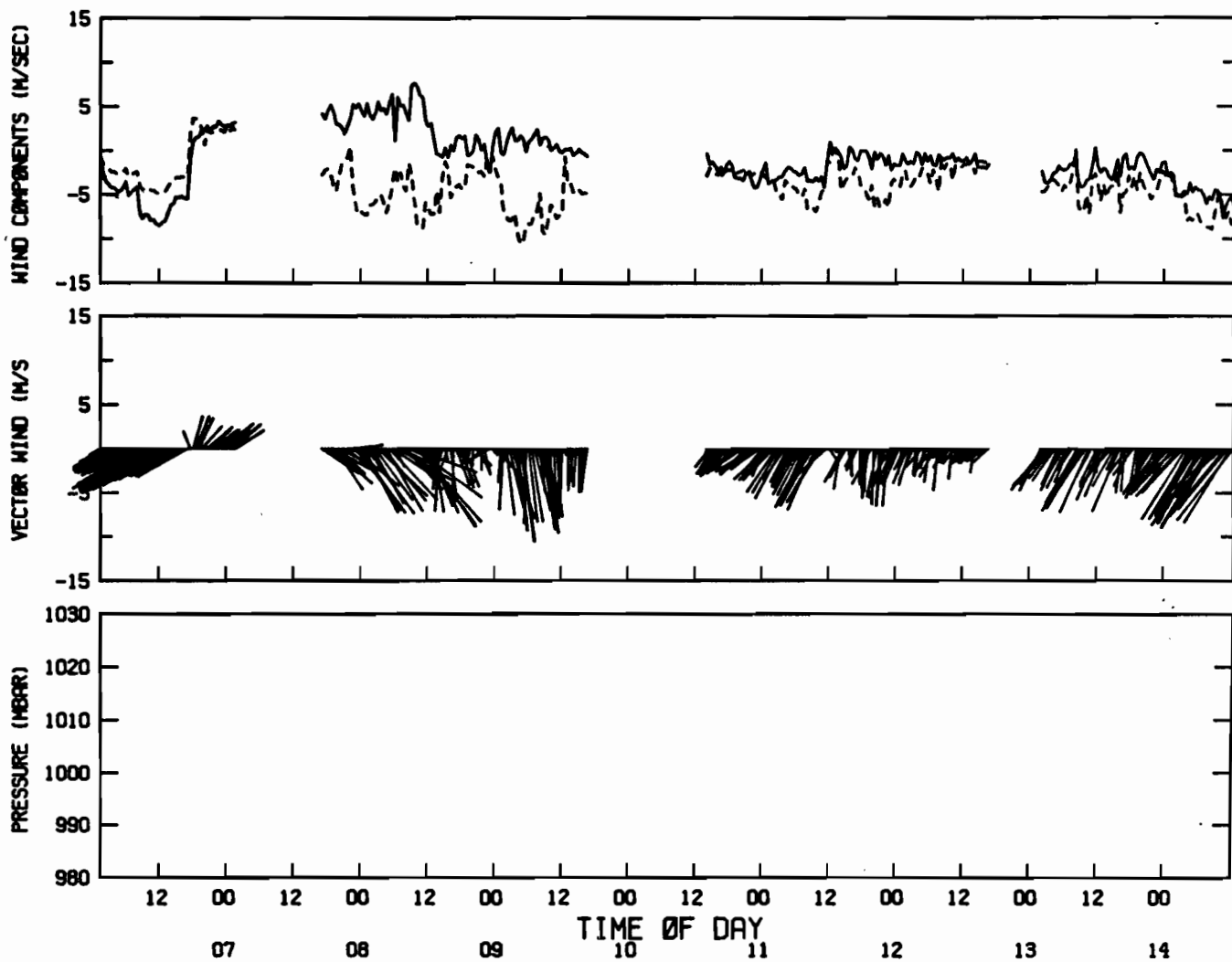
TIME SERIES PLOT FOR APEX ICE STATION C
6 FEB 85 TO 2 APR 85 INTERVAL= 90.0 MINS



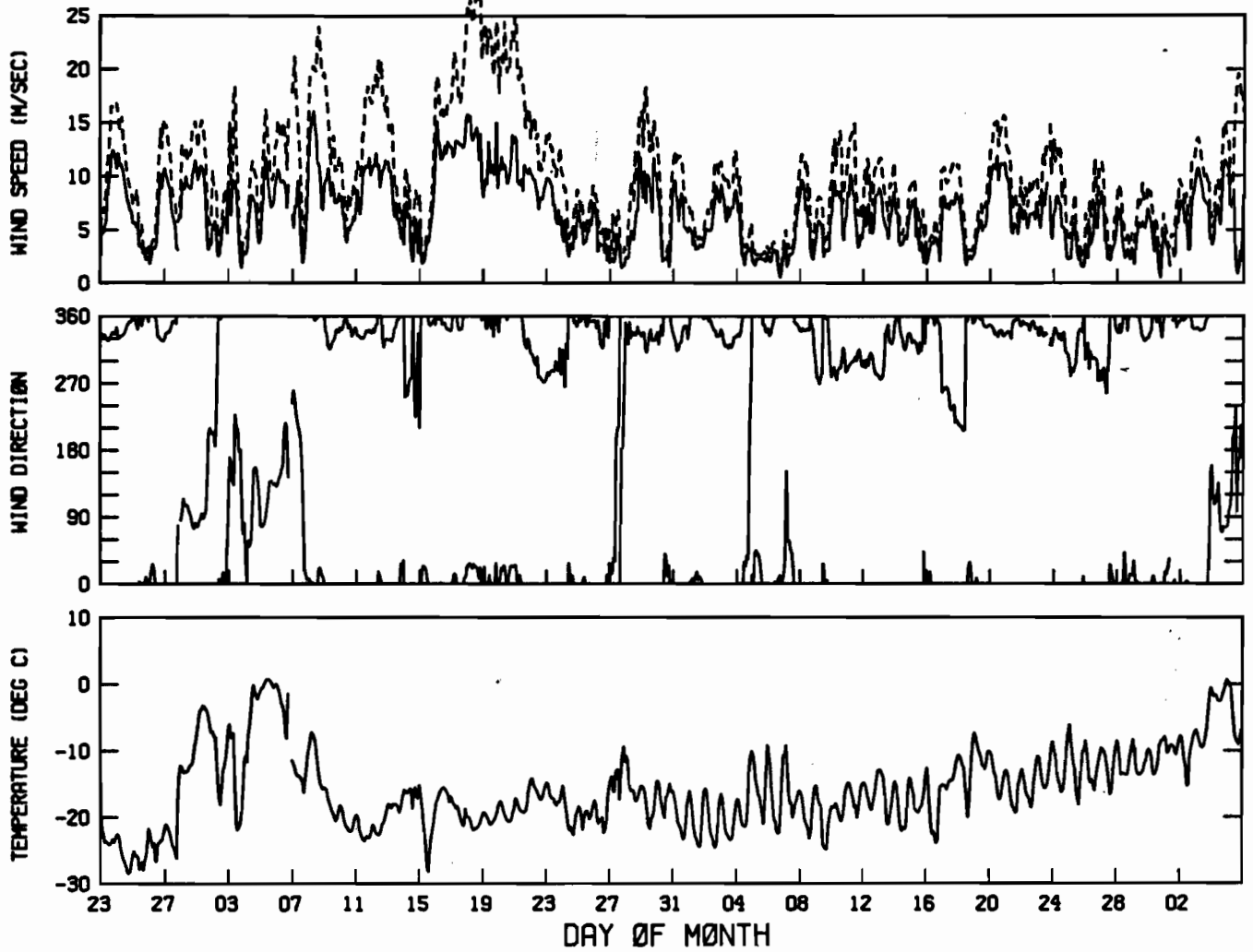
TIME SERIES PLOT FOR APEX ICE STATION C
6 FEB 85 TO 14 FEB 85 INTERVAL= 30.0 MINS



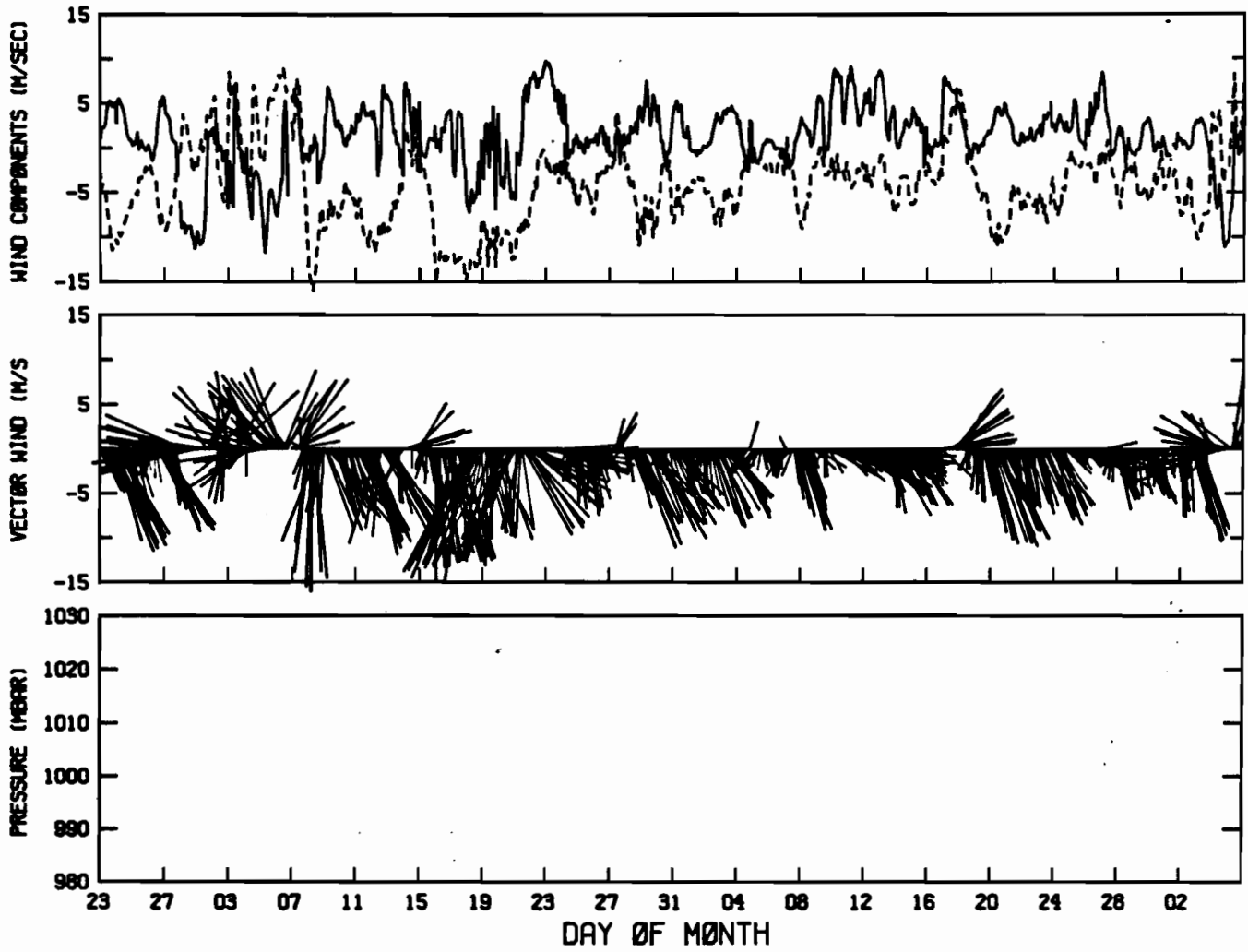
TIME SERIES PLOT FOR APEX ICE STATION C
6 FEB 85 TO 14 FEB 85 INTERVAL= 30.0 MINS



TIME SERIES PLOT FOR APEX ICE STATION D
22 FEB 85 TO 5 MAY 85 INTERVAL= 120.0 MINS



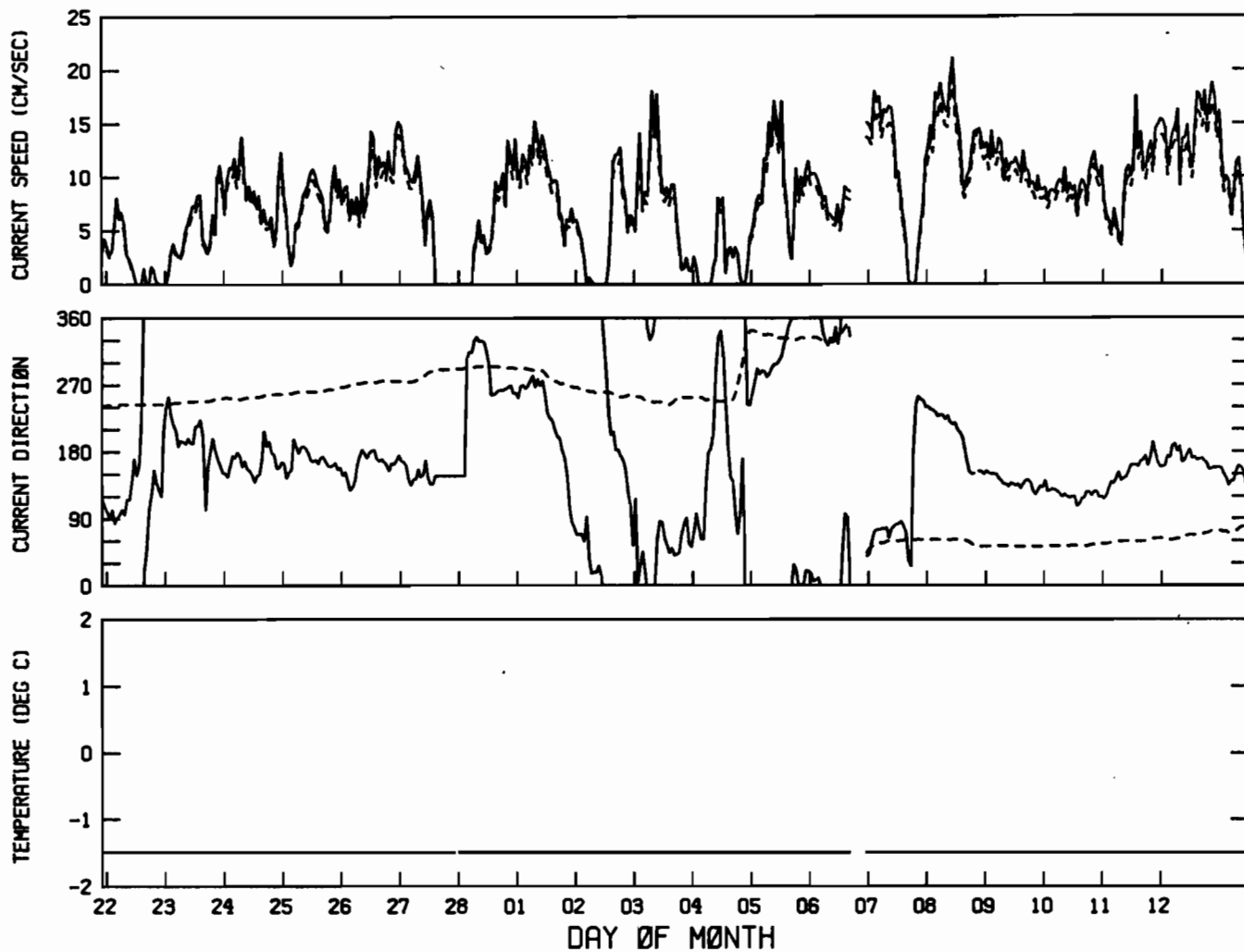
TIME SERIES PLOT FOR APEX ICE STATION D
22 FEB 85 TO 5 MAY 85 INTERVAL= 120.0 MINS



Appendix D. GOES Oceanographic Data

Please see section 2.2 for a description of the GOES instrumentation and sampling.

TIME SERIES PLOT FOR APEX ICE STATION A
21 FEB 85 TO 13 MAR 85 INTERVAL= 60.0 MINS



TIME SERIES PLOT FOR APEX ICE STATION B
23 FEB 85 TO 30 MAR 85 INTERVAL= 60.0 MINS

